PALACKÝ UNIVERSITY OLOMOUC

Faculty of Science

Department of Cell Biology and Genetics

ENDOGENOUS AND XENOBIOTIC INDOLES AS MODULATORS OF THE AHR AND PXR SIGNALLING PATHWAYS

Ph.D. Thesis

Author:	**Mgr. Barbora Vyhlídalová**
Study program:	P1527 Biology
Study branch:	Molecular and Cell Biology
Form of study:	Present
Supervisor:	**Prof. RNDr. Zdeněk Dvořák, DrSc. *et* Ph.D.**
Submitted:	22th August 2022

Olomouc 2022

I hereby declare that the presented Ph.D. thesis is based on my research conducted at the Department of Cell Biology and Genetics, Faculty of Science, Palacký University Olomouc, in the period September 2017-August 2022. The co-authors agree with the inclusion of the published results. All literature sources cited in this thesis are listed in the "References" section.

Olomouc 22th August 2022   ……………………………

                                                                                Mgr. Barbora Vyhlídalová

ACKNOWLEDGEMENT

I would like to express my heartfelt thanks to all those who supported me, provided me valuable advice, and co-operated with me during the conduct of my study and writing of my thesis.

My particular gratitude goes to my supervisor, Prof. RNDr. Zdeněk Dvořák, DrSc. *et* Ph.D. for his professional guidance, patience, and help, consistent and factual remarks, and advice throughout my study. I also appreciate the opportunity to be part of his research group. His ideas, perceptions, knowledge, creativity, and friendship are first-class examples of leadership not only to a group of scientists, but also to the Department of Cell Biology and Genetics.

Furthermore, I would like to acknowledge my colleagues - Mgr. Iveta Zůvalová, Ph.D. and Mgr. Karolína Poulíková. They both shared their laboratory skills and knowledge with me, especially at the beginning of my Ph.D. study. My long-time friend Karolína supported and motivated me and stood by me always in this chapter of my life.

In addition, my thanks go to my colleagues from the Department of Cell Biology and Genetics for the friendly working environment.

Lastly but not the least, I am very grateful to my family for their unceasing support and encouragement. In particular, my husband has constantly encouraged me, even in the difficult moments of my Ph.D. study.

Data presented in this thesis are contained in the following publications:

Vyhlidalova B., Poulikova K., Bartonkova I., Krasulova K., Vanco J., Travnicek Z., Mani S., Dvorak Z. (2019). Mono-methylindoles induce CYP1A genes and inhibit CYP1A1 enzyme activity in human hepatocytes and HepaRG cells. *Toxicol Lett,* 313: 66-76. **[IF$_{2019}$ 3.569]**

Vyhlidalova B., Bartonkova I., Jiskrova E., Li H., Mani S., Dvorak, Z. (2020). Differential activation of human pregnane X receptor PXR by isomeric mono-methylated indoles in intestinal and hepatic in vitro models. *Toxicol Lett,* 324: 104-110. **[IF$_{2020}$ 4.374]**

Vyhlidalova B., Krasulova K., Pecinkova P., Marcalikova A., Vrzal R., Zemankova L., Vanco J., Travnicek Z., Vondracek J., Karasova M., Mani S., Dvorak, Z. (2020). Gut Microbial Catabolites of Tryptophan Are Ligands and Agonists of the Aryl Hydrocarbon Receptor: A Detailed Characterization. *Int. J. Mol. Sci,* 21(7): 2614. **[IF$_{2020}$ 5.924]**

Illes P., Krasulova K., **Vyhlidalova B.**, Poulikova K., Marcalikova A., Pecinkova P., Sirotova N., Vrzal R., Mani S., Dvorak, Z. (2020). Indole microbial intestinal metabolites expand the repertoire of ligands and agonists of the human pregnane X receptor. *Toxicol Lett,* 334: 87-93. **[IF$_{2020}$ 4.374]**

Bibliographic identification

First name and surname	Mgr. Barbora Vyhlídalová
Title	Endogenous and xenobiotic indoles as modulators of AhR and PXR signalling pathways
Type of thesis	Ph.D.
Department	Department of Cell Biology and Genetics
Supervisor	prof. RNDr. Zdeněk Dvořák, DrSc. et Ph.D.
The year of presentation	2022

Abstract

The human microbiome produces diverse metabolites that affect human health. A distinct class of microbial catabolites is formed from dietary tryptophan, some of which have already been described as ligands of the aryl hydrocarbon receptor (AhR) and the pregnane X receptor (PXR). Both receptors act as sensors for endogenous and exogenous compounds, and thus regulate gene expression of drug-metabolizing enzymes. In addition, both AhR and PXR play pivotal roles in various physiological and pathophysiological processes. For this reason, these receptors are important therapeutic targets for existing and novel compounds. However, not all microbial tryptophan catabolites have been systematically studied in relation to AhR and PXR, which would be significant to general intestinal health. Tryptophan catabolites contain indole in their structure, which is considered a biologically active component. Thus, endogenous and xenobiotic indole derivatives have been the subject of many studies and may have both beneficial and deleterious biological effects through these receptors.

In the present thesis, I have investigated the effects of tryptophan catabolites and mono-methylated indoles on the activities of AhR and PXR and the subsequent molecular events involved in these signalling pathways. Appropriate human and mouse intestinal and hepatic *in vitro* cell models were used for the study. Our findings showed that mono-methylated indoles are ligands and partial agonists of human PXR that induce PXR-regulated genes in human intestinal cells. Mono-methylated indoles display dual effects on the

AhR-CYP1A signalling pathway in human intestinal and liver cells. On the one hand, they are AhR-dependent inducers of CYP1A genes, and on the other hand, they are inhibitors of CYP1A1 catalytic activity. In addition, this study demonstrated that the tryptophan catabolites are low-potency agonists of AhR, and their effects on AhR may differ substantially, as they may behave as full agonists, partial agonists, or even ligand-selective antagonists of human AhR. The findings of this study, for the first time, showed that indole-3-acetamide, indole-3-pyruvate, indole-3-acrylate, and indole-3-ethanol were among the strongest AhR ligands within the microbial tryptophan pathway and that indole and indole-3-acetamide are ligands and agonists of human PXR. In conclusion, this study comprehensively characterised the interactions of gut microbial tryptophan catabolites and synthetic mono-methylated indoles with AhR and PXR, which may expand the current understanding of their potential roles inhuman intestinal health and disease. Furthermore, these findings would expand the potential drug repertoire through the concept of indole-based mimicry.

Bibliografická identifikace

Jméno a příjmení	Mgr. Barbora Vyhlídalová
Titul	Endogenní a xenobiotické indoly jako modulátory signálních drah AhR a PXR
Typ práce	Ph.D.
Pracoviště	Katedra buněčné biologie a genetiky
Školitel	prof. RNDr. Zdeněk Dvořák, DrSc. et Ph.D.
Rok obhajoby práce	2022

Abstrakt

Lidský mikrobiom produkuje rozmanité metabolity, které ovlivňují lidské zdraví. Jedna skupina mikrobiálních katabolitů je tvořena z tryptofanu přijatého v potravě, z nichž některé již byly popsány jako ligandy aryl uhlovodíkového receptoru (AhR) a pregnanového X receptoru (PXR). Oba receptory působí jako xenoreceptory endogenních i exogenních sloučenin a regulují tak genovou expresi enzymů metabolizujících léčiva. Kromě toho AhR i PXR hrají významnou roli v různých fyziologických a patofyziologických procesech. Z tohoto důvodu jsou tyto receptory významným terapeutickým cílem pro stávající i nové látky. Doposud však nebyly systematicky studovány všechny známé tryptofanové katabolity ve vztahu k AhR a PXR, což by byl jedinečný a přímo aplikovatelný přístup ke střevnímu zdraví všeobecně. Tryptofanové katabolity obsahují ve své struktuře indol, který je považován za biologicky aktivní část. Předmětem mnoha studií jsou tedy endogenní I xenobiotické deriváty indolu, které mohou mít prostřednictvím těchto receptorů, jak příznivé, tak negativní biologické účinky.

V předkládané disertační práci jsem se zabývala studiem účinků tryptofanových katabolitů a mono-methylovaných indolů na aktivitu AhR a PXR receptoru a následné molekulární děje účastnící se těchto signálních drah. Pro studium byly použity vhodné *in vitro* modely lidských a myších, střevních a jaterních buněk. Naše zjištění ukázala, že mono-methylované indoly jsou ligandy a parciální agonisté lidského PXR, které indukují PXR cílové geny v lidských střevních buňkách. Zároveň mono-methylované indoly mají dvojí účinek na AhR-CYP1A signální dráhu v lidských střevních a jaterních buňkách.

Jednak indukují expresi CYP1A genů prostřednictvím AhR, ale na druhé straně jsou inhibitory CYP1A1 katalytické aktivity. Dále jsme prokázali, že tryptofanové katabolity jsou AhR agonisté s nízkou účinností, avšak jejich působení na AhR se může podstatně lišit, protože se mohou chovat jako úplní agonisté, částeční agonisté nebo dokonce ligandově selektivní antagonisté lidského AhR. Výsledky této studie poprvé ukázaly, že indol-3-acetamid, indol-3-pyruvát, indol-3-akrylát a indol-3-etanol patří mezi nejsilnější ligandy AhR v rámci mikrobiální tryptofanové dráhy a že indol a indol-3-acetamid jsou ligandy a agonisté lidského PXR. Závěrem lze říci, že tato studie komplexně charakterizovala interakce střevních mikrobiálních katabolitů tryptofanu a syntetických mono-methylovaných indolů s AhR a PXR, což může rozšířit současné chápání o jejich potencionálních rolích v lidském střevním zdraví a onemocněních. Navíc tato zjištění jsou zásadní pro rozšíření potencionálního repertoáru léčiv prostřednictvím konceptu mimikry na bázi indolů.

Klíčová slova	Indolové deriváty, střevní mikrobiom, pregnanový X receptor, aryl uhlovodíkový receptor, cytochrom 450, střevní záněty
Počet stran	130
Počet příloh	4
Jazyk	Angličtina

CONTENT

LIST OF SYMBOLS AND ABBREVIATIONS

3-MMI/3-MI	3-methylindole
5-HT	5-hydroxytryptamine/serotonin
5-HTP	5-hydroxytryptophan
AADC	Aromatic amino acid decarboxylase
ABC	ATP-binding cassette transporters
ADME	Absorption, distribution, metabolism, and excretion
AF-1/2	Activation function 1/2
AhR	Aryl hydrocarbon receptor
AhRR	Aryl hydrocarbon receptor repressor
AR	Androgen receptor
ARNT	Aryl hydrocarbon receptor nuclear translocator
ATP	Adenosine triphosphate
BaP	Benzo[a]pyrene
BCRP	Breast cancer resistance protein
bHLH	Basic helix loop helix
CAR	Constitutive androstane receptor
CBP	Cyclic adenosine monophosphate Response Element Binding protein
CCRP	Cytoplasmic CAR retention protein
ChIP	Chromatin immunoprecipitation
Co-IP	Co-immunoprecipitation
CRISPR	Clustered Regularly Interspaced Short Palindromic Repeats
CS-FBS	Charcoal-stripped foetal bovine serum
CYP	Cytochrome P450
DBD	DNA binding domain
DME	Drug metabolizing enzyme
DMEM	Dulbecco´s modified Eagle´s medium
DMSO	Dimethylsulfoxide
DNA	Deoxyribonucleic acid
DR	Direct repeat
DRE	Dioxin response element
DSS	Dextran sulfate sodium salt

EC$_{50}$	Half maximal effective concentration
ECACC	European Collection of Authenticated Cell Cultures
ER	Estrogen receptor
ER	Everted repeat
ERAP140	Estrogen receptor-associated protein 140
FBS	Foetal bovine serum
FICZ	6-formylindolo[3,2-b]carbazole
FMO	Flavin containing monooxygenase
FXR	Farnesoid X receptor
GAPDH	Glyceraldehyde 3-phosphate dehydrogenase
GI	Gastrointestinal
GPR35	G Protein-Coupled Receptor 35
GR	Glucocorticoid receptor
GST	Glutathione S-transferase
HAH	Halogenated aromatic hydrocarbon
Hsp90	Heat shock protein 90
IA	Indole-3-aldehyde
IAA	Indole-3-acetate
IAC	Indole-3-acrylate
IAD	Indole-3-acetamide
IAL	Indole-3-acrylate
IBD	Inflammatory bowel disease
IC$_{50}$	Half maximal inhibitory concentration
IDO	Indoleamine 2,3-dioxygenase
IET	Indole-3-ethanol
ILA	Indole-3-lactate
IND	Indole
IPA	Indole-3-propionate
IPY	Indole-3-pyruvate
IR	Inverted repeat
KLF-6	Krüppel-like factor 6
LBD	Ligand binding domain
LXR	Liver X receptor
MDR	Multidrug resistance

MEM	Minimal essential medium
MICT	Microbial intestinal catabolite of tryptophan
MMI	Mono-methylated indole
MR	Mineralocorticoid receptor
MRP	Multidrug resistance associated protein
NAT	N-acetyltransferase
NCoR1/2	Nuclear receptor corepressor
NES	Nuclear export signal
NF-κB	Nuclear factor kappa B
NGFI-B	Nerve growth factor-induced clone B
NLS	Nuclear localization signal
NR	Nuclear receptor
OAT	Organic anion transporter
OATP	Organic anion transporting polypeptide
OCT	Organic cation transporter
p23	Prostaglandin E Synthase 3
p300	Transcriptional coactivator
PAH	Polycyclic aromatic hydrocarbon
PAS	Perion-ARNT-Single minded
PBS	Phosphate buffered saline
PCB	Polychlorinated biphenyl
PCDD	Polychlorinated dibenzo-p-dioxins
PCDF	Polychlorinated dibenzofurans
P-gp	P glycoprotein
POP	Persistent organic pollutant
PPAR	Peroxisome proliferator-activated receptor
PR	Progesterone receptor
PXR	Pregnane X receptor
PXRRE	PXR responsive element
qPCR	Quantitative polymerase chain reaction
RAR	Retinoic acid receptor
RE	Response element
RIF	Rifampicin
ROR	Retinoic acid receptor-related orphan receptors

RNA	Ribonucleic acid
RXR	Retinoid X receptor
SCFA	Short chain fatty acid
SF 1	Steroidogenic factor 1
SLC	Solute carrier family
SMRT	Silencing mediator of retinoic acid and thyroid hormone receptor
SRC	Steroid receptor coactivator
SULT	Sulfotransferase
TA	Tryptamine
TAD	Transactivation domain
TCDD	2,3,7,8-tetrachlorodibenzo-p-dioxin
TCDF	2,3,7,8-tetrachlorodibenzofuran
TDO	Tryptophan 2,3-dioxygenase
TEACOP	Trace-extended aromatic condensation products
TLR4	Toll like receptor 4
TnaA	Tryptophanase A
TpH1/2	Tryptophan hydroxylase 1/2
TR	Thyroid receptor
TR-FRET	Time-resolved fluorescence energy transfer
Trp	Tryptophan
UGT	UDP glucuronosyltransferase
VDR	Vitamin D receptor
XAP2	Aryl hydrocarbon receptor interacting protein
XRE	Xenobiotic response element

1 INTRODUCTION

The gastrointestinal microbiota plays an important role in the maintenance of gut health and host nutrition. In addition, microbes have been extensively studied due to their ability to affect the functions of distant organs and send signal across the gut-brain and gut-liver axes. The imbalance of the normal intestinal microbiome has been linked to dysbiosis and the etiology of several diseases, such as inflammatory bowel disease (IBD), diabetes, atopy, and obesity (Bull et Plummer, 2014; Wishart, 2019).

Among a wide range of intestinal microbial metabolites, indoles have been found to be involved in the crosstalk between several organs and host physiology. Most indole-based molecules exert biological functions through receptor-mediated signal transduction pathways, including the aryl hydrocarbon receptor (AhR) and the pregnane X receptor (PXR) that are expressed in various cell types within the gut (epithelial cells, fibroblasts, and immune cells) (Kumar et al., 2021). A variety of xenobiotic and dietary indoles, in addition to microbial indoles, have been described as ligands of AhR and PXR.

AhR and PXR have become promising targets for the treatment of different diseases, such as immune disorders, inflammatory diseases, and specific tumours. The identification of ligands with defined health-promoting effects and/or pharmaceutical properties for AhR and PXR is a key strategy for the development of new drugs targeting these receptors (Mulero-Navarro et Fernandez-Salguero, 2016). Our group recently described PXR-mediated intestinal anti-inflammatory effects of newly designed compounds that structurally mimick microbial indole-based catabolites (Dvorak et al., 2020). A number of reports suggests that dietary and microbial indoles exhibit both agonist and antagonist activities for AhR and/or the PXR and may modulate gastrointestinal immune cells, increase barrier function, and inhibit intestinal inflammation (Hubbard et al., 2015a; Venkatesh et al., 2014; Zelante et al., 2013).

AhR and PXR are xenobiotic receptors that act as transcription factors for the regulation of their target genes. PXR is a member of the nuclear receptor family, whereas AhR belongs to the basic-helix-loop-helix-Period/ARNT/Single minded (bHLH-PAS) family, but both show functional analogy. These receptors

are well-described regulators of drug-metabolizing enzymes and the transcriptional activities of drug transporters, which include members of the cytochrome P450 family. Although the CYP genes are primarily induced by xenobiotics, they are also induced by endobiotics (Larigot et al., 2018). Besides their roles as xenosensors, both AhR and PXR are involved in various cellular and biological processes, such as immune responses, carcinogenesis, cell migration, metabolic diseases, and DNA damage (Bock, 2017; Gutierrez-Vazquez et Quintana, 2018; Hakkola et al., 2016; Chai et al., 2020; Kolluri et al., 2017; Qiu et al., 2016). Different ligands may have varying physiological and cellular effects. It is generally known that the sustained activation of these receptors by endogenous ligands is essential for proper cell function; however, exogenous ligands have deleterious effects on human health (Stejskalova et al., 2011). These ligand-specific biologic responses are caused by the interaction of AhR and PXR with other transcription factors and the direct recruitment of distinct coactivators, leading to the expression of different target genes (e.g. CYPs and pro-inflammatory or anti-inflammatory cytokines) (Gutierrez-Vazquez et Quintana, 2018; Poulain-Godefroy et al., 2020). Microbiota-derived compounds may be considered pseudo-endogenous ligands and may have dual effects on human health (Murray et Perdew, 2020). AhR is involved in the regulation of intestinal innate and mucosal immunity and its activity can be modulated by intestinal indole-based microbiota-derived metabolites (Schiering et al., 2017). Therefore, it is necessary to know and investigate the metabolic fate and effects of these compounds in organisms. This knowledge should be crucial for the development of new indole-based compounds as potential drugs for different diseases, such as IBD.

2 AIMS

The main goal of this study was to evaluate the effects of microbial intestinal catabolites of tryptophan (MICTs) and mono-methylated indoles (MMIs) on the AhR and PXR signalling pathways. The objectives of the study were to investigate the *in vitro* effects of the test compounds on:

1) The transcriptional activities of AhR and PXR in human cancer cell lines

2) The expression of AhR and PXR target genes in human cancer cell lines, immortalised hepatic progenitor cell lines, and primary human hepatocytes

3) The molecular functions of AhR and PXR, including nuclear translocation, heterodimerisation, and DNA binding

3 THEORETICAL BACKGROUND

3.1 Biotransformation

The human body is daily exposed to a wide range of chemicals, such as drugs, environmental pollutants, cosmetics, and dietary factors (e.g. food additives or colouring). Although most compounds are generally harmless, some may be potentially toxic. Therefore, organisms have developed a detoxification system through which these foreign substances, referred to as xenobiotics, are metabolised and subsequently excreted from the body to maintain homeostasis (Croom, 2012; Johnson et al., 2012). This process is known as biotransformation, and it involves chemical modification of the structure of xenobiotics, leading to reduced biological activity and potential toxicity. Most xenobiotics that enter the body are lipophilic. The general principle of biotransformation is the conversion of lipophilic xenobiotics into more hydrophilic (water-soluble) products that are readily excreted in the urine, bile, and/or faeces (Ashrap et al., 2017; Johnson et al., 2012; Meyer, 1996). In general, the fate of a xenobiotic in a living organism involves absorption, distribution, metabolism, and excretion (ADME). Drug-metabolizing enzymes (DMEs) and membrane transporters, whose expression is regulated by xenoreceptors, steroid receptors, and ligand-activated transcription factors, play important roles in the ADME processes (Omiecinski et al., 2011; Tibbitts et al., 2016; Wang et al., 2012).

The elimination of xenobiotics involves transport processes and biotransformation reactions. Biotransformation reactions are divided into two phases (phase I and phase II), and these phases are directly involved in the chemical transformation of compounds. Most of these processes take place in the liver, but biotransformation enzymes are also found in the extrahepatic tissues, such as the intestine, kidney, lung, and skin (Meyer, 1996; Phang-Lyn et Llerena, 2021). The transportation of xenobiotics and their metabolites has been described as phase 0 and phase III of biotransformation (Doring et Petzinger, 2014; Petzinger et Geyer, 2006; Vrzal et al., 2004). Importantly, each phase performs a specific function, as described below, in the fate of the compounds. Moreover, substances produced by the action of biotransformation enzymes (metabolites) may be inactive or have properties that are different

from those of the parent compound, and these properties determine their behaviour in an organism. In addition, drug-metabolizing enzymes have been exploited in the design of pharmacologically inactive prodrugs that are converted to active molecules in the body, and the resulting active metabolites are able to produce the desired therapeutic effects (Katzung, 2004). Typical examples are prodrugs used for the treatment of hypertension (e.g. enalapril, ramipril) (Wang et al., 2016). This strategy overcomes the problems associated with absorption barrier, route of administration, metabolism, excretion, toxicology, and site-specific delivery (Zhang et Tang, 2018).

3.1.1 Phase I

The phase I reactions lead to the chemical conversion of a hydrophobic xenobiotic to more polar molecules by the introduction of hydroxyl (-OH), amino (-NH2), sulfhydryl (-SH), or carboxyl (-COOH) functional polar groups into the molecule of the parent compound (Holcapek et al., 2008; Komives et Gullner, 2005). The main reactions that take place in phase I of biotransformation are oxidation, reduction, and hydrolysis. These reactions are catalysed by enzyme systems, such as flavin-containing monooxygenases (FMOs), NAD(P)H:quinone oxidoreductases (NQOs), amine oxidases, alcohol dehydrogenases, esterase, peroxidase, and the well-known cytochrome P450s (CYPs) family (Gan et al., 2016). The phase I metabolite is more polar, compared with the parent compound and can be eliminated from the body directly or can enter into phase II of biotransformation (Jancova et al., 2010).

The cytochrome P450 enzymes are classified as a superfamily of hemoproteins that are essential for xenobiotic metabolism. CYPs are primarily located in the membranes of the endoplasmic reticulum and mitochondria (Bernhardt, 2006; Neve et Ingelman-Sundberg, 2010). The structure of CYPs contains noncovalently bound iron protoporphyrin IX as a heme prosthetic group (Phillips et al., 2006). They are named cytochromes P450 for their unusual spectral properties and their hemoprotein character. In their reduced state, CYPs can bind carbon monoxide, and this CO-bound CYP complex typically shows maximum absorbance in UV-VIS spectrum at 450 nm (Bernhardt, 2006). Based on the percentage of amino-acid sequence similarity, CYPs have been grouped into families, subfamilies, and individual

isoforms. As at 2021, 57 CYP human genes, categorised into 18 families and 44 subfamilies, have been identified (Esteves et al., 2021). In addition, individual isoforms may differ in tissue distribution as well as catalytic specificity and may also exhibit different affinities for the substrate (Meyer, 1996). Although a large number of enzymes from different CYP families are involved in endobiotic metabolism, such as lipids, steroids, and vitamins, only a few isoforms belonging only to families 1, 2, and 3 are responsible for the metabolism of exogenous substances, including 70–80 % of all clinically used drugs. These include CYP1A1, CYP1A2, CYP1B1, CYP2A6, CYP2B6, CYP2C8, CYP2C9, CYP2C19, CYP2D6, CYP2E1, CYP2J2, CYP3A4, and CYP3A5 (Wilkinson, 2005; Zanger et Schwab, 2013). CYPs catalyse mainly oxidative reactions, especially (*O*-, *S*-, and *N*-) dealkylation, aliphatic and aromatic hydroxylation, (*S*- and *N*-) oxygenation, epoxidation, dehydrogenation, oxidative deamination, and oxidative desulfuration. However, CYPs can also catalyse reductive (such as azoreduction, nitroreduction, and reductive dehalogenation) and isomerization reactions (Casarett et al., 1996; Omiecinski et al., 2011; Vrzal et al., 2004). The unique combination of environmental, physiological, patho-physiological, and genetic factors causes interindividual and intraindividual distinctions in the expression and activity of human CYPs (Meyer, 1996; Zanger et Schwab, 2013). CYPs exhibit multiple genetic polymorphisms that vary with populations and ethnicity. CYP2C9, CYP2C19, and CYP2D6 are isoforms with the highest genetic variability in humans conducing diverse pharmacogenetic phenotypes characterised as poor, intermediate, extensive, and ultrarapid metabolisers. Other intrinsic factors, including age, gender, hormone levels, and pathological states (e.g. inflammation, infection, and cancer) influence drug response through the regulation of CYP expression. (Esteves et al., 2021; Zanger et Schwab, 2013). Drugs, steroids, dietary factors, alcohol, and cigarette smoke are environmental factors that can cause intraindividual variation and the induction or inhibition of drug-metabolizing enzymes (Meyer, 1996).

3.1.2 Phase II

In phase II, the polar metabolites undergo conjugation reactions that are catalysed by conjugation enzymes, particularly by different transferases, such as sulfotransferase (SULT), glutathione S-transferase (GST), UDP-glucuronosyltransferase (UGT), N-acetyltransferase (NAT), and different methyltransferases (Negishi et al., 2001). The reactive metabolites are conjugated to a small hydrophilic endogenous conjugating agent, which contains ionisable groups. Common conjugating agents of phase II are sulfate, glutathione, glucuronic acid, methyl and acetyl groups, and amino acids. The phase II products, generally referred to as conjugates, are more hydrophilic than the compounds entering the reaction, and therefore, they are more easily excreted (Negishi et al., 2001). Phase I may not always precede phase II in the biotransformation process. If the foreign substance already contains a functional group suitable for conjugation reaction of phase II, phase I is not necessary. Conversely, if the phase I metabolite is sufficiently polar for excretion from the organism, it is no longer subject to phase II (Bock et al., 1987; Esteves et al., 2021; Jancova et al., 2010)

3.1.3 Phase III

Phase III is similar to phase 0, as both are associated with the transport of compounds and their metabolites in and out of the cells. In particular, water-soluble or charged compounds are virtually unable to spontaneously cross the phospholipid membrane barrier (Doring et Petzinger, 2014; Jančová, 2012). For this reason, they must be transported across the cell membrane by specific membrane transporters. Transporters can be divided into two main groups according to the direction of transport. First, the uptake transporters transport the substrates into the cell during phase 0 (Petzinger et Geyer, 2006). Second, the efflux transporters are responsible for exporting the substrates out of the cell during phase III (Ishikawa, 1992). The uptake transporters include the solute carrier (SLC) transporter family, such as organic anion transporting polypeptides (OATPs), organic anion transporters (OATs), and organic cation transporters (OCTs) (Klaassen et Lu, 2008; Roth et al., 2012). The efflux transporters include the ATP binding cassette (ABC) transporter family, such as P-glycoprotein (P-gp; also called multidrug resistance protein 1, MDR1), breast

cancer resistance protein (BCRP), and members of multidrug resistance associated proteins (MRPs) (Kim, 2002; Noguchi et al., 2014). The members of both families mediate the transport of a large number of structurally diverse compounds with overlapping substrate specificities within the families (Roth et al., 2012). Transporters are expressed on the plasma membrane of the cells mainly in the liver, kidney, intestine, and the endothelium of the blood-brain barrier, and they play important role in drug disposition and drug-drug interactions (Benadiba et Maor, 2016; International Transporter et al., 2010; Lee et al., 2017).

3.2 Nuclear receptors

The nuclear receptor (NR) superfamily regulates diverse biological processes, including endogenous signalling, reproduction, inflammation, development, and metabolism (Gustafsson, 2016; Kininis et Kraus, 2008). The glucocorticoid receptor, which was cloned in 1985, was the first cloned member of NRs (Govindan et al., 1985). A phylogenetic tree connecting 65 known nuclear receptor types in vertebrates, arthropods, and nematodes was constructed based on sequence alignments and phylogenetic studies. A total of six evolutionary families of unequal size have been classified:

1) *Thyroid hormone receptor-like family*: this large group contains thyroid hormone receptor (TR), retinoic acid receptor (RAR), vitamin D receptor (VDR), peroxisome proliferator-activated receptors (PPARs) as well as orphan (or deorphanised) receptors, such as liver X receptor (LXR) and pregnane X receptor (PXR).

2) *Retinoid X receptor-like family*: this group includes retinoid X receptor (RXR), COUP-TFII, and HNF-4.

3) *Estrogen receptor-like family*: this family includes the steroid receptors with estrogen receptor (ER), glucocorticoid receptor (GR), progesterone receptor (PR), androgen receptor (AR), and estrogen-related receptors (ERRs).

4) *Nerve growth factor IB-like family*: this small group contains receptors for growth factors.

5) *Steroidogenic factor-like family*: this family includes steroidogenic factor 1 (NR5A1) and the receptor related to the *Drosophila* FTZ-F1.

6) *Germ cell nuclear factor-like family*: this family contains only the GCNF1 receptor (NR6A1), which does not fit well into any other subfamilies.

Nevertheless, a subfamily 0 has also been described. This family includes NRs that contain incomplete DNA or ligand-binding domain (Germain et al., 2006; Nuclear Receptors Nomenclature, 1999).

Despite the diversity in the shape, size, and charges of activating ligands, NRs share a common structural organization. The N-terminal region (A/B domain) is a highly disordered domain that varies greatly in both size and

sequence between members of NRs. A/B domain contains the activation function-1 region (AF-1), which interacts with several co-regulatory proteins in a cell- and promoter-specific manner (Kumar et Thompson, 2003). Moreover, the A/B domain is a target for post-translational modification (e.g. acetylation, phosphorylation, and SUMOylation), which can lead to transcriptional initiation or repression (Anbalagan et al., 2012). The central DNA-binding domain (DBD; C domain) is the most conserved region among all the NR domains (Danielsen, 2001). The DBD contains a P-box, which is a short motif responsible for DNA-binding specificity and is involved in the dimerization of NRs, including the formation of both heterodimers and homodimers. A linker region (D domain) is located between the DBD and the ligand-binding domain (LBD) (Pawlak et al., 2012; Robinson-Rechavi et al., 2003). This region acts as a flexible hinge and contains the nuclear localization signal (NLS), which may overlap on the C domain. NLS drives the subcellular distribution of NRs (Haelens et al., 2007). The C-terminal ligand-binding domain (E domain) is a multi-functional unit comprising, in addition to the ligand binding pocket, homo- and heterodimerisation interfaces and a comodulator binding region (Pawlak et al., 2012). Another activation function-2 region (AF-2), which is involved in the recruitment of transcriptional co-activators and co-repressors in a ligand-dependent manner, is located within the LBD (O'Malley et al., 2008; Wolf et al., 2008). Moreover, the LBD is moderately conserved in sequence, and the variability across NRs allows them to recognise a diverse cadre of ligands (Moras et Gronemeyer, 1998; Weatherman et al., 1999). In addition to the aforementioned domains, some receptors contain F domain situated in the C-terminus of NRs. The F domain sequence is extremely variable, and the function is unknown (Kumar et al., 1987).
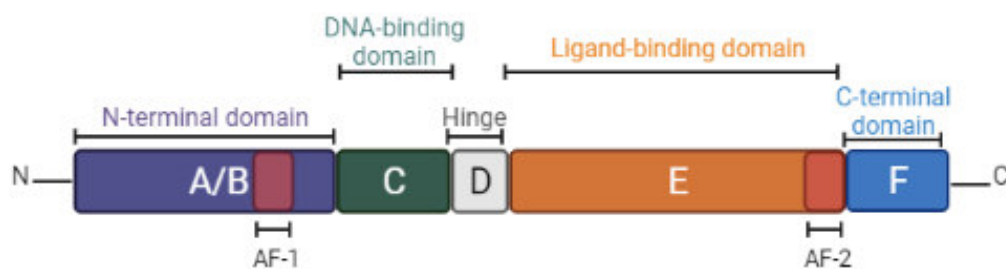

Figure 1: Domain structure of nuclear receptors. The structure and functions of each domain is described in the text. Adopted from Pawlak et al., (2012).

25

All nuclear receptors modulate gene transcription through the interaction with the specific DNA sequence known as response elements (REs). The RE is a nucleotide sequence composed of one or two hexameric half-site motifs. REs form palindromes arranged in direct (DRs), inverted (IRs), or everted repeats (ERs) separated by a spacer of varying length and sequence (Pawlak et al., 2012). The NR superfamily can be divided into subgroups based on their dimerization patterns. The first group consists of the steroid receptors, which include estrogen receptor (ER), androgen receptor (AR), progesterone receptor (PR), glucocorticoid receptor (GR), and mineralocorticoid receptor (MR). These receptors act as homodimers that bind to a degenerated set of response elements containing inverted repeats of a hexameric half-site. These inverted repeats are separated by three base pairs spacer (IR3) (Beato et al., 1995; Schwabe et al., 1993). The second group of receptors form heterodimers with retinoid X receptor (RXR) and recognise two copies of half-site motifs arranged as DRs, IRs, or ERs. The core contains 5´-AGGTCA-3´ sequence. This group of receptors include endocrine receptors (e.g. thyroid hormone receptor, TR; retinoic acid receptor, RAR; vitamin D receptor, VDR) and orphan or adopted orphan receptors (pregnane X receptor, PXR; peroxisome proliferator-activated receptor, PPAR; and farnesoid X receptor, FXR) (Butt et Walfish, 1996). The last group consists of receptors, mainly orphan, which efficiently bind to DNA as monomers, such as SF-1, ROR, Rev-erb, and NGFI-B (Germain et al., 2006).

Nuclear receptors, together with AhR, a member of the bHLH-PAS family act as transcription factors to regulate their target genes. In addition to the regulation of xenobiotic metabolism, numerous other functions of AhR and PXR have been characterised since their discovery. The individual receptors are described in the following sections.

3.2.1 Aryl hydrocarbon receptor

AhR is a ligand-inducible transcription factor belonging to the family of bHLH-PAS proteins. PAS family proteins members, including AhR, are involved in the regulation of many physiological processes, such as organ development, neurogenesis, metabolism of xenobiotics, circadian rhythms, and stress response to hypoxia (Crews, 1998; Gonzalez et Fernandez-Salguero, 1998). AhR nuclear translocator (ARNT) and AhR repressor (AhRR) also belong to the bHLH-PAS group of proteins. Both of them are essential in the AhR signalling pathway (Hahn et al., 2009; Kikuchi et al., 2003; Whitlock, 1999).

For the first time, AhR was identified in 1976 as a receptor that mediates the toxic effects of xenobiotic ligands; specifically, it mediated the toxicity of 2,3,7,8-tetrachlorodibenzo-p-dioxin (TCDD), a byproduct of the synthesis of 2,4,5-trichlorophenoxyacetit acid (Poland et al., 1976). AhR is highly expressed in the human placenta, lung, liver, intestine, kidney, skin, and spleen (Abel et Haarmann-Stemmann, 2010). The gene encoding human AhR is located on chromosome 7p21 and contains 11 exons (Ema et al., 1994).

The AhR protein structure includes several functional domains essential for interaction with other proteins (Yamaguchi et Kuo, 1995). The N-terminal region contains a highly conserved bHLH domain characterised by amino acid sequence and two amphipathic α-helices connected by a loop. bHLH is responsible for binding transcription factors to specific sequences of DNA and for protein-protein interactions; hence, it is referred to as DNA-binding domain (DBD) (Murre et al., 1989). It is followed by the PAS domain in the central region of AhR. The PAS domain contains approximately 250–300 amino acids, comprising of two incomplete PAS motifs (PAS-A and PAS-B). These motifs mediate ligand binding (ligand-binding domain, LBD) and heterodimerisation with structural analog proteins, known as ARNT, and chaperone proteins, such as heat shock protein 90 (Hsp90) (Hogenesch et al., 2000). The last glutamine-rich (Q-rich) transactivation domain (TAD) is located in the C-terminal region of AhR. TAD is characterised by variable length and plays important role in transcription initiation after DNA binding (Yamaguchi et Kuo, 1995).

The unliganded AhR resides in the cell cytosol and forms a complex with two Hsp90 molecules and one molecule of prostaglandin E synthase 3 (p23) and immunophilin-like protein (XAP2; also known as AIP or ARA9)

(Petrulis et Perdew, 2002). This chaperone complex protects AhR from surreptitious nuclear translocation and keeps it in a state that is capable of ligand binding (Pongratz et al., 1992). Ligand binding results in the dissociation of chaperone complex, except of one molecule of Hsp90. Subsequently, this molecule allows conformational changes of AhR. This translocates active AhR into the nucleus (McGuire et al., 1994). Upon entry, Hsp90 is released and AhR heterodimerises with ARNT. The AhR/ARNT complex interacts with DNA at dioxin response elements (DRE; also known as xenobiotic response elements, XRE). DRE contains rigidly defined sequence (5´-TNGCGTG-3´) that is located near the promoter regions of target genes (Swanson et al., 1995). Subsequently, the heterodimer AhR/ARNT activates gene transcription in the presence of transcriptional co-activators and co-factors, such as CREB-binding protein (CBP), estrogen receptor-associated protein 140 (ERAP140), nuclear receptor coactivator (SRC), and p300 (Beischlag et al., 2002; Kobayashi et al., 1997; Kumar et al., 1999; Wang et Hankinson, 2002).

Following transcriptional activation, the liganded AhR is exported out of the nucleus back to the cytosol through nuclear export signal sequence (NES). After that, AhR undergoes rapid degradation through the ubiquitin-proteasome pathway (Davarinos et Pollenz, 1999; Zhao et al., 2019). Ubiquitinylation is a post-translation modification process catalysed by three enzymes, ubiquitin-activating enzyme (E1), ubiquitin-conjugating enzyme (E2), and ubiquitin-ligase (E3). This reaction requires covalent binding of ubiquitin protein and AhR. Upon chemical modification of AhR on its Lys residues, AhR is targeted for degradation in 26S proteasome (Hershko et Ciechanover, 1998; Ma et Baldwin, 2000). In addition, SUMOylation is another post-translation modification implicated in the regulation of AhR. SUMOylation inhibits AhR ubiquitinylation and thereby reinforces its stability (Xing et al., 2012). Moreover, AhR functions are regulated by a negative feedback mechanism. AhR, among other genes, also induces the expression of its competitive repressor, which is known as AhR repressor (AhRR). AhRR competes with AhR for ARNT binding in order to form a heterodimer. Subsequently, transcriptional inactive AhRR/ARNT dimer may interact with DRE, and thereby block AhR transcriptional activity (Mimura et al., 1999).
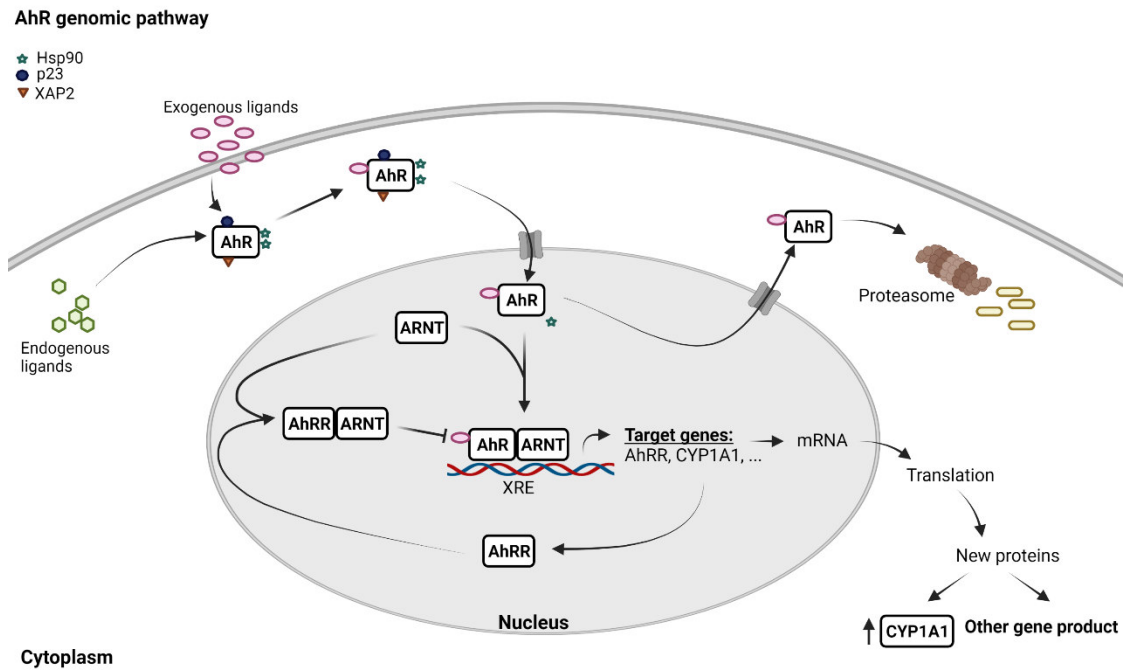
Figure 2: Mechanism of AhR/ARNT signalling pathway. The activation process is described in detail in the text above. Adopted from (Denison et Nagy, 2003; Larigot et al., 2018).

In addition to the aforementioned AhR:ARNT canonical pathway, AhR frequently interacts in a non-canonical manner with other receptor-mediated signalling pathways (e.g. nuclear factor-κB (NF-κB) or Krüppel-like factor 6 (KLF6)). These interactions could explain the pleiotropic actions induced by the structural diversity of AhR ligands (Denison et Faber, 2017; Puga et al., 2000; Sorg, 2014). In the non-canonical pathway, ligand-activated AhR dimerises with nuclear proteins, other than ARNT, and these unique heterodimers trigger gene expression, through the interaction with DNA at responsive elements that are distinct from DRE, to regulate a unique set of genes (Denison et Faber, 2017). For example, NF-κB is involved in diverse cellular processes, including cell differentiation, proliferation, and apoptosis, and it has a significant role in adaptive and innate immunity. NF-κB is composed of five subunits (p50, RelA, p52, c-Rel, and RelB), where RelA and RelB may interact with AhR (Vogel et al., 2007). However, the complex AhR:RelA appears to be transcriptional non-active in the activities of CYP1A1 and IL-6 genes (Jensen et al., 2003; Tian et al., 1999). In contrast, the AhR/RelB interaction leads to increased DRE reporter activity of CYP1A1 and mediates the transcription of NF-κB target genes, such as IL-8 and other chemokines, by binding to DNA responsive element RelBAhRE (Vogel et Matsumura, 2009). Ligand-mediated AhR

29

activation may also lead to heterodimerisation with KLF6 to form a complex that binds to non-consensus DRE sequence (nc-DRE). The complex regulates the expression of target genes, such as p21^{CIP1}, which mediate cell cycle control. In addition to these unique AhR heterodimers, the agonist-activated AhR can trigger gene expression through its ability to function as a coactivator for other transcription factors (Denison et Faber, 2017). For example, ligand-activated AhR/ARNT dimer directly interacts with estrogen receptors. This association results in the recruitment of unliganded estrogen receptor and the coactivator p300 to estrogen-responsive elements, leading to the activation of target gene transcription and estrogenic effects (Ohtake et al., 2003).

AhR has been considered a transcriptional mediator of xenoprotective and drug-metabolizing genes for a long time; however, its role in many physiological (organ development, cell cycle regulation, apoptosis, tumour suppression, immune response, and in endocrine and host-microbiome signalling) and pathophysiological processes (inflammation and carcinogenesis) has been reported (Fujii-Kuriyama et Kawajiri, 2010; Larigot et al., 2018; Tkachenko et al., 2016). AhR-target genes that are involved in xenobiotic metabolism include prototype phase I enzymes (ubiquitously-expressed CYP1A1, mainly hepatic CYP1A2, and extrahepatic CYP1B1), phase II enzymes (such as NADPH:quinone oxidoreductase (NQO1), glutathione S-transferase A2 (GSTA2), UDP-glucuronosyltransferase 1A1, and UGT1A6), and human conjugate transporter ABCG2 (Bock, 2019; Nebert, 2017; Rothhammer et Quintana, 2019). In addition to these enzymes, AhR is a regulator of proteins involved in the aforementioned processes. Examples of such AhR target genes are p21^{CIP1}, p27^{KIP1}, c-jun, junD, Bax, Fillagrin, IL-2, PAI-1, BAFF, IL-10, and IL-22. The regulatory effects of AhR on the expression of many genes are specific to the cell type (Bock et Kohle, 2006; Lamas et al., 2018).

Currently, numerous exogenous and endogenous ligands of AhR have been described. Most of them are planar, hydrophobic, and polycyclic compounds. Exogenous ligands are those that are taken in from the environment and are not normally found in our bodies. The first group of exogenous ligands are environmental pollutants, which together belong to a large group known as persistent organic pollutants (POPs). POPs are

persistent toxic chemicals that can adversely affect human health and the environment. The most commonly encountered POPs are polycyclic aromatic hydrocarbons (PAHs) and halogenated aromatic hydrocarbons (HAHs) (e.g. polychlorinated biphenyls (PCBs), polychlorinated dibenzo-*p*-dioxins (PCDDs), and polychlorinated dibenzofurans (PCDFs)) (Denison et Nagy, 2003; Langenbach, 2013; Vogel et al., 2020). PAHs are a class of organic compounds, consisting of two or more fused aromatic rings (e.g. anthracene, benzo[a]pyrene, and 3-methylcholanthrene). Natural emission sources of PAHs come from natural forest fire, volcanic eruptions, and moorland fire caused by lightning flashes. Anthropogenic emission sources of PAHs can be of industrial, mobile, domestic, or agricultural origin (e.g. incomplete combustion from industrial waste incineration, coal-tar pitch production, asphalt industries, exhaust from refineries, and power production; exhaust from vehicles; garbage burning and wood burning, grilled food and cigarette smoke) (Patel et al., 2020). HAHs are a large group of industrial chemicals, containing at least one atom of a halogen (chloride, fluoride, bromide, iodide) and a benzene ring in their structure. The dioxin group includes the prototype AhR ligand, 2,3,7,8-tetrachlorodibenzo-*p*-dioxin (TCDD), which is by far the most effective xenobiotic AhR inducer (Denison et al., 2002a). Interestingly, naturally occurring compounds have also been identified as AhR ligands. This second group of exogenous ligands includes plant polyphenolics, alkaloids, and dietary compounds. Polyphenols represent a large group of organic compounds that can be divided into four classes (phenolic acids, flavonoids, stilbenes, and lignans). These compounds are frequently found in fruits, vegetables, cereals and beverages. For example, quercetin and resveratrol are well-known flavonoids with both agonist and antagonist AhR effects, while berberine is an alkaloid with AhR activity (Ciolino et al., 1999; Guyot et al., 2013; Nguyen et Bradfield, 2008; Stejskalova et al., 2011). An example of dietary AhR active compound is glucobrassicin (indole-containing compound), which is derived from cruciferous plants, such as broccoli or Brussels sprouts, and it is converted into indole-3-carbinol, an AhR ligand and agonist, during digestion. Subsequently, indole-3-carbinol succumbs to condensation reactions, resulting in the production of other indole derivatives (e.g. 3,3'-diindolylmethan), which may act as an additional dietary ligands of AhR (Dvorak et al., 2021; Heath-

Pagliuso et al., 1998). The third group of exogenous AhR ligands are synthetic compounds, such as pharmaceutical drugs, synthetic flavonoids, and pesticides. For instance, benzimidazole derivatives (omeprazole and lansoprazole) are proton pump inhibitors used in the treatment of gastroesophageal reflux disease and peptic ulcer disease, which are also AhR activators and inducers of CYP1A genes (Stejskalova et al., 2011). Furthermore, drugs used to treat migraine (avitriptan and donitriptan), containing an indole core in their structure, have recently been described by our research group as low-affinity ligands and weak AhR agonists (Vyhlidalova et al., 2020b). Another example of drugs as AhR ligands are dihydropiridine calcium channel blockers (e.g. benidipine, isradipine, and felodipine) used as anti-hypertensives and in the treatment of angina pectoris. It is worth noting that these drugs have enantiospecific effects on AhR (Stepankova et al., 2016), as does the azole antifungal ketoconazole (Novotna et al., 2014). Pesticides have different chemical nature, such as organophosphates (e.g. chlorpyrifos), phenyl amides (e.g. propanil), and imidazoles (prochloraz) (Jayaraj et al., 2016; Long et al., 2003; Takeuchi et al., 2008). The latter group of exogenous AhR ligands also includes synthetic compounds, such as kinase inhibitors (e.g. SP600125) or synthetic flavonoids (e.g. 6,2',4'-trimethoxyflavone (TMF) and 3'-methoxy-4'-nitroflavone (MNF). In addition to these unique AhR heterodimers, the agonist-activated AhR can trigger gene expression through its ability to function as a coactivator for other transcription factors (Stejskalova et al., 2011).
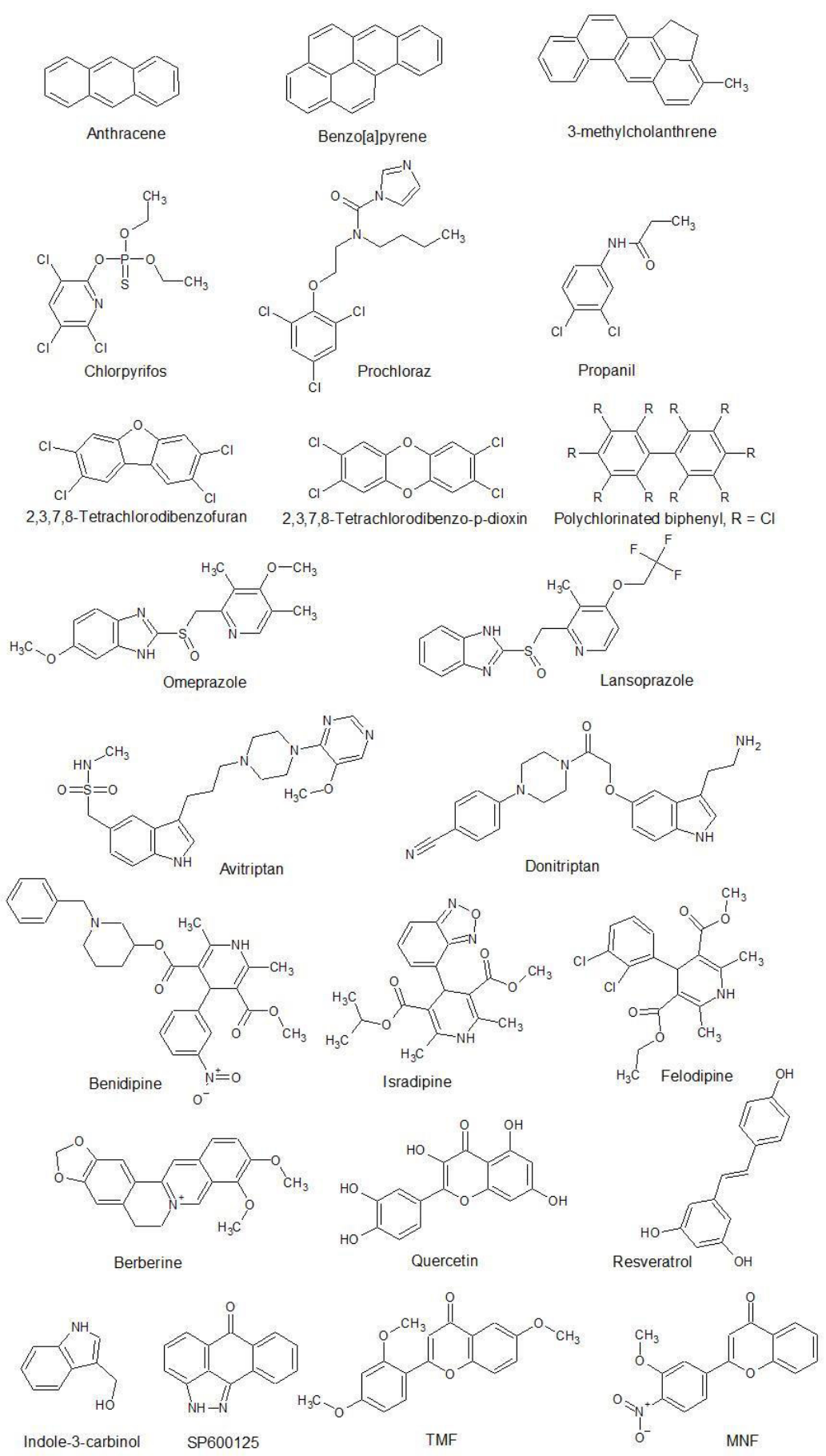
Figure 3: Chemical structures of selected exogenous AhR ligands

Endogenous ligands of AhR are those compounds that are endogenously synthesised in higher organisms. Endogenous AhR ligands particularly include tryptophan metabolites, but they may also include heme metabolites (e.g. bilirubin, biliverdin, hemin), eicosanoids (e.g. arachidonic acid metabolites such as lipoxin 4A and prostaglandins), and indigoids (indigo and indirubin) (Stejskalova et al., 2011). Tryptophan metabolites represent a large group of compounds (e.g. tryptamine, indole-3-acetate) and have been extensively described in this thesis (see chapter 3.3.1). It is worth noting here that 6-formylindolo[3,2-b]carbazole (FICZ), an oxidative photoproduct of tryptophan formed by UV irradiation-exposed skin, can also activate AhR (Rannug et al., 1995).
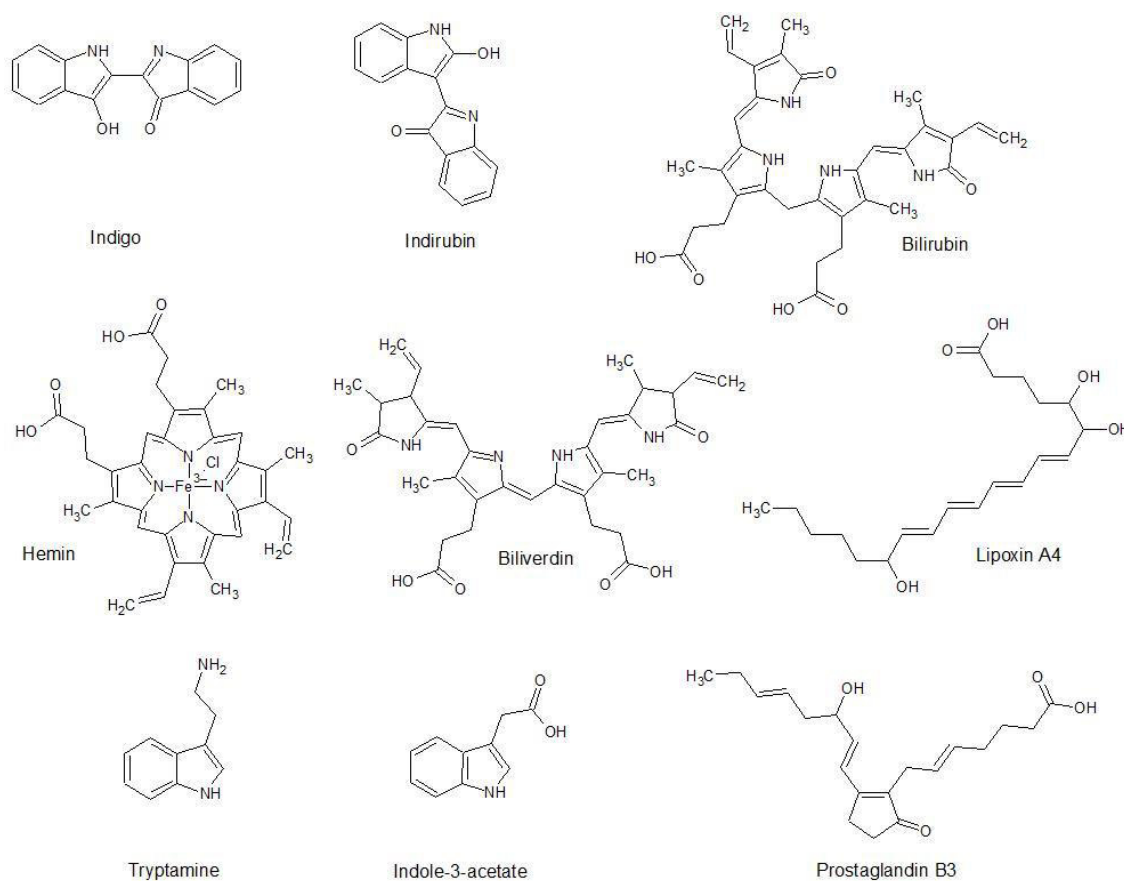

Figure 4: Chemical structures of selected endogenous AhR ligands

3.2.2 Pregnane X Receptor

PXR is a ligand-activated transcription factor and a member of nuclear receptor I family. The PXR is a key regulator of biotransformation enzymes and drug transporters involved in detoxification (Kliewer et al., 1998; Waxman, 1999). The human PXR gene (NR1I2) is located on chromosome 3 (3q1-q13.3) and contains 10 exons separated by nine introns (Hustert et al., 2001; Zhang et al., 2001). The PXR is frequently expressed in the human liver, intestine, and to a lesser extent, kidney. Tissues, such as lung, uterus, bone marrow, and stomach, display low or even no PXR expression (Pavek et Dvorak, 2008).

The structure of the PXR domain differs from those of the others NRs. For instance, the N-terminal region of PXR does not have a ligand-independent activation domain (activation function 1, AF1) (Timsit et Negishi, 2007). The highly conserved DBD domain formed by two zinc fingers is responsible for heterodimerisation. For PXR, the retinoid X receptor alpha (RXRα) is its heterodimerisation partner. In addition, DBD is responsible for the recognition of specific DNA sequences in the regulatory regions of target genes (Berg, 1989; Klug et Schwabe, 1995). The LBD-PXR is composed of a three-layered α-helical sandwich and five-stranded antiparallel β-sheets. This domain is able to bind large scale of structurally diverse compounds. The promiscuity of PXR ligands has been explained by the X-ray crystal structure of PXR-LBD. The structure revealed huge, spherical cavity in the PXR ligand-binding pocket. In addition, there is approximately 60 residues long region in this pocket that distinguishes PXR-LBD from other members of NR (Chrencik et al., 2005; Timsit et Negishi, 2007). The ligand-binding pocket of PXR is mainly composed of hydrophobic residues and a couple of crucial polar and charged residues permitting interactions with ligands in multiple orientations (Ostberg et al., 2002).

The PXR cellular localization is not fully understood. The non-active mPXR is primarily maintained in the cytoplasm of untreated liver cells in complex with chaperones, such as heat shock protein 90 (Hsp90) or cytoplasmic CAR retention protein (CCRP) (Kliewer et al., 1998; Pavek et Dvorak, 2008; Tebbens et al., 2018). Upon ligand binding, mPXR dissociates from the complex and translocates into the nucleus in mouse hepatocytes. In the nucleus, the PXR-RXRα heterodimer binds to specific sequence in DNA

to regulate gene transcription. Nevertheless, nuclear localization of human PXR has been detected in mammalian tumour-derived cell lines. hPXR is associated with a corepressor complex in the absence of ligand in the nucleus (Pavek et Dvorak, 2008; Tebbens et al., 2018). This complex is formed by nuclear receptor corepressor 1 (NCoR1) and silencing mediator of retinoic acid and thyroid hormone receptor (SMRT, also known as NCoR2), which inhibit PXR transcriptional activity (Johnson et al., 2006; Kliewer et al., 1998).

Ligands bind to the PXR after they enter the cells. Once the ligand is bound, the PXR changes conformation, thereby causing the release of the corepressors from the complex. The corepressors are replaced by other coactivators, such as steroid receptor co-activator 1 (SRC-1) and SRC-3 with intrinsic histone acetyl-transferase activity (Moore et al., 2006). Together, this multi-protein complex leads to chromatin remodelling and subsequent gene transcription of target genes (Pondugula et Mani, 2013). Transcription-active PXR-RXRα heterodimer binds to regulatory DNA sequences with 5´-AGGTCA-3´ motif, known as PXR responsive element (PXRRE). PXR binds to miscellaneous PXRRE represented by direct repeats (DR-3, DR-4, and DR-5) and everted repeats (ER-6 and ER-8) (Kliewer et al., 1998; Orans et al., 2005). It has been recently reported that the receptor has a high binding preference for a novel motif DR-$(5n + 4)$ (Cui et al., 2010). Cytochrome P450 3A4 (CYP3A4), one of the most important PXR target genes, contains the DR-3 element in its enhancer as well as the ER-6 element located in the proximal promoter of the CYP3A4 gene (Blumberg et al., 1998; Goodwin et al., 1999).
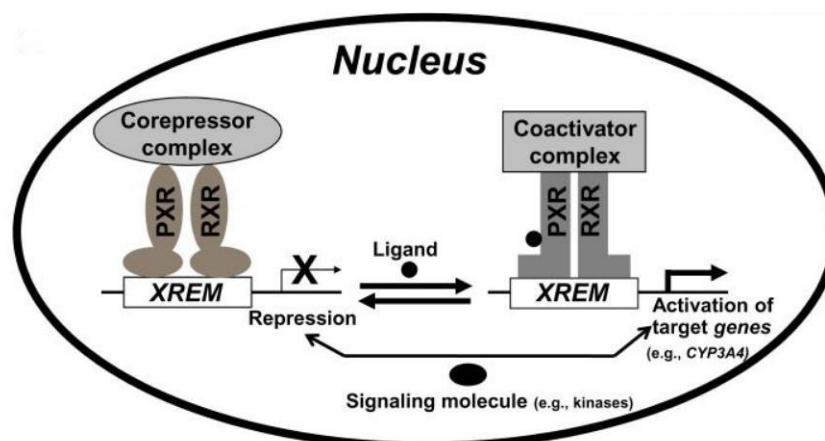

Figure 5: Mechanism of PXR-induced target gene expression (Pondugula et al., 2009b). The activation process is described in detail in the text above.

Apart from being the regulator of the CYP3A4 gene, PXR is also a major metabolic regulator of other genes that are involved in phase I of biotransformation. These include cytochrome P450s (such as CYP2B6, CYP2B9, CYP2C8, CYP2C29, CYP2C19, CYP3A5, CYP3A7, and CYP3A23), aldehyde and alcohol dehydrogenases, and carboxylesterases. In addition, the production of several enzymes involved in heme production and the P450 reaction cycle are regulated by PXR (Orans et al., 2005; Tebbens et al., 2018). PXR also controls the expression of phase II drug metabolism genes encoding UDP-glucuronosyl-transferases (UGT), glutathione *S*-transferase (GST), and sulfotransferases (SULT) (Staudinger et al., 2011). Furthermore, PXR regulates the expression of genes encoding phase III transporters. In particular, that includes multidrug resistance protein 1 (MDR1), multidrug resistance protein family (MRP), and organic anion transporting polypeptide-2 (OATP-2) (Geick et al., 2001; Orans et al., 2005; J. Staudinger et al., 2001; Teng et al., 2003). PXR also plays an important role in the regulation of endogenous metabolism, where it is involved in adrenal steroid homeostasis. The activation of hPXR in mice increases the plasma levels of corticosterone and aldosterone. This increase is accompanied by the elevated expression of adrenal steroidogenic enzymes: Cyp11a1, Cyp11b1, Cyp11b2, and 3β-hydroxysteroid dehydrogenase (Zhai et al., 2007). Furthermore, PXR is involved in the regulation of glucose and lipid metabolism. Glucose-6-phosphatase (G6Pase) and phosphoenolpyruvate carboxykinase (PEPCK1) are key enzymes involved in gluconeogenesis, and their expression is downregulated by PXR, leading to a decrease in glucose levels; conversely, ligand-activated PXR promotes the ynthesis of triglyceride and reduces β-oxidation and ketogenesis (di Masi et al., 2009; J. Zhou et al., 2006). PXR also regulates cholesterol and bile acid levels, where it represses the expression of cholesterol 7α-hydroxylase (CYP7A1), which catalyses the rate-limiting step in the classical pathway for the conversion of cholesterol to bile acids (J. L. Staudinger et al., 2001). Other PXR-target genes, such as CYP3A, SULT2A, MRP, and OATP-2, are also involved in bile acid metabolism and transport (Ihunnah et al., 2011). Other functions of PXR include bilirubin detoxification and vitamin metabolism. In addition, PXR plays a critical role in inflammation; its activation by rifampicin attenuates NF-κB target genes, such as prostaglandin-endoperoxide synthase 2

(COX-2), tumour necrosis factor alpha (TNFα), and several interleukins (IL-1α, IL-1β, and IL-6), which facilitates immune response and inflammation. Conversely, activated NF-κB inhibits PXR activity and its functions (C. Zhou et al., 2006).

PXR is activated by a wide range of structurally unrelated chemicals, which included xenobiotics and endobiotics. A large group of xenobiotic PXR ligands are drugs, including antibiotics (rifampicin), imidazole antifungals (clotrimazole), sedatives (phenobarbital), antihypertensive drugs (nifedipine and spironolactone), or anticancer drugs (tamoxifen and taxol) (Honkakoski et al., 2003). Additionally, the components of frequently used herbal remedies (St. John´s Wort containing hyperforin, Gugulipid containing guggul extract, Kava Kava containing kavalactones) and dietary supplements, including carotenoids and vitamins (vitamin K_2 and vitamin E), also bind to PXR (Carazo et al., 2019; Chang, 2009; Landes et al., 2003; Staudinger et al., 2006). Environmental pollutants, such as organochlorine pesticides and polybrominated diphenyl ether flame retardants, have also been identified as PXR ligands (Coumoul et al., 2002; Pacyniak et al., 2007). Endogenous PXR ligands include certain bile acid (lithocholic acid) and their precursors (deoxycholic acid), progesterone, pregnenolone, and cholesterol (Wilson et al., 2020; Zhang et al., 2001; Zhuo et al., 2014). Recent studies have revealed that the products of gut microflora derived from tryptophan, such as indole 3-propionic acid (IPA) in combination with indole, are responsible for PXR activation in intestinal epithelial cells (Venkatesh et al., 2014).
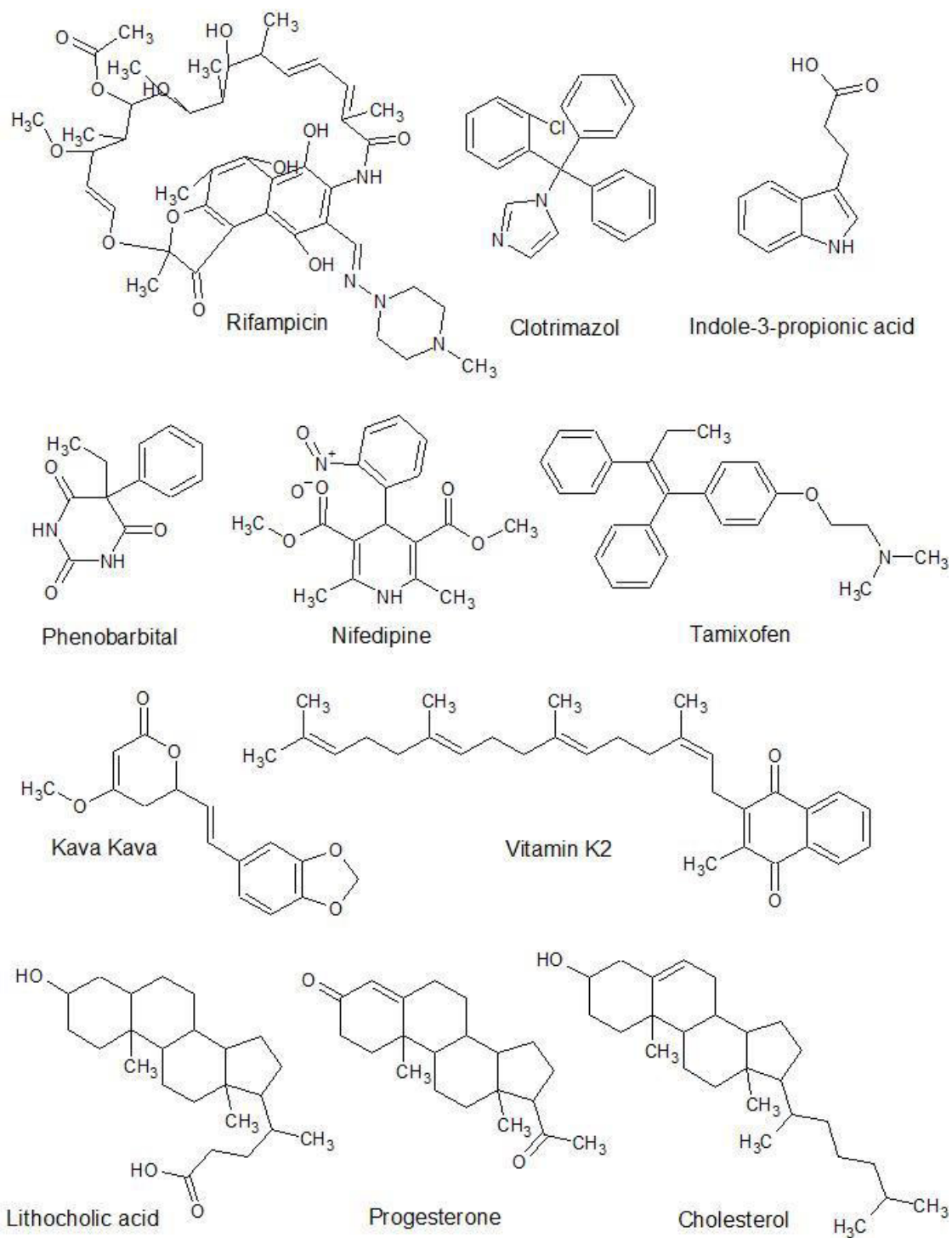
Figure 6: Chemical structures of selected PXR-active compounds

3.3 Microbiome and its role in intestinal physiology

The gastrointestinal tract (GI) is the largest mucosal surface of the human body colonised by several trillion microbes that coexist in symbiosis with the host and its immune system (Stockinger et al., 2014). The microbial community plays an important role in the maintenance of host health and nutrition (Tremaroli et Backhed, 2012). The disruption of the balance among bacterial species or in microbiota has been associated with the etiology of IBD, cancer, obesity, allergy, diabetes, and asthma. A mutualistic relationship between the microbiome and the host is mediated by specific ligand-receptor interactions. Microbiota produce molecules that serve as ligands, which are crucial for the maintenance of immune homeostasis (Holmes et al., 2011; Saha et al., 2016).

The gut of an infant is assumed to be sterile before birth (Escherich, 1988). Recently, scientific reports have provided evidence that bacterial colonization (e.g. by *Bifidobacterium*, *Lactobacillus*, and *Enterococcus*) begins when the foetus is in the lower uterus (Aagaard et al., 2014; Jimenez et al., 2008; Perez-Munoz et al., 2017). However, extensive bacterial colonization comes during childbirth through maternal transmission or from the outside environment (caesarean delivery). The large intestine is mostly populated by facultative anaerobic bacterial strains, such as *Escherichia coli* and *Streptococcus spp.* These are nutritionally undemanding, and therefore, they are able to create a strongly anaerobic environment for the development of other strains, such as *Bifidobacterium*, *Clostridium*, *Eubacterium, Lactobacillus*, and *Bacteroides*, and sometimes *Ruminococcus* (Cummings et al., 2004; Macfarlane et Macfarlane, 1997; Matamoros et al., 2013). *Bifidobacterium* is a dominant bacterial genus in the infant gut microbiota. The infant gut microflora slowly develops and expands to include other species before reaching the adult state around 3 years of age (Matamoros et al., 2013). The early composition and diversity of the infant microbiome are influenced by infant nutrition (breast milk or formula diet) and by the use of antibiotics and probiotics (Jandhyala et al., 2015). Despite the enormous inter-individual variability, the gut microbiome in adults is considered relatively stable and predominantly represented by only two phyla. These are the phylum

of gram-positive (G$^+$) *Firmicutes* and the phylum of gram-negative (G$^-$) *Bacteroidetes*. All the aforementioned genera fall into these phyla (Flint et al., 2007; Walker et al., 2011). Arumugam et al. proposed an effective classification of the microbiota in the human population into three enterotypes, each enriched by different bacterial genera: *Bacteroides* (enterotype 1), *Prevotella* (enterotype 2), and *Ruminococcus* (enterotype 3) (Arumugam et al., 2011). Adult diet (vegan-based or meat-based) also influences the composition of the gut microbiome. A plant-based diet leads to an increase in *Bacteroidetes* at the phylum level and a higher abundance of *Prevotella* at the genus level, while a meat-based diet promotes the abundance of the *Bacteroide*s genus (Tomova et al., 2019). The use of certain drugs negatively affects the human microbiome of adults. Indeed, the use of antibiotics alters the composition of the gut microbiota and reduces resistance against colonization by *Clostridium difficile*, a pathogenic bacterium that causes colitis (Fletcher et al., 2021). In addition to bacteria, the microbiome is composed of other microorganisms, such as viruses, fungi, archaea, and protozoans (Sekirov et al., 2010).
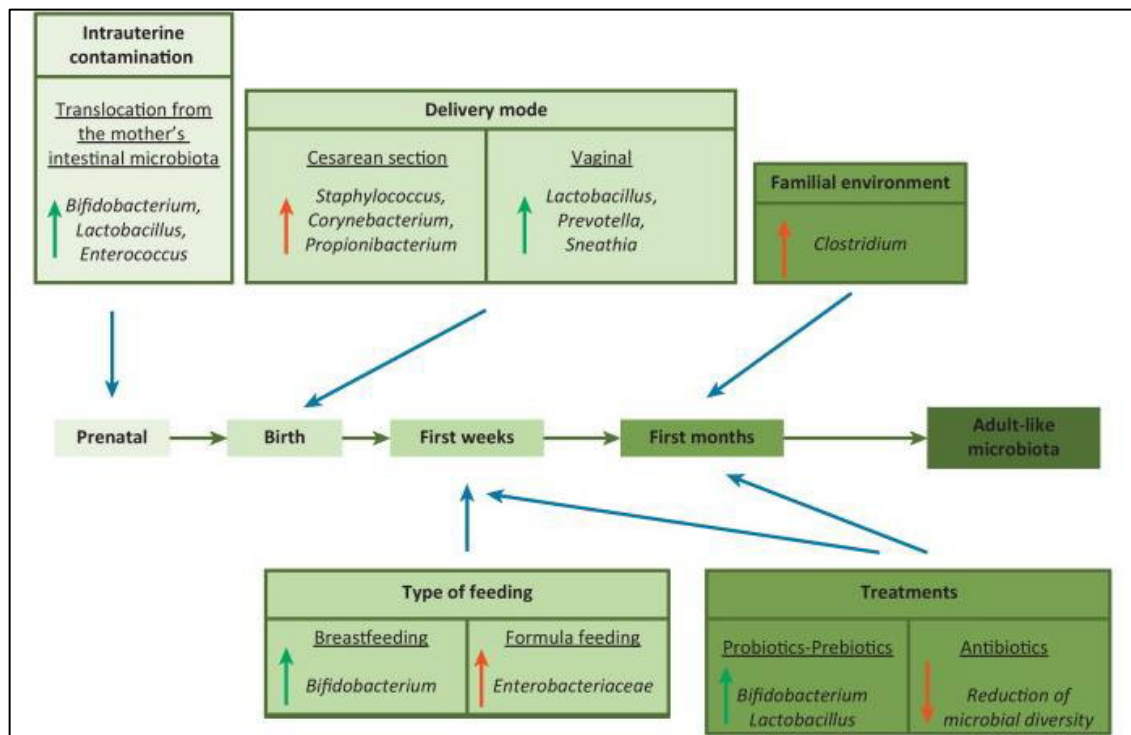

Figure 7: Impact of external factors on the intestinal microbiota of an infant. Green arrows show beneficial modification; red arrows show modification considered detrimental to healthy development (Matamoros et al., 2013).

The intestinal microflora provides several beneficial functions. One of the main ones is the breakdown of carbohydrates, proteins, and, to a lesser extent, fats that escape digestion in the upper intestine. Proteins are cleaved into small molecules, such as peptides or amino acids (Oliphant et Allen-Vercoe, 2019). The products of carbohydrate fermentation by bacteria are short-chain fatty acids (SCFAs), such as acetate, propionate, and butyrate, which are produced in the approximate molar ratio of 60:20:20 and are absorbed by colonocytes (Boets et al., 2017). They play an important role in human energy metabolism and contribute to the maintenance of colonic integrity (Cook et Sellin, 1998; Vinolo et al., 2011). These three SCFAs also differ in tissue distribution. While butyrate is the preferred energy source for intestinal epithelial cells, the fractions of acetate and propionate that are not consumed by the colonic mucosa are transported to other tissues (den Besten et al., 2013b). Propionate is almost all sequestrated in the liver, where it may act as a gluconeogenic substrate or be oxidised (De Vadder et al., 2014). Moreover, it inhibits cholesterol synthesis in the hepatic tissue. Thus, the cholesterol-lowering effects of fibre may be secondary to propionate production in the colon (Jenkins, 1989). Acetate largely escapes splanchnic extraction and is therefore available in the peripheral circulation to adipose tissues, where it can be utilised for lipogenesis or oxidised by muscle (den Besten et al., 2013a). Another function of microbiome is the biotransformation of exogenous dietary polyphenols (e.g. flavanols, flavanones, tannins, lignans, and chlorogenic acid) by bacteria (Marin et al., 2015). Furthermore, the enzymes present in these microorganisms have the capability to metabolise drugs and other xenobiotics rapidly (Sousa et al., 2008). Most drugs are delivered orally and may encounter commensal microorganisms in the small and large intestine. The modification of compounds by intestinal microorganisms can lead to activation (e.g. sulfasalazine), inactivation (e.g. digoxin), or conversion to toxic metabolites (e.g. sorivudine) with local or systemic pharmacological effects (Zimmermann et al., 2019). However, reactions mediated by the gut microbiota differ from those mediated by hepatic metabolism. In particular, oxidation and conjugation reactions take place in the liver to produce high-molecular-weight polar compounds (see chapter 3.1.1. and 3.1.2.). However, the gut microbiota is involved in reductive and hydrolytic reactions that produce low-molecular-weight non-polar

metabolites (Wilson et Nicholson, 2017). The microbiota can also influence the expression and activity of drug-metabolizing enzymes and transporters, and they can even alter the expression and activity of their regulators (transcription factors) through metabolites that are produced from components of the ingested food and that act as signalling molecules (Swanson, 2015). Colonic bacteria can also synthesise essential micronutrients, such as vitamins (e.g. B vitamins (thiamine and riboflavin) and vitamin K) (Biesalski, 2016). Moreover, the intestinal microbiota drive the metabolism of endogenous compounds. For instance, the secondary bile acids (deoxycholic acid and lithocholic acid) are metabolised from primary bile acids through intestinal bacteria (Ridlon et Bajaj, 2015). Bile acids facilitate the absorption of lipids and lipid-soluble vitamins and are involved in maintaining intestinal barrier function (Kang et al., 2019; Swanson, 2015).

All processes lead to the production of innumerable microbial metabolites, which are depended on the gut microbiota composition. These metabolites serve as signalling molecules with both local and system effects (after being absorbed into the bloodstream) and may have potentially beneficial but also deleterious effects on human health (Oliphant et Allen-Vercoe, 2019). For example, microbial tryptophan metabolites contribute to the maintenance of intestinal homeostasis. Gut microbiota dysbiosis in IBD is characterised by depleted diversity, reduced abundance of microbial tryptophan producers, and enriched pro-inflammatory microbes (Nishida et al., 2018; Roager et Licht, 2018). Altered microbiota composition is also associated with metabolic disorders (altered bile acid metabolism is associated with hepatic steatosis, glucose and lipid dysmetabolism, or SCFA with diabetes) (Agus et al., 2021). Besides metabolite production, intestinal microflora also protects the organism against the colonization of pathogenic microorganisms (Jandhyala et al., 2015). Currently, the three most studied categories of microbiota-derived metabolites with a role in intestinal physiology appear to be SCFAs, secondary bile acids, and tryptophan catabolites (Blacher et al., 2017).

3.3.1 Tryptophan metabolism

Tryptophan is an essential aromatic amino acid. It is produced from the degradation of dietary proteins. Tryptophan is present in common protein-rich foods (such as milk, fish, poultry, and cheese) as well as in some other foods (such as oats, bananas, chocolate or even wine) (Krautkramer et al., 2021). In addition, it is has the lowest occurrence in proteins (Santiveri et Jimenez, 2010). At the same time, it is also the least abundant free amino acid in the cells (Bennett et al., 2009). However, tryptophan undergoes a wide array of enzymatic and chemical conversions (Alkhalaf et Ryan, 2015).

Tryptophan is metabolised in the GI through the three major metabolic pathways (kynurenine pathway, serotonin pathway, and direct transformation of tryptophan into indole derivatives mediated by gut microbiota) (Agus et al., 2018). Even though tryptophan is so important for protein synthesis, most of it (more than 95 %) is degraded through the kynurenine pathway in the gut. The first step of this pathway is mediated by the rate-limiting enzyme indoleamine 2,3-dioxygenase (IDO1). Gut microbiota control IDO1 expression and the activity of IDO1 also affects the composition of the microbial community. Tryptophan is converted to kynurenine by two other rate-limiting enzymes-tryptophan 2,3-dioxygenase (TDO) and IDO2. However, these two enzymes are expressed in the liver (Hoglund et al., 2019; Krautkramer et al., 2021; Peters, 1991). The kynurenine pathway generates numerous metabolites, generally known as "kynurenines" (e.g. kynurenic acid and quinolinic acid), and the final product is NAD^+. Kynurenine and its derivatives exert distinct biological effects on immune response, inflammation, and neurotransmission. Such effects are mediated by AhR signalling and G protein-coupled receptor (GPR35) (Krautkramer et al., 2021; Platten et al., 2019). Although most studies report kynurenine as an AhR ligand, Seok et al. demonstrated that kynurenine acts only as a pro-ligand of AhR and requires chemical transformations to act as a receptor agonist. Kynurenine is not directly responsible for AhR activation; its condensation products, namely trace-extended aromatic condensation products (TEACOPs), which are active at picomolar levels, are direct activators of AhR (Seok et al., 2018).

Only a minor fraction of ingested tryptophan (approximately 1–2 %) is utilised for the synthesis of serotonin (5-HT) in the brain and gut and that

of melatonin in the pineal gland through the serotonin pathway (Bai et al., 2017; Hoglund et al., 2019). More than 90 % of neurotransmitter 5-HT is produced in enterochromaffin cells in the gut through a two-stage enzymatic reaction. Under physiological conditions, 5-HT does not cross the blood-brain barrier. The first step in the serotonin pathway is catalysed by tryptophan hydroxylase 1 enzyme (TpH1), which generates 5-hydroxytryptophan (5-HTP). 5-HTP is further converted by aromatic amino acid decarboxylase (AADC) to 5-HT (Agus et al., 2018; El-Merahbi et al., 2015). Peripheral 5-HT is an important signalling molecule that binds to specific 5-HT receptors in the gastrointestinal tract. Serotonin-activated receptors transmit signals from the gut to intrinsic or extrinsic neurons, thereby affecting intestinal peristalsis and secretion, motility, absorption of nutrients, and vasodilation (Mawe et Hoffman, 2013; Walther et al., 2003). The role of gut microbiota in the regulation of intestinal 5-HT production has been demonstrated in germ-free mice, which showed reduced intestinal 5-HT production (Reigstad et al., 2015; Yano et al., 2015). The remaining amount of 5-HT is produced in the brain through tryptophan hydroxylase 2 enzyme (TpH2), where it plays an integrative role in behavioural and neuroendocrine stress response (Agus et al., 2018).

The rest of the ingested tryptophan (approximately 4–6 %) is directly metabolised to indole and its derivatives by gut microbiota (Yokoyama et Carlson, 1979), as detailed in "Chapter 3.4.1."
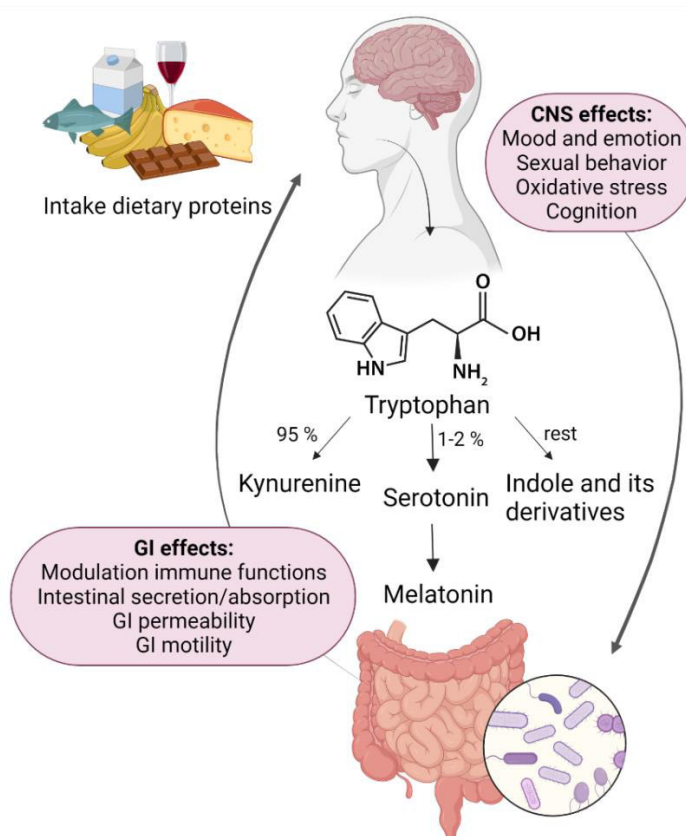
Figure 8: Schematic illustration of tryptophan metabolism and the microbiome gut brain axis. Adopted from (Gheorghe et al., 2019).

3.3.2 AhR/PXR as mediators of host-microbiota interplay

Microbiota-produced metabolites and co-metabolites play important roles as ligands for AhR and PXR. As suggested by a growing body of evidence, these interactions facilitate bidirectional communication between the host and the microbiota, thereby modulating the host physiology (Marinelli et al., 2019). This chapter focuses on the importance of AhR and PXR in inflammatory diseases, as well as metabolites produced by bacteria, such as short-chain fatty acids (SCFAs) and secondary bile acids, and their relevance in the context of AhR and PXR.

Both receptors are involved in intestinal barrier functions and in the regulation of a wide range of immune cell populations (e.g. regulatory T cells (Tregs), innate lymphoid cells-3 (ILC-3), helper T cells (Th cells), and many types of B cells, which is relevant to the pathogenesis of many diseases, such as IBD, multiple sclerosis (MS), rheumatoid arthritis (RA), cancer, and obesity (Brave et al., 2015; Gao et al., 2018; Qiu et Zhou, 2013). AhR and PXR activation have immunomodulatory effects through interaction with the NF-κB

signalling pathway, leading to the expression of a number of cytokines and chemokines (Mencarelli et al., 2011; Vogel et Matsumura, 2009).

Rodent models of chemical-induced colitis have been used for studies on chronic intestinal inflammation. Interestingly, results from animal experiments and studies on IBD patients have shown that colonic epithelial cells may have reduced expression of AhR and PXR and the availability of their ligands is low during inflammation, highlighting the clinical relevance of these pathways in IBD pathologies. AhR activation by ligand administration and AhR knock-down in mice suppressed and enhanced DSS-induced colitis, respectively, suggesting that AhR activation plays a beneficial role in IBD (Furumatsu et al., 2011; Marinelli et al., 2019). This hypothesis was further supported by a recent study that showed that IBD-associated single nucleotide polymorphism (SNP) within the CARD9 gene affects microbiota composition, reduce the production of bacterial AhR ligands, and subsequently influence intestinal inflammation (Lamas et al., 2016). As a different and specific example, our recent study demonstrated that targeting AhR with microbial metabolite mimics alleviates experimental colitis in mice (Grycova et al., 2022). The opposite effect was demonstrated in a study by Monteleone et al., where an AhR antagonist led to the production of more inflammatory cytokines and less IL-22, and the mice developed severe colitis (Monteleone et al., 2011). IL-22 is an essential mediator in inflammation and mucous production, as well as in protective roles against pathogens, wound healing, and tissue regeneration, and its expression is dependent on AhR (Arshad et al., 2020; Parks et al., 2015). The amelioration of inflammatory response in DSS-induced colitis in mice has also been repeatedly observed after the administration of PXR-specific agonists (Mencarelli et al., 2010; Shah et al., 2007).

Different studies have investigated the role of SCFAs produced by microbiota in relation to AhR. Jin et al. showed that SCFAs synergistically enhanced basal and ligand-induced transcriptional activity of AhR (Jin et al., 2017). Furthermore, Rosser et al. recently demonstrated reduced SCFA levels in patients with rheumatoid arthritis and rheumatoid mice, compared with those observed in healthy controls, which further highlights the importance of microbial metabolites in immune diseases. The same authors showed that butyrate supplementation augmented AhR ligand availability by supporting the

growth and metabolism of tryptophan bacteria, which increased the production of the major metabolite of serotonin-5-hydroxyindole-3-acetic acid (5-HIAA). 5-HIAA, in turn, activated AhR-dependent gene transcription of IL-10 in B cells, resulting in the amelioration of arthritis (Rosser et al., 2020).

Furthermore, secondary bile acids produced by microbiota (deoxycholic and lithocholic) can induce strong activation of PXR. Lithocholic acid causes cholestasis, which is a liver disease that is characterised by a cessation or impairment of bile flow, nutritional imbalances related to malabsorption of lipids and fat-soluble vitamins, and irreversible liver damage induced by the accumulation of toxins normally secreted by bile. PXR mediates the biotransformation of lithocholic acid, and Staudinger et al. demonstrated that PXR activation ameliorated severe lithocholic acid-induced liver injury (Shah et John, 2022; J. L. Staudinger et al., 2001). Furthermore, bile acids derived from microbes contribute to IBD and host immune surveillance (Shah et al., 2007; Wilson et al., 2020). Other diseases, such as liver cirrhosis, liver cancer, and obesity are also associated with changes in the intestinal bile acid pool. However, the mechanism associated with these bile acid-microbiome-disease remains to be elucidated (Heinken et al., 2019).

The gut microbiota profoundly influences the inflammatory state through the production of immunomodulatory metabolites, making it an attractive target for well-founded microbe- and/or metabolite-based therapies (Gasaly et al., 2021). These indicate the interactions of microbial metabolites with receptors and the potential relevance in various pathological conditions. However, these approaches require further comprehensive scientific investigation with clear characterisation of metabolites and their functions in organisms.

3.4 Test compounds

3.4.1 Microbial intestinal catabolites of tryptophan (MICTs)

Tryptophan formed from nutrient digestion may serve as a substrate for enzymes in the gut microbiota. Direct bacterial transformation of tryptophan leads to the production of various catabolites, which includes indole (IND), tryptamine (TA), 3-methylindole (3-MMI; skatole), indole-3-acrylate (IAC), indole-3-lactate (ILA), indole-3-pyruvate (IPY), indole-3-propionate (IPA), indole-3-acetate (IAA), indole-3-ethanol (IET), indole-3-acetamide (IAD), indole-3-aldehyde (IA), and indole-3-acetaldehyde (IAL) (Roager et Licht, 2018). Some of these microbial indole derivatives have already been identified as AhR and PXR ligands, through which they affect intestinal barrier integrity and immune response (Lamas et al., 2016; Venkatesh et al., 2014; Zelante et al., 2013). All MICTs, except IAL, were analysed in this work, and their effects on AhR and the PXR signalling pathways were determined. Structurally, these indole derivatives are aromatic bicyclic molecules that are composed of benzene fused to a pyrrole ring carrying different substituents at position 3.

Tryptophan is transformed by many Gram-positive and Gram-negative bacteria species, such as *Escherichia coli*, *Vibrio cholera, Bacteroides*, and *Clostridium,* into indole. The conversion to indole is induced by the enzymatic activity of tryptophanase (TnaA). Although indole has been known for > 100 years, the exploration of its detailed biological functions has only begun recently (Roager et Licht, 2018). Indole is the main tryptophan metabolite; it is an intracellular signalling molecule involved in the regulation of a number of biological processes (e.g. regulation of bacterial sporulation and virulence, bacterial motility, biofilm formation, and antibiotics resistance) (Li et Young, 2013). It has been reported that indole activates AhR, resulting in increased production of interleukin-22 (IL-22). IL-22 is a protein that controls the secretion of antimicrobial peptides and protects against pathogenic infections (Levy et al., 2017). The intestinal concentrations of MICTs are mostly unknown. Relatively high levels of indole (0.25–6 mM) have been detected in the faecal samples of healthy adults (Dong et al., 2020; Dvorak et al., 2020; Hubbard et al., 2015b; Jin et al., 2014; Lamas et al., 2016; Roager et Licht, 2018). Different bacterial species generate various MICTs through different metabolic pathways.

For instance, *Peptostreptococcus* metabolises tryptophan to IPA and IAC, while *Clostridium sporogenes* triggers tryptophan conversion into TA, ILA, and IPA (Roager et Licht, 2018).

Tryptophan decarboxylation induced by tryptophan decarboxylase enzyme leads to the production of tryptamine, which is another regulator of intestinal motility and immune functions (Williams et al., 2014; Wlodarska et al., 2015). Tryptamine is able to inhibit IDO1 enzyme, which subsequently influences immune surveillance (Tourino et al., 2013). In addition, TA acts as a ligand for AhR, and through AhR, it regulates intestinal immunity in DSS-induced colitis in mice by suppressing the expression of pro-infllammatory cytokines (Islam et al., 2017). TA is also responsible for serotonin release from enteroendocrine cells (Takaki et al., 1985).

A part of tryptophan may be metabolised to other indole derivatives by gut microbiota. The effects of indole derivatives on intestinal homeostasis have also been reported. Some *Clostridium*, *Bacteroides*, *Peptostreptococcus*, and *E. coli* spp convert tryptophan to tryptamine and indole-3-pyruvate, which are then metabolised to ILA, IAC, IPA, and IAA. Similarly, *Lactobacillus* are capable of converting tryptophan into IA and ILA in the presence of aromatic amino acid aminotransferase and an indolelactate dehydrogenase (Gao et al., 2018; Roager et Licht, 2018). Recent studies have shown that IPA can decrease intestinal permeability through the regulation of junctional proteins and maintain intestinal homeostasis through suppressed expression of cytokines, including TNF-α and IL-6, and these are mediated by the PXR and Toll-like receptor 4 (TLR4) pathway (Venkatesh et al., 2014). Furthermore, commensal *Lactobacilli* is able to produce IA from tryptophan. IA conduces to increased production of IL-22 through AhR in intestinal immune cells. Thus, it provides resistance against *Candida albicans* colonization and mucosal protection against inflammation (Zelante et al., 2013). IA also triggers AhR-dependent IL-10 expression in the intestine and subsequent expansion of goblet cells, thereby strengthening the intestinal barrier through mucus production (Powell et al., 2020). It has been reported that the concentration of IAA in the faecal samples of healthy individuals is 5 µM (Lamas et al., 2016), while the concentrations of other indole derivatives (e.g. IPA, TA, ILA, IA) in the human gut have not yet been determined.

Finally, 3-methylindole (skatole) is an intestinal microbiota-derived metabolite of tryptophan (Jensen et al., 1995), which is synthesised from IAA by *Bacteroides* and *Clostridium* in the presence of indoleacetate decarboxylase. 3-MMI has been extensively studied due to its typical faecal odour and the occurrence of this odour in pork (Roager et Licht, 2018). Skatole formation is a two-step process mediated by at least two different bacterial species. This possibly explains the high variable intestinal concentration of 3 MMI. The concentration of IAA, the precursor of skatole, is another rate-limiting factor (Gao et al., 2018). Skatole exerts bacteriostatic effects on Gram-negative enterobacteria, such as *Salmonella*, *Shigella*, and *Escherichia*. Therefore, it may affect the composition of intestinal microbiota (Yokoyama et Carlson, 1979). Apart from this function, skatole can activate human AhR in a dose-dependent manner, but can only exhibit modest activation of mouse AhR. Such skatole-mediated activation of human AhR within the GI tract may regulate intestinal homeostasis (Hubbard et al., 2015a).
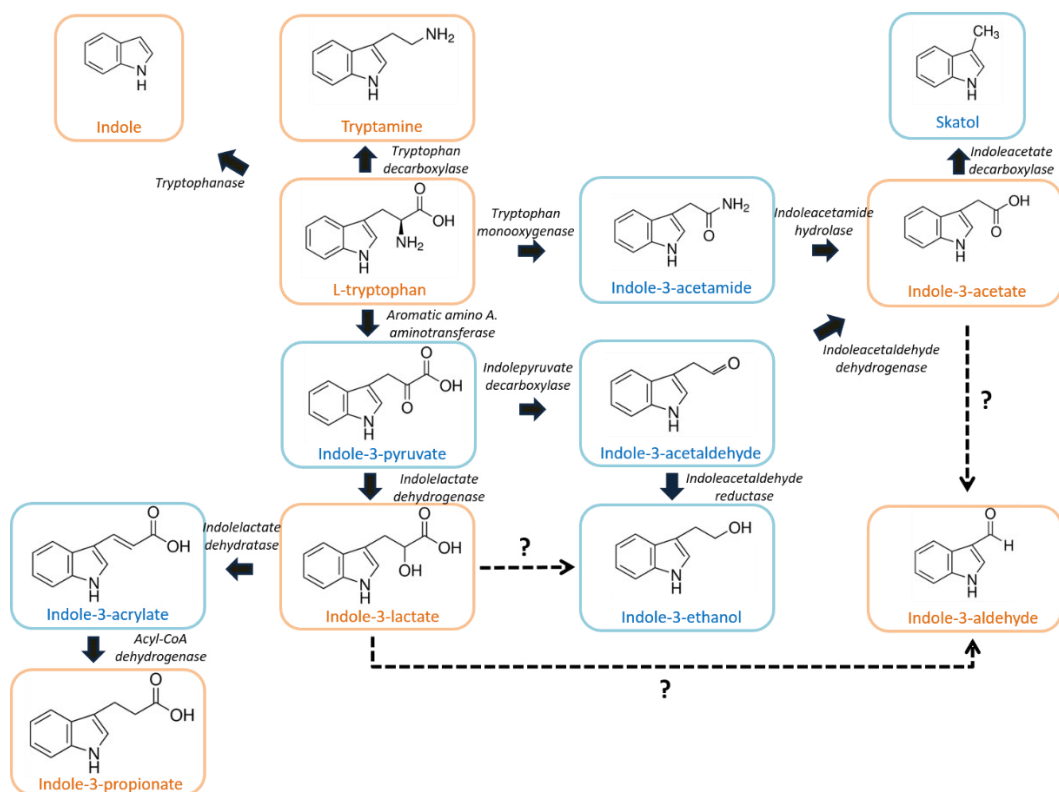

Figure 9: Microbial generation of tryptophan catabolites in the human gut. Overview of the different ways microbes degrade tryptophan in the human gut. The metabolites framed in orange colour represent the most commonly detected tryptophan catabolites in the human gut. Dashed lines represent pathways where no enzymes have been identified. Adopted from (Roager et Licht, 2018).

3.4.2 Mono-methylated indoles (MMIs)

This section is on the effects of seven MMI isomers on the AhR and PXR signalling pathways. Several studies monitored the biological processes of some MMIs connected to these signalling pathways. However, for most MMIs, these mechanisms remain unknown. MMIs differ from each other in the position of attached methyl group on the indole core. While 3-MMI is a microbial catabolite formed from dietary tryptophan in intestines (described above), the other MMIs isomers are xenobiotics. Rasmussen et al. demonstrated that 3-MMI is a partial agonist of human AhR and an inducer of CYP1A1, CYP1A2, and CYP1B1 genes in HepG2 cell line and primary human hepatocytes, which was later confirmed also by other researchers (Rasmussen et al., 2016; Stepankova et al., 2018). The same authors also showed that indole-3-carbinol (skatole metabolite) is a more potent inducer of human AhR than skatole (Rasmussen et al., 2016). Skatole also induces the expression of CYP1A1 mRNA and protein in primary normal bronchial epithelial cells at physiologically relevant concentrations (Weems et Yost, 2010). Using a reporter gene assay, Hubbard el al. showed that 3-MMI, but not 1-MMI or 2-MMI activates AhR. However, experiments were carried out with only up to 10 µM concentrations of MMI (Hubbard et al., 2015a). 3-MMI, as well as xenobiotic 2-MMI, induced ethoxy-resorufin-O-deethylase activity in Zebrafish (Brown et al., 2015) and Atlantic killifish embryos (Brown et al., 2016).

Apart from 3-methylindole, the metabolism of the other tested MMIs is unknown. Because many AhR ligands are also PXR ligands (approx. 88 % overlap for dual activators: PubChem Bioassay ID434939 and PubChem Bioassay ID2796), it is reasonable to assume that indoles might also be PXR ligands.
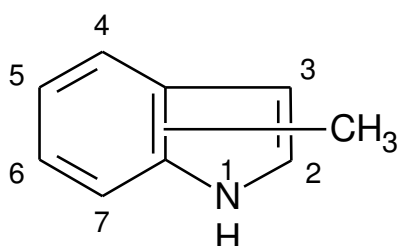

Figure 10: Chemical structure of mono-methylated indoles

4 MATERIALS AND METHODS

4.1 Biological materials

4.1.1 Cancer cell lines

The human Caucasian colon adenocarcinoma cell line LS180 (ECACC No. 87021202) and mouse hepatoma cell line Hepa-1c1c7 (ECACC No. 95090613) were purchased from the European Collection of Authenticated Cell Cultures (ECACC). Human Caucasian colon adenocarcinoma cell line LS174T (ATCC: CL-188; 7 000 3535) (Synthego Corporation, Redwood City, CA, USA) was used, as the parental cell line, to develop the PXR-knockout variant LS174T PXR-KO, utilizing CRISPR/Cas9 technology, as recently described (Dvorak et al., 2020). Human Caucasian colon adenocarcinoma cell lines HT-29 wild-type and AHR knock-out variant clone E4 were a generous gift from prof. RNDr. Jan Vondráček Ph.D. (IBP Brno, Czech Republic). The AHR knock-out variant, a clone E4 of HT-29 cell line, was generated using CRISPR/Cas9 as previously described (Vyhlidalova et al., 2020a). Stably transfected reporter gene cell line AZ-AhR (Novotna et al., 2011) and the polyclonal population of LS174T (RM12-PXR) cells with stably transfected pReceiver-M12 expression plasmid (Illes et al., 2020) were developed in our laboratory. All the cell lines, except for Hepa-1c1c7, were maintained in Dulbecco´s modified Eagle´s medium (DMEM) supplemented with 10 % foetal bovine serum or 10 % charcoal-stripped foetal bovine serum, 2 mM L-glutamine, 1 % non-essential amino acids, 100 U/ml streptomycin, and 100 µg/ml penicillin. The Hepa-1c1c7 cell line was cultured in minimal essential medium without nucleosides (MEM) enriched with 10 % foetal bovine serum and 2 mM L-glutamine. All used cells were incubated at 37 °C and 5 % CO_2.

4.1.2 Primary and progenitor hepatic cell lines and immortalised keratinocytes

Human immortal keratinocyte cell line HaCaT was kindly donated by *P. Boukamp* (IUF Düsseldorf, Germany) and was cultured in DMEM as earlier described.

Three human hepatoma HepaRG^{TM}-derived cell lines (5F Clone control cells, AHR knock-out (AHR-KO) and PXR-knock-out (PXR-KO)) were obtained

from Sigma Aldrich (Prague, Czech Republic) and incubated according to the manufacturer's instructions.

Primary cultures of human hepatocytes were of dual origins: (i) cultures in a monolayer batch marked with "HEP" were purchased from Biopredic International (Rennes, France); (ii) cultures from multi-organ donors marked with "LH" were prepared at the Faculty of Medicine, Palacký University Olomouc. The liver tissues were obtained from the University Hospital Olomouc, Czech Republic, and the tissue acquisition protocol complied with the requirements/regulations issued by "Ethical Committee of the University Hospital Olomouc, Czech Republic" and with transplantation Law #285/2002 Coll. Primary human hepatocyte cultures were maintained in serum-free ISOM medium (Isom et al., 1985; Pichard-Garcia et al., 2002). The age and sex of each donor are mentioned below (Table 1). The cells were incubated at 37 °C with 5 % CO_2.

Table 1: Age and gender of donors of used primary human cultures

Batch number	Sex	Age
HEP200565	Female	21
HEP200570	Male	64
HEP200571	Male	77
HEP220993	Female	76
HEP2201020	Male	75
HEP2201021	Male	66
LH75	Female	75
LH79	Male	60

4.2 Compounds and reagents

DMEM, MEM, foetal bovine serum (FBS), charcoal-stripped foetal bovine serum (CS-FBS), non-essential amino-acids, L-glutamine, penicillin, streptomycin, dimethyl sulfoxide (DMSO, D8418), rifampicin (RIF, R3501, Lot 0000104692, purity ≥ 97 %), hygromycin B, TRI Reagent®, Triton™ X-100, D-luciferin, coenzyme A, adenosine triphosphate (ATP), bovine serum albumin, benzo[a]pyrene (BaP, B1760, Lot SLB0038V, purity 99 %), 6-formylindolo[3,2-b]carbazole (FICZ, SML1489, Lot 0000026018, purity 99.5 %), 1-methylindole (193984, Lot BGBC4251V, purity ≥ 97 %),

2-methylindole (M51407, Lot BCBF7494V, purity 98 %), 3-methylindole (M51458, Lot STBK2264, purity 98 %), 5-methylindole (222410, Lot STBF3756V, purity 99 %), 6-methylindole (246328, Lot MKBJ2514V, purity 97 %), 7-methylindole (M51490, Lot MKBP5287V, purity 97 %), indole-3-aldehyde (129445, Lot STBH5988, purity 97 %) and indole-3-ethanol (T90301, Lot BCBW9114, purity 97 %) were purchased from Sigma Aldrich (Prague, Czech Republic). 4-methylindole (E020483, Lot AH160074, purity 98 %) was obtained from Energy Chemical (Shanghai, China). Tryptamine (SC-206065, Lot E0218, purity 99.9 %), indole-3-propionate (SC-255215, Lot E0218, purity ≥ 98 %), indole-3-acetamide, (SC-255213, Lot K0618, purity ≥ 98 %), indole-3-pyruvate (SC-218597, Lot K1218, purity ≥ 95 %), indole-3-acetate (SC-254494, Lot A2218, purity ≥ 99 %), indole-3-lactate (SC-489732, Lot B2321, purity 99.7 %), indole-3-acrylate (SC-272496, Lot K1618, purity 98.4 %), indole (SC-257606, Lot J0918, purity ≥ 98 %), primary mouse monoclonal antibodies against CYP1A1 (sc-393979, A-9), CYP1A2 (sc-53614, 3B8C1), CYP3A4 (sc-53850, HL3), ARNT-1 (sc-17812, G-3), AhR (sc-133088, A-3) and AhR labeled with Alexa fluor 488 (sc-133088 AF488, A-3), PXR rabbit polyclonal antibody (sc-25381, H-160), normal rabbit IgG (sc-2027) were acquired from Santa Cruz Biotechnology (Santa Cruz, CA, USA). Other primary antibodies against AhR (rabbit monoclonal; 83200S, D5S6H) and β-actin (mouse monoclonal; 3700S, 8H10D10) as well as anti-mouse secondary antibody conjugated to horseradish peroxidase (7076S) were purchased from Cell Signalling Technology (Danvers, MA, USA). An anti-PXR (mouse monoclonal; PP-H4417-00) antibody was obtained from Perseus Proteomics, Int. (Tokyo, Japan). WesternSure® PREMIUM Chemiluminescent Substrate was purchased from LI-COR Biotechnology (Lincoln, NE, USA), whereas reagents for Simple Western blotting by Sally Sue™, a goat anti-mouse secondary horseradish conjugated antibody, and antibody diluent were acquired from ProteinSimple (San Jose, CA, USA). Luciferase lysis buffer, FuGENE® HD Transfection Reagent, and P450-Glo™ CYP1A1 assay were purchased from Promega (Madison, WI, USA). M-MuLV Reverse Transcriptase and Random Primers 6 were acquired from New England Biolabs (Ipswith, MA, USA). UPL probes and oligonucleotide primers used in qPCR reactions were designed by Universal ProbeLibrary Assay Design Center and synthesised by Sigma

Aldrich (Prague, Czech Republic), while LightCycler® 480 Probes Master was purchased from Roche Diagnostic Corporation (Prague, Czech Republic). 2,3,7,8-tetrachlorodibenzo-p-dioxin (TCDD, RPE-029) was from Ultra Scientific (North Kingstown, RI, USA). 2,3,7,8-tetrachlorodibenzofuran (TCDF, Amb17620425, Lot 51207-31-9) was from Ambinter (Orléans, France). DAPI (4',6-diamino-2-phenylindole) was from Serva (Heidelberg, Germany). [^{3}H]-TCDD (ART 1642, Lot 181018, purity 98.6 %) was purchased from American Radiolabeled Chemicals (St. Louis, MO, USA). Bio-Gel® HTP Hydroxyapatite (1300420, Lot 64079675) was obtained from Bio-Rad Laboratories (Hercules, CA, USA). LanthaScreen^{TM} TR-FRET PXR (SXR) Competitive Binding Assay Kit and Pierce^{TM} Co-Immunoprecipitation Kit were acquired from Thermo Fisher Scientific (Waltham, MA, USA). All other chemicals were of the highest quality commercially available.

4.3 Methods

4.3.1 Reporter gene assay

To investigate AhR transcriptional activity, stably transfected AZ-AhR cells were used (Novotna et al., 2011). LS180 cells, transiently transfected with human PXR expression vector pSG5-PXR, (kindly provided by Dr. S. Kliewer, University of Texas, Dallas, US) and a chimeric p3A4-luc reporter construct (Pavek et al., 2010) through lipofection (FuGENE® HD Transfection reagent), were used to study PXR transcriptional activity. The cells were seeded at a density of 25×10^3/well in 96-well plates and allowed to stabilise for 24 h. The cells were incubated for 24 h with tested compounds and/or vehicle (DMSO; 0.1 % v/v), in the presence (antagonist mode) or absence (agonist mode) of TCDD (13.5 nM), FICZ (22.6 µM), or BaP (15.8 µM) for AhR activity and RIF (10 µM) for PXR activity. In another experiment, the cells were incubated for 24 h with culture media aspired from human hepatocytes cultures that had been previously incubated for 0 h and 24 h with vehicle (DMSO; 0.1 % v/v), TCDD (5 nM), and mono-methylindoles (MMIs; 200 µM). This different approach of treating cells using collected culture media was applied to understand MMI metabolism (see chapter 5.1.4. and 5.1.5). Following cell

lysis, luciferase activity was measured using a Tecan Infinite M200 Pro Plate Reader (Schoeller Instruments, Czech Republic).

4.3.2 mRNA isolation and quantitative reverse transcriptase polymerase chain reaction (qRT-PCR)

LS180 cells were used to explore mRNA expression levels of PXR target genes (CYP3A4 and MDR1). They were transiently transfected with a pSG5-hPXR expression vector through lipofection (FuGENE® HD Transfection reagent).

The cells were seeded in 12-well plates and stabilised for 24 h (48 h for primary human hepatocytes). Cultured cells were incubated for 24 h with vehicle (DMSO; 0.1 % v/v) or examined compounds in the presence (antagonist mode) or absence (agonist mode) of TCDD (5 nM or 10 nM) or RIF (10 μM), respectively. Total RNA was isolated by using TRI Reagent® according to the manufacturer's protocol. The concentration and quality of the RNA was determined with a NanoDrop™ Lite Spectrophotometer (Thermo Fisher Scientific, MA, USA). The isolated RNA (1000 ng) was used for cDNA synthesis using M-MuLV reverse transcriptase and Random Primers 6. The reverse transcription was carried out at 42 °C for 60 min, and the cDNA sample was diluted in ratio 1:4 with PCR-grade water. qRT-PCR was performed on LightCycler® 480 Instrument II (Roche Diagnostic Corporation, Prague, Czech Republic) using the LightCycler® Probes Master. The levels of all mRNAs were determined using the Universal Probes Library probes in combination with specific primers (Table 2). An activation step was conducted at 95 °C for 10 min, followed by 45 cycles of PCR (denaturation at 95 °C for 10 s; annealing with elongation at 60 °C for 30 s). All measurements were carried out in triplicates. The data were processed by the delta-delta C_t method and normalised to GAPDH as the housekeeping gene.

Table 2: Primer sequences with appropriate Universal Probes Library (UPL) numbers

Gene	Forward Primer (5′ → 3′)	Reverse Primer (5′ → 3′)	UPL no.
GAPDH	CTCTGCTCCTCCTGTTCGAC	ACGACCAAATCCGTTGACTC	60
CYP1A1	CCAGGCTCCAAGAGTCCA	AGGGATCTTGGAGGTGGCT	33
CYP1A2	ACAACCCTGCCAATCTCAAG	GGGAACAGACTGGGACAATG	34
CYP3A4	TGTGTTGGTGAGAAATCTGAGG	CTGTAGGCCCCAAAGACG	38
MDR1	CCTGGAGCGGTTCTACGA	TGAACATTCAGTCGCTTTATTTCT	147

4.3.3 Simple western blotting by Sally Sue^{TM}

The protein levels of CYP1A1, CYP1A2, CYP3A4, and β-actin in the total protein extracts prepared from primary human hepatocytes were determined. The cells were stabilised for 48 h before treatment, followed by incubation for 24 h with MMIs, TCDD (5 nM), RIF (10 μM), and/or vehicle (DMSO; 0.1 % v/v). After incubation, the cells were washed once in phosphate buffered saline (PBS) and centrifuged (4600 rpm/5 min/4 °C). Total protein extracts were prepared by resuspending the pellets in non-denaturizing ice cold lysis buffer (150 mM NaCl, 10 mM Tris (pH 7.2), 0.1 % (w/v), Triton X-100, anti-phosphatase cocktail, anti-protease cocktail, 1 % (v/v) sodium deoxycholate, and 5 mM EDTA). The suspension was vortexed and centiruged (13,200 rpm/ 15 min/4 °C). The supernatant was collected and the concentration of proteins was determined using Bradford reagent. Target proteins were detected by using automated capillary electrophoresis Sally Sue^{TM} Simple Western System (ProteinSimple^{TM}, San Jose CA, USA) and handled in accordance with the ProteinSimple manual. Primary antibodies for CYP1A1 (dilution 1:100), CYP1A2 (dilution 1:1000), CYP3A4 (dilution 1:5000 to 1:20000), and β-actin (dilution 1:1000) were used, and detection was performed using a horseradish conjugated secondary antibody on a chemiluminescent substrate. The data were analysed using Compass Software version 2.6.5.0 (ProteinSimple^{TM}). CYP signals were normalised to β-actin signal as a loading control and expressed as fold induction over negative control (DMSO).

4.3.4 Time resolved-fluorescence resonance energy transfer

The LanthaScreen^{TM} TR-FRET PXR (SXR) Competitive Binding Assay Kit (Thermo Fisher Scientific, Waltham, MA, USA) was used to determine the binding of MMIs, indole-3-acetamide, and indole at PXR. The experiments were performed in a volume of 20 μl in 384-well black plate with tested compounds prepared in serial dilution (from 11-points to 13-points), at concentrations ranging from 0.05 μM to 500 μM. Vehicle (DMSO) and SR12813 (100 μM) were used as negative and positive control, respectively. The plate was incubated for 1 h at room temperature in the dark. Subsequently, using the 340 nm excitation filter, the fluorescent signals were measured at 495 nm and 520 nm on the Tecan Infinite F200 Pro Plate Reader (Achoeller Instruments, Czech

Republic). For the TR-FRET ratio, the emission signal at 520 nm was divided by the emission signal at 495 nm. Binding assays were done in quadruplicates (technical replicates) in at least three independent experiments (biological replicates), and the IC_{50} values were calculated.

4.3.5 Chromatin immunoprecipitation assay

4.3.5.1 Detection of AhR binding to CYP1A1 promoter

LS180 cells were seeded in a 60-mm cell culture dish (4×10^6), and the following day, the cells were incubated with vehicle (DMSO; 0.1 % v/v), TCDD (10 nM), or the test compounds (indole 1000 µM, indole-3-acrylate 100 µM, others 200 µM) for 90 min at 37 °C. Chromatin immunoprecipitation assay (ChIP) procedure was performed in accordance with the manufacturer's protocol in the manual for the SimpleChIP Plus Enzymatic Chromatin IP Kit (Magnetic Beads; Cell Signalling Technology, Leiden, The Netherlands) and as previously described (Stepankova et al., 2018). Immunoprecipitation was achieved by the addition of 5 µl anti-AhR antibody (D5S6H, Cell Signalling Technology) to 25 µg of digested chromatin. The amplification of CYP1A1 promoter DNA was carried out with PCR using the following primers:

Forward   5'-AGCTAGGCCATGCCAAAT-3'

Reverse   5'-AAGGGTCTAGGTCTGCGTGT-3'

The data are expressed as the fold enrichment to vehicle-treated cells. The end point PCR product was separated using 2 % agarose gel electrophoresis.

4.3.5.2 Detection of PXR binding to MDR1 promoter

LS174T cells with stably transfected pReceiver-M12 expression plasmid (RM12-PXR) were seeded in a 60-mm cell culture dish (3 million) and allowed to stabilise. The following day, the cells were maintained in DMEM with 10 % CS-FBS containing vehicle (DMSO; 0.1% v/v), RIF (10 µM), indole-3-acetamide (IAD, 200 µM), and indole (IND, 1000 µM) for 20 h at 37 °C. ChIP assay was performed as previously described (Stepankova et al., 2018) with small modifications: a) 5 µl of anti-PXR antibody (PP-H4417-00, Perseus Proteomics Int.) was used against 30 µg of DNA; b) MDR1 promoter DNA was amplified by PCR using the following primers:

Forward   5'-GAGTGAACGTTACCTCATTGAAC-3'

Reverse   5'-CCGAAATGGCTTTTGAATTG-3'

The data were analysed as previously described, and the amplicon was electrophoresed on 2 % agarose gel after PCR.

4.3.5.3 Detection of PXR binding to CYP3A4 promoter

LS174T cells were transiently transfected with pSG5-PXR expression plasmid, plated in 150-mm cell culture dish, and grown to confluence. The cells were incubated with vehicle (DMSO; 0.1 % v/v), RIF (10 µM), and 1-MMI (200 µM) for 24 h at 37 °C. ChIP procedure was carried out as previously decribed (Dvorak et al., 2020) and 2 µg of anti-PXR antibody (SC-25381, H-160, Santa Cruz Biotechnology) was used for immunoprecipitation. Purified chromatin DNA was used to perform PCR amplification for CYP3A4 promoter DNA with the following primers:

Forward   5'-AGAGACAAGGGCAAGAGAG-3'
Reverse   5'-CTCTTTGCTGGGCTAGTGCA-3'

Next, the PCR products were resolved on 1.5 % agarose gel.

4.3.6 Protein Co-Immunoprecipitation

- **Detection of the formation of the AhR-ARNT heterodimer**

The formation of AhR-ARNT heterodimer was studied in cell lysates from intestinal LS180 cells, which were incubated with vehicle (DMSO; 0.1 % v/v), TCDD (10 nM), and the tested compounds-indole (IND, 1000 µM), indole-3-pyruvate (IPY, 200 µM), 3-methylindole (3-MMI, 200 µM), tryptamine (TA, 200 µM), indole-3-acrylate (IAC, 200 µM), and indole-3-acetamide (IAD, 200 µM) for 90 min at 37 °C. The Pierce^{TM} Co-Immunoprecipitation Kit (Thermo Fisher Scientific, Waltham, MA, USA) and covalently coupled AhR antibody (mouse monoclonal, sc-133088, A-3, Santa Cruz Biotechnology) were used. Eluted protein complexes, in parallel with total parental lysates, were separated on 8 % SDS-PAGE gels, followed by western blot analysis and immuno-detection with ARNT-1 antibody (mouse monoclonal, sc-17812, G-3, Santa Cruz Biotechnology). Chemiluminescent detection was performed using horseradish peroxidase-conjugated anti-mouse secondary antibody (7076S, Cell Signalling Technology) and WesternSure® PREMIUM Chemiluminescent Substrate (LI-COR Biotechnology) by C-DiGit® Blot Scanner (LI-COR Biotechnology).

4.3.7 Competitive Radio-Ligand Binding Assay

The ligand binding assay was carried out using cytosolic protein extracts isolated from murine hepatoma Hepa1c1c7 cells as previously described (Denison et al., 2002b). In brief, cytosolic protein (2 mg/ml) was incubated for 2 h at room temperature with 2 nM [^{3}H]-TCDD in the presence of vehicle (DMSO; negative control; 0.1% v/v), FICZ (positive control; 0.01 nM-10 nM), TCDF (non-specific binding; 200 nM), or increasing concentration of MICT. Next, the hydroxyapatite slurry was added to the samples and the suspension was kept on ice and washed three times with HEGT buffer. The hydroxyapatite pellet was resuspended in a scintillation cocktail, and radioactivity was determined using a liquid scintillation counter. The specific binding of [^{3}H]-TCDD was defined as the difference between total radioactivity and radioactivity of non-specific reaction (TCDF). Binding assays were performed in triplicates (technical replicates), in at least two independent experiments, and the IC$_{50}$ values were calculated where necessary.

4.3.8 High-performance liquid chromatography

High performance liquid chromatography (HPLC) was used to determine the levels of tryptophan in the samples of culture media isolated from the growing cells at 2 h intervals from 0 h to 24 h. A simple gradient HPLC method using an Agilent 1260 Infinity system (consisting of a quaternary gradient pump, autosampler, column thermostat, and diode array detector (DAD)) was used. The starting mobile phase mix consisted of 90 % of 0.2 % trifluoroacetic acid (TFA) and 10 % of acetonitrile (MeCN), and during the run, a linear gradient was applied up to 15 min, increasing the percentage of MeCN to 90 %. A post time of 5 min was applied to achieve the proper starting conditions for the next run. The stable mobile phase flow of 0.5 ml/min was applied at the reverse phase chromatographic column Agilent Poroshell 120 EC-C18, 4.6 × 50 mm, 2.7 μm particle size. The DAD detector was set to detect at the following wavelengths: 290 ± 4 nm (A), 254 ± 4 nm (B), 210 ± 4 nm (C), and 275 ± 4 nm (D, used for quantification of tryptophan levels) with a reference range of wavelengths of 820 ± 100 nm. The sample volume applied to the column was 10 μl in all the cases. An external calibration in the concentration range of 0.7 μM–112.0 μM was used, giving a straight calibration curve with

$R^2 = 0.9999$. The peak of tryptophan was identified at $t_R = 5.0 \pm 0.1$ min, and it was completely resolved from other peaks in the chromatogram. The individual determinations were done in duplicate, and the concentration levels were expressed as mean values ± sample standard deviations.

4.3.9 Liquid chromatography/mass spectrometry

Liquid chromatography/mass spectrometry (LC/MS) analysis was used to determine MMI metabolites in the culture media samples. Three cultures of primary human hepatocytes (LH75, HEP200565, and HEP200570) were incubated with 200 µM MMIs for 24 h. Thereafter, culture media were aspired and used for reporter gene assay in AZ-AhR cells (*vide supra*) and for LC/MS analysis. Briefly, a previously described method (Zhang et al., 2014) with slight modification was used for the separation of the metabolites using the UHPLC Dionex UltiMate 3000 (Thermo Fisher Scientific) coupled with the LCQ Fleet™ Ion Trap Mass Spectrometer (Thermo) in a positive ionization mode. The mobile phase consisted of water supplemented with 0.1 % trifluoroacetic acid (TFA) and acetonitrile supplemented with 0.1 % of TFA. During the 18-min analysis, the mobile phase gradient comprised 95 % of water for 1 min, followed by the linear gradient to 15 min down to 5 % of water, followed by the rapid linear gradient to 18 min reconstituting the starting 95% of water. The stable mobile phase flow of 0.5 mL/min was applied at the reverse-phase chromatographic column Agilent Poroshell 120 EC-C18, 4.6 × 50 mm, 2.7 µm particle size. The PDA detector was set to the detection wavelengths of 254 ± 4 nm, 210 ± 4 nm, 225 ± 4 nm (used for quantification of residual levels of MMI), and 350 ± 4 nm, and the MS analyser was set to detect the mass range of 50-2000 m/z. The sample volume applied to the column was 10 µl in all the cases. All samples were analysed in three parallel determinations and the LC/MS data were analysed using the Thermo Excalibur 2.2 Qual Browser (Thermo).

4.3.10 Nuclear translocation of AhR

LS180 cells (60,000 cells/well) were plated on poly-D-lysine-coated 8-well chambered slides (94.6140.802, Sarstedt, Nümbrecht, Germany) and allowed to grow overnight. Next, the cells were incubated for 90 min with DMSO (0.1 % v/v), TCDD (10 nM), IND (1000 µM), 3-MMI (200 µM), TA

(200 µM), IPY (200 µM), IAD (200 µM), and IAC (100 µM). The staining procedure has earlier been described (Stepankova et al., 2018). The primary anti-AhR antibody used was Alexa Fluor 488 labelled mouse monoclonal (sc-133088, Santa Cruz Biotechnology, U.S.A.). The nuclei were stained with 4',6-diamino-2-phenylindole (DAPI), and the cells were enclosed by VectaShield® Antifade Mounting Medium (Vector Laboratories Inc., U.S.A.). The images were captured using an IX73 fluorescence microscope (Olympus, Tokyo, Japan). The immunofluorescence signal intensity (of the AhR antibody) in the nucleus was visually evaluated. To calculate the percentage number of cells, approximately 500 cells from at least four randomly selected fields of view in each specimen were used.

4.3.11 CYP1A1 enzyme activity

The P450-Glo™ CYP1A1 cell-based assay was used to determine CYP1A1 catalytic activity in primary human hepatocytes and intestinal LS180 cells. The amount of luminescence produced was directly proportional to CYP1A1 activity. Experiments were carried out in two layouts: (i) Assessment of CYP1A1 induction and degradation by MMI: The cells were incubated with MMIs (0.1 µM–200 µM), vehicle (DMSO; 0.1 % v/v), and 5 nM TCDD for 24 h. Next, the enzyme substrate luciferin-CEE was added for additional 3 h; (ii) Assessment of the inhibition of TCDD-induced CYP1A1 by MMIs: The cells were pre-incubated with TCDD for 24 h, followed by the addition of enzyme substrate luciferin-CEE with MMIs for another 3 h. Each reaction was performed in duplicates, and two independent experiments were performed for each replicate. Net luminescence signals were determined by subtracting background luminescence values (no-cell control) from treated and untreated values. CYP1A1 catalytic activity was evaluated by plotting fold induction against MMI concentrations.

4.3.12 Statistical analysis

In order to determine significantly different results with respect to negative or positive control, one-way analysis of variance (ANOVA), followed by Dunnett's test, was applied. A p-value < 0.05 indicated statistical significance. The normality of the data was tested using the Shapiro-Wilk normality test. All calculations (including IC_{50} and EC_{50}) and curve fittings were performed using GraphPad Prism version 8.0 for Windows (GraphPad Software, La Jolla, CA, USA).

5 RESULTS

5.1 Effects of MMIs on the AhR signalling pathway

5.1.1 Effects of MMIs on the mRNA expression of CYP1A1 and CYP1A2 in HepaRG cells

Non-toxic concentrations of MMIs, as determined by MTT test using AZ-AhR cells, were used for analysis (Stepankova et al., 2018).

In the first series of experiments, we examined the induction of CYP1A1 and CYP1A2 mRNAs, which are prototypical AhR-regulated genes. The study was performed in human progenitor hepatic cells, HepaRG, which are highly competent to express xenobiotic-metabolizing enzymes. Control clone (5 F) and AhR knock-out variant of HepaRG cells (AhR-KO) were incubated for 24 h with vehicle (DMSO; 0.1 % v/v), model CYP1A inducer dioxin (TCDD; 5 nM), and MMIs (200 µM). The expression of CYP1A genes was determined through RT-PCR. Dioxin strongly induced CYP1A1 (44-fold and 93-fold) and CYP1A2 (34-fold and 50-fold) mRNA in two consecutive passages of 5F-HepaRG cells. 4-methylindole and 6-methylindole induced CYP1A genes with efficacy similar to that of TCDD (~100 %). Medium CYP1A induction was achieved with 1-methylindole (~15 %), 3-methylindole (~50 %), 5-methylindole (~20 %), and 7-methylindole (~20 %), while 2-methylindole was nearly inactive. The induction of CYP1A genes by MMIs in AhR-KO-HepaRG cells ceased, which corroborated the involvement of AhR in the induction of CYP1A1 and CYP1A2 mRNAs in HepaRG cells.
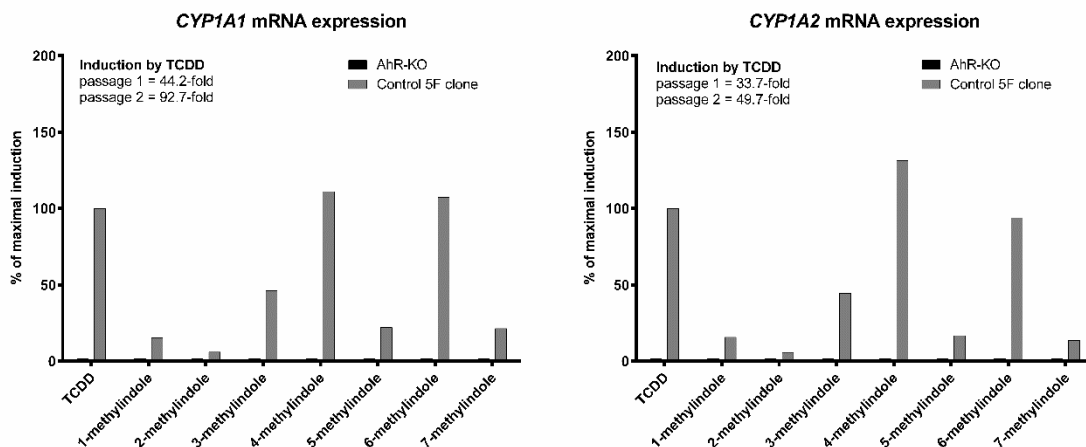
Figure 11: Effects of MMIs on the mRNA expression of CYP1A1 and CYP1A2 in HepaRG cells. AhR knock-out (AHR-KO) and control 5F Clone of HepaRG cells were incubated for 24 h with the vehicle (DMSO; 0.1 % v/v), dioxin (TCDD; 5 nM), and MMIs (200 μM). The mRNA expression of CYP1A1 and CYP1A2 was determined by RT-PCR, and the data were normalised to GAPDH mRNA level. The bar graphs show the percentage of maximal induction achieved by TCDD in the control 5F Clone of HepaRG expressed as the means of two consecutive cell passages. RT-PCR analysis was carried out in triplicates.

5.1.2 Effects of MMIs on CYP1A1 and CYP1A2 expression in primary human hepatocytes

We also examined the effects of MMIs on the expression of CYP1A1 and CYP1A2 mRNAs and proteins in three different primary cultures of human hepatocytes. Human hepatocytes were incubated for 24 h with vehicle (DMSO; 0.1% v/v), dioxin (TCDD; 5 nM), and MMIs (200 μM). The expression of CYP1A genes was determined by using RT-PCR. The levels of CYP1A1 and CYP1A2 proteins were determined with quantitative automated western-blot analyser SallySue. Dioxin strongly induced the protein and mRNA expression of CYP1A1 and CYP1A2 in all the three human hepatocyte cultures. The effects of MMI were highly consistent between individual human hepatocytes cultures, and the changes in the mRNA expression of CYP1A1 and CYP1A2 followed the same trend as those of CYP1A1 and CYP1A2 proteins. MMIs methylated at positions 4, 5, 6, and 7 were strong inducers of CYP1A1 and CYP1A2. 1-methylindole and 3-methylindole achieved medium induction of CYP1A, whereas 2-methylindole had no effect. The effects of MMIs on CYP1A expression in human hepatocytes were in accordance with those observed in HepaRG cells except with 7-methylindole, which exerted a moderate induction of CYP1A in HepaRG and LS180 intestinal cells (Stepankova et al., 2018), but a strong induction in all human hepatocytes cultures. This indicated a possible metabolic

66

transformation of 7-methylindole by human hepatocytes into a derivative with increased AhR-activity.
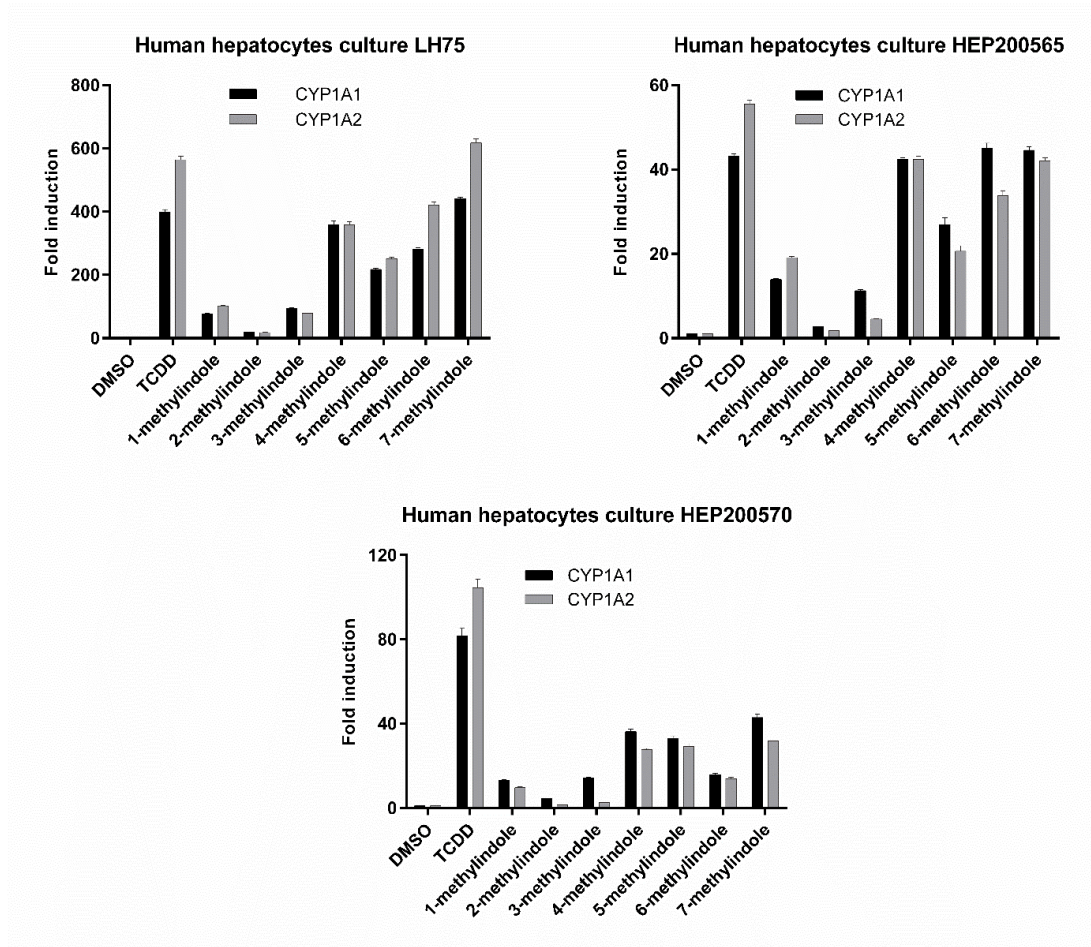

Figure 12: Effects of MMIs on the mRNA expression of CYP1A1 and CYP1A2 in primary human hepatocytes. Primary human hepatocytes cultures obtained from three liver tissue donors (LH75, HEP200565, and HEP200570) were incubated for 24 h with the vehicle (DMSO; 0.1 % v/v), dioxin (TCDD; 5 nM), and MMIs (200 µM). The expression of CYP1A1 and CYP1A2 mRNAs was determined by using reverse transcription polymerase chain reaction (RT-PCR), and the data were normalised to GAPDH mRNA level. The data of each hepatocytes culture are expressed as the means ± standard deviation from triplicate RT-PCR measurements.
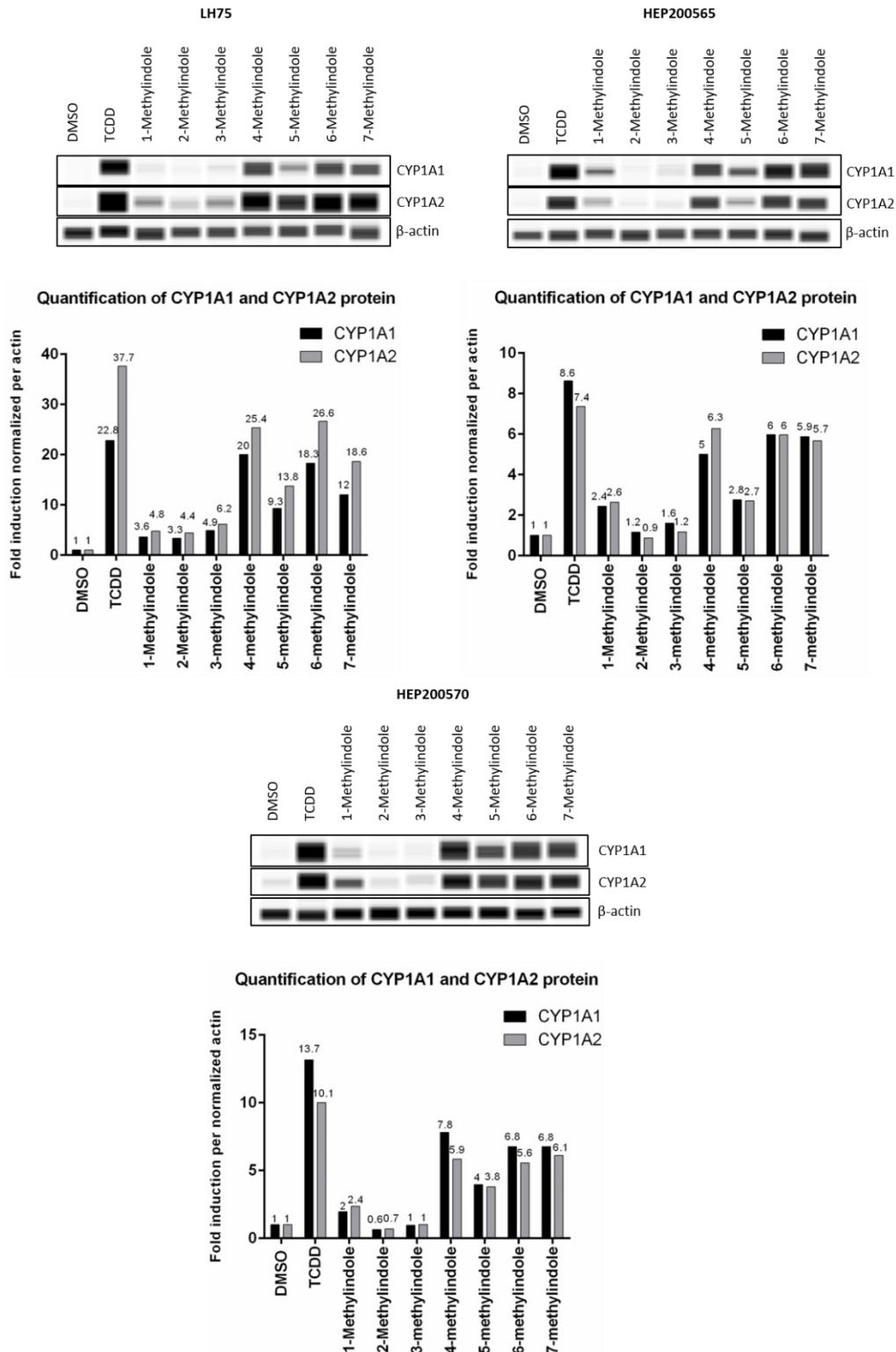
Figure 13: Effects of MMIs on the protein expression of CYP1A1 and CYP1A2 in primary human hepatocytes. Primary human hepatocytes obtained from three donors (n = 3) were incubated for 24 h with the vehicle (DMSO; 0.1 % v/v), dioxin (TCDD; 5 nM), and MMIs (200 µM). The levels of CYP1A1 and CYP1A2 proteins were determined using quantitative automated western-blot analyser SallySue. Upper panels within each hepatocyte culture: Records of CYP1A1, CYP1A2, and β-actin proteins from SallySue software. Lower panels within each hepatocyte culture: Bar graphs show quantified CYP1A1 and CYP1A2 proteins, normalised to the β-actin levels. Note: The presented data are intensity band generated by ProteinSimple software from automated capillary electrophoresis analysis.

5.1.3 Effects of MMIs on CYP1A1 catalytic activity in cultured human hepatocytes and LS180 cells

To study the functional endpoint of AhR-dependent gene induction, the effects of MMIs on CYP1A1 catalytic activity in primary human hepatocytes and intestinal LS180 cells were determined. Experiments were carried out in two layouts: (i) Assessment of the CYP1A1 amount (induction or degradation): The cells were incubated with MMIs in the concentration range of 0.1 µM–200 µM; followed by the addition of the enzyme substrate luciferin-CEE for 3 h (Figure 14); (ii) Assessment of the inhibition of TCDD-induced CYP1A1: The cells were pre-incubated with 5 nM TCDD for 24 h, followed by incubation with the enzyme substrate luciferin-CEE along with MMIs (0.1 µM–200 µM) for additional 3 h (Figure 15).

1-MMI and 7-MMI displayed dose-dependent induction of CYP1A1 activity, but with a weaker efficacy, compared with that of TCDD in human hepatocytes. The induction of CYP1A1 enzyme activity by TCDD in human HEP200571 and HEP220993 hepatocyte cultures was 11-fold and 153-fold, respectively. Inverse U-shaped, concentration-dependent profiles of CYP1A1 induction, peaking between 5 µM and 25 µM, were observed for 4-MMI, 5-MMI, and 6-MMI. No induction was observed in human hepatocytes incubated with 2-MMI and 3-MMI (Figure 14A, layout (i)). All the tested MMIs dose-dependently inhibited the catalytic activity of CYP1A1 in human hepatocytes pre-incubated with TCDD, with IC_{50} values ranging from 1.2 µM to 23.8 µM (Figure 15A, layout (ii)).

The induction of CYP1A1 catalytic activity in LS180 cells by TCDD ranged from 150-fold to 250-fold, compared with vehicle-treated cells. All tested MMIs induced CYP1A1 catalytic activity in LS180 cells, but with different concentration-response patterns. 1-MMI, 3-MMI, 5-MMI, and 7-MMI yielded dose-dependent profile, while 2-MMI, 4-MMI, and 6-MMI yielded inverse U shape profiles, peaking at 25 µM. Maximal relative efficacies of MMI ranged from 2 % to 25 %, compared with that of 5 nM TCDD (Figure 14B, layout (i)). CYP1A1 catalytic activity in TCDD-pre-incubated LS180 cells were inhibited in a concentration-dependent manner by all MMIs, with IC_{50} values ranging from 3.4 µM to 11.4 µM (Figure 15B, layout (ii)).
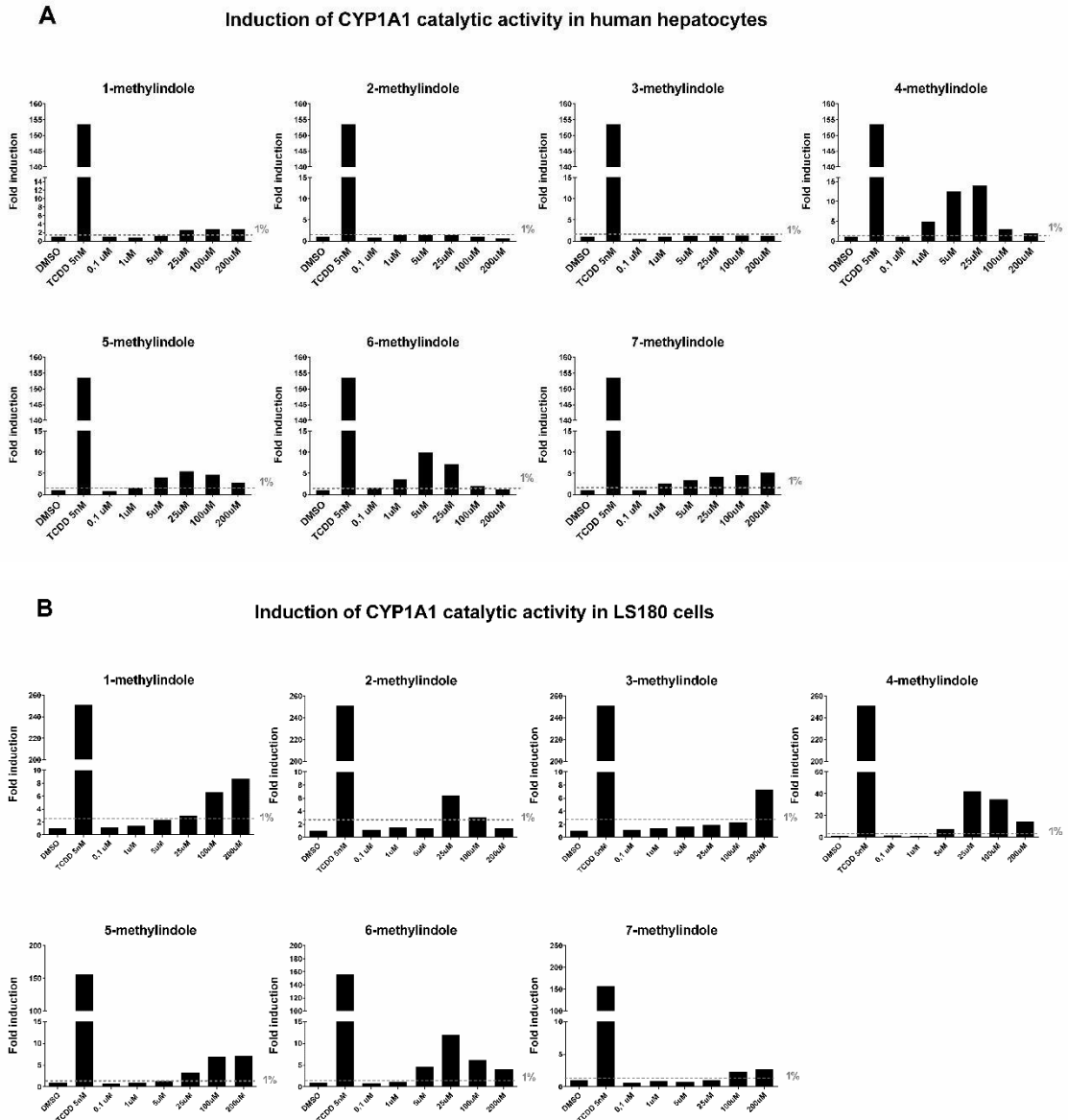
Figure 14: Effects of MMIs on the induction of the catalytic activity of CYP1A1 in primary human hepatocytes and LS180 cells. Primary human hepatocytes obtained from two donors (n = 2,cultures HEP200571 and HEP220993) and intestinal LS180 cells were seeded on 12-well plates and stabilised. Thereafter, the cells were incubated with MMIs (0.1 µM, 1 µM, 5 µM, 25 µM, 100 µM, and 200 µM), TCDD (5 nM) and vehicle (DMSO; 0.1 % v/v) for 24 h. Specific CYP1A1 substrate luciferin-CEE was then added to the cells for additional 3 h. Net luminescence signals were determined by subtracting background luminescence values (no-cell control) from treated and untreated values. The induction of CYP1A1 catalytic activity was evaluated by plotting fold induction against MMI concentrations. Incubations were performed in two parallel wells (technical duplicates). **Panel A**: Bar graphs show data from culture HEP220993 of primary human hepatocytes. **Panel B**: Experiments were performed in two consecutive passages in LS180 cells. Bar graphs show a representative experiment.
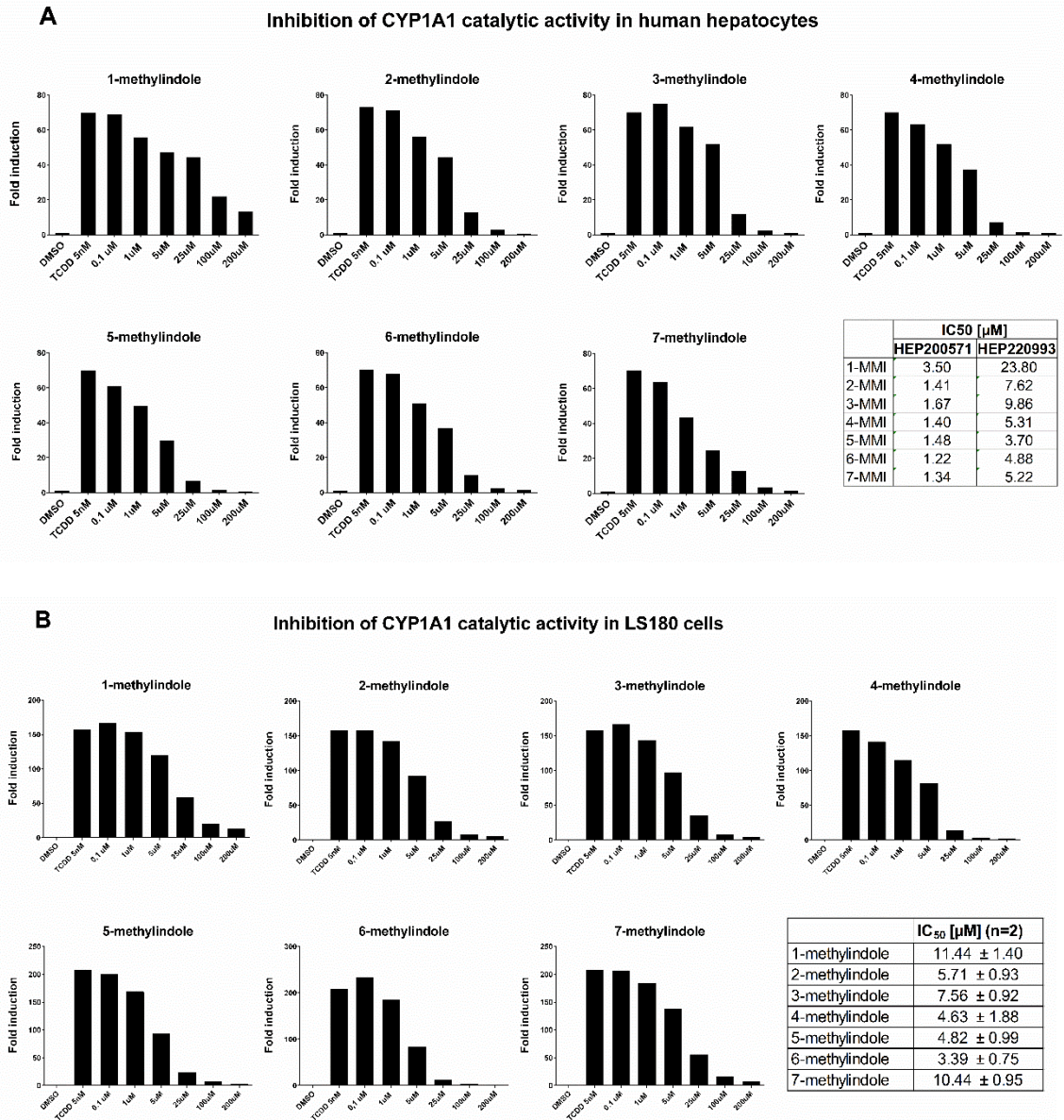
A. Inhibition of CYP1A1 catalytic activity in human hepatocytes

IC50 [µM]		
	HEP200571	HEP220993
1-MMI	3.50	23.80
2-MMI	1.41	7.62
3-MMI	1.67	9.86
4-MMI	1.40	5.31
5-MMI	1.48	3.70
6-MMI	1.22	4.88
7-MMI	1.34	5.22

B. Inhibition of CYP1A1 catalytic activity in LS180 cells

	IC_{50} [µM] (n=2)
1-methylindole	11.44 ± 1.40
2-methylindole	5.71 ± 0.93
3-methylindole	7.56 ± 0.92
4-methylindole	4.63 ± 1.88
5-methylindole	4.82 ± 0.99
6-methylindole	3.39 ± 0.75
7-methylindole	10.44 ± 0.95

Figure 15: Inhibitory effects of MMIs on TCDD-induced catalytic activity of CYP1A1 in primary human hepatocytes and LS180 cells. Primary human hepatocytes obtained from two donors (n = 2, cultures HEP200571 and HEP220993) and intestinal LS180 cells were seeded at 12-well plate and stabilised, prior to the pre-incubation with 5 nM TCDD for 24 h. Thereafter, MMIs (0.1 µM, 1 µM, 5 µM, 25 µM, 100 µM, 200 µM) in the mixture with specific CYP1A1 substrate luciferin-CEE were added to the cells for 3 h. Incubations were performed in two parallel wells (technical duplicates). The values of IC_{50} were calculated and inserted in the each panel (bottom right). **Panel A**: Bar graphs show data from culture HEP220993 of primary human hepatocytes. **Panel B**: Experiments were performed in two consecutive passages in LS180 cells. Bar graphs show a representative experiment.

71

5.1.4 Effects of MMIs and their metabolites on the transcriptional activity of AhR

Indoles undergo cytochrome P450-mediated oxidative metabolic transformation, as documented literature (Gillam et al., 2000). In order to find out, whether biotransformation alters AhR agonist activity of parental MMIs, we collected culture media from human hepatocytes, which were incubated for 0 h and 24 h with MMIs and we applied them AZ-AhR reporter cells. Firstly, we proved that the application of culture medium from human hepatocytes ISOM does not influence the responsivity of AZ-AhR cells to AhR agonists as compared to the common DMEM medium (Figure 16D). Culture media from three cultures of human hepatocytes (LH75, HEP200565, HEP200570) incubated with 4-methylindole and 6-methylindole, displayed drastically reduced AhR-agonist activity in AZ-AhR cells as compared to media not incubated with human hepatocytes. At a lesser extent, AhR-agonist activity of 3-methylindole also decreased. In contrast, 7-methylindole gained strong AhR-agonist activity after the incubation with human hepatocytes (Figure 16A, B, C). These data reveal that human hepatic cells transform MMIs into metabolites with altered AhR-agonist activities.
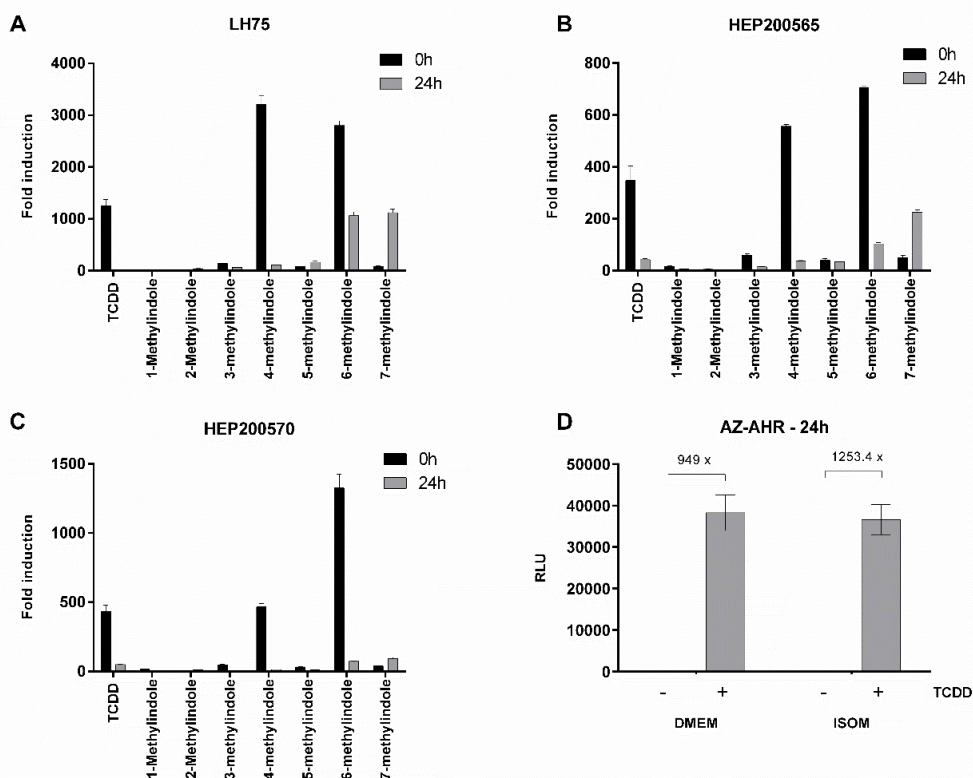
Figure 16: Effects of MMIs metabolites on transcriptional activation of AhR - reporter gene assay. Primary human hepatocytes (LH75, HEP200565, HEP2000570) were incubated for 0 h and 24 h with MMIs (200 µM). Thereafter, AZ-AhR cells were treated with culture medium from hepatocytes cultures for 24 h (**Panels A, B, C**). Next, the AZ-AhR cells were lysed and luciferase activity was measured. Data are expressed as a fold induction of luciferase activity over vehicle-treated cells and they are the mean ± standard deviation from triplicates. **Panel D**: Responsivity of AZ-AhR to TCDD (5 nM; 24 h) in DMEM and ISOM culture media.

5.1.5 Metabolism of MMIs in primary human hepatocytes

Culture media from three cultures of human hepatocytes previously incubated with MMIs were analysed by using LC/MS. The concentration of parental MMIs in the culture media decreased markedly after incubation with human hepatocytes, and no residual MMI was detected in the 1-MMI treated samples after 24 h. For samples treated with other MMIs, residual MMI concentrations ranged from 6.3 to 35.9 % of the initial 200 µM concentration, and differences were noticeable among the three cultures of hepatocytes employed (Figure 17A). The decreased MMI in the media may involve metabolic transformation, active uptake by human hepatocytes, degradation in the media, or non-specific binding. Based on the previously published metabolic studies (Lanza et Yost, 2001; Zhang et al., 2014), we also focused on identifying classes of putative MMI metabolites using selective molecular

mass search. In this study, we were able to identify two main types of metabolites in the cell culture media after 24 h of incubation. The first one represent the various derivatives of mono-oxidated MMIs, such as hydroxylated or monomethyl-oxindole derivatives. They were detected in the region of t_R = 7.0–7.5 min and represented by the molecular peak at 148.10 m/z in the mass spectrum (Figure 17D and Figure 17E) corresponding to the mono-protonated species.

In this region, we observed significant differences between the chromatograms obtained for specific MMIs. The most pronounced differences were observed between the chromatograms obtained for 2-MMI and 7-MMI (see the highlighted region in Figure 17B), whereas the peak at t_R = 7.16 min was only observed in the chromatogram for 7-MMI. The second major type of metabolites consisted of MMI derivatives conjugated to glutathione.They were observed at t_R ≈ 9.70 min, 11.15 min, and 11.60 min (Figure 17C) and represented by a molecular peak at 437.13 m/z in the mass spectra corresponding to the [GS–MMI+H]$^+$ species.
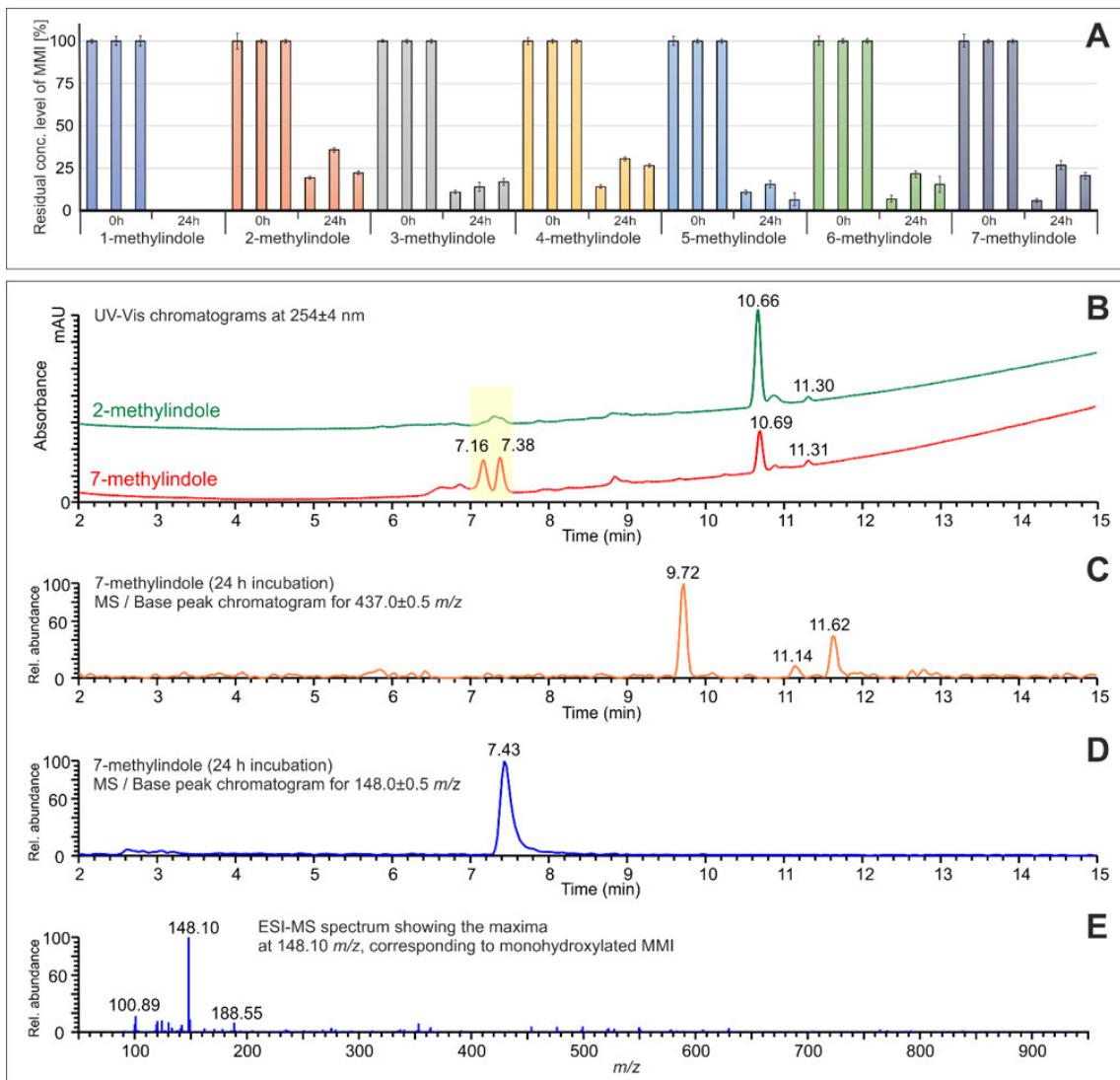
Figure 17: Liquid Chromatography/Mass Spectrometry analysis of mono-methylindoles metabolites. **Panel A**: The quantitative evaluation of residual MMI levels in culture media after 24 h incubation with human hepatocytes (cultures LH75, HEP200565, and HEP200570); **Panel B**: The comparison of UV/Vis chromatograms for the 2-MMI and 7-MMI samples showing the significant differences in the region of mono-oxidated metabolites (highlighted in yellow); **Panel C**: The base-peak chromatogram for the mass range of 437.0 ± 0.5 m/z, showing the GSH-conjugated metabolites of 7-MMI at t_R = 9.72 min, 11.14 min, and 11.62 min; **Panel D**: The base-peak chromatogram for the mass range of 148.0±0.5 m/z, showing the broad peak of mono-oxidated metabolites of 7-MMI at t_R = 7.43 min; **Panel E**: Mass spectrum, corresponding to the mono-oxidated species of 7-MMI with the maxima at 148.10 m/z, i.e. [MMI+H]+ species.

5.2 Effects of MMIs on the PXR signalling pathway

5.2.1 Effects of MMIs on the transcriptional activity of PXR

We examined the agonistic and antagonistic effects of individual MMIs on PXR in LS180 cells transiently transfected with human PXR expression vector and p3A4-luc reporter plasmid. The cells were incubated for 24 h with vehicle (DMSO; 0.1 % v/v) and MMIs in the absence (agonist mode) or presence (antagonist mode) of model PXR agonist rifampicin (RIF; 10 µM). All MMIs were tested at the concentration range of 10–200 µM. The PXR-dependent luciferase activity induced by RIF ranged from 13-fold to 24-fold, compared with that induced by vehicle-treated cells in three consecutive cell passages. MMIs activated PXR in a dose-dependent manner and the potency was comparable at all the test concentrations, with EC_{50} values ranging from 22.1 µM to 75.7 µM. The relative efficacy of MMIs at 200 µM, compared with that at 10 µM RIF ranged from 34 % to 111 %. The RIF-inducible PXR activity was slightly, dose-dependently decreased by the test MMI samples, but the IC_{50} value was reached only for 3-MMI (153.63 ± 39.17 µM). Taken together, the data revealed the partial agonist effect of MMI on PXR.

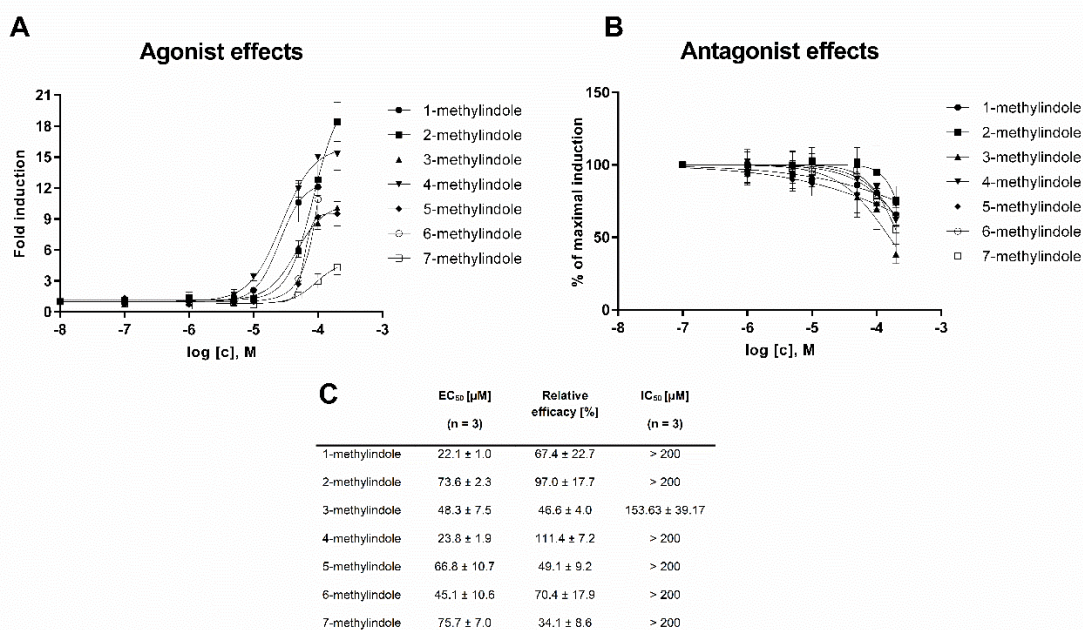| C	EC_{50} [µM] (n = 3)	Relative efficacy [%]	IC_{50} [µM] (n = 3)
1-methylindole	22.1 ± 1.0	67.4 ± 22.7	> 200
2-methylindole	73.6 ± 2.3	97.0 ± 17.7	> 200
3-methylindole	48.3 ± 7.5	46.6 ± 4.0	153.63 ± 39.17
4-methylindole	23.8 ± 1.9	111.4 ± 7.2	> 200
5-methylindole	66.8 ± 10.7	49.1 ± 9.2	> 200
6-methylindole	45.1 ± 10.6	70.4 ± 17.9	> 200
7-methylindole	75.7 ± 7.0	34.1 ± 8.6	> 200

Figure 18: Effects of MMIs on the transcriptional activity of PXR-reporter gene assay. Cell line LS180 was transiently co-transfected with p3A4-luc reporter plasmid and PXR expression vector and incubated for 24 h with vehicle (DMSO, 0.1 % v/v) and/or the tested compounds (10 nM–200 µM). Incubations were in the presence (antagonist mode) or in the absence (agonist mode) of PXR ligand rifampicin (RIF, 10 µM). Experiments were performed in three consecutive cell passages. Each treatment was carried out in four technical replicates (culture

wells). Representative experiments from one cell passage are shown in the plots. **Panel A**: Agonist mode. Data are expressed as a fold induction over a negative control. **Panel B**: Antagonist mode. Data are expressed as a percentage of maximal induction attained by 10 µM rifampicin. **Panel C**: The table shows EC_{50}, IC_{50}, and relative efficacy values. Relative efficacies (%) were obtained by dividing the maximal induction attained by tested compound by the induction attained by 10 µM rifampicin. Relative efficacy values are expressed as a mean ± standard deviation from three independent experiments.

5.2.2 Effects of MMIs on CYP3A4 and MDR1 expression in human hepatic and intestinal cells

We evaluated the effects of MMIs on the expression of CYP3A4 and MDR1, which are typical PXR-dependent genes, in human hepatic and intestinal cells. Rifampicin, a model ligand and activator of PXR, induced CYP3A4 and MDR1 mRNAs by approximately 6-folds and 8-folds, respectively, in human colon adenocarcinoma cell line LS180 transiently transfected with PXR expression vector. 1-methylindole and 2-methylindole significantly induced CYP3A4 (cca 2-folds) and MDR1 (cca-5 folds) mRNAs. In addition, significant induction of MDR1 mRNA, but not CYP3A4 mRNA, was achieved by 4-methylindole (4-fold) and 5-methylindole (2-fold) (Figure 19A, Figure 19B). In primary human hepatocytes cultures from three different liver donors, rifampicin significantly induced CYP3A4 and MDR1 mRNAs. The effects of MMIs on PXR-regulated genes in human hepatocytes displayed inter-individual pattern dependent on liver tissue donor. The effects were overall negative; however, 1-MMI, 2-MMI, and 4-MMI weakly induced CYP3A4 mRNA expression (borderline induction > 5 % of that by RIF), but only in one hepatocytes culture LH75 (Figure 19C, Figure 19D). Similarly, the level of CYP3A4 protein was only increased by 2-MMI in hepatocytes culture LH75 (Figure 19E). Notably, unlike in cell lines, human hepatocytes are fully metabolically active; hence, gene induction comprises the effects of both maternal compounds and their metabolites. Furthermore, we used wild type (control 5F clone) and PXR-knock out (PXR-KO) variant of human hepatic progenitor HepaRG cells to confirm PXR role in MMI-induced CYP3A4/MDR1 induction. Rifampicin induced CYP3A4 mRNA in 5F-HepaRG cells (8-folds), but not in PXR-KO-HepaRG cells. Significant induction of CYP3A4 mRNA was observed for 1-MMI (5-folds) and 2-MMI (4-folds) only in wild type 5F-HepaRG cells (Figure 19F), which was consistent with CYP3A4 induction pattern

observed in LS180 cells (Figure 19A). Additionally, these data confirm that CYP3A4 induction by 1-MMI and 2-MMI is PXR-dependent.
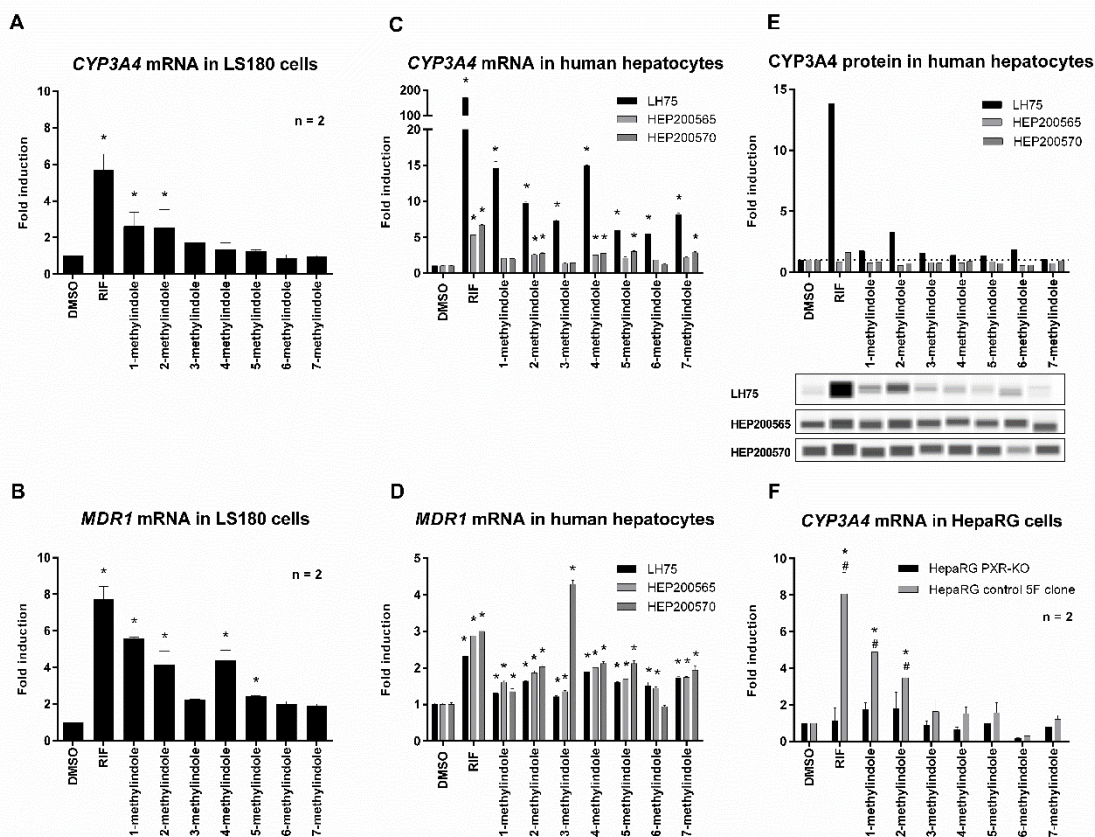

Figure 19: Effects of mono-methylated indoles on the expression of CYP3A4 and MDR1 genes in human hepatic and intestinal cells. Cultured cells were incubated for 24 h with the vehicle (DMSO; 0.1 % v/v), rifampicin (RIF; 10 µM), and/or MMIs (200 µM). The levels of CYP3A4 and MDR1 mRNA were determined by RT-PCR, and the data were normalised per GAPDH mRNA level. Each measurement was done in triplicates (technical replicates). * = value significantly different from negative control ($p < 0.05$). # = value significantly different from control 5F clone ($p < 0.05$). Graphs show mean ± standard deviation and are expressed as a fold induction over negative control. The levels of CYP3A4 protein were normalised per β-actin levels (quantitation by SallySue software), and the data are expressed as a fold induction over negative control. **Panel A,B**: Incubations were performed in two consecutive passages of LS180 cells transiently transfected with PXR vector. **Panel C, D, E**: Primary human hepatocytes from three different donors, (LH75, HEP200565, and HEP200570). **Panel F**: Incubations were performed in two consecutive passages of HepaRG (control clone and PXR-KO) cells.

5.2.3 PXR binding in CYP3A4 promoter

The capability of MMIs to enhance the binding of PXR to the promoter of its target gene was assessed by ChIP. The incubation of intestinal LS174T cells, transiently transfected with PXR expression vector, with 1-MMI (200 µM, selected as lead PXR-activate MMI) resulted in the slight enrichment of the CYP3A4 promoter with PXR. These data reveal that the induction of CYP3A4 by MMIs involves increased PXR binding at the CYP3A4 promoter.
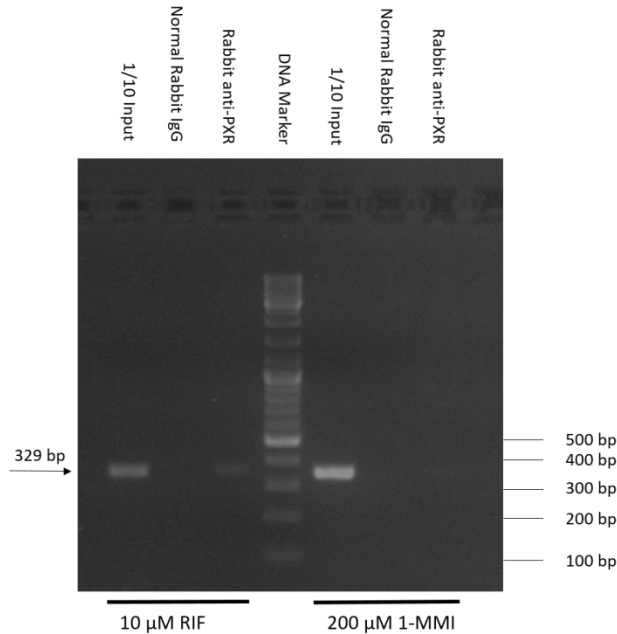

Figure 20: Effect of 1-MMI on the binding of PXR to DNA. LS174T cells transiently transfected with PXR expression vector were incubated with vehicle (DMSO; 0.1 % v/v), rifampicin (RIF; 10 µM), and 1-MMI (200 µM) for 24 h. Chromatin Immunoprecipitation (ChIP) was performed as described in the 'Methods' section. The purified chromatin (anti-PXR) was subjected to PCR reaction using CYP3A4 promoter primers and PXR products resolved on 1.5 % agarose gel.

5.2.4 Binding of MMIs to the ligand-binding domain of PXR

Competitive ligand binding assay, based on the principle of time-resolved fluorescence resonance energy (TR-FRET), was used to assess the binding of MMIs to the ligand-binding domain of the human PXR. All the tested MMIs, with the exception of 7-MMI, dose-dependently displaced fluorescent PXR ligand Fluormone^{TM} from PXR-LBD. Typical, class-I (Shukla et al., 2009) full-length sigmoid curve, was recorded for 1-MMI ($IC_{50} = 36.8 \pm 9.1$ µM) and 4-MMI ($IC_{50} = 81.6 \pm 9.1$ µM). These data imply that these compounds are weak ligands of PXR.
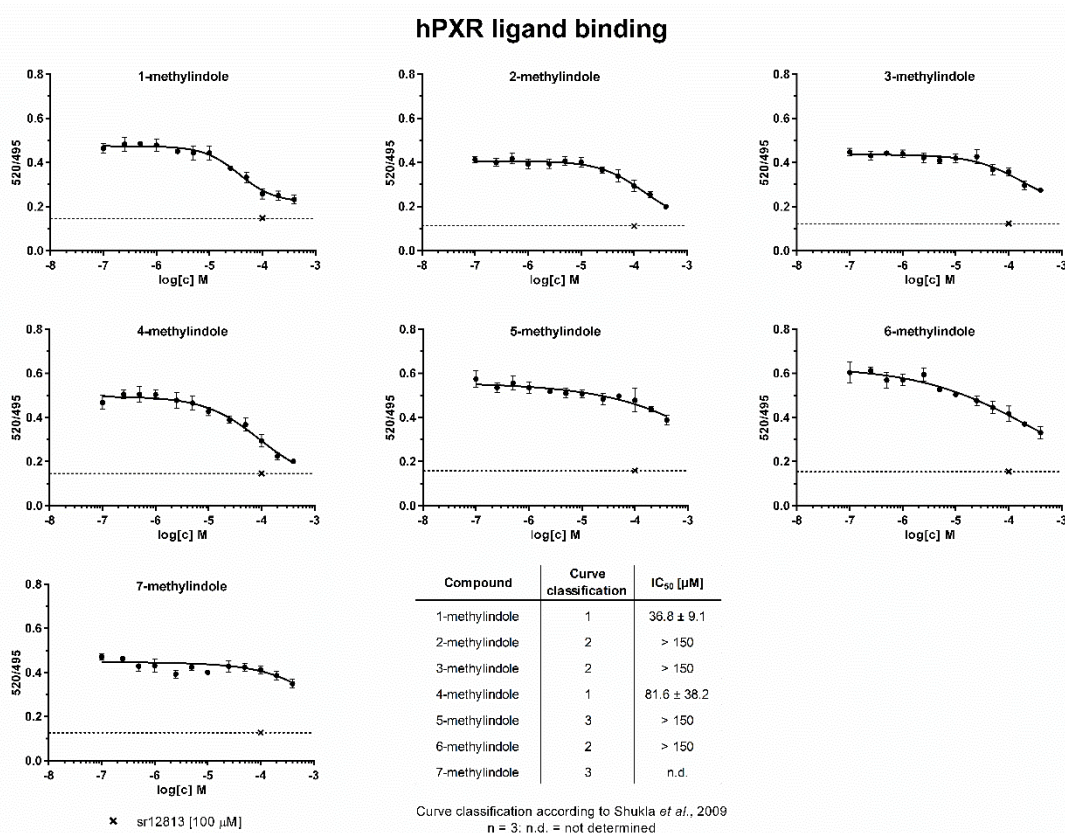
Figure 21: Binding of MMIs at PXR-TR FRET assay. TR-FRET ratios 520/495 nm were plotted against the concentrations of the tested compounds. Half-maximal inhibitory concentration (IC_{50}) values were obtained from interpolated standard curves (sigmoidal, variable, and slopes), and are shown in table together with curve classification. Experiments were performed three times (n = 3) and the representative plots are shown. The presented data are mean ± SE from quadruplicates (technical replicates). Positive control SR12813 (100 µM) is depicted as a single point at the dashed line inserted in each plot.

5.3 Effects of microbial intestinal catabolites of tryptophan (MICTs) on the AhR signalling pathway

5.3.1 Levels of tryptophan in culture medium

Because our focus in this part of the work was to assess the biological activity of tryptophan metabolites and common cell culture media and fetal bovine serum contain tryptophan, which might potentially affect AhR-mediated background activity, we first verified the appropriateness of tryptophan-containing media for such a study. Using HPLC, we determined the concentration of tryptophan in the cultures of AZ-AhR, LS174T, and HaCaT cells over a 24 h period. The initial concentration of tryptophan in the culture medium containing 10 % serum was approximately 75 µM, and it slowly and linearly decreased, down to approximately 60 µM after 24 h incubation, regardless of the cell-type b (Figure 22A). Therefore, tryptophan concentration in cell cultures can be considered to be stable over the time of incubation. Tryptophan did not activate AhR up to 100 µM concentration in AZ-AHR cells cultures when using tryptophan-free/serum-free medium, whereas both TCDD and IND induced luciferase activity by 10000-folds and 500-folds, respectively (Figure 22B). Finally, by comparing TCDD- and IND-induced AhR activation in AZ-AhR cells cultured in conventional, tryptophan-free, serum-free, and tryptophan-free/serum-free media, we concluded that the presence of tryptophan in the culture medium would not interfere with MICT assay under normal cell culture conditions (Figure 22C).
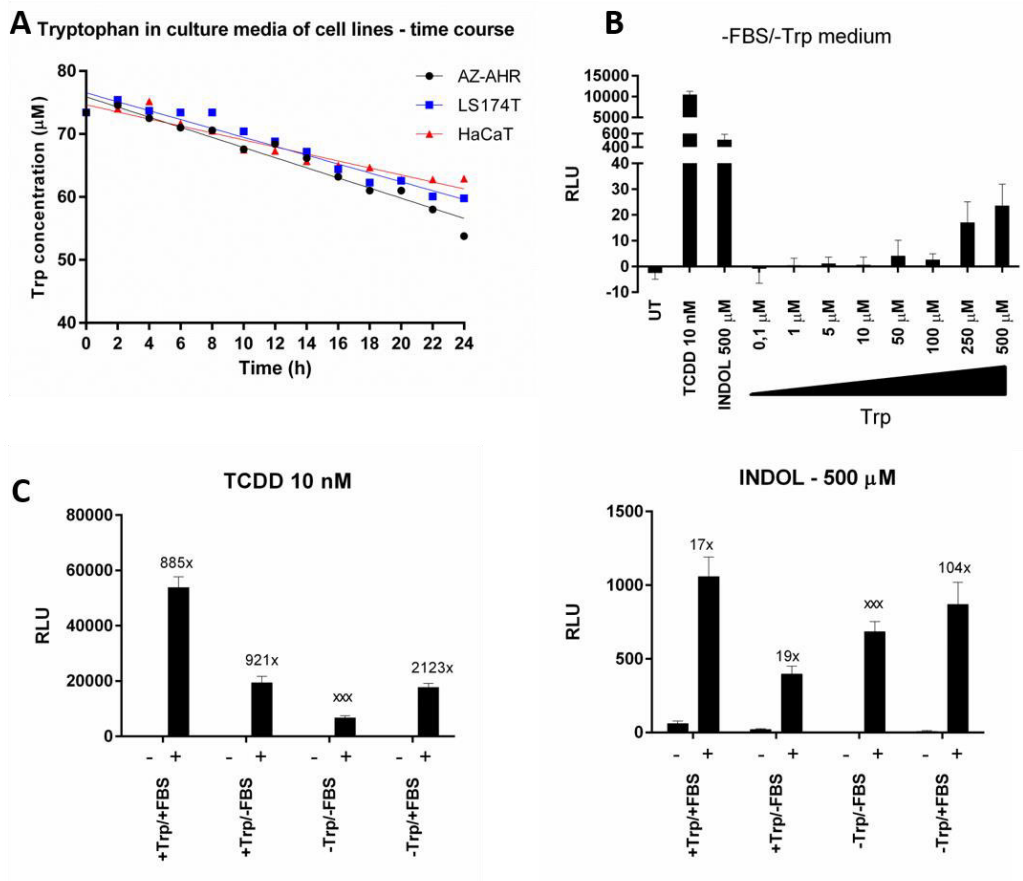
Figure 22: Effects of tryptophan (TrP) on AhR activity in culture medium. Panel A: Time-course of Trp levels in culture media from hepatic (AZ-AhR), instestinal (LS174T), and skin (HaCaT) cells as determined by HPLC. **Panel B**: Induction of AhR-dependent luciferase activity in AZ-AHR cells incubated for 24 h with TCDD, Indole, and Trp in Trp/serum-free culture medium. **Panel C**: Induction of AhR-dependent luciferase activity in AZ-AHR cells incubated for 24 h with TCDD and Indole in standard (+Trp/+FBS), serum-free (+Trp/-FBS), Trp-free (-Trp/+FBS), and Trp-free/serum-free (-Trp/-FBS) culture media.

5.3.2 Effects of MICTs on the transcriptional activity of AhR

In the first series of experiments, we examined the effects of MICTs on the transcriptional activity of human AhR by conducting a reporter gene assay. For this purpose, stably transfected AZ-AhR cells were incubated for 24 h with vehicle (DMSO; 0.1 % v/v) and individual MICTs in the absence (agonist mode) or presence (antagonist mode) of typical AhR full agonists (TCDD, BaP and FICZ). All compounds were tested at concentrations of up to 200 µM, except for IAC (the maximum concentration was 100 µM due to solubility limitations) and IND (10 mM, given its known high intestinal concentration). The model AhR agonists were applied at fixed concentrations corresponding to their EC_{80} (TCDD = 13.5 nM; BaP = 15.8 µM; and FICZ = 22.6 µM). All the MICTs activated the AhR in a dose-dependent

manner; however, the plateau was not reached, and their relative efficacy values differed substantially. IND, IPY, and IAD (fold inductions of 200-600-fold) displayed a high efficacy agonism. The agonists with average efficacy included 3-MMI, TA, IET, and IAC (fold inductions 40–100-fold). In contrast, the agonists that were almost inactive were IPA, IAA, ILA, and IA ($\approx$ 8-fold induction). The relative potency of MICT was rather low, with their EC_{50} values ranging from 42 µM to 103 µM. A notable exception was IND, with EC_{50} of approximately 1.5 mM (Figure 23). IA, IND, and TA displayed dose-dependent antagonistic effects against all the agonists. In contrast, IET, IAC, ILA, IAA, and IPA exhibited no antagonistic effects against any of the full agonists. We observed a ligand-selective antagonism for 3-MMI, which dose-dependently inhibited AhR activation by TCDD and BaP, but not by FICZ. Interestingly, IAD and IPY had dual effects on ligand-activated AhR. These two compounds antagonised TCDD, but potentiated the agonistic effects of BaP and FICZ (Figure 24).
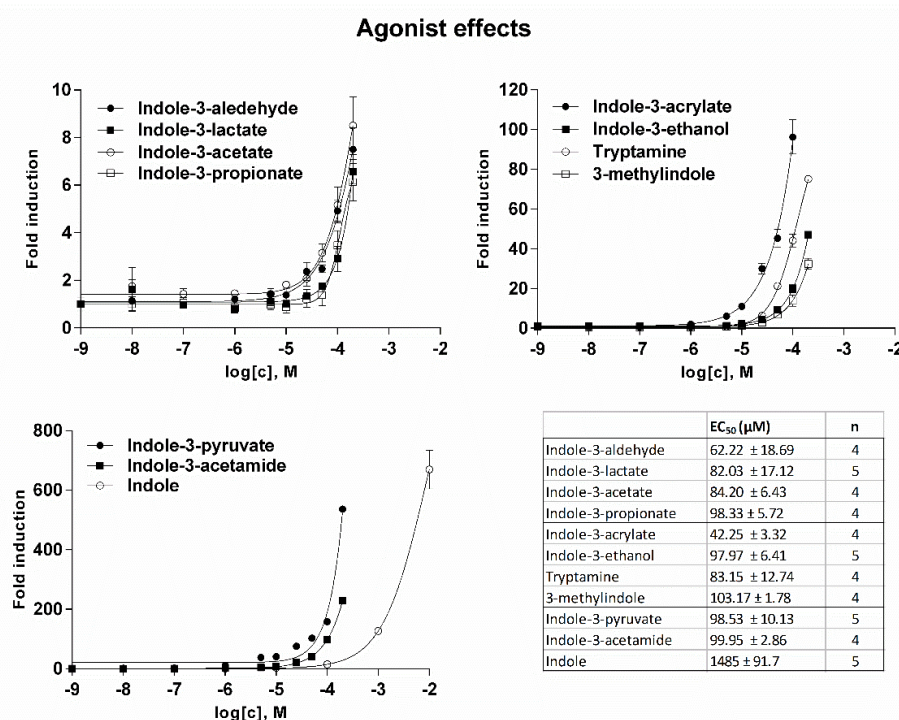

Agonist effects

	EC_{50} (µM)	n
Indole-3-aldehyde	62.22 ± 18.69	4
Indole-3-lactate	82.03 ± 17.12	5
Indole-3-acetate	84.20 ± 6.43	4
Indole-3-propionate	98.33 ± 5.72	4
Indole-3-acrylate	42.25 ± 3.32	4
Indole-3-ethanol	97.97 ± 6.41	5
Tryptamine	83.15 ± 12.74	4
3-methylindole	103.17 ± 1.78	4
Indole-3-pyruvate	98.53 ± 10.13	5
Indole-3-acetamide	99.95 ± 2.86	4
Indole	1485 ± 91.7	5

Figure 23: Effects of MICTs on the transcriptional activity of AhR (agonist mode)-reporter gene assay. AZ-AhR cells were incubated for 24 h with vehicle (DMSO; 0.1 % v/v) and increasing concentrations of MICTs. Following treatment, the cells were lysed and luciferase activity was measured. Experiments were performed at least in four consecutive cell passages. Incubations were performed in quadruplicates (technical replicates). Bar graphs show data from a representative experiment and are expressed as a fold induction of luciferase activity over control cells. The inserted table shows the number of cell passages and the EC_{50} values of the tested compounds.
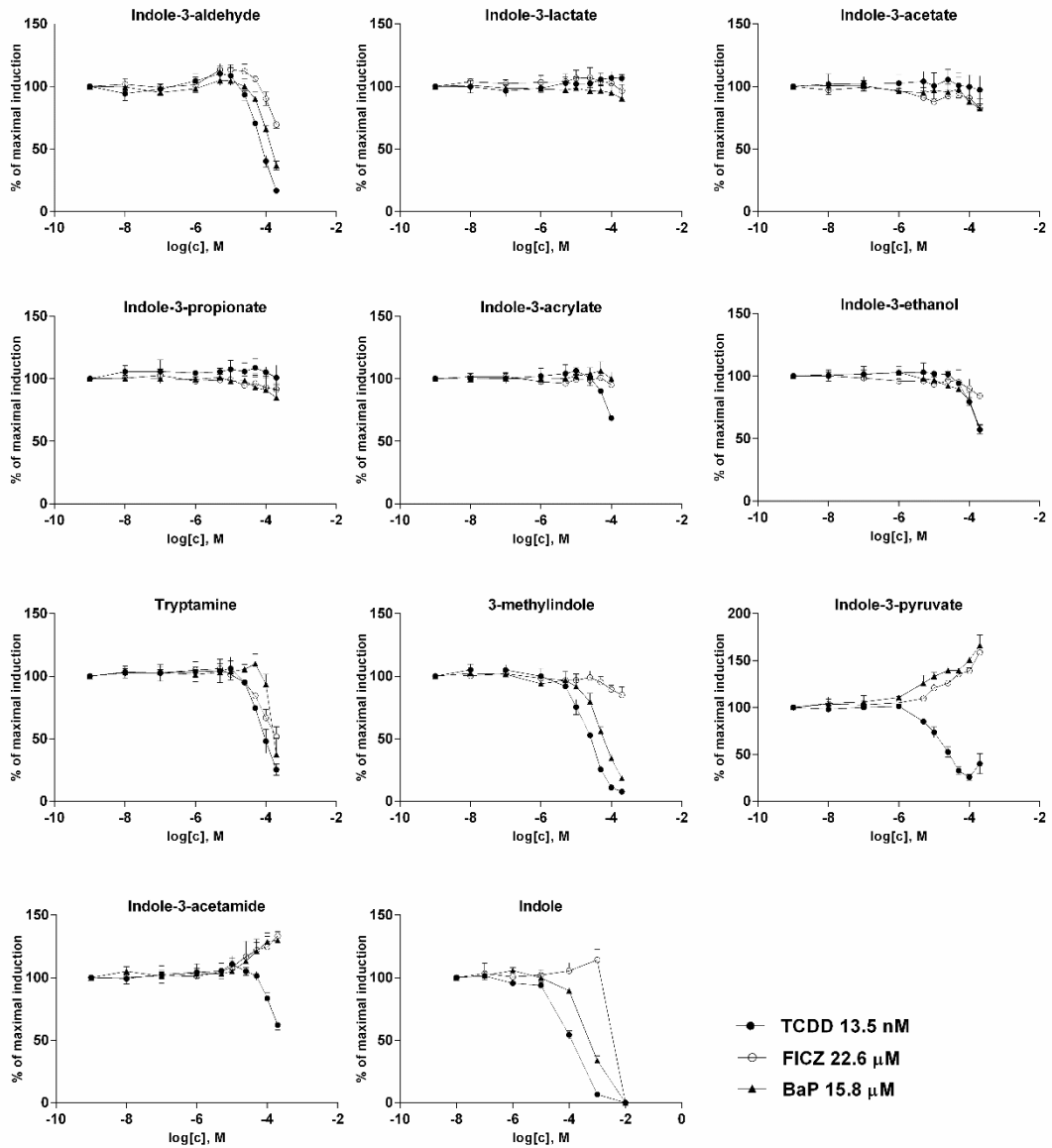
Antagonist effects

Figure 24: Effects of MICTs on the transcriptional activity of AhR (antagonist mode) - reporter gene assay. AZ-AhR cells were incubated for 24 h with vehicle (DMSO; 0.1 % v/v) and increasing concentrations of MICTs. Following treatment, the cells were lysed, and luciferase activity was measured. Experiments were performed at least in four consecutive cell passages. Incubations were performed in quadruplicates (technical replicates). Bar graphs show data from a representative experiment and are expressed as a fold induction of luciferase activity over control cells. The inserted table shows the number of cell passages and the EC_{50} values of the tested compounds.

5.3.3 Binding of MICTs to the ligand-binding domain of AhR

The ability of MICT to bind AhR was investigated by competitive radio-ligand binding assay using cytosols from Hepa1c1c7 mouse hepatoma cells. FICZ, a high-affinity AhR ligand, competitively inhibited $[^3H]$-TCDD from binding to AhR ($IC_{50} \approx 2$ nM). We identified low-affinity AhR ligands among the tested MICTs, including 3-MMI ($IC_{50} = 72$ μM), IPY ($IC_{50} = 55$ μM), IAD ($IC_{50} = 44$ μM), and very low-affinity ligands comprising IAC ($IC_{50} = 710$ μM), IET ($IC_{50} = 1540$ μM), and IND ($IC_{50} = 1130$ μM) (Figure 25). Figure 26 shows a comprehensive chart and "heat map," summarizing AhR binding affinities of individual MICT, as well as their respective agonistic and antagonistic effects towards AhR.
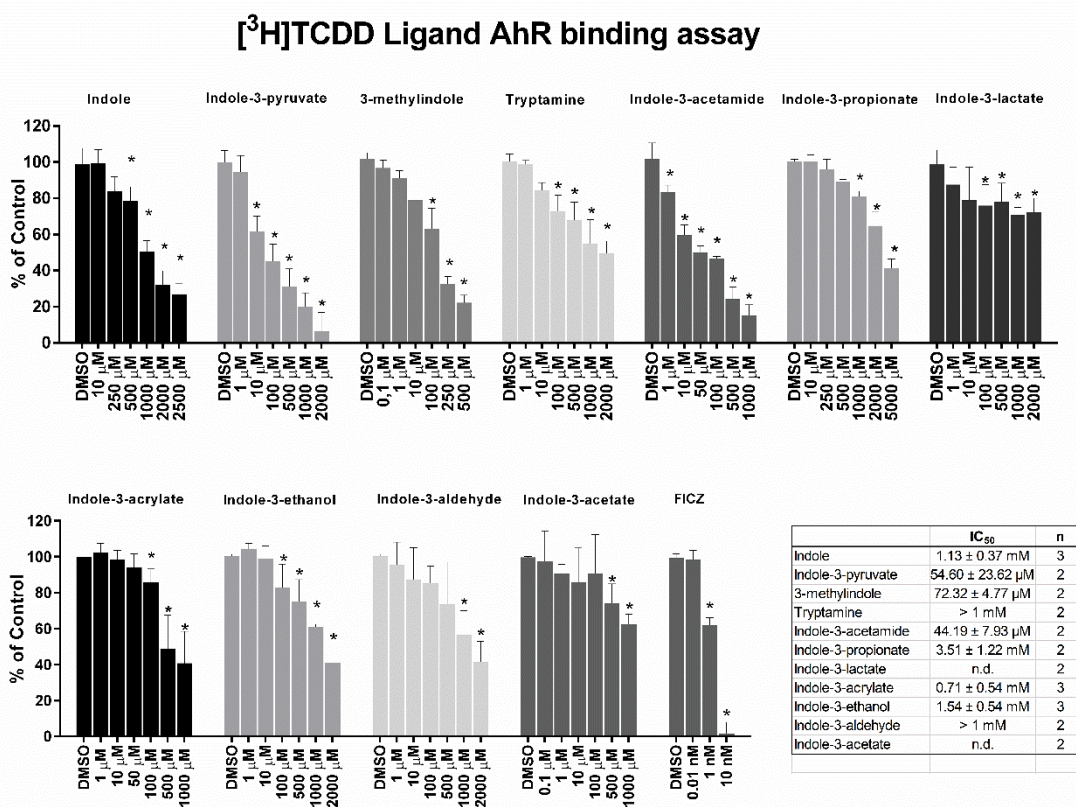
Figure 25: Binding of MICTs at AhR – competitive radio ligand binding assay. Cytosols from Hepa1c1c7 cells were incubated with vehicle (negative control; 0.1 % v/v), FICZ (positive control; 0.01 nM–10 nM), TCDF (non-specific binding; 200 nM), and increasing doses of MICT in the presence of 2 nM [3H]-TCDD. The specific binding of [3H]-TCDD was determined as a difference between total and non-specific (200 nM; TCDF) reactions (value for vehicle DMSO; 0.1 % v/v = corresponds to *specific binding of [3H]-TCDD = 100 %*). At least two independent experiments were performed and the incubations were done in triplicates in each experiment (technical replicates). The error bars represent the mean ± standard deviation. * = significantly different from the vehicle ($p < 0.05$). The inserted table shows the number of repeats and the IC_{50} values of each MICT.
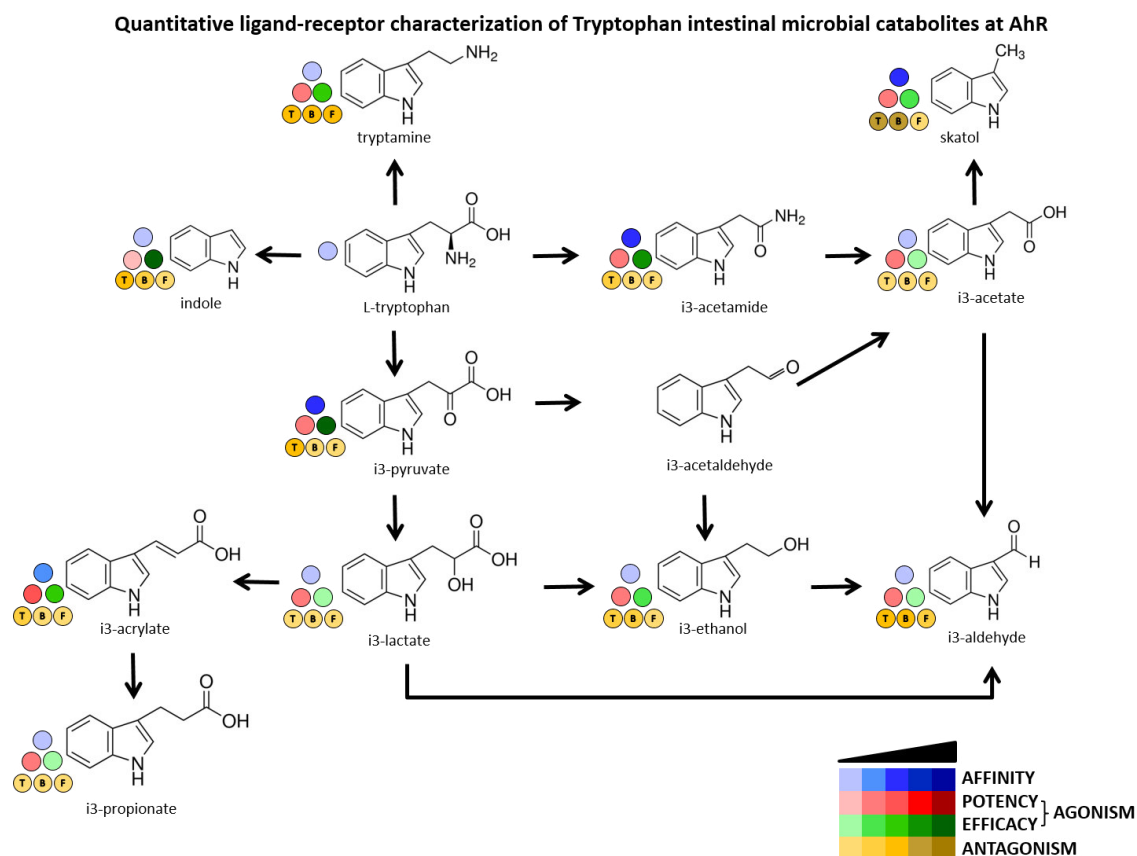
Figure 26: Quantitative characterisation of interactions between MICT and AhR.
The scheme depicts intestinal microbial catabolism of tryptophan, and the source data come from Figures 23, 24, and 25. **Blue scale** refers to the affinity of MICT (ligand binding). **Red & Green scales** quantify relative agonist effects of MICT; Red ≈ potency (EC_{50}), Green ≈ efficacy (EMAX). **Brown scale** quantify relative antagonist effects (IC_{50}) of MICT, against three different agonists used at EC_{80} concentration and designated as "T" = TCDD, "B" = BaP, "F" = FICZ.

5.3.4 Effects of MICTs on *CYP1A1* mRNA expression in human hepatic and intestinal cells

MICTs behaved as ligands and full/partial agonists of AhR; hence, we studied their effects on the induction of CYP1A1 expression, a prototypical AhR target gene. We incubated intestinal and hepatic cells with MICT for 24 h and measured CYP1A1 mRNA levels by using qRT-PCR. IND, IPY, 3-MMI, TA, IAC, and IAD caused strong induction of CYP1A1 mRNA in intestinal LS180 cells (Figure 27A), which was consistent with the reporter gene assay data (except for IET). We also observed antagonistic effects in LS180 cells co-incubated with TCDD, particularly by IND, 3-MMI, IPY, and IA, and to a lesser extent by IAA, IPA, ILA, and IAC (Figure 27B). This profile was not consistent with the results of the reporter gene assay, which could be attributed to cell-type differences. In colon HT-29 cells, IPY, IAC, and IAD caused strong

induction of CYP1A1 mRNA, while IND, 3-MMI, and TA had a weaker effect. The qualitative profiles of CYP1A1 mRNA induction in both intestinal cell models were identical. Moreover, in the AhR knock-out HT-29 variant, the induction of CYP1A1 mRNA by TCDD and MICTs was nullified, which corroborated the role of AhR in MICT-dependent CYP1A1 induction (Figure 27C). Finally, in primary cultures of human hepatocytes derived from three different donors, IND, 3-MMI, IPY, IAD, IAC, but not TA, induced CYP1A1 mRNA (Figure 27D). The lack of induction by TA could be, in part, related to its extensive hepatic metabolism.
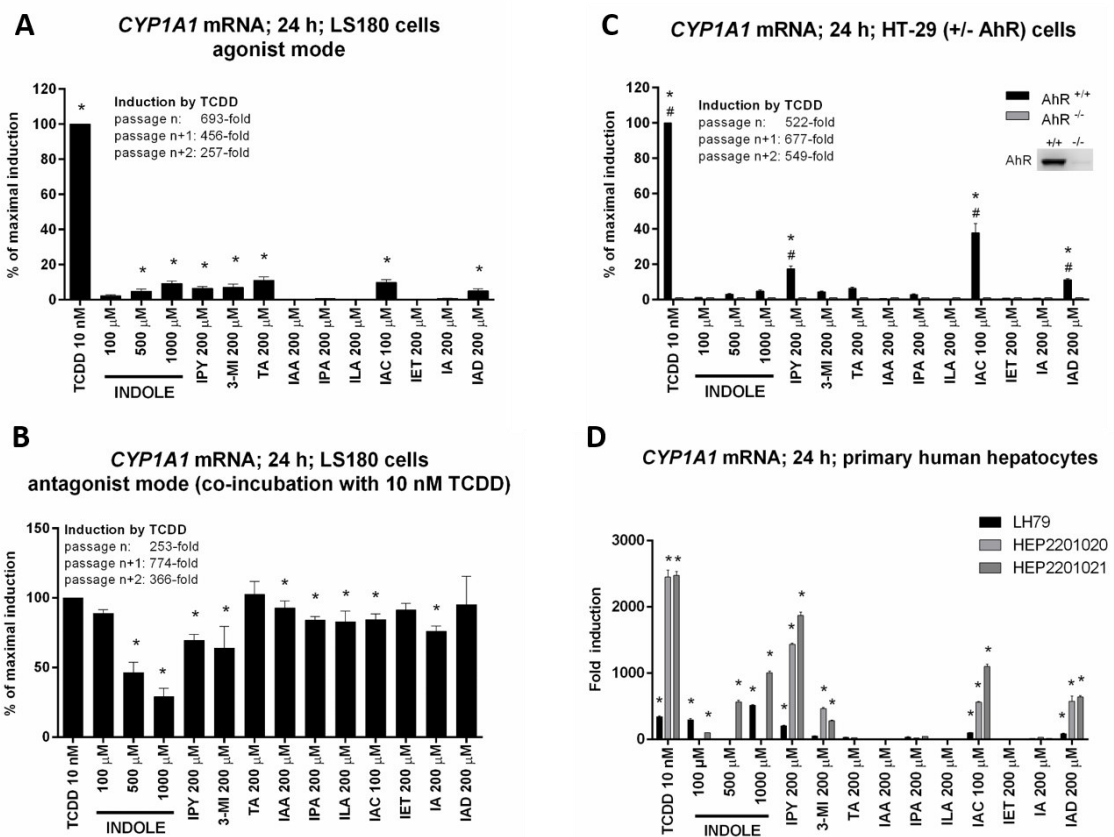
Figure 27: Effects of MICT on the expression of CYP1A1 mRNA in human hepatic and intestinal cells. Cultured cells were incubated with the vehicle (DMSO; 0.1 % v/v) and MICTs in the presence or absence of TCDD (10 nM) for 24 h. RT-PCR was used to determine the mRNA level of CYP1A1, and the data were normalised per GAPDH mRNA level. Each measurement was done in triplicates (technical replicates). * = value significantly different from negative control ($p < 0.05$). **Panel A, B**: Experiments in three consecutive passages of human colon adenocarcinoma cell line LS180 in the absence (A) and the presence (B) of 10 nM TCDD. Bar graphs show the percentage of maximal induction attained by TCDD and are expressed as mean ± standard deviation. **Panel C**: Experiments in three consecutive passages of wild-type (AhR+/+) and AhR-knockout (AhR-/-) HT-29 cells. The bar graph shows a percentage of maximal induction achieved by TCDD. Data are expressed as mean ± standard deviation. #value significantly different from HT-29 wild-type (AhR+/+) ($p < 0.05$). Insert western blot image confirms AhR knock-out. **Panel D**: Primary human hepatocytes from three different donors (LH79, HEP2201020, and HEP2201021). The bar graph shows a fold induction of CYP1A1 mRNA over vehicle-incubated cells.

5.3.5 Effects of lead MICTs on molecular functions of AhR

IND, 3-MMI, IPY, IAD, IAC, and TA were selected as lead AhR-active MICTs and tested for their ability to trigger the molecular functions of AhR in LS180 cells. Following ligand binding, AhR translocated to the nucleus, where it formed a heterodimer with ARNT, which then bound DRE motifs at the promoters of its target genes. According to immune-fluorescence detection (Figure 28), all tested MICTs triggered a large nuclear translocation of AhR that was similar in intensity to that elicited by TCDD. Consequently, protein co-immune-precipitation assay confirmed that IND, 3-MMI, IPY, IAD, IAD, and TA induced the formation of AhR-ARNT heterodimer (Figure 29). Finally, all lead MICTs, as well as TCDD, enhanced AhR binding to the promoter of CYP1A1 gene, as indicated by the results of the ChIP assay (Figure 30).
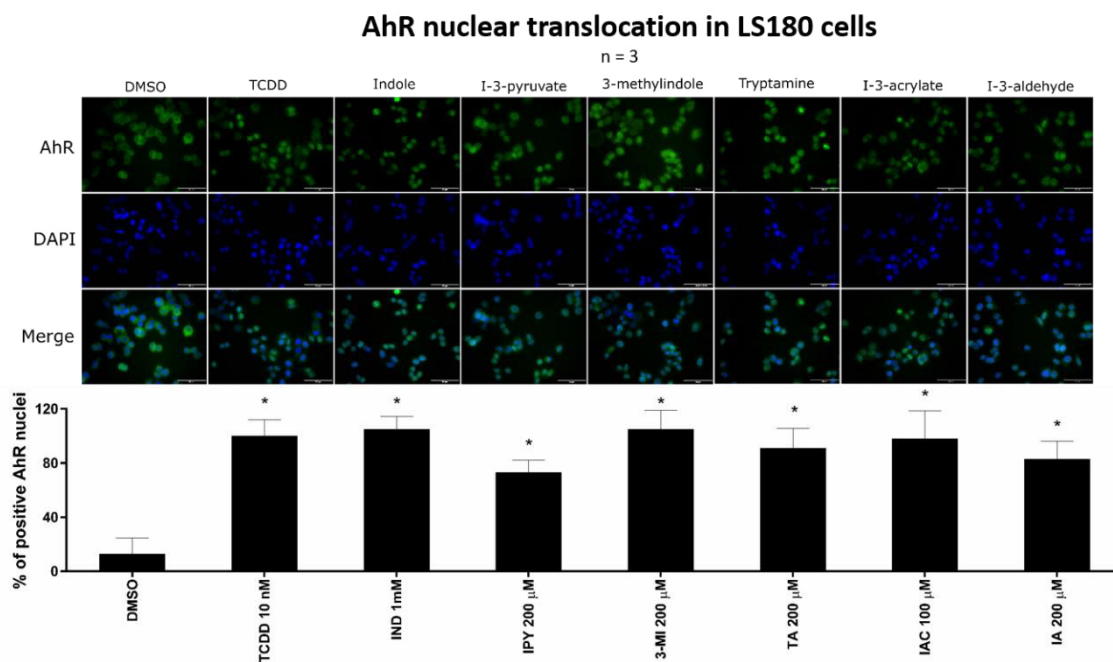

Figure 28: Effect of MICTs on the nuclear translocation of AhR. Intestinal LS180 cells were incubated for 90 min with vehicle (DMSO; 0.1 % v/v), TCDD (10 nM), and MICTs. Experiments were performed in three consecutive cell passages with all tested compounds in duplication. Fluorescence images depict sub-cellular localization of AhR visualised with Alexa Fluor 488 labelled primary antibody (upper panels) and nuclear staining by DAPI (lower panels). Representative micrographs are shown. The bar graph shows the percentage of AhR-positive nuclei (mean ± standard deviation; n =3), relative to TCDD-treated cells (also ref. below in Table 3). * = value significantly different from negative control (p < 0.05).

Table 3: AhR nuclear translocation–quantification of immunofluorescence. AhR translocation was evaluated visually depending on the distinct signal intensity of AhR antibody in the nucleus and cytosol. To determine the percentage translocation, approximately one hundred cells from at least four randomly selected fields of view in each replicate were used.

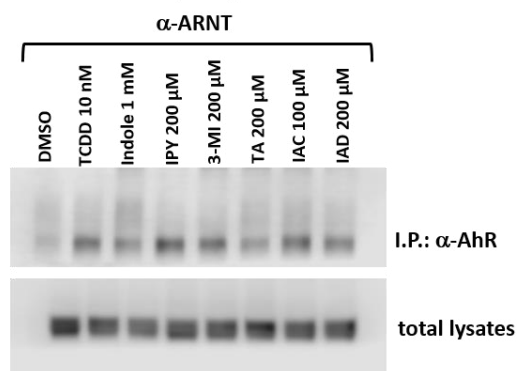| incubation		# fields	∑ cells	# positive AhR nuclei	% positive AhR nuclei	% relative AhR nuclei	Ø % AhR positive nuclei
Vehicle (DMSO)	exp 1	4	316	17	5	9	
	exp 2	11	545	19	3	4	13 ± 11.6
	exp 3	11	553	90	16	26	
10 nM TCDD	exp 1	7	318	171	54	100	
	exp 2	14	555	430	77	100	100 ± 11.8
	exp 3	11	538	330	61	100	
1 mM Indol	exp 1	6	335	203	61	113	
	exp 2	9	338	248	73	95	105 ± 9.2
	exp 3	12	500	323	65	107	
200 µM 3MI	exp 1	6	407	264	65	120	
	exp 2	9	329	236	72	94	105 ± 13.8
	exp 3	13	603	375	62	102	
200 µM TA	exp 1	6	421	187	44	81	
	exp 2	11	319	208	65	84	91 ± 14.6
	exp 3	12	527	346	66	108	
200 µM IPY	exp 1	7	326	136	42	78	
	exp 2	9	295	176	60	78	73 ± 9.0
	exp 3	11	514	194	38	62	
100 µM IAC	exp 1	6	393	199	51	94	
	exp 2	9	356	218	61	79	98 ± 20.4
	exp 3	11	499	366	73	120	
200 µM IAD	exp 1	7	377	175	46	85	
	exp 2	9	344	252	73	95	83 ± 13.1
	exp 3	11	538	228	42	69	

Figure 29: Effects of MICTs on the formation of the AhR-ARNT heterodimer. Intestinal LS180 cells were incubated with TCDD, MICT, and vehicle (DMSO; 0.1 % v/v) for 90 min. Protein co-immunoprecipitation of ARNT was carried out as described in the 'Methods' section. Representative immunoblots of immuno-precipitated protein eluates and total cell lysates are shown. Experiments were performed in two consecutive cell passages.
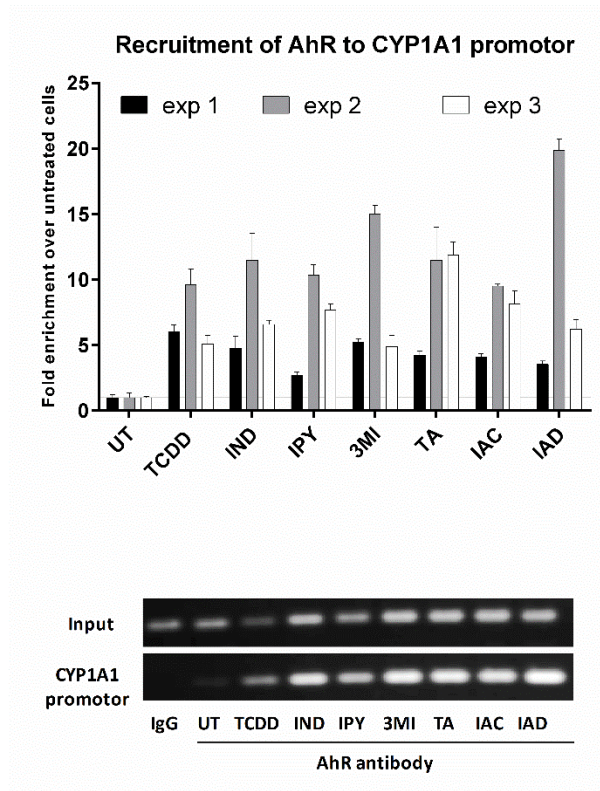
Figure 30: Effect of MICTs on AhR binding to DNA. LS180 cells were incubated with vehicle, TCDD, and test compounds as described in the 'Methods" section, followed by Chromatin Immunoprecipitation (ChIP) analysis. Bar graphs show the enrichment of CYP1A1 promoter by AhR, compared with that observed in vehicle treated cells. The entire protocol was carried out in three consecutive cell passages. The data are expressed as fold enrichment to vehicle-treated cells and show mean ± standard deviation from duplicates (technical replicates). DNA fragments amplified by PCR were resolved on 2 % agarose gel (representative record from "exp 2" is shown).

5.4 Effects of MICTs on the PXR signalling pathway

5.4.1 Effects of MICTs on the transcriptional activity of PXR

The ability of MICTs to activate human PXR was examined in human intestinal LS180 cells, which were transiently transfected with human PXR expression vector and p3A4-luc reporter plasmid. The tested MICTs, vehicle (DMSO; 0.1 % v/v), rifampicin (RIF; 10 µM), and a model PXR activator were incubated with cells for 24 h. Cytotoxicity assay for MICTs was also performed, and none of the tested compounds was cytotoxic to LS180 cells (data not shown). IAD dose-dependently activated PXR and increased PXR-dependent luciferase activity approximately by 15-folds at a concentration of 200 µM. However, the EC_{50} value was not calculated because the plateau was not reached. IND activated PXR only at the highest concentration (1 mM). The relative efficacy of both IAD and IND in the highest applied concentrations was comparable with that by 10 µM RIF. IET and TA were weak, but significant activators of PXR. The other MICTs did not activate PXR.

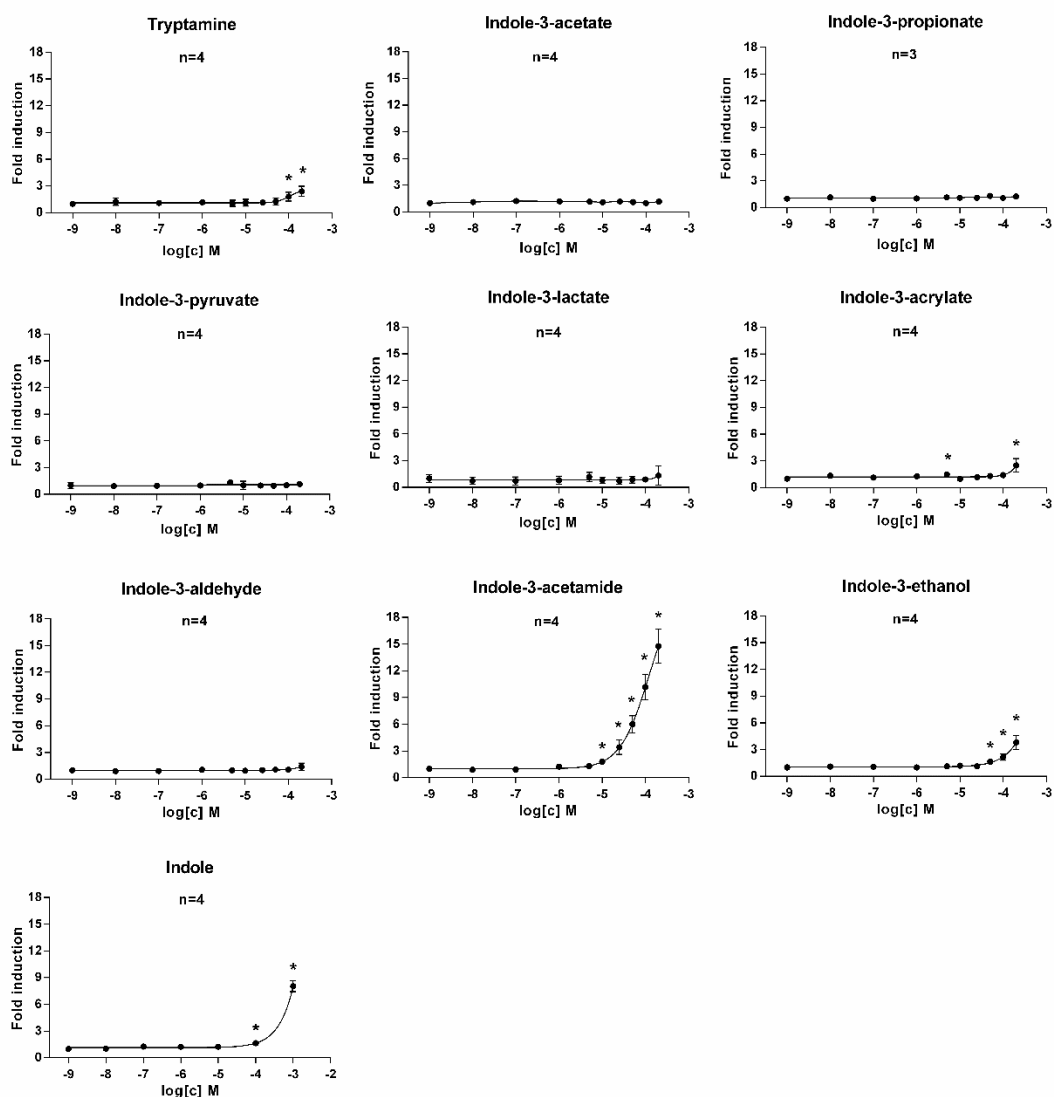# hPXR transcriptional activity

Figure 31: Effects of MICT on the transcriptional activity of PXR (agonist mode)–reporter gene assay. LS180 cells transiently co-transfected with p3A4-luc reporter plasmid and PXR expression vector were incubated for 24 h with increasing concentrations of MICTs. After treatment, the cells were lysed and luciferase activity was measured. The analyses were performed in quadruplicates (technical replicates). The data represent the means ± standard deviation from at least three consecutive cell passages (biological replicates) and are expressed as a fold induction of luciferase activity over the luciferase activity of the cells treated with the lowest concentration (1 nM). * = value significantly different from the cells exposed to the lowest concentration of examined compound ($p < 0.05$). Note: These data have already been presented by Ms. Natália Sirotová in her bachelor thesis entitled "Effects of gut microbiota metabolites on transcriptional activity of pregnane X receptor (PXR)" Ms. Sirotová performed the reporter gene analysis and presented this data in the publication. For completeness of the study results, these data are also presented in this thesis.

5.4.2 Effects of MICTs on *CYP3A4* and *MDR1* mRNA expression in human hepatic and intestinal cells

We examined if MICTs could induce CYP3A4 and MDR1, which are typical PXR-regulated genes, in human hepatic and intestinal cells. We incubated primary human hepatocytes and human intestinal LS174T cells with the MICTs for 24 h. The mRNA levels of PXR-target genes were measured by using RT-PCR. Almost none of the MICTs induced CYP3A4 and MDR1 mRNAs in LS174T, except for IND and IAD. In comparison with 10 µM RIF, the relative efficacies of IND/IAD were ≈ 10 % and ≈ 40 % for CYP3A4 and MDR1, respectively (Figure 32A). IND and IAD weakly induced CYP3A4 mRNA (≈ 8 % relative efficacy) only in LH79 primary human hepatocytes culture, but not in HEP2201020 and HEP2201021 cultures (Figure 32B). Because MDR1 gene is poorly inducible in hepatic cells, its expression level in primary human hepatocytes was not assessed. Additionally, we performed comparative analysis of the mRNA transcription patters of CYP3A4 and MDR1 in wild-type LS174T, PXR-knockout LS174T, and LS180 cells transiently transfected with human PXR expression plasmid (Figure 32C). RIF, IND, and IAD induced both CYP3A4 and MDR1 mRNAs in wild-type LS174T cells, which was consistent with the data from compound screening. These effects were not observed in PXR-knockout variant of LS174T cells, revealing PXR-dependent induction of CYP3A4 and MDR1 by IND and IAD. In LS180 cells transiently over-expressing the human PXR, we observed an induction of MDR1 mRNA by RIF (8-folds), IND (2-folds), and IAD (5-folds); however the induction of CYP3A4 mRNA was weak (2-folds for RIF).
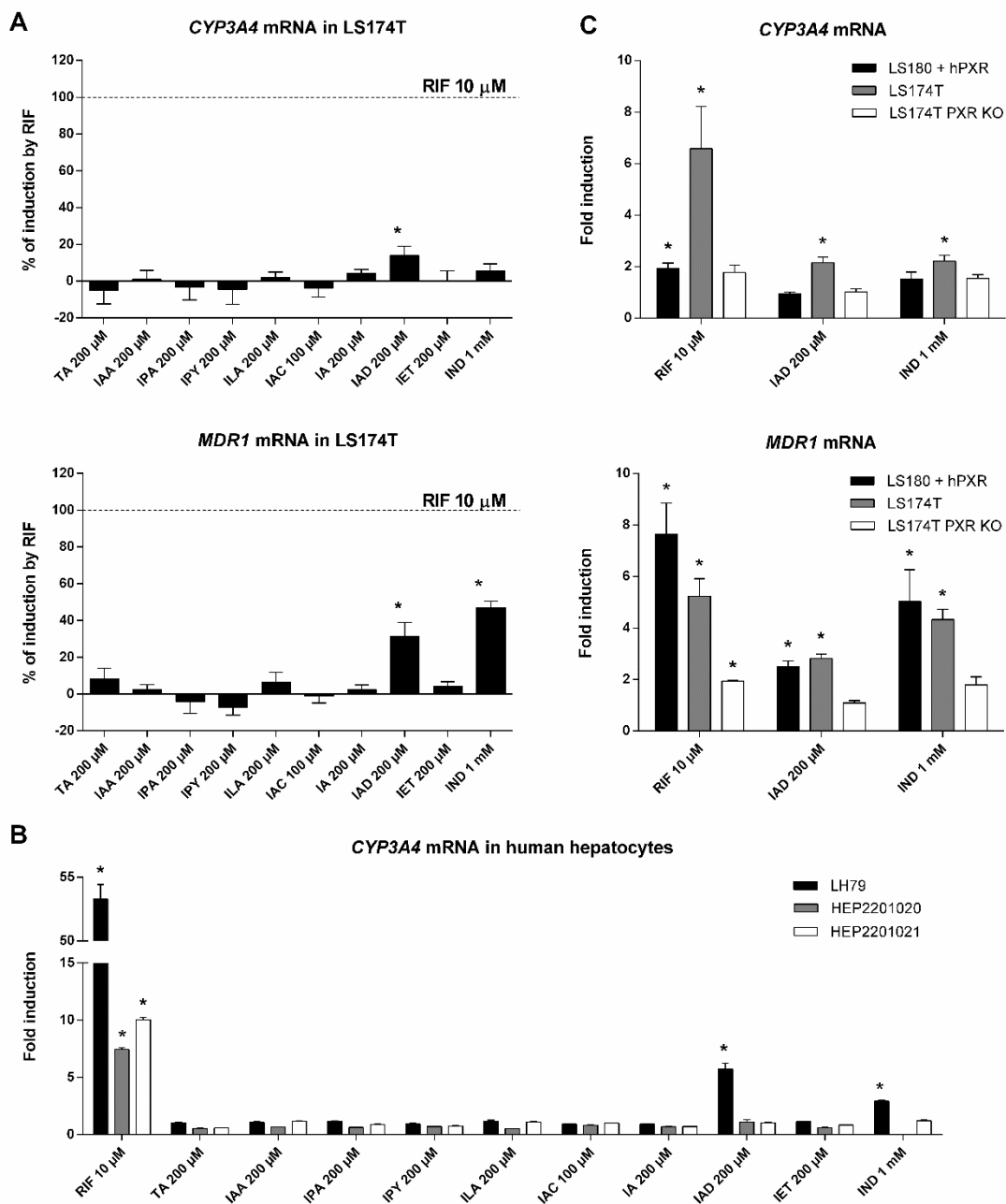
Figure 32: Effects of MICTs on the mRNA expression of CYP3A4 and MDR1 in human hepatic and intestinal cells. Panel A: LS174T cells were treated with MICTs, vehicle (DMSO; 0.1% v/v), or rifampicin (RIF; 10 µM) for 24 h. The levels of CYP3A4 and MDR1 were determined by qRT-PCR and are expressed as a percentage of induction attained by RIF (10 µM). The data represent the means ± standard deviation from three consecutive cell passages. **Panel B**: Human hepatocytes were exposed to MICTs, vehicle (DMSO; 0.1 % v/v), or rifampicin (RIF; 10 µM). After 24 h, qRT-PCR was performed and the level of CYP3A4 mRNA was determined. The data for each hepatocyte culture are expressed as a fold induction ± standard deviation over the vehicle-treated cells (DMSO; 0.1 % v/v). **Panel C**: LS180 cells transiently transfected with PXR expression plasmid, LS174T cells and LS174T PXR-KO cells were exposed to indole-3-acetamide (IAD; 200 µM), indole (IND; 1 mM), vehicle (DMSO; 0.1 % v/v), or rifampicin (RIF; 10 µM) for 24 h. The levels of CYP3A4 and MDR1 were determined by qRT-PCR and are expressed as a fold induction over the vehicle-treated cells (DMSO; 0.1 % v/v). The data represent the means ± standard deviation from three consecutive cell passages. * = value significantly different from negative control ($p < 0.05$).

5.4.3 Binding of IND and IAD to the ligand-binding domain of PXR

Cell-free, competitive ligand-binding assay (Time-Resolved Fluorescence Resonance Energy Transfer; TR-FRET) was used to assess the binding of IND and IAD to the ligand-binding domain of the human PXR. Both IND (IC_{50} = 292 μM) and IAD (IC_{50} = 10 μM) caused dose-dependent displacement of the fluorescent ligand from PXR-LBD. This implies that both compounds are orthosteric ligands of the human PXR that directly bind to the receptor.

hPXR ligand binding

IND: IC_{50} = 292.33 ± 69.72 μM (n = 4)
IAD: IC_{50} = 10.10 ± 2.32 μM (n = 3)
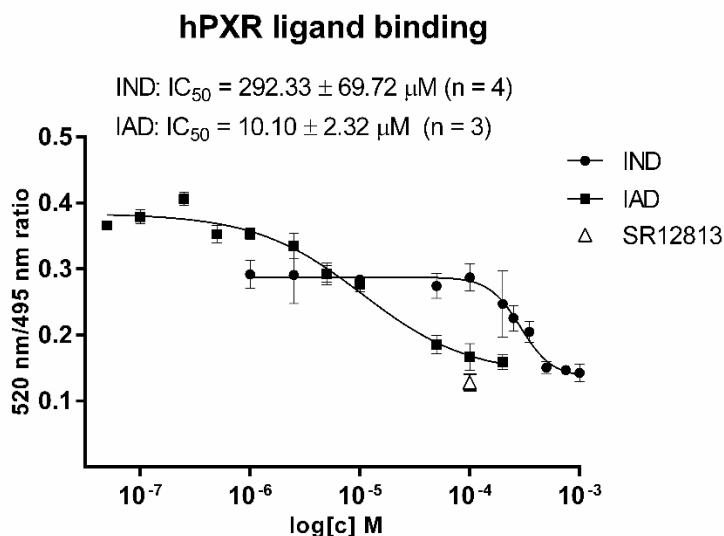
Figure 33: Binding of IND and IAD at PXR-TR FRET assay. TR-FRET 520/495 ratios were plotted against the concentrations of the test compounds. Half-maximal inhibitory concentrations (IC_{50} values) were obtained from interpolated standard curves (sigmoidal, variable slopes) and are inserted in the plot. Experiments were performed at least three times (n = 3) and the representative plots are shown. The presented data are mean ± standard error from quadruplicates (technical replicates). Positive control SR12813 (100 μM) is depicted as a single point (triangle symbol).

5.4.4 PXR binding in MDR1 promoter

The capability of IND and IAD to augment PXR binding to the MDR1 promoter was examined using ChIP assay. The incubation of intestinal LS174T cells stably over-expressing PXR with both IND and IAD resulted in the enrichment of the MDR1 promoter with PXR. These findings were consistent with previous data, where we found out that IND and IAD bound to PXR, activated PXR, and induced PXR-dependent genes.
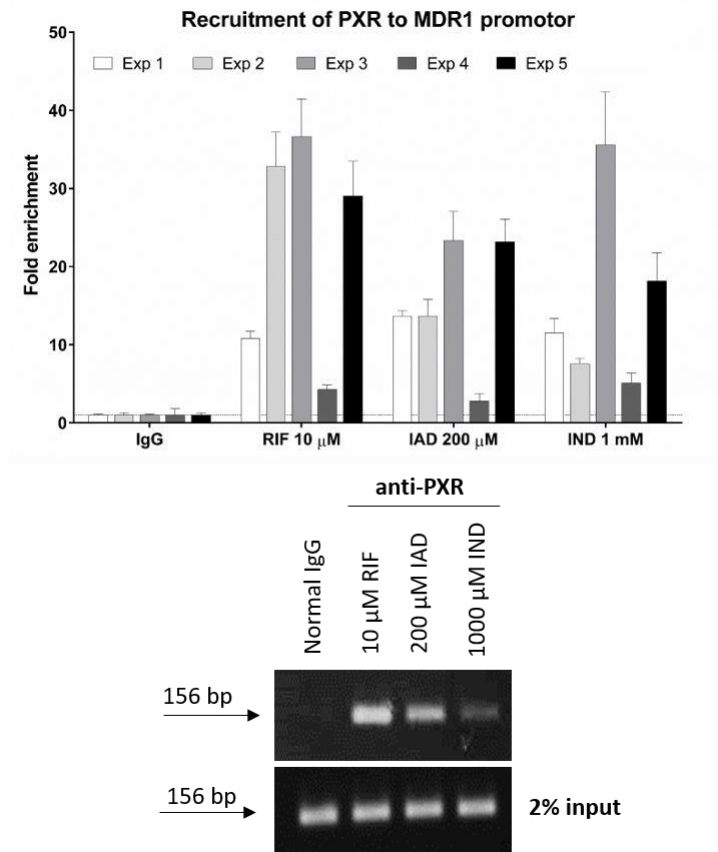

Figure 34: Effect of MICTs on the binding of PXR to DNA. RM12-PXR cells were incubated with vehicle (DMSO; 0.1 % v/v), rifampicin (RIF; 10 µM), IAD (200 µM), and IND (1000 µM) for 20 h. The cells were then subjected to ChIP analysis using anti-PXR antibody and RT-PCR amplification of MDR1 promotor primers. Experiments were performed in five consecutive cell passages. Bar graphs show enrichment of MDR1 promoter with PXR as the fold increase in signal relative to the background signal, that is, normal (mock) IgG. Representative DNA fragments amplified by polymerase chain reaction and analysed on a 2 % agarose gel are shown.

6 DISCUSSION

Compounds with an indole ring in their structure, including synthetic compounds, endogenous substances, or microbial products, are ligands of AhR and PXR (Dvorak et al., 2021; Hubbard et al., 2015a; Venkatesh et al., 2014). Both receptors, originally thought to be xenobiotic sensors, play many physiological roles and are involved in a number of pathophysiological processes and the etiology of many diseases. Thus, the use of indole moiety as a pharmacophore in therapeutic targeting of PXR and AhR has become a challenge in pharmacotherapy (Chen et al., 2020; Pondugula et al., 2015; Venkatesh et al., 2014). The bottleneck of this approach is the fact that AhR and PXR have both beneficial and detrimental effects on ligands. Therapeutic targeting is hindered by the fact that many compounds are dual activators of AhR and PXR, and in addition, there is a mutual functional cross-talk between these receptors (Rasmussen et al., 2017). Therefore, different therapeutic outcomes are expected for AhR-selective and PXR-selective ligands, compared with dual AhR/PXR activators. Given the important roles of AhR and PXR in human gut health, it is vital to investigate the effects of indole derivatives on the AhR and PXR signalling pathways. These indole-based compounds could potentially serve as therapeutics for different diseases, such as IBDs, through the activation of AhR and/or PXR.

In the present study, I systematically investigated the effects of the entire series of MMIs and 11 known human microbial intestinal tryptophan catabolites on the activities and functions of AhR and PXR. *In vitro* models of primary human hepatocytes, human hepatic progenitor cell lines, and cancer cell lines were used. The compounds were tested using various experimental approaches to determine the transcriptional activities of AhR and PXR, mRNA and protein expression levels of target genes, CYP1A1 catalytic activity, protein-protein interactions, DNA-protein interactions, and metabolism of the test compounds.

The first series of experiments published in *Toxicology Letters* in 2019 (appendix I.) was performed as the follow-up study, where Stepankova et al. showed that the relative efficacy of individual MMI at AhR differed substantially. For instance, the efficacy of 4-MMI and 6-MMI as AhR agonists were

approximately 25-folds higher than that of 3-MMI (skatole), while 2-MMI was nearly inactive at AhR (Stepankova et al., 2018). Given that a very subtle change in the chemical structures of MMIs, such as a shift in methyl moiety at indole ring, results in a dramatic impact on their activities at AhR, we subjected MMIs to further investigation. We demonstrated that MMIs induced CYP1A1 and CYP1A2 genes in HepaRG human hepatic progenitor cells through AhR-dependent mechanisms. MMIs also induced the mRNA and protein expression of CYP1A1 and CYP1A2 in the primary cultures of human hepatocytes. The relative efficacy of MMIs in HepaRG and primary human hepatocytes were similar to those detected previously for CYP1A1 in LS180 intestinal cancer cells (Stepankova et al., 2018), with one exception. Although 7-MMI was a weak inducer of CYP1A1 in LS180 and HepaRG cells, it was a very strong inducer of CYP1A genes in three cultures of human hepatocytes. Because primary human hepatocytes possess more sophisticated system for xenobiotic metabolism than cell lines, the plausible explanation for the strong increase in the ability to induce CYP1A genes by 7-MMI may be its metabolic conversion to a highly AhR-active product. The hypothesis of 7-MMI metabolic activation was supported by results demonstrating increased AhR activation in transgenic reporter gene AZ-AhR cells induced by culture media from human hepatocytes incubated 24 h with 7-MMI, compared with media containing 7-MMI without prior incubation. In contrast, we also observed loss of AhR agonist activity of 4-MMI after incubation with human hepatocytes. The dramatic decline in MMI concentrations in culture media after 24 h incubation with human hepatocytes indicated either metabolic degradation or active cellular uptake of parental MMI. Through LC/MS analysis, we observed the formation of various derivatives of mono-oxidated MMIs (mono-hydroxylated MMIs ormono-methyl-oxindole derivatives) and GSH-conjugates of MMIs in cell culture media. Significant differences in the amounts and types of mono-oxidated metabolites were observed in the samples. Conjugation with a large polar glutathione molecule and/or introduction of hydroxyl groups into the indole skeleton could compromise AhR agonist activity of MMIs, which has also been observed by other authors (Heath-Pagliuso et al., 1998). Speculatively, this could be a reason for a loss of AhR agonist activity for 4-MMI. On the other hand, the formation of mono-methyl-oxindoles could

lead to the formation of condensed products analogous to indigo and indirubin, which are potent AhR agonists (Adachi et al., 2001). This could be the reason for the acquisition of AhR agonist activity by 7-MMI. Collectively, distinct metabolic signatures for individual MMIs might result in no change, loss, or gain of AhR agonist activity. The activators of AhR and inducers of CYP1A genes are often the inhibitors of CYP1A enzymes. Indeed, the effects of MMIs on CYP1A1 enzyme activity in cultured LS180 cells and in primary human hepatocytes involved both the inhibition of catalytic activity and increase in CYP1A1 amount by induction, but with a different concentration-response pattern.

Results reported in *Toxicology Letters* in 2020 (appendix II.) showed differential effects on the PXR-CYP3A4 signalling pathway by MMIs in human hepatic and intestinal cells. We identified 1-MMI as the most PXR-active derivate across all performed assays and observed the induction of PXR-regulated CYP3A4 gene in intestinal LS180 cells and in hepatic progenitor cells HepaRG, but not in primary human hepatocytes. Direct interaction of PXR ligand-binding domain with 1-MMI was revealed using TR-FRET assay as well as ChIP assay, and the results showed 1-MMI-induced increase in PXR binding in the promoter of CYP3A4. The discrepancy in CYP3A4 expression in cell lines and primary human hepatocytes could be due to increased or decreased activities in metabolically competent human hepatocytes; similarly as in previous study (Vyhlidalova et al., 2019). 1-MMI is also a partial agonist of PXR as shown by the reporter gene assay. The absence of CYP3A4 induction by MMIs in primary human hepatocytes would predestine these compounds as intestinal-selective PXR modulators, having no systemic effects from a therapeutic standpoint.

Overall, the activation of AhR and PXR by MMIs depends on the position of the methyl moiety attached to the indole ring. The highly efficacious agonists of AhR have the methyl groups attached at positions 4, 5, and 6 on the indole ring, whereas powerful PXR agonists include MMIs with a methyl group attached at positions 1 and 2. Furthermore, MMIs induce PXR genes in a tissue-specific manner, suggesting that the lead PXR-active 1-MMI, resulting from this study may be considered a selective intestinal PXR activator. PXR is a physiologic regulator of intestinal barrier permeability and its activation is

reduced in patients with IBD intestinal inflammatory diseases, largely through loss of endogenous ligands (Venkatesh et al., 2014; Wilson et al., 2020). Engaging appropriate activation of PXR in the setting of colitis with suitable ligands that are essentially non-toxic to the host and have locally (gut-specific) limited pharmacology (no systemic exposure) is a novel approach in the treatment of intestinal pathologies. While medicinal chemistry research teams have focused on the development of indole-based drugs, they have not specifically targeted them as PXR ligands (Chadha et Silakari, 2017). Although indole-like structures are known to bind and activate PXR (Dring et al., 2010; Pondugula et al., 2015), only recently has there been increased interest in the direct structure-activity relationship (SAR) between indoles compounds and PXR (Dvorak et al., 2020; Li et al., 2021). 1-MMI could thus be a suitable candidate for the treatment of PXR-responsive pathologies, such as inflammatory pathologies of the gastrointestinal tract.

In the study published in *International Journal of Molecular Sciences* in 2020 (appendix III.), we comprehensively described, for the first time, the effects of all known human MICTs on AhR activity and functions. We found that MICTs: (i) displaced [3H]-TCDD from the AhR in the ligand-binding assay; (ii) activated AhR in reporter gene assays; (iii) induced AhR target gene expression; (iv) triggered nuclear translocation of AhR; (v) induced the formation of AhR-ARNT heterodimer; and (vi) enhanced binding of AhR to CYP1A1 promoter. The results showed that MICTs act as ligands and agonists of AhR to different extent, as summarised in Table 4. We focused on the effects of MICTs occurring at biologically relevant concentrations after 24 h. Due to the concentrations used and the extensive metabolism of indole compounds, the plateau was not reached in the reporter gene assays and EC_{50} values were estimated. In the follow-up study, the effects of MICT were determined after 4 h and almost all MICTs reached a plateau (unpublished data). The relative efficacy was almost the same, compared with that of model AhR ligand TCDD; however, the EC_{50} values were significantly reduced after 4 h, compared with that observed at 24 h. For example, the estimated EC_{50} for indole was 1485 ± 91.7 µM after 24 h, while EC_{50} for indole after 4 h was 37 ± 17 µM. Hubbard et al. observed dose-dependent indole-induced increase in AhR transcriptional activity with EC_{50} of 3 µM in HepG2 cells after 4 h (Hubbard et

al., 2015a), which was relatively consistent with our findings from 30 experiments.

Table 4: Summary of MICT effects on the AhR-CYP1A1 pathway

Compound	Affinity (IC_{50})	Potency (EC_{50})	Efficacy (E_{MAX})	Antagonism (IC_{50})	Gene expression	AhR cell functions (translocation; heterodimerisation; DNA-binding
Indole	very low	very low	high	yes – all ligands	strong inducer	highly active – all parameters
Skatole	low	low	medium	ligand selective	strong inducer	highly active – all parameters
Tryptamine	no	low	medium	yes – all ligands	strong inducer	highly active – all parameters
I3-acetamide	low	low	high	none	strong inducer	highly active – all parameters
I3-acetate	no	low	low	none	inactive	not tested
I3-acrylate	very low	low	medium	none	strong inducer	highly active – all parameters
I3-aldehyde	no	low	low	yes – all ligands	inactive	not tested
I3-ethanol	very low	low	medium	ligand selective	inactive	not tested
I3-lactate	no	low	low	none	inactive	not tested
I3-propionate	no	low	low	none	inactive	not tested
I3-pyruvate	low	low	high	ligand selective	strong inducer	highly active – all parameters

The study published in *Toxicology Letters* in 2020 (appendix IV.) was focused on the effects of MICT on PXR activity and consecutive molecular events. We defined IND as a low-affinity (IC_{50} = 292 μM) ligand of the hPXR, which exhibited low-potency and high-efficacy agonist effects on PXR. IND concentration in faeces have been detected in the range of 250 μM to 6000 μM (Dvorak et al., 2020; Hubbard et al., 2015b; Jin et al., 2014; Lamas et al., 2016; Roager et Licht, 2018), which is sufficient to activate intestinal PXR. We also identified IAD as a medium-affinity (IC_{50} = 10 μM) ligand of PXR; however, intestinal or faecal concentrations of IAD are unknown. The other MICTs were inactive to PXR.

Our findings suggest that small structural changes in the indole molecule lead to differential activation of AhR and PXR receptors; therefore, studying structure-activity relationship of compounds that are focused on specific target is essential for development new drugs. This study demonstrated that indole is identified as a dual activator of both receptor, but its 3-substituted metabolites bind to AhR and PXR with various affinity, potency and efficacy. Although mono-methyl substitution at any position of the indole ring increases PXR

activity, we found that 3-substituted indoles with mono-carboxylic acids (acetate, acrylate, lactate, propionate, and pyruvate) as well as with aldehyde group are very weak or even inactive toward PXR. In contrast, all of these exhibited higher potency and efficacy to AHR than PXR. Interestingly, IPA does not activate human PXR in intestinal cells, but Venkatesh et al. demonstrated the agonistic effects of IPA in combination with indole in mice, which additionally had strong PXR-mediated anti-inflammatory effects (Venkatesh et al., 2014). Substitution with hydroxyethyl or hydroxyamine moieties exerted weak agonist effects on PXR, while acetamide moiety exerted strong PXR activation. Indole-3-acetamide also binds to AhR with similar affinity and potency to PXR, but PXR showed higher relative potency at the same metabolite concentration than AhR. However, we did not find any commonality between the structures of the studied indoles in relation to AhR activity, as was the case for PXR.

The mechanisms through which MICTs can affect host health and disease are well defined; hence, there is a growing interest in these molecules and their therapeutic applications. In this context, there are studies that used chemical modifications of indole derivatives to activate AhR or PXR as a potential therapeutic target, especially in IBDs (Dvorak et al., 2020; Grycova et al., 2022; Li et al., 2021). For example, our group recently published that replacing the methyl ester moiety in the microbial metabolite 2-(1'H-indole-3'-carbonyl)-thiazole-4-carboxylic acid methyl ester (ITE), found in porcine lungs, with an *N*-methylacetamide group leads to improved metabolic stability while maintaining the AhR agonist activity. Moreover, this ITE analogue alleviated DSS-induced colitis in mice (Grycova et al., 2022). Another study described indole microbial metabolites-based mimics as selective ligands of human PXR with anti-inflammatory activity *in vitro* and *in vivo.* The basic PXR-active entity was 1-(phenylsulfonyl)-indol-2-yl scaffold. The new introduction of the unsubstituted indol-2-yl group led to the acquisition of AhR activity and the AhR/PXR-dual agonists. Moreover, the removal of phenyl sulfonyl substituent resulted in AhR-superactive compounds (Dvorak et al., 2020; Li et al., 2021). Thus, minimal changes in the structure of indole metabolites could lead to more potent, receptor-selective drug-like molecules.

It is debatable whether the search for receptor-selective compounds is the correct strategy or whether dual activators may also be beneficial. Given the

known lack of activation of both AhR and PXR in IBD patients, a positive effect can be expected when dual activators are used. However, there is need to study if simultaneous activation of AhR and PXR may lead to receptor interactions that may enhance therapeutic outcome or lead to interference that may alter cellular function. The latter claim is supported by the study from Rasmussen et al., where they demonstrated reduced expression of the PXR target gene CYP3A4 and PXR by AhR ligands in human hepatocytes and HepaRG cells; however, the mechanism of this cross-talk is still elusive (Rasmussen et al., 2017). Moreover, Gerbal-Chaloin et al. described that enzymatic modification of the AhR ligands may cause an interference of the PXR signalling pathway with AhR signalling pathway. They showed that omeprazole (an AhR agonist) is efficiently converted from omeprazole-suphide (an AhR antagonist) by PXR-induced CYP3A4 activity in primary human hepatocytes (Gerbal-Chaloin et al., 2006). However, it is not clear if similar interactions also occur with indole derivatives.

However, pharmacological activation of AhR and PXR still has its limitations. Excessive activation of these receptors results in tissue-specific effects, some of which are not desirable. For example, long-term overactivation of AhR lead to pathophysiological conditions, such as carcinogenesis, anaemia, and alteration of liver functions, including lipid (steroid, phospholipid and fatty acids) and carbohydrate metabolism (Kim et al., 2020; Pierre et al., 2014). Similarly, the systemic overstimulation of PXR can lead to adverse drug interactions and hepatic steatosis, and it has the potential to accelerate the development of *de novo* malignancies (Abdel-Razik et al., 2018; Cheng et al., 2012). Thus, the goal of therapy targeting AhR and PXR, for example in IBD, where their activation is insufficient, is the restoration of normal activation of these receptors (as if the system were replaced with endogenous ligands) and not overstimulation.

Overall, our studies expand the list of indole derivatives that can act as ligands for PXR and/or AhR. Our findings may pave way for the design of new indole-based therapeutic scaffolds for the treatment of different diseases, such as IBDs, in which both receptors are supposed to play an important role. However, the impact of MICTs (or their derivatives) on intestinal health requires further study, as they occur as complex mixtures within intestines and

understanding their cumulative effects on AhR and PXR might be a clue for therapeutic targeting of these receptors.

7 CONCLUSION

The present thesis focused on the effects of 7 MMIs and 11 MICTs on the AhR and PXR signalling pathways. The major findings are:

(i)   MMIs are agonists of AhR. The overall effects of MMIs on the AhR-CYP1A pathway in human cells involve the induction of CYP1A genes, the inhibition of CYP1A1 catalytic activity, and the combined action of parental compounds and their metabolites.

(ii)   MMIs are partial agonists of PXR that induce PXR-regulated genes in intestinal cells, but not in primary human hepatocytes. The major PXR-active 1-MMI showed only negligible AhR activity, allowing 1-MMI to be considered as intestinal PXR-selective activator.

(iii)   MICTs are low-potency agonists of AhR that induce CYP1A1 mRNA in intestinal cells and primary human hepatocytes as well as trigger all other molecular events of the AhR signalling pathway.

(iv)   Indole and indole-3-acetamide are agonists of PXR and inducers of PXR-regulated genes in intestinal cells.

The data suggest that the position of the methylated group on the indole ring may be responsible for the preference of the compound for AhR/PXR binding. Furthermore, we found that indole and indole-3-acetamide are dual activators of AhR and PXR in intestinal cells, which could facilitate the understanding of the role of microbial catabolites in human physiology and pathophysiology.

My experimental contributions to the published work:

Vyhlidalova B., Poulikova K., Bartonkova I., Krasulova K., Vanco J., Travnicek Z., Mani S., Dvorak Z. (2019). Mono-methylindoles induce CYP1A genes and inhibit CYP1A1 enzyme activity in human hepatocytes and HepaRG cells. *Toxicol Lett,* 313: 66-76 **[IF$_{2019}$ 3.569]**. Contribution: reporter gene assay, mRNA isolation and qRT-PCR analysis, protein isolation and analysis

Vyhlidalova B., Bartonkova I., Jiskrova E., Li H., Mani S., Dvorak, Z. (2020). Differential activation of human pregnane X receptor PXR by isomeric mono-methylated indoles in intestinal and hepatic in vitro models. *Toxicol Lett,* 324: 104-110. **[IF$_{2020}$ 4.372]**. Contribution: reporter gene assay, mRNA isolation and qRT-PCR analysis, protein isolation and analysis, TR-FRET assay

Vyhlidalova B., Krasulova K., Pecinkova P., Marcalikova A., Vrzal R., Zemankova L., Vanco J., Travnicek Z., Vondracek J., Karasova M., Mani S., Dvorak, Z. (2020). Gut Microbial Catabolites of Tryptophan Are Ligands and Agonists of the Aryl Hydrocarbon Receptor: A Detailed Characterization. *Int. J. Mol. Sci,* 21(7): 2614. **[IF$_{2020}$ 5.923]**. Contribution: determination of tryptophan amount in cultures media using reporter gene assay, mRNA isolation and qRT-PCR analysis, protein isolation and analysis

Illes P., Krasulova K., **Vyhlidalova B.**, Poulikova K., Marcalikova A., Pecinkova P., Sirotova N., Vrzal R., Mani S., Dvorak, Z. (2020). Indole microbial intestinal metabolites expand the repertoire of ligands and agonists of the human pregnane X receptor. *Toxicol Lett,* 334: 87-93. **[IF$_{2020}$ 4.372]**. Contribution: mRNA isolation and qRT-PCR analysis

8 REFERENCES

Aagaard, K., Ma, J., Antony, K.M., Ganu, R., Petrosino, J., Versalovic, J. (2014). The placenta harbors a unique microbiome. *Sci Transl Med*, 6, 237ra65.

Abdel-Razik, A., Mousa, N., Shabana, W., Refaey, M., Elzehery, R., Elhelaly, R., Zalata, K., Abdelsalam, M., Eldeeb, A.A., Awad, M., Elgamal, A., Attia, A., El-Wakeel, N., Eldars, W. (2018). Rifaximin in nonalcoholic fatty liver disease: hit multiple targets with a single shot. *Eur J Gastroenterol Hepatol*, 30, 1237-1246.

Abel, J., Haarmann-Stemmann, T. (2010). An introduction to the molecular basics of aryl hydrocarbon receptor biology. *Biol Chem*, 391, 1235-48.

Adachi, J., Mori, Y., Matsui, S., Takigami, H., Fujino, J., Kitagawa, H., Miller, C.A., Kato, T., Saeki, K., Matsuda, T. (2001). Indirubin and indigo are potent aryl hydrocarbon receptor ligands present in human urine. *Journal of Biological Chemistry*, 276, 31475-31478.

Agus, A., Clement, K., Sokol, H. (2021). Gut microbiota-derived metabolites as central regulators in metabolic disorders. *Gut*, 70, 1174-1182.

Agus, A., Planchais, J., Sokol, H. (2018). Gut Microbiota Regulation of Tryptophan Metabolism in Health and Disease. *Cell Host Microbe*, 23, 716-724.

Alkhalaf, L.M., Ryan, K.S. (2015). Biosynthetic manipulation of tryptophan in bacteria: pathways and mechanisms. *Chem Biol*, 22, 317-28.

Anbalagan, M., Huderson, B., Murphy, L., Rowan, B.G. (2012). Post-translational modifications of nuclear receptors and human disease. *Nucl Recept Signal*, 10, e001.

Arshad, T., Mansur, F., Palek, R., Manzoor, S., Liska, V. (2020). A Double Edged Sword Role of Interleukin-22 in Wound Healing and Tissue Regeneration. *Front Immunol*, 11, 2148.

Arumugam, M., Raes, J., Pelletier, E., Le Paslier, D., Yamada, T., Mende, D.R., Fernandes, G.R., Tap, J., Bruls, T., Batto, J.M., Bertalan, M., Borruel, N., Casellas, F., Fernandez, L., Gautier, L., Hansen, T., Hattori, M., Hayashi, T., Kleerebezem, M., Kurokawa, K., Leclerc, M., Levenez, F., Manichanh, C., Nielsen, H.B., Nielsen, T., Pons, N., Poulain, J., Qin, J., Sicheritz-Ponten, T., Tims, S., Torrents, D., Ugarte, E., Zoetendal, E.G., Wang, J., Guarner, F., Pedersen, O., de Vos, W.M., Brunak, S., Dore, J., Meta, H.I.T.C., Antolin, M., Artiguenave, F., Blottiere, H.M., Almeida, M., Brechot, C., Cara, C., Chervaux, C., Cultrone, A., Delorme, C., Denariaz, G., Dervyn, R., Foerstner, K.U., Friss, C., van de Guchte, M., Guedon, E., Haimet, F., Huber, W., van Hylckama-Vlieg, J., Jamet, A., Juste, C., Kaci, G., Knol, J., Lakhdari, O., Layec, S., Le Roux, K., Maguin, E., Merieux, A., Melo Minardi, R., M'Rini, C., Muller, J., Oozeer, R., Parkhill, J., Renault, P., Rescigno, M., Sanchez, N., Sunagawa, S., Torrejon, A., Turner, K., Vandemeulebrouck, G., Varela, E., Winogradsky, Y., Zeller, G., Weissenbach, J., Ehrlich, S.D., Bork, P. (2011). Enterotypes of the human gut microbiome. *Nature*, 473, 174-80.

Ashrap, P., Zheng, G., Wan, Y., Li, T., Hu, W., Li, W., Zhang, H., Zhang, Z., Hu, J. (2017). Discovery of a widespread metabolic pathway within and among phenolic xenobiotics. *Proc Natl Acad Sci U S A*, 114, 6062-6067.

Bai, M., Liu, H., Xu, K., Oso, A.O., Wu, X., Liu, G., Tossou, M.C., Al-Dhabi, N.A., Duraipandiyan, V., Xi, Q., Yin, Y. (2017). A review of the immunomodulatory role of dietary tryptophan in livestock and poultry. *Amino Acids*, 49, 67-74.

Beato, M., Herrlich, P., Schutz, G. (1995). Steroid hormone receptors: many actors in search of a plot. *Cell*, 83, 851-7.

Beischlag, T.V., Wang, S., Rose, D.W., Torchia, J., Reisz-Porszasz, S., Muhammad, K., Nelson, W.E., Probst, M.R., Rosenfeld, M.G., Hankinson, O. (2002). Recruitment of the NCoA/SRC-1/p160 family of transcriptional coactivators by the aryl hydrocarbon receptor/aryl hydrocarbon receptor nuclear translocator complex. *Mol Cell Biol*, 22, 4319-33.

Benadiba, M., Maor, Y. (2016). Importance of ABC Transporters in Drug Development. *Curr Pharm Des*, 22, 5817-5829.

Bennett, B.D., Kimball, E.H., Gao, M., Osterhout, R., Van Dien, S.J., Rabinowitz, J.D. (2009). Absolute metabolite concentrations and implied enzyme active site occupancy in Escherichia coli. *Nat Chem Biol*, 5, 593-9.

Berg, J.M. (1989). DNA binding specificity of steroid receptors. *Cell*, 57, 1065-8.

Bernhardt, R. (2006). Cytochromes P450 as versatile biocatalysts. *J Biotechnol*, 124, 128-45.

Biesalski, H.K. (2016). Nutrition meets the microbiome: micronutrients and the microbiota. *Ann N Y Acad Sci*, 1372, 53-64.

Blacher, E., Levy, M., Tatirovsky, E., Elinav, E. (2017). Microbiome-Modulated Metabolites at the Interface of Host Immunity. *J Immunol*, 198, 572-580.

Blumberg, B., Sabbagh, W., Jr., Juguilon, H., Bolado, J., Jr., van Meter, C.M., Ong, E.S., Evans, R.M. (1998). SXR, a novel steroid and xenobiotic-sensing nuclear receptor. *Genes Dev*, 12, 3195-205.

Bock, K.W. (2017). Human and rodent aryl hydrocarbon receptor (AHR): from mediator of dioxin toxicity to physiologic AHR functions and therapeutic options. *Biol Chem*, 398, 455-464.

Bock, K.W. (2019). Aryl hydrocarbon receptor (AHR): From selected human target genes and crosstalk with transcription factors to multiple AHR functions. *Biochem Pharmacol*, 168, 65-70.

Bock, K.W., Kohle, C. (2006). Ah receptor: Dioxin-mediated toxic responses as hints to deregulated physiologic functions. *Biochemical Pharmacology*, 72, 393-404.

Bock, K.W., Lilienblum, W., Fischer, G., Schirmer, G., Bock-Henning, B.S. (1987). The role of conjugation reactions in detoxication. *Arch Toxicol*, 60, 22-9.

Boets, E., Gomand, S.V., Deroover, L., Preston, T., Vermeulen, K., De Preter, V., Hamer, H.M., Van den Mooter, G., De Vuyst, L., Courtin, C.M., Annaert, P., Delcour, J.A., Verbeke, K.A. (2017). Systemic availability and metabolism of colonic-derived short-chain fatty acids in healthy subjects: a stable isotope study. *J Physiol*, 595, 541-555.

Brave, M., Lukin, D.J., Mani, S. (2015). Microbial control of intestinal innate immunity. *Oncotarget*, 6, 19962-3.

Brown, D.R., Clark, B.W., Garner, L.V., Di Giulio, R.T. (2015). Zebrafish cardiotoxicity: the effects of CYP1A inhibition and AHR2 knockdown following exposure to weak aryl hydrocarbon receptor agonists. *Environ Sci Pollut Res Int*, 22, 8329-38.

Brown, D.R., Clark, B.W., Garner, L.V., Di Giulio, R.T. (2016). Embryonic cardiotoxicity of weak aryl hydrocarbon receptor agonists and CYP1A inhibitor fluoranthene in the Atlantic killifish (Fundulus heteroclitus). *Comp Biochem Physiol C Toxicol Pharmacol*, 188, 45-51.

Bull, M.J., Plummer, N.T. (2014). Part 1: The Human Gut Microbiome in Health and Disease. *Integr Med (Encinitas)*, 13, 17-22.

Butt, T.R., Walfish, P.G. (1996). Human nuclear receptor heterodimers: opportunities for detecting targets of transcriptional regulation using yeast. *Gene Expr*, 5, 255-68.

Carazo, A., Mladenka, P., Pavek, P. (2019). Marine Ligands of the Pregnane X Receptor (PXR): An Overview. *Mar Drugs*, 17.

Casarett, L.J., Klaassen, C.D., Amdur, M.O., Doull, J. (1996). Casarett and Doull's toxicology : the basic science of poisons, 5th ed. *McGraw-Hill, Health Professions Division*, New York.

Ciolino, H.P., Daschner, P.J., Yeh, G.C. (1999). Dietary flavonols quercetin and kaempferol are ligands of the aryl hydrocarbon receptor that affect CYP1A1 transcription differentially. *Biochem J*, 340 (Pt 3), 715-22.

Cook, S.I., Sellin, J.H. (1998). Review article: short chain fatty acids in health and disease. *Aliment Pharmacol Ther*, 12, 499-507.

Coumoul, X., Diry, M., Barouki, R. (2002). PXR-dependent induction of human CYP3A4 gene expression by organochlorine pesticides. *Biochem Pharmacol*, 64, 1513-9.

Crews, S.T. (1998). Control of cell lineage-specific development and transcription by bHLH-PAS proteins. *Genes Dev*, 12, 607-20.

Croom, E. (2012). Metabolism of xenobiotics of human environments. *Prog Mol Biol Transl Sci*, 112, 31-88.

Cui, J.Y., Gunewardena, S.S., Rockwell, C.E., Klaassen, C.D. (2010). ChIPing the cistrome of PXR in mouse liver. *Nucleic Acids Res*, 38, 7943-63.

Cummings, J.H., Antoine, J.M., Azpiroz, F., Bourdet-Sicard, R., Brandtzaeg, P., Calder, P.C., Gibson, G.R., Guarner, F., Isolauri, E., Pannemans, D., Shortt, C., Tuijtelaars, S., Watzl, B. (2004). PASSCLAIM--gut health and immunity. *Eur J Nutr*, 43 Suppl 2, II118-II173.

Danielsen, M. (2001). Bioinformatics of nuclear receptors. *Methods Mol Biol*, 176, 3-22.

Davarinos, N.A., Pollenz, R.S. (1999). Aryl hydrocarbon receptor imported into the nucleus following ligand binding is rapidly degraded via the cytosplasmic proteasome following nuclear export. *J Biol Chem*, 274, 28708-15.

De Vadder, F., Kovatcheva-Datchary, P., Goncalves, D., Vinera, J., Zitoun, C., Duchampt, A., Backhed, F., Mithieux, G. (2014). Microbiota-generated metabolites promote metabolic benefits via gut-brain neural circuits. *Cell*, 156, 84-96.

den Besten, G., Lange, K., Havinga, R., van Dijk, T.H., Gerding, A., van Eunen, K., Muller, M., Groen, A.K., Hooiveld, G.J., Bakker, B.M., Reijngoud, D.J. (2013a). Gut-derived short-chain fatty acids are vividly assimilated into host carbohydrates and lipids. *Am J Physiol Gastrointest Liver Physiol*, 305, G900-10.

den Besten, G., van Eunen, K., Groen, A.K., Venema, K., Reijngoud, D.J., Bakker, B.M. (2013b). The role of short-chain fatty acids in the interplay between diet, gut microbiota, and host energy metabolism. *J Lipid Res*, 54, 2325-40.

Denison, M.S., Faber, S.C. (2017). And Now for Something Completely Different: Diversity in Ligand-Dependent Activation of Ah Receptor Responses. *Curr Opin Toxicol*, 2, 124-131.

Denison, M.S., Nagy, S.R. (2003). Activation of the aryl hydrocarbon receptor by structurally diverse exogenous and endogenous chemicals. *Annu Rev Pharmacol Toxicol*, 43, 309-34.

Denison, M.S., Pandini, A., Nagy, S.R., Baldwin, E.P., Bonati, L. (2002a). Ligand binding and activation of the Ah receptor. *Chem Biol Interact*, 141, 3-24.

Denison, M.S., Rogers, J.M., Rushing, S.R., Jones, C.L., Tetangco, S.C., Heath-Pagliuso, S. (2002b). Analysis of the aryl hydrocarbon receptor (AhR) signal transduction pathway. *Curr Protoc Toxicol*, Chapter 4, Unit4 8.

di Masi, A., De Marinis, E., Ascenzi, P., Marino, M. (2009). Nuclear receptors CAR and PXR: Molecular, functional, and biomedical aspects. *Mol Aspects Med*, 30, 297-343.

Dong, F., Hao, F., Murray, I.A., Smith, P.B., Koo, I., Tindall, A.M., Kris-Etherton, P.M., Gowda, K., Amin, S.G., Patterson, A.D., Perdew, G.H. (2020). Intestinal microbiota-derived tryptophan metabolites are predictive of Ah receptor activity. *Gut Microbes*, 12, 1-24.

Doring, B., Petzinger, E. (2014). Phase 0 and phase III transport in various organs: combined concept of phases in xenobiotic transport and metabolism. *Drug Metab Rev*, 46, 261-82.

Dring, A.M., Anderson, L.E., Qamar, S., Stoner, M.A. (2010). Rational quantitative structure-activity relationship (RQSAR) screen for PXR and CAR isoform-specific nuclear receptor ligands. *Chem Biol Interact*, 188, 512-25.

Dvorak, Z., Kopp, F., Costello, C.M., Kemp, J.S., Li, H., Vrzalova, A., Stepankova, M., Bartonkova, I., Jiskrova, E., Poulikova, K., Vyhlidalova, B., Nordstroem, L.U., Karunaratne, C.V., Ranhotra, H.S., Mun, K.S., Naren, A.P., Murray, I.A., Perdew, G.H., Brtko, J., Toporova, L., Schon, A., Wallace, B.D., Walton, W.G., Redinbo, M.R., Sun, K., Beck, A., Kortagere, S., Neary, M.C., Chandran, A., Vishveshwara, S., Cavalluzzi, M.M., Lentini, G., Cui, J.Y., Gu, H., March, J.C., Chatterjee, S., Matson, A., Wright, D., Flannigan, K.L., Hirota, S.A., Sartor, R.B., Mani, S. (2020). Targeting the pregnane X receptor using microbial metabolite mimicry. *EMBO Mol Med*, 12, e11621.

Dvorak, Z., Poulikova, K., Mani, S. (2021). Indole scaffolds as a promising class of the aryl hydrocarbon receptor ligands. *Eur J Med Chem*, 215, 113231.

El-Merahbi, R., Loffler, M., Mayer, A., Sumara, G. (2015). The roles of peripheral serotonin in metabolic homeostasis. *FEBS Lett*, 589, 1728-34.

Ema, M., Matsushita, N., Sogawa, K., Ariyama, T., Inazawa, J., Nemoto, T., Ota, M., Oshimura, M., Fujii-Kuriyama, Y. (1994). Human arylhydrocarbon receptor: functional expression and chromosomal assignment to 7p21. *J Biochem*, 116, 845-51.

Escherich, T. (1988). The intestinal bacteria of the neonate and breast-fed infant. 1884. *Rev Infect Dis*, 10, 1220-5.

Esteves, F., Rueff, J., Kranendonk, M. (2021). The Central Role of Cytochrome P450 in Xenobiotic Metabolism-A Brief Review on a Fascinating Enzyme Family. *J Xenobiot*, 11, 94-114.

Fletcher, J.R., Pike, C.M., Parsons, R.J., Rivera, A.J., Foley, M.H., McLaren, M.R., Montgomery, S.A., Theriot, C.M. (2021). Clostridioides difficile exploits toxin-mediated inflammation to alter the host nutritional landscape and exclude competitors from the gut microbiota. *Nat Commun*, 12, 462.

Flint, H.J., Duncan, S.H., Scott, K.P., Louis, P. (2007). Interactions and competition within the microbial community of the human colon: links between diet and health. *Environ Microbiol*, 9, 1101-11.

Fujii-Kuriyama, Y., Kawajiri, K. (2010). Molecular mechanisms of the physiological functions of the aryl hydrocarbon (dioxin) receptor, a multifunctional regulator that senses and responds to environmental stimuli. *Proc Jpn Acad Ser B Phys Biol Sci*, 86, 40-53.

Furumatsu, K., Nishiumi, S., Kawano, Y., Ooi, M., Yoshie, T., Shiomi, Y., Kutsumi, H., Ashida, H., Fujii-Kuriyama, Y., Azuma, T., Yoshida, M. (2011). A role of the aryl hydrocarbon receptor in attenuation of colitis. *Dig Dis Sci*, 56, 2532-44.

Gan, J., Ma, S., Zhang, D. (2016). Non-cytochrome P450-mediated bioactivation and its toxicological relevance. *Drug Metab Rev*, 48, 473-501.

Gao, J., Xu, K., Liu, H., Liu, G., Bai, M., Peng, C., Li, T., Yin, Y. (2018). Impact of the Gut Microbiota on Intestinal Immunity Mediated by Tryptophan Metabolism. *Front Cell Infect Microbiol*, 8, 13.

Gasaly, N., de Vos, P., Hermoso, M.A. (2021). Impact of Bacterial Metabolites on Gut Barrier Function and Host Immunity: A Focus on Bacterial Metabolism and Its Relevance for Intestinal Inflammation. *Front Immunol*, 12, 658354.

Geick, A., Eichelbaum, M., Burk, O. (2001). Nuclear receptor response elements mediate induction of intestinal MDR1 by rifampin. *J Biol Chem*, 276, 14581-7.

Gerbal-Chaloin, S., Pichard-Garcia, L., Fabre, J.M., Sa-Cunha, A., Poellinger, L., Maurel, P., Daujat-Chavanieu, M. (2006). Role of CYP3A4 in the regulation of the aryl hydrocarbon receptor by omeprazole sulphide. *Cell Signal*, 18, 740-50.

Germain, P., Staels, B., Dacquet, C., Spedding, M., Laudet, V. (2006). Overview of nomenclature of nuclear receptors. *Pharmacol Rev*, 58, 685-704.

Gheorghe, C.E., Martin, J.A., Manriquez, F.V., Dinan, T.G., Cryan, J.F., Clarke, G. (2019). Focus on the essentials: tryptophan metabolism and the microbiome-gut-brain axis. *Curr Opin Pharmacol*, 48, 137-145.

Gillam, E.M., Notley, L.M., Cai, H., De Voss, J.J., Guengerich, F.P. (2000). Oxidation of indole by cytochrome P450 enzymes. *Biochemistry*, 39, 13817-24.

Gonzalez, F.J., Fernandez-Salguero, P. (1998). The aryl hydrocarbon receptor: studies using the AHR-null mice. *Drug Metab Dispos*, 26, 1194-8.

Goodwin, B., Hodgson, E., Liddle, C. (1999). The orphan human pregnane X receptor mediates the transcriptional activation of CYP3A4 by rifampicin through a distal enhancer module. *Mol Pharmacol*, 56, 1329-39.

Govindan, M.V., Devic, M., Green, S., Gronemeyer, H., Chambon, P. (1985). Cloning of the human glucocorticoid receptor cDNA. *Nucleic Acids Res*, 13, 8293-304.

Grycova, A., Joo, H., Maier, V., Illes, P., Vyhlidalova, B., Poulikova, K., Sladekova, L., Nadvornik, P., Vrzal, R., Zemankova, L., Pecinkova, P., Poruba, M., Zapletalova, I., Vecera, R., Anzenbacher, P., Ehrmann, J., Ondra, P., Jung, J.W., Mani, S., Dvorak, Z. (2022). Targeting the Aryl Hydrocarbon Receptor with Microbial Metabolite Mimics Alleviates Experimental Colitis in Mice. *J Med Chem*.

Gustafsson, J.A. (2016). Historical overview of nuclear receptors. *J Steroid Biochem Mol Biol*, 157, 3-6.

Gutierrez-Vazquez, C., Quintana, F.J. (2018). Regulation of the Immune Response by the Aryl Hydrocarbon Receptor. *Immunity*, 48, 19-33.

Guyot, E., Chevallier, A., Barouki, R., Coumoul, X. (2013). The AhR twist: ligand-dependent AhR signaling and pharmaco-toxicological implications. *Drug Discov Today*, 18, 479-86.

Haelens, A., Tanner, T., Denayer, S., Callewaert, L., Claessens, F. (2007). The hinge region regulates DNA binding, nuclear translocation, and transactivation of the androgen receptor. *Cancer Res*, 67, 4514-23.

Hahn, M.E., Allan, L.L., Sherr, D.H. (2009). Regulation of constitutive and inducible AHR signaling: complex interactions involving the AHR repressor. *Biochem Pharmacol*, 77, 485-97.

Hakkola, J., Rysa, J., Hukkanen, J. (2016). Regulation of hepatic energy metabolism by the nuclear receptor PXR. *Biochim Biophys Acta*, 1859, 1072-1082.

Heath-Pagliuso, S., Rogers, W.J., Tullis, K., Seidel, S.D., Cenijn, P.H., Brouwer, A., Denison, M.S. (1998). Activation of the Ah receptor by tryptophan and tryptophan metabolites. *Biochemistry*, 37, 11508-15.

Heinken, A., Ravcheev, D.A., Baldini, F., Heirendt, L., Fleming, R.M.T., Thiele, I. (2019). Systematic assessment of secondary bile acid metabolism in gut microbes reveals distinct metabolic capabilities in inflammatory bowel disease. *Microbiome*, 7, 75.

Hershko, A., Ciechanover, A. (1998). The ubiquitin system. *Annu Rev Biochem*, 67, 425-79.

Hogenesch, J.B., Gu, Y.Z., Moran, S.M., Shimomura, K., Radcliffe, L.A., Takahashi, J.S., Bradfield, C.A. (2000). The basic helix-loop-helix-PAS protein MOP9 is a brain-specific heterodimeric partner of circadian and hypoxia factors. *J Neurosci*, 20, RC83.

Hoglund, E., Overli, O., Winberg, S. (2019). Tryptophan Metabolic Pathways and Brain Serotonergic Activity: A Comparative Review. *Front Endocrinol (Lausanne)*, 10, 158.

Holcapek, M., Kolarova, L., Nobilis, M. (2008). High-performance liquid chromatography-tandem mass spectrometry in the identification and determination of phase I and phase II drug metabolites. *Anal Bioanal Chem*, 391, 59-78.

Holmes, E., Li, J.V., Athanasiou, T., Ashrafian, H., Nicholson, J.K. (2011). Understanding the role of gut microbiome-host metabolic signal disruption in health and disease. *Trends Microbiol*, 19, 349-59.

Honkakoski, P., Sueyoshi, T., Negishi, M. (2003). Drug-activated nuclear receptors CAR and PXR. *Ann Med*, 35, 172-82.

Hubbard, T.D., Murray, I.A., Bisson, W.H., Lahoti, T.S., Gowda, K., Amin, S.G., Patterson, A.D., Perdew, G.H. (2015a). Adaptation of the human aryl hydrocarbon receptor to sense microbiota-derived indoles. *Sci Rep*, 5, 12689.

Hubbard, T.D., Murray, I.A., Perdew, G.H. (2015b). Indole and Tryptophan Metabolism: Endogenous and Dietary Routes to Ah Receptor Activation. *Drug Metab Dispos*, 43, 1522-35.

Hustert, E., Zibat, A., Presecan-Siedel, E., Eiselt, R., Mueller, R., Fuss, C., Brehm, I., Brinkmann, U., Eichelbaum, M., Wojnowski, L., Burk, O. (2001). Natural protein variants of pregnane X receptor with altered transactivation activity toward CYP3A4. *Drug Metab Dispos*, 29, 1454-9.

Chadha, N., Silakari, O. (2017). Indoles as therapeutics of interest in medicinal chemistry: Bird's eye view. *Eur J Med Chem*, 134, 159-184.

Chai, S.C., Wright, W.C., Chen, T. (2020). Strategies for developing pregnane X receptor antagonists: Implications from metabolism to cancer. *Med Res Rev*, 40, 1061-1083.

Chang, T.K. (2009). Activation of pregnane X receptor (PXR) and constitutive androstane receptor (CAR) by herbal medicines. *AAPS J*, 11, 590-601.

Chen, J., Haller, C.A., Jernigan, F.E., Koerner, S.K., Wong, D.J., Wang, Y., Cheong, J.E., Kosaraju, R., Kwan, J., Park, D.D., Thomas, B., Bhasin, S., De La Rosa, R.C., Premji, A.M., Liu, L., Park, E., Moss, A.C., Emili, A., Bhasin, M., Sun, L., Chaikof, E.L. (2020). Modulation of lymphocyte-mediated tissue repair by rational design of heterocyclic aryl hydrocarbon receptor agonists. *Sci Adv*, 6, eaay8230.

Cheng, J., Krausz, K.W., Tanaka, N., Gonzalez, F.J. (2012). Chronic exposure to rifaximin causes hepatic steatosis in pregnane X receptor-humanized mice. *Toxicol Sci*, 129, 456-68.

Chrencik, J.E., Orans, J., Moore, L.B., Xue, Y., Peng, L., Collins, J.L., Wisely, G.B., Lambert, M.H., Kliewer, S.A., Redinbo, M.R. (2005). Structural disorder in the complex of human pregnane X receptor and the macrolide antibiotic rifampicin. *Mol Endocrinol*, 19, 1125-34.

Ihunnah, C.A., Jiang, M., Xie, W. (2011). Nuclear receptor PXR, transcriptional circuits and metabolic relevance. *Biochim Biophys Acta*, 1812, 956-63.

Illes, P., Krasulova, K., Vyhlidalova, B., Poulikova, K., Marcalikova, A., Pecinkova, P., Sirotova, N., Vrzal, R., Mani, S., Dvorak, Z. (2020). Indole microbial intestinal metabolites expand the repertoire of ligands and agonists of the human pregnane X receptor. *Toxicol Lett*, 334, 87-93.

International Transporter, C., Giacomini, K.M., Huang, S.M., Tweedie, D.J., Benet, L.Z., Brouwer, K.L., Chu, X., Dahlin, A., Evers, R., Fischer, V., Hillgren, K.M., Hoffmaster, K.A., Ishikawa, T., Keppler, D., Kim, R.B., Lee, C.A., Niemi, M., Polli, J.W., Sugiyama, Y., Swaan, P.W., Ware, J.A., Wright, S.H., Yee, S.W., Zamek-Gliszczynski, M.J., Zhang, L. (2010). Membrane transporters in drug development. *Nat Rev Drug Discov*, 9, 215-36.

Ishikawa, T. (1992). The ATP-dependent glutathione S-conjugate export pump. *Trends Biochem Sci*, 17, 463-8.

Islam, J., Sato, S., Watanabe, K., Watanabe, T., Ardiansyah, Hirahara, K., Aoyama, Y., Tomita, S., Aso, H., Komai, M., Shirakawa, H. (2017). Dietary tryptophan alleviates dextran sodium sulfate-induced colitis through aryl hydrocarbon receptor in mice. *J Nutr Biochem*, 42, 43-50.

Isom, H.C., Secott, T., Georgoff, I., Woodworth, C., Mummaw, J. (1985). Maintenance of differentiated rat hepatocytes in primary culture. *Proc Natl Acad Sci U S A*, 82, 3252-6.

Jancova, P., Anzenbacher, P., Anzenbacherova, E. (2010). Phase II drug metabolizing enzymes. *Biomed Pap Med Fac Univ Palacky Olomouc Czech Repub*, 154, 103-16.

Jančová, P. (2012). Phase II Drug Metabolism, *IntechOpen*, sine loco.

Jandhyala, S.M., Talukdar, R., Subramanyam, C., Vuyyuru, H., Sasikala, M., Nageshwar Reddy, D. (2015). Role of the normal gut microbiota. *World J Gastroenterol*, 21, 8787-803.

Jayaraj, R., Megha, P., Sreedev, P. (2016). Organochlorine pesticides, their toxic effects on living organisms and their fate in the environment. *Interdiscip Toxicol*, 9, 90-100.

Jenkins, D.J. (1989). The link between colon fermentation and systemic disease. *Am J Gastroenterol*, 84, 1362-4.

Jensen, B.A., Leeman, R.J., Schlezinger, J.J., Sherr, D.H. (2003). Aryl hydrocarbon receptor (AhR) agonists suppress interleukin-6 expression by bone marrow stromal cells: an immunotoxicology study. *Environ Health*, 2, 16.

Jensen, M.T., Cox, R.P., Jensen, B.B. (1995). 3-Methylindole (skatole) and indole production by mixed populations of pig fecal bacteria. *Appl Environ Microbiol*, 61, 3180-4.

Jimenez, E., Marin, M.L., Martin, R., Odriozola, J.M., Olivares, M., Xaus, J., Fernandez, L., Rodriguez, J.M. (2008). Is meconium from healthy newborns actually sterile? *Research in Microbiology*, 159, 187-193.

Jin, U.H., Cheng, Y., Park, H., Davidson, L.A., Callaway, E.S., Chapkin, R.S., Jayaraman, A., Asante, A., Allred, C., Weaver, E.A., Safe, S. (2017). Short Chain Fatty Acids Enhance Aryl Hydrocarbon (Ah) Responsiveness in Mouse Colonocytes and Caco-2 Human Colon Cancer Cells. *Sci Rep*, 7, 10163.

Jin, U.H., Lee, S.O., Sridharan, G., Lee, K., Davidson, L.A., Jayaraman, A., Chapkin, R.S., Alaniz, R., Safe, S. (2014). Microbiome-derived tryptophan metabolites and their aryl hydrocarbon receptor-dependent agonist and antagonist activities. *Mol Pharmacol*, 85, 777-88.

Johnson, D.R., Li, C.W., Chen, L.Y., Ghosh, J.C., Chen, J.D. (2006). Regulation and binding of pregnane X receptor by nuclear receptor corepressor silencing mediator of retinoid and thyroid hormone receptors (SMRT). *Mol Pharmacol*, 69, 99-108.

Johnson, C.H., Patterson, A.D., Idle, J.R., Gonzalez, F.J. (2012). Xenobiotic metabolomics: major impact on the metabolome. *Annu Rev Pharmacol Toxicol*, 52, 37-56.

Kang, J.D., Myers, C.J., Harris, S.C., Kakiyama, G., Lee, I.K., Yun, B.S., Matsuzaki, K., Furukawa, M., Min, H.K., Bajaj, J.S., Zhou, H., Hylemon, P.B. (2019). Bile Acid 7alpha-Dehydroxylating Gut Bacteria Secrete Antibiotics that Inhibit Clostridium difficile: Role of Secondary Bile Acids. *Cell Chem Biol*, 26, 27-34 e4.

Katzung, B.G. (2004). Basic & clinical pharmacology, 9th ed. *Lange Medical Books/McGraw Hill*, New York.

Kikuchi, Y., Ohsawa, S., Mimura, J., Ema, M., Takasaki, C., Sogawa, K., Fujii-Kuriyama, Y. (2003). Heterodimers of bHLH-PAS protein fragments derived from AhR, AhRR, and Arnt prepared by co-expression in Escherichia coli: characterization of their DNA binding activity and preparation of a DNA complex. *J Biochem*, 134, 83-90.

Kim, D.J., Venkataraman, A., Jain, P.C., Wiesler, E.P., DeBlasio, M., Klein, J., Tu, S.S., Lee, S., Medzhitov, R., Iwasaki, A. (2020). Vitamin B12 and folic acid alleviate symptoms of nutritional deficiency by antagonizing aryl hydrocarbon receptor. *Proc Natl Acad Sci U S A*, 117, 15837-15845.

Kim, R.B. (2002). Transporters and xenobiotic disposition. *Toxicology*, 181-182, 291-7.

Kininis, M., Kraus, W.L. (2008). A global view of transcriptional regulation by nuclear receptors: gene expression, factor localization, and DNA sequence analysis. *Nucl Recept Signal*, 6, e005.

Klaassen, C.D., Lu, H. (2008). Xenobiotic transporters: ascribing function from gene knockout and mutation studies. *Toxicol Sci*, 101, 186-96.

Kliewer, S.A., Moore, J.T., Wade, L., Staudinger, J.L., Watson, M.A., Jones, S.A., McKee, D.D., Oliver, B.B., Willson, T.M., Zetterstrom, R.H., Perlmann, T., Lehmann, J.M. (1998). An orphan nuclear receptor activated by pregnanes defines a novel steroid signaling pathway. *Cell*, 92, 73-82.

Klug, A., Schwabe, J.W. (1995). Protein motifs 5. Zinc fingers. *FASEB J*, 9, 597-604.

Kobayashi, A., Numayama-Tsuruta, K., Sogawa, K., Fujii-Kuriyama, Y. (1997). CBP/p300 functions as a possible transcriptional coactivator of Ah receptor nuclear translocator (Arnt). *J Biochem*, 122, 703-10.

Kolluri, S.K., Jin, U.H., Safe, S. (2017). Role of the aryl hydrocarbon receptor in carcinogenesis and potential as an anti-cancer drug target. *Arch Toxicol*, 91, 2497-2513.

Komives, T., Gullner, G. (2005). Phase I xenobiotic metabolic systems in plants. *Z Naturforsch C J Biosci*, 60, 179-85.

Krautkramer, K.A., Fan, J., Backhed, F. (2021). Gut microbial metabolites as multi-kingdom intermediates. *Nat Rev Microbiol*, 19, 77-94.

Kumar, M.B., Tarpey, R.W., Perdew, G.H. (1999). Differential recruitment of coactivator RIP140 by Ah and estrogen receptors. Absence of a role for LXXLL motifs. *J Biol Chem*, 274, 22155-64.

Kumar, P., Lee, J.H., Lee, J. (2021). Diverse roles of microbial indole compounds in eukaryotic systems. *Biol Rev Camb Philos Soc*, 96, 2522-2545.

Kumar, R., Thompson, E.B. (2003). Transactivation functions of the N-terminal domains of nuclear hormone receptors: protein folding and coactivator interactions. *Mol Endocrinol*, 17, 1-10.

Kumar, V., Green, S., Stack, G., Berry, M., Jin, J.R., Chambon, P. (1987). Functional domains of the human estrogen receptor. *Cell*, 51, 941-51.

Lamas, B., Natividad, J.M., Sokol, H. (2018). Aryl hydrocarbon receptor and intestinal immunity. *Mucosal Immunol*, 11, 1024-1038.

Lamas, B., Richard, M.L., Leducq, V., Pham, H.P., Michel, M.L., Da Costa, G., Bridonneau, C., Jegou, S., Hoffmann, T.W., Natividad, J.M., Brot, L., Taleb, S., Couturier-Maillard, A., Nion-Larmurier, I., Merabtene, F., Seksik, P., Bourrier, A., Cosnes, J., Ryffel, B., Beaugerie, L., Launay, J.M., Langella, P., Xavier, R.J., Sokol, H. (2016). CARD9 impacts colitis by altering gut microbiota metabolism of tryptophan into aryl hydrocarbon receptor ligands. *Nat Med*, 22, 598-605.

Landes, N., Birringer, M., Brigelius-Flohe, R. (2003). Homologous metabolic and gene activating routes for vitamins E and K. *Mol Aspects Med*, 24, 337-44.

Langenbach, T. (2013). Persistence and Bioaccumulation of Persistent Organic Pollutants (POPs), *IntechOpen*, sine loco.

Lanza, D.L., Yost, G.S. (2001). Selective dehydrogenation/oxygenation of 3-methylindole by cytochrome p450 enzymes. *Drug Metab Dispos*, 29, 950-3.

Larigot, L., Juricek, L., Dairou, J., Coumoul, X. (2018). AhR signaling pathways and regulatory functions. *Biochim Open*, 7, 1-9.

Lee, S.C., Arya, V., Yang, X., Volpe, D.A., Zhang, L. (2017). Evaluation of transporters in drug development: Current status and contemporary issues. *Adv Drug Deliv Rev*, 116, 100-118.

Levy, M., Blacher, E., Elinav, E. (2017). Microbiome, metabolites and host immunity. *Curr Opin Microbiol*, 35, 8-15.

Li, G., Young, K.D. (2013). Indole production by the tryptophanase TnaA in Escherichia coli is determined by the amount of exogenous tryptophan. *Microbiology (Reading)*, 159, 402-410.

Li, H., Illes, P., Karunaratne, C.V., Nordstrom, L.U., Luo, X., Yang, A., Qiu, Y., Kurland, I.J., Lukin, D.J., Chen, W., Jiskrova, E., Krasulova, K., Pecinkova, P., DesMarais, V.M., Liu, Q., Albanese, J.M., Akki, A., Longo, M., Coffin, B., Dou, W., Mani, S., Dvorak, Z. (2021). Deciphering structural bases of intestinal and hepatic selectivity in targeting pregnane X receptor with indole-based microbial mimics. *Bioorg Chem*, 109, 104661.

Long, M., Laier, P., Vinggaard, A.M., Andersen, H.R., Lynggaard, J., Bonefeld-Jorgensen, E.C. (2003). Effects of currently used pesticides in the AhR-CALUX assay: comparison between the human TV101L and the rat H4IIE cell line. *Toxicology*, 194, 77-93.

Ma, Q., Baldwin, K.T. (2000). 2,3,7,8-tetrachlorodibenzo-p-dioxin-induced degradation of aryl hydrocarbon receptor (AhR) by the ubiquitin-proteasome pathway. Role of the transcription activaton and DNA binding of AhR. *J Biol Chem*, 275, 8432-8.

Macfarlane, G.T., Macfarlane, S. (1997). Human colonic microbiota: ecology, physiology and metabolic potential of intestinal bacteria. *Scand J Gastroenterol Suppl*, 222, 3-9.

Marin, L., Miguelez, E.M., Villar, C.J., Lombo, F. (2015). Bioavailability of dietary polyphenols and gut microbiota metabolism: antimicrobial properties. *Biomed Res Int*, 2015, 905215.

Marinelli, L., Martin-Gallausiaux, C., Bourhis, J.M., Beguet-Crespel, F., Blottiere, H.M., Lapaque, N. (2019). Identification of the novel role of butyrate as AhR ligand in human intestinal epithelial cells. *Sci Rep*, 9, 643.

Matamoros, S., Gras-Leguen, C., Le Vacon, F., Potel, G., de La Cochetiere, M.F. (2013). Development of intestinal microbiota in infants and its impact on health. *Trends Microbiol*, 21, 167-73.

Mawe, G.M., Hoffman, J.M. (2013). Serotonin signalling in the gut--functions, dysfunctions and therapeutic targets. *Nat Rev Gastroenterol Hepatol*, 10, 473-86.

McGuire, J., Whitelaw, M.L., Pongratz, I., Gustafsson, J.A., Poellinger, L. (1994). A cellular factor stimulates ligand-dependent release of hsp90 from the basic helix-loop-helix dioxin receptor. *Mol Cell Biol*, 14, 2438-46.

Mencarelli, A., Migliorati, M., Barbanti, M., Cipriani, S., Palladino, G., Distrutti, E., Renga, B., Fiorucci, S. (2010). Pregnane-X-receptor mediates the anti-inflammatory activities of rifaximin on detoxification pathways in intestinal epithelial cells. *Biochem Pharmacol*, 80, 1700-7.

Mencarelli, A., Renga, B., Palladino, G., Claudio, D., Ricci, P., Distrutti, E., Barbanti, M., Baldelli, F., Fiorucci, S. (2011). Inhibition of NF-kappaB by a PXR-dependent pathway mediates counter-regulatory activities of rifaximin on innate immunity in intestinal epithelial cells. *Eur J Pharmacol*, 668, 317-24.

Meyer, U.A. (1996). Overview of enzymes of drug metabolism. *J Pharmacokinet Biopharm*, 24, 449-59.

Mimura, J., Ema, M., Sogawa, K., Fujii-Kuriyama, Y. (1999). Identification of a novel mechanism of regulation of Ah (dioxin) receptor function. *Genes Dev*, 13, 20-5.

Monteleone, I., Rizzo, A., Sarra, M., Sica, G., Sileri, P., Biancone, L., MacDonald, T.T., Pallone, F., Monteleone, G. (2011). Aryl hydrocarbon receptor-induced signals up-regulate IL-22 production and inhibit inflammation in the gastrointestinal tract. *Gastroenterology*, 141, 237-48, 248 e1.

Moore, D.D., Kato, S., Xie, W., Mangelsdorf, D.J., Schmidt, D.R., Xiao, R., Kliewer, S.A. (2006). International Union of Pharmacology. LXII. The NR1H and NR1I receptors: constitutive androstane receptor, pregnene X receptor, farnesoid X receptor alpha, farnesoid X receptor beta, liver X receptor alpha, liver X receptor beta, and vitamin D receptor. *Pharmacol Rev*, 58, 742-59.

Moras, D., Gronemeyer, H. (1998). The nuclear receptor ligand-binding domain: structure and function. *Curr Opin Cell Biol*, 10, 384-91.

Mulero-Navarro, S., Fernandez-Salguero, P.M. (2016). New Trends in Aryl Hydrocarbon Receptor Biology. *Front Cell Dev Biol*, 4, 45.

Murray, I.A., Perdew, G.H. (2020). How Ah Receptor Ligand Specificity Became Important in Understanding Its Physiological Function. *International Journal of Molecular Sciences*, 21.

Murre, C., McCaw, P.S., Baltimore, D. (1989). A new DNA binding and dimerization motif in immunoglobulin enhancer binding, daughterless, MyoD, and myc proteins. *Cell*, 56, 777-83.

Nebert, D.W. (2017). Aryl hydrocarbon receptor (AHR): "pioneer member" of the basic-helix/loop/helix per-Arnt-sim (bHLH/PAS) family of "sensors" of foreign and endogenous signals. *Prog Lipid Res*, 67, 38-57.

Negishi, M., Pedersen, L.G., Petrotchenko, E., Shevtsov, S., Gorokhov, A., Kakuta, Y., Pedersen, L.C. (2001). Structure and function of sulfotransferases. *Arch Biochem Biophys*, 390, 149-57.

Neve, E.P., Ingelman-Sundberg, M. (2010). Cytochrome P450 proteins: retention and distribution from the endoplasmic reticulum. *Curr Opin Drug Discov Devel*, 13, 78-85.

Nguyen, L.P., Bradfield, C.A. (2008). The search for endogenous activators of the aryl hydrocarbon receptor. *Chem Res Toxicol*, 21, 102-16.

Nishida, A., Inoue, R., Inatomi, O., Bamba, S., Naito, Y., Andoh, A. (2018). Gut microbiota in the pathogenesis of inflammatory bowel disease. *Clin J Gastroenterol*, 11, 1-10.

Noguchi, K., Katayama, K., Sugimoto, Y. (2014). Human ABC transporter ABCG2/BCRP expression in chemoresistance: basic and clinical perspectives for molecular cancer therapeutics. *Pharmgenomics Pers Med*, 7, 53-64.

Novotna, A., Korhonova, M., Bartonkova, I., Soshilov, A.A., Denison, M.S., Bogdanova, K., Kolar, M., Bednar, P., Dvorak, Z. (2014). Enantiospecific effects of ketoconazole on aryl hydrocarbon receptor. *PLoS One*, 9, e101832.

Novotna, A., Pavek, P., Dvorak, Z. (2011). Novel stably transfected gene reporter human hepatoma cell line for assessment of aryl hydrocarbon receptor transcriptional activity: construction and characterization. *Environ Sci Technol*, 45, 10133-9.

Nuclear Receptors Nomenclature, C. (1999). A unified nomenclature system for the nuclear receptor superfamily. *Cell*, 97, 161-3.

O'Malley, B.W., Qin, J., Lanz, R.B. (2008). Cracking the coregulator codes. *Curr Opin Cell Biol*, 20, 310-5.

Ohtake, F., Takeyama, K., Matsumoto, T., Kitagawa, H., Yamamoto, Y., Nohara, K., Tohyama, C., Krust, A., Mimura, J., Chambon, P., Yanagisawa, J., Fujii-Kuriyama, Y., Kato, S. (2003). Modulation of oestrogen receptor signalling by association with the activated dioxin receptor. *Nature*, 423, 545-50.

Oliphant, K., Allen-Vercoe, E. (2019). Macronutrient metabolism by the human gut microbiome: major fermentation by-products and their impact on host health. *Microbiome*, 7, 91.

Omiecinski, C.J., Vanden Heuvel, J.P., Perdew, G.H., Peters, J.M. (2011). Xenobiotic metabolism, disposition, and regulation by receptors: from biochemical phenomenon to predictors of major toxicities. *Toxicol Sci*, 120 Suppl 1, S49-75.

Orans, J., Teotico, D.G., Redinbo, M.R. (2005). The nuclear xenobiotic receptor pregnane X receptor: recent insights and new challenges. *Mol Endocrinol*, 19, 2891-900.

Ostberg, T., Bertilsson, G., Jendeberg, L., Berkenstam, A., Uppenberg, J. (2002). Identification of residues in the PXR ligand binding domain critical for species specific and constitutive activation. *Eur J Biochem*, 269, 4896-904.

Pacyniak, E.K., Cheng, X., Cunningham, M.L., Crofton, K., Klaassen, C.D., Guo, G.L. (2007). The flame retardants, polybrominated diphenyl ethers, are pregnane X receptor activators. *Toxicol Sci*, 97, 94-102.

Parks, O.B., Pociask, D.A., Hodzic, Z., Kolls, J.K., Good, M. (2015). Interleukin-22 Signaling in the Regulation of Intestinal Health and Disease. *Front Cell Dev Biol*, 3, 85.

Patel, A.B., Shaikh, S., Jain, K.R., Desai, C., Madamwar, D. (2020). Polycyclic Aromatic Hydrocarbons: Sources, Toxicity, and Remediation Approaches. *Front Microbiol*, 11, 562813.

Pavek, P., Dvorak, Z. (2008). Xenobiotic-induced transcriptional regulation of xenobiotic metabolizing enzymes of the cytochrome P450 superfamily in human extrahepatic tissues. *Curr Drug Metab*, 9, 129-43.

Pavek, P., Pospechova, K., Svecova, L., Syrova, Z., Stejskalova, L., Blazkova, J., Dvorak, Z., Blahos, J. (2010). Intestinal cell-specific vitamin D receptor (VDR)-mediated transcriptional regulation of CYP3A4 gene. *Biochem Pharmacol*, 79, 277-87.

Pawlak, M., Lefebvre, P., Staels, B. (2012). General molecular biology and architecture of nuclear receptors. *Curr Top Med Chem*, 12, 486-504.

Perez-Munoz, M.E., Arrieta, M.C., Ramer-Tait, A.E., Walter, J. (2017). A critical assessment of the "sterile womb" and "in utero colonization" hypotheses: implications for research on the pioneer infant microbiome. *Microbiome*, 5, 48.

Peters, J.C. (1991). Tryptophan nutrition and metabolism: an overview. *Adv Exp Med Biol*, 294, 345-58.

Petrulis, J.R., Perdew, G.H. (2002). The role of chaperone proteins in the aryl hydrocarbon receptor core complex. *Chem Biol Interact*, 141, 25-40.

Petzinger, E., Geyer, J. (2006). Drug transporters in pharmacokinetics. *Naunyn Schmiedebergs Arch Pharmacol*, 372, 465-75.

Phang-Lyn, S., Llerena, V.A. (2021). Biochemistry, Biotransformation, StatPearls. Treasure Island (FL).

Phillips, I.R., Phillips, I.R., Shephard, E.A., SpringerLink (2006). Cytochrome P450 protocols, 2nd ed. *Humana Press : Imprint: Humana*, Totowa, N.J

Pierre, S., Chevallier, A., Teixeira-Clerc, F., Ambolet-Camoit, A., Bui, L.C., Bats, A.S., Fournet, J.C., Fernandez-Salguero, P., Aggerbeck, M., Lotersztajn, S., Barouki, R., Coumoul, X. (2014). Aryl hydrocarbon receptor-dependent induction of liver fibrosis by dioxin. *Toxicol Sci*, 137, 114-24.

Pichard-Garcia, L., Gerbal-Chaloin, S., Ferrini, J.B., Fabre, J.M., Maurel, P. (2002). Use of long-term cultures of human hepatocytes to study cytochrome P450 gene expression. *Methods Enzymol*, 357, 311-21.

Platten, M., Nollen, E.A.A., Rohrig, U.F., Fallarino, F., Opitz, C.A. (2019). Tryptophan metabolism as a common therapeutic target in cancer, neurodegeneration and beyond. *Nat Rev Drug Discov*, 18, 379-401.

Poland, A., Glover, E., Kende, A.S. (1976). Stereospecific, high affinity binding of 2,3,7,8-tetrachlorodibenzo-p-dioxin by hepatic cytosol. Evidence that the binding species is receptor for induction of aryl hydrocarbon hydroxylase. *J Biol Chem*, 251, 4936-46.

Pondugula, S.R., Flannery, P.C., Abbott, K.L., Coleman, E.S., Mani, S., Samuel, T., Xie, W. (2015). Diindolylmethane, a naturally occurring compound, induces CYP3A4 and MDR1 gene expression by activating human PXR. *Toxicol Lett*, 232, 580-9.

Pondugula, S.R., Mani, S. (2013). Pregnane xenobiotic receptor in cancer pathogenesis and therapeutic response. *Cancer Letters*, 328, 1-9.

Pongratz, I., Mason, G.G., Poellinger, L. (1992). Dual roles of the 90-kDa heat shock protein hsp90 in modulating functional activities of the dioxin receptor. Evidence that the dioxin receptor functionally belongs to a subclass of nuclear receptors which require hsp90 both for ligand binding activity and repression of intrinsic DNA binding activity. *J Biol Chem*, 267, 13728-34.

Poulain-Godefroy, O., Boute, M., Carrard, J., Alvarez-Simon, D., Tsicopoulos, A., de Nadai, P. (2020). The Aryl Hydrocarbon Receptor in Asthma: Friend or Foe? *Int J Mol Sci*, 21.

Powell, D.N., Swimm, A., Sonowal, R., Bretin, A., Gewirtz, A.T., Jones, R.M., Kalman, D. (2020). Indoles from the commensal microbiota act via the AHR and IL-10 to tune the cellular composition of the colonic epithelium during aging. *Proc Natl Acad Sci U S A*, 117, 21519-21526.

Puga, A., Barnes, S.J., Dalton, T.P., Chang, C., Knudsen, E.S., Maier, M.A. (2000). Aromatic hydrocarbon receptor interaction with the retinoblastoma protein potentiates repression of E2F-dependent transcription and cell cycle arrest. *J Biol Chem*, 275, 2943-50.

Qiu, J., Zhou, L. (2013). Aryl hydrocarbon receptor promotes RORgammat(+) group 3 ILCs and controls intestinal immunity and inflammation. *Semin Immunopathol*, 35, 657-70.

Qiu, Z., Cervantes, J.L., Cicek, B.B., Mukherjee, S., Venkatesh, M., Maher, L.A., Salazar, J.C., Mani, S., Khanna, K.M. (2016). Pregnane X Receptor Regulates Pathogen-Induced Inflammation and Host Defense against an Intracellular Bacterial Infection through Toll-like Receptor 4. *Sci Rep*, 6, 31936.

Rannug, U., Rannug, A., Sjoberg, U., Li, H., Westerholm, R., Bergman, J. (1995). Structure elucidation of two tryptophan-derived, high affinity Ah receptor ligands. *Chem Biol*, 2, 841-5.

Rasmussen, M.K., Balaguer, P., Ekstrand, B., Daujat-Chavanieu, M., Gerbal-Chaloin, S. (2016). Skatole (3-Methylindole) Is a Partial Aryl Hydrocarbon Receptor Agonist and Induces CYP1A1/2 and CYP1B1 Expression in Primary Human Hepatocytes. *PLoS One*, 11, e0154629.

Rasmussen, M.K., Daujat-Chavanieu, M., Gerbal-Chaloin, S. (2017). Activation of the aryl hydrocarbon receptor decreases rifampicin-induced CYP3A4 expression in primary human hepatocytes and HepaRG. *Toxicol Lett*, 277, 1-8.

Reigstad, C.S., Salmonson, C.E., Rainey, J.F., 3rd, Szurszewski, J.H., Linden, D.R., Sonnenburg, J.L., Farrugia, G., Kashyap, P.C. (2015). Gut microbes promote colonic serotonin production through an effect of short-chain fatty acids on enterochromaffin cells. *FASEB J*, 29, 1395-403.

Ridlon, J.M., Bajaj, J.S. (2015). The human gut sterolbiome: bile acid-microbiome endocrine aspects and therapeutics. *Acta Pharm Sin B*, 5, 99-105.

Roager, H.M., Licht, T.R. (2018). Microbial tryptophan catabolites in health and disease. *Nat Commun*, 9, 3294.

Robinson-Rechavi, M., Escriva Garcia, H., Laudet, V. (2003). The nuclear receptor superfamily. *J Cell Sci*, 116, 585-6.

Rosser, E.C., Piper, C.J.M., Matei, D.E., Blair, P.A., Rendeiro, A.F., Orford, M., Alber, D.G., Krausgruber, T., Catalan, D., Klein, N., Manson, J.J., Drozdov, I., Bock, C., Wedderburn, L.R., Eaton, S., Mauri, C. (2020). Microbiota-Derived Metabolites Suppress Arthritis by Amplifying Aryl-Hydrocarbon Receptor Activation in Regulatory B Cells. *Cell Metab*, 31, 837-851 e10.

Roth, M., Obaidat, A., Hagenbuch, B. (2012). OATPs, OATs and OCTs: the organic anion and cation transporters of the SLCO and SLC22A gene superfamilies. *Br J Pharmacol*, 165, 1260-87.

Rothhammer, V., Quintana, F.J. (2019). The aryl hydrocarbon receptor: an environmental sensor integrating immune responses in health and disease. *Nat Rev Immunol*, 19, 184-197.

Saha, S., Rajpal, D.K., Brown, J.R. (2016). Human microbial metabolites as a source of new drugs. *Drug Discov Today*, 21, 692-8.

Santiveri, C.M., Jimenez, M.A. (2010). Tryptophan residues: scarce in proteins but strong stabilizers of beta-hairpin peptides. *Biopolymers*, 94, 779-90.

Sekirov, I., Russell, S.L., Antunes, L.C., Finlay, B.B. (2010). Gut microbiota in health and disease. *Physiol Rev*, 90, 859-904.

Seok, S.H., Ma, Z.X., Feltenberger, J.B., Chen, H., Chen, H., Scarlett, C., Lin, Z., Satyshur, K.A., Cortopassi, M., Jefcoate, C.R., Ge, Y., Tang, W., Bradfield, C.A., Xing, Y. (2018). Trace derivatives of kynurenine potently activate the aryl hydrocarbon receptor (AHR). *J Biol Chem*, 293, 1994-2005.

Shah, R., John, S. (2022). Cholestatic Jaundice, StatPearls. Treasure Island (FL).

Shah, Y.M., Ma, X., Morimura, K., Kim, I., Gonzalez, F.J. (2007). Pregnane X receptor activation ameliorates DSS-induced inflammatory bowel disease via inhibition of NF-kappaB target gene expression. *Am J Physiol Gastrointest Liver Physiol*, 292, G1114-22.

Shukla, S.J., Nguyen, D.T., Macarthur, R., Simeonov, A., Frazee, W.J., Hallis, T.M., Marks, B.D., Singh, U., Eliason, H.C., Printen, J., Austin, C.P., Inglese, J., Auld, D.S. (2009). Identification of pregnane X receptor ligands using time-resolved fluorescence resonance energy transfer and quantitative high-throughput screening. *Assay Drug Dev Technol*, 7, 143-69.

Schiering, C., Wincent, E., Metidji, A., Iseppon, A., Li, Y., Potocnik, A.J., Omenetti, S., Henderson, C.J., Wolf, C.R., Neberts, D.W., Stockinger, B. (2017). Feedback control of AHR signalling regulates intestinal immunity. *Nature*, 542, 242-245.

Schwabe, J.W., Chapman, L., Finch, J.T., Rhodes, D. (1993). The crystal structure of the estrogen receptor DNA-binding domain bound to DNA: how receptors discriminate between their response elements. *Cell*, 75, 567-78.

Sorg, O. (2014). AhR signalling and dioxin toxicity. *Toxicol Lett*, 230, 225-33.

Sousa, T., Paterson, R., Moore, V., Carlsson, A., Abrahamsson, B., Basit, A.W. (2008). The gastrointestinal microbiota as a site for the biotransformation of drugs. *Int J Pharm*, 363, 1-25.

Staudinger, J., Liu, Y., Madan, A., Habeebu, S., Klaassen, C.D. (2001). Coordinate regulation of xenobiotic and bile acid homeostasis by pregnane X receptor. *Drug Metab Dispos*, 29, 1467-72.

Staudinger, J.L., Ding, X., Lichti, K. (2006). Pregnane X receptor and natural products: beyond drug-drug interactions. *Expert Opin Drug Metab Toxicol*, 2, 847-57.

Staudinger, J.L., Goodwin, B., Jones, S.A., Hawkins-Brown, D., MacKenzie, K.I., LaTour, A., Liu, Y., Klaassen, C.D., Brown, K.K., Reinhard, J., Willson, T.M., Koller, B.H., Kliewer, S.A. (2001). The nuclear receptor PXR is a lithocholic acid sensor that protects against liver toxicity. *Proc Natl Acad Sci U S A*, 98, 3369-74.

Staudinger, J.L., Xu, C., Biswas, A., Mani, S. (2011). Post-translational modification of pregnane x receptor. *Pharmacol Res*, 64, 4-10.

Stejskalova, L., Dvorak, Z., Pavek, P. (2011). Endogenous and exogenous ligands of aryl hydrocarbon receptor: current state of art. *Curr Drug Metab*, 12, 198-212.

Stepankova, M., Bartonkova, I., Jiskrova, E., Vrzal, R., Mani, S., Kortagere, S., Dvorak, Z. (2018). Methylindoles and Methoxyindoles are Agonists and Antagonists of Human Aryl Hydrocarbon Receptor. *Mol Pharmacol*, 93, 631-644.

Stepankova, M., Krasulova, K., Doricakova, A., Kurka, O., Anzenbacher, P., Dvorak, Z. (2016). Optical isomers of dihydropyridine calcium channel blockers display enantiospecific effects on the expression and enzyme activities of human xenobiotics-metabolizing cytochromes P450. *Toxicol Lett*, 262, 173-186.

Stockinger, B., Di Meglio, P., Gialitakis, M., Duarte, J.H. (2014). The aryl hydrocarbon receptor: multitasking in the immune system. *Annu Rev Immunol*, 32, 403-32.

Swanson, H.I. (2015). Drug Metabolism by the Host and Gut Microbiota: A Partnership or Rivalry? *Drug Metab Dispos*, 43, 1499-504.

Swanson, H.I., Chan, W.K., Bradfield, C.A. (1995). DNA binding specificities and pairing rules of the Ah receptor, ARNT, and SIM proteins. *J Biol Chem*, 270, 26292-302.

Takaki, M., Mawe, G.M., Barasch, J.M., Gershon, M.D., Gershon, M.D. (1985). Physiological responses of guinea-pig myenteric neurons secondary to the release of endogenous serotonin by tryptamine. *Neuroscience*, 16, 223-40.

Takeuchi, S., Iida, M., Yabushita, H., Matsuda, T., Kojima, H. (2008). In vitro screening for aryl hydrocarbon receptor agonistic activity in 200 pesticides using a highly sensitive reporter cell line, DR-EcoScreen cells, and in vivo mouse liver cytochrome P450-1A induction by propanil, diuron and linuron. *Chemosphere*, 74, 155-65.

Tebbens, J.D., Azar, M., Friedmann, E., Lanzendorfer, M., Pavek, P. (2018). Mathematical Models in the Description of Pregnane X Receptor (PXR)-Regulated Cytochrome P450 Enzyme Induction. *Int J Mol Sci*, 19.

Teng, S., Jekerle, V., Piquette-Miller, M. (2003). Induction of ABCC3 (MRP3) by pregnane X receptor activators. *Drug Metab Dispos*, 31, 1296-9.

Tian, Y., Ke, S., Denison, M.S., Rabson, A.B., Gallo, M.A. (1999). Ah receptor and NF-kappaB interactions, a potential mechanism for dioxin toxicity. *J Biol Chem*, 274, 510-5.

Tibbitts, J., Canter, D., Graff, R., Smith, A., Khawli, L.A. (2016). Key factors influencing ADME properties of therapeutic proteins: A need for ADME characterization in drug discovery and development. *MAbs*, 8, 229-45.

Timsit, Y.E., Negishi, M. (2007). CAR and PXR: the xenobiotic-sensing receptors. *Steroids*, 72, 231-46.

Tkachenko, A., Henkler, F., Brinkmann, J., Sowada, J., Genkinger, D., Kern, C., Tralau, T., Luch, A. (2016). The Q-rich/PST domain of the AHR regulates both ligand-induced nuclear transport and nucleocytoplasmic shuttling. *Sci Rep*, 6, 32009.

Tomova, A., Bukovsky, I., Rembert, E., Yonas, W., Alwarith, J., Barnard, N.D., Kahleova, H. (2019). The Effects of Vegetarian and Vegan Diets on Gut Microbiota. *Front Nutr*, 6, 47.

Tourino, M.C., de Oliveira, E.M., Belle, L.P., Knebel, F.H., Albuquerque, R.C., Dorr, F.A., Okada, S.S., Migliorini, S., Soares, I.S., Campa, A. (2013). Tryptamine and dimethyltryptamine inhibit indoleamine 2,3 dioxygenase and increase the tumor-reactive effect of peripheral blood mononuclear cells. *Cell Biochem Funct*, 31, 361-4.

Tremaroli, V., Backhed, F. (2012). Functional interactions between the gut microbiota and host metabolism. *Nature*, 489, 242-9.

Venkatesh, M., Mukherjee, S., Wang, H., Li, H., Sun, K., Benechet, A.P., Qiu, Z., Maher, L., Redinbo, M.R., Phillips, R.S., Fleet, J.C., Kortagere, S., Mukherjee, P., Fasano, A., Le Ven, J., Nicholson, J.K., Dumas, M.E., Khanna, K.M., Mani, S. (2014). Symbiotic bacterial metabolites regulate gastrointestinal barrier function via the xenobiotic sensor PXR and Toll-like receptor 4. *Immunity*, 41, 296-310.

Vinolo, M.A., Rodrigues, H.G., Nachbar, R.T., Curi, R. (2011). Regulation of inflammation by short chain fatty acids. *Nutrients*, 3, 858-76.

Vogel, C.F., Matsumura, F. (2009). A new cross-talk between the aryl hydrocarbon receptor and RelB, a member of the NF-kappaB family. *Biochem Pharmacol*, 77, 734-45.

Vogel, C.F., Sciullo, E., Li, W., Wong, P., Lazennec, G., Matsumura, F. (2007). RelB, a new partner of aryl hydrocarbon receptor-mediated transcription. *Mol Endocrinol*, 21, 2941-55.

Vogel, C.F.A., Van Winkle, L.S., Esser, C., Haarmann-Stemmann, T. (2020). The aryl hydrocarbon receptor as a target of environmental stressors - Implications for pollution mediated stress and inflammatory responses. *Redox Biol*, 34, 101530.

Vrzal, R., Ulrichova, J., Dvorak, Z. (2004). Aromatic hydrocarbon receptor status in the metabolism of xenobiotics under normal and pathophysiological conditions. *Biomed Pap Med Fac Univ Palacky Olomouc Czech Repub*, 148, 3-10.

Vyhlidalova, B., Krasulova, K., Pecinkova, P., Marcalikova, A., Vrzal, R., Zemankova, L., Vanco, J., Travnicek, Z., Vondracek, J., Karasova, M., Mani, S., Dvorak, Z. (2020a). Gut Microbial Catabolites of Tryptophan Are Ligands and Agonists of the Aryl Hydrocarbon Receptor: A Detailed Characterization. *Int J Mol Sci*, 21.

Vyhlidalova, B., Krasulova, K., Pecinkova, P., Poulikova, K., Vrzal, R., Andrysik, Z., Chandran, A., Mani, S., Dvorak, Z. (2020b). Antimigraine Drug Avitriptan Is a Ligand and Agonist of Human Aryl Hydrocarbon Receptor That Induces CYP1A1 in Hepatic and Intestinal Cells. *Int J Mol Sci*, 21.

Vyhlidalova, B., Poulikova, K., Bartonkova, I., Krasulova, K., Vanco, J., Travnicek, Z., Mani, S., Dvorak, Z. (2019). Mono-methylindoles induce CYP1A genes and inhibit CYP1A1 enzyme activity in human hepatocytes and HepaRG cells. *Toxicol Lett*, 313, 66-76.

Walker, A.W., Ince, J., Duncan, S.H., Webster, L.M., Holtrop, G., Ze, X., Brown, D., Stares, M.D., Scott, P., Bergerat, A., Louis, P., McIntosh, F., Johnstone, A.M., Lobley, G.E., Parkhill, J., Flint, H.J. (2011). Dominant and diet-responsive groups of bacteria within the human colonic microbiota. *ISME J*, 5, 220-30.

Walther, D.J., Peter, J.U., Bashammakh, S., Hortnagl, H., Voits, M., Fink, H., Bader, M. (2003). Synthesis of serotonin by a second tryptophan hydroxylase isoform. *Science*, 299, 76.

Wang, S., Hankinson, O. (2002). Functional involvement of the Brahma/SWI2-related gene 1 protein in cytochrome P4501A1 transcription mediated by the aryl hydrocarbon receptor complex. *J Biol Chem*, 277, 11821-7.

Wang, X., Wang, G., Shi, J., Aa, J., Comas, R., Liang, Y., Zhu, H.J. (2016). CES1 genetic variation affects the activation of angiotensin-converting enzyme inhibitors. *Pharmacogenomics J*, 16, 220-30.

Wang, Y.M., Ong, S.S., Chai, S.C., Chen, T. (2012). Role of CAR and PXR in xenobiotic sensing and metabolism. *Expert Opin Drug Metab Toxicol*, 8, 803-17.

Waxman, D.J. (1999). P450 gene induction by structurally diverse xenochemicals: central role of nuclear receptors CAR, PXR, and PPAR. *Arch Biochem Biophys*, 369, 11-23.

Weatherman, R.V., Fletterick, R.J., Scanlan, T.S. (1999). Nuclear-receptor ligands and ligand-binding domains. *Annu Rev Biochem*, 68, 559-81.

Weems, J.M., Yost, G.S. (2010). 3-Methylindole metabolites induce lung CYP1A1 and CYP2F1 enzymes by AhR and non-AhR mechanisms, respectively. *Chem Res Toxicol*, 23, 696-704.

Whitlock, J.P., Jr. (1999). Induction of cytochrome P4501A1. *Annu Rev Pharmacol Toxicol*, 39, 103-25.

Wilkinson, G.R. (2005). Drug metabolism and variability among patients in drug response. *N Engl J Med*, 352, 2211-21.

Williams, B.B., Van Benschoten, A.H., Cimermancic, P., Donia, M.S., Zimmermann, M., Taketani, M., Ishihara, A., Kashyap, P.C., Fraser, J.S., Fischbach, M.A. (2014). Discovery and characterization of gut microbiota decarboxylases that can produce the neurotransmitter tryptamine. *Cell Host Microbe*, 16, 495-503.

Wilson, A., Almousa, A., Teft, W.A., Kim, R.B. (2020). Attenuation of bile acid-mediated FXR and PXR activation in patients with Crohn's disease. *Sci Rep*, 10, 1866.

Wilson, I.D., Nicholson, J.K. (2017). Gut microbiome interactions with drug metabolism, efficacy, and toxicity. *Transl Res*, 179, 204-222.

Wishart, D.S. (2019). Metabolomics for Investigating Physiological and Pathophysiological Processes. *Physiol Rev*, 99, 1819-1875.

Wlodarska, M., Kostic, A.D., Xavier, R.J. (2015). An integrative view of microbiome-host interactions in inflammatory bowel diseases. *Cell Host Microbe*, 17, 577-91.

Wolf, I.M., Heitzer, M.D., Grubisha, M., DeFranco, D.B. (2008). Coactivators and nuclear receptor transactivation. *J Cell Biochem*, 104, 1580-6.

Xing, X., Bi, H., Chang, A.K., Zang, M.X., Wang, M., Ao, X., Li, S., Pan, H., Guo, Q., Wu, H. (2012). SUMOylation of AhR modulates its activity and stability through inhibiting its ubiquitination. *J Cell Physiol*, 227, 3812-9.

Yamaguchi, Y., Kuo, M.T. (1995). Functional analysis of aryl hydrocarbon receptor nuclear translocator interactions with aryl hydrocarbon receptor in the yeast two-hybrid system. *Biochem Pharmacol*, 50, 1295-302.

Yano, J.M., Yu, K., Donaldson, G.P., Shastri, G.G., Ann, P., Ma, L., Nagler, C.R., Ismagilov, R.F., Mazmanian, S.K., Hsiao, E.Y. (2015). Indigenous bacteria from the gut microbiota regulate host serotonin biosynthesis. *Cell*, 161, 264-76.

Yokoyama, M.T., Carlson, J.R. (1979). Microbial metabolites of tryptophan in the intestinal tract with special reference to skatole. *Am J Clin Nutr*, 32, 173-8.

Zanger, U.M., Schwab, M. (2013). Cytochrome P450 enzymes in drug metabolism: regulation of gene expression, enzyme activities, and impact of genetic variation. *Pharmacol Ther*, 138, 103-41.

Zelante, T., Iannitti, R.G., Cunha, C., De Luca, A., Giovannini, G., Pieraccini, G., Zecchi, R., D'Angelo, C., Massi-Benedetti, C., Fallarino, F., Carvalho, A., Puccetti, P., Romani, L. (2013). Tryptophan catabolites from microbiota engage aryl hydrocarbon receptor and balance mucosal reactivity via interleukin-22. *Immunity*, 39, 372-85.

Zhai, Y., Pai, H.V., Zhou, J., Amico, J.A., Vollmer, R.R., Xie, W. (2007). Activation of pregnane X receptor disrupts glucocorticoid and mineralocorticoid homeostasis. *Mol Endocrinol*, 21, 138-47.

Zhang, C.H., Ma, S.G., Delarosa, E.M., Tay, S., Sodhi, J., Musinipally, V., Chang, P., Pai, R., Halladay, J.S., Misner, D., Kenny, J.R., Hop, C.E.C.A., Khojasteh, S.C. (2014). For a series of methylindole analogs, reactive metabolite formation is a poor predictor of intrinsic cytotoxicity in human hepatocytes. *Toxicology Research*, 3, 184-190.

Zhang, J., Kuehl, P., Green, E.D., Touchman, J.W., Watkins, P.B., Daly, A., Hall, S.D., Maurel, P., Relling, M., Brimer, C., Yasuda, K., Wrighton, S.A., Hancock, M., Kim, R.B., Strom, S., Thummel, K., Russell, C.G., Hudson, J.R., Jr., Schuetz, E.G., Boguski, M.S. (2001). The human pregnane X receptor: genomic structure and identification and functional characterization of natural allelic variants. *Pharmacogenetics*, 11, 555-72.

Zhang, Z., Tang, W. (2018). Drug metabolism in drug discovery and development. *Acta Pharm Sin B*, 8, 721-732.

Zhao, H., Chen, L., Yang, T., Feng, Y.L., Vaziri, N.D., Liu, B.L., Liu, Q.Q., Guo, Y., Zhao, Y.Y. (2019). Aryl hydrocarbon receptor activation mediates kidney disease and renal cell carcinoma. *J Transl Med*, 17, 302.

Zhou, C., Tabb, M.M., Nelson, E.L., Grun, F., Verma, S., Sadatrafiei, A., Lin, M., Mallick, S., Forman, B.M., Thummel, K.E., Blumberg, B. (2006). Mutual repression between steroid and xenobiotic receptor and NF-kappaB signaling pathways links xenobiotic metabolism and inflammation. *J Clin Invest*, 116, 2280-2289.

Zhou, J., Zhai, Y., Mu, Y., Gong, H., Uppal, H., Toma, D., Ren, S., Evans, R.M., Xie, W. (2006). A novel pregnane X receptor-mediated and sterol regulatory element-binding protein-independent lipogenic pathway. *J Biol Chem*, 281, 15013-20.

Zhuo, W., Hu, L., Lv, J., Wang, H., Zhou, H., Fan, L. (2014). Role of pregnane X receptor in chemotherapeutic treatment. *Cancer Chemother Pharmacol*, 74, 217-27.

Zimmermann, M., Zimmermann-Kogadeeva, M., Wegmann, R., Goodman, A.L. (2019). Mapping human microbiome drug metabolism by gut bacteria and their genes. *Nature*, 570, 462-467.

9 CURRICULUM VITAE

Personal information

Name: Barbora Vyhlídalová

Maiden name: Jenčíková

Date of birth: 10. 01. 1993

Residence: Edvarda Beneše 333/13, Olomouc

Nationality: Czech

E-mail: vyhlidalovabara@gmail.com

Office: Department of Cell Biology and Genetics

Palacký University in Olomouc, Faculty of Science

Šlechtitelů 27

783 71 Olomouc

Czech Republic

(+420) 585 634 909

Education

Present study 2017 - 2022

PhD study in Molecular and Cell Biology in the Department of Cell Biology and Genetics, Faculty of Science, Palacký University in Olomouc

Thesis topic: Endogenous and xenobiotic indoles as modulators of the AhR and PXR signalling pathways

PhD supervisor: prof. RNDr. Zdeněk Dvořák, DrSc. et Ph.D. (moulin@email.cz)

Completed study 2015 - 2017

Master´s program in Molecular and Cell Biology, Palacký University in Olomouc

Thesis topic: Expression of opioid receptors and its influence on the treatment of gastrointestinal cancer patients

Completed study 2012 - 2015

Bachelor´s program in Molecular and Cell Biology, Palacký University in Olomouc

Thesis topic: Prognostic and predictive value of matrix metalloproteinases in colorectal cancer patients

Teaching experience

Practical courses in Genetics

Practical courses in Cell Biology II

Practical courses in Molecular Biology

Research fellowship

<u>September - November 2016</u>

Short-term research stays at University of Linköping, Department of Oncology, Institute of Clinical and Experimental Medicine, Sweden (3 months)

Participation in projects (researcher)

22-00355S – Microbial metabolite mimicry in pharmacological modulation of intestinal health (2022 – 2024)

20-00449S - Microbial catabolites of tryptophan as modulators of intestinal health via AHR (2020 - 2022)

19-00236S - The role of intestinal microbiome indole metabolites in the control of gastro-hepatic regulation of lipid and xenobiotic metabolism (2019 - 2021)

NV19-05-00220 - Activators of human aryl hydrocarbon receptor (AHR) in the therapy of inflammatory bowel disease (2019 - 2022)

Student projects IGA UP – PrF 2018-005, PrF 2019-003, PrF 2020-006, PrF 2021-005, and PrF 2022-009 of the Palacký University Olomouc

Publications

Abbott K. L., Chaudhury C. S., Chandra, A., Vishveshwara S., Dvorak Z., Jiskrova E., Poulikova K., **Vyhlidalova B.**, Mani S. and Pondugula S. R. (2019). Belinostat, at Its Clinically Relevant Concentrations, Inhibits Rifampicin-Induced CYP3A4 and MDR1 Gene Expression. *Mol Pharmacol*, 95(3): 324-334 **[IF$_{2019}$ 3.664]**

Vyhlidalova B., Poulikova K., Bartonkova I., Krasulova K., Vanco J., Travnicek Z., Mani S. and Z. Dvorak (2019). Mono-methylindoles induce CYP1A genes and inhibit CYP1A1 enzyme activity in human hepatocytes and HepaRG cells. *Toxicol Lett*, 313, 66-76 **[IF$_{2019}$ 3.569]**

Vyhlidalova B., Bartonkova I., Jiskrova E., Li H., Mani S. and Dvorak Z. (2020). Differential activation of human pregnane X receptor PXR by isomeric mono-methylated indoles in intestinal and hepatic in vitro models. *Toxicol Lett*, 324: 104-110 **[IF$_{2020}$ 4.374]**

Dvorak Z., Kopp F., Costello C. M., Kemp J. S., Li H., Vrzalova A., Stepankova M., Bartonkova I., Jiskrova E., Poulikova K., **Vyhlidalova B.**, Nordstroem L. U., Karunaratne C. V., Ranhotra H. S., Mun K. S., Naren A. P., Murray I. A., Perdew G. H., Brtko J., Toporova L., Schon A., Wallace W. G., Walton W. G., Redinbo M. R., Sun K., Beck A., Kortagere S., Neary M. C., Chandran A., Vishveshwara S., Cavalluzzi M. M., Lentini G., Cui J. Y., Gu H., March J. C., Chatterjee S., Matson A., Wright D., Flannigan K. L., Hirota S. A., Sartor R. B. and Mani S. (2020). Targeting the pregnane X receptor using microbial metabolite mimicry. *EMBO Mol Med*, 12(4): e11621 **[IF$_{2020}$ 12.137]**

Vyhlidalova B., Krasulova K., Pecinkova P., Marcalikova A., Vrzal R., Zemankova L., Vanco J., Travnicek Z., Vondracek J., Karasova M., Mani S., Dvorak Z. (2020). Gut Microbial Catabolites of Tryptophan Are Ligands and Agonists of the Aryl Hydrocarbon Receptor: A Detailed Characterization. *Int J Mol Sci*, 21(7): 2614 **[IF$_{2020}$ 5.924]**

Vyhlidalova B., Krasulova K., Pecinkova P., Poulikova K., Vrzal R., Andrysik Z., Chandran A., Mani S. and Dvorak Z. (2020). Antimigraine Drug Avitriptan Is a Ligand and Agonist of Human Aryl Hydrocarbon Receptor that Induces CYP1A1 in Hepatic and Intestinal Cells. *Int J Mol Sci* 21(8):2799 **[IF$_{2020}$ 5.924]**

Illes P., Krasulova K., **Vyhlidalova B.**, Poulikova K., Marcalikova A., Pecinkova P., Sirotova N., Vrzal R., Mani S. and Dvorak Z. (2020). Indole microbial intestinal metabolites expand the repertoire of ligands and agonists of the human pregnane X receptor. *Toxicol Lett*, 334: 87-93 **[IF$_{2020}$ 4.374]**

Grycova A., Joo H., Maier V., Illes P., **Vyhlidalova B.**, Poulikova K., Sladekova L., Nadvornik P., Vrzal R., Zemankova L., Pecinkova P., Poruba M., Zapletalova I., Vecera R., Anzenbacher P., Ehrmann J., Ondra P., Jung J.-W., Mani S., Dvorak Z. (2022). Targeting the aryl hydrocarbon receptor with microbial metabolite mimics alleviates experimental colitis in mouse. *J Med Chem* 65(9):6859-6868 **[IF$_{2021}$ 8.039]**

Conference reports

Vyhlidalova B., Poulikova K., Bartonkova I., Dvorak Z.: Methylindoles activate human pregnane X receptor. *International Meeting on 22nd MDO and 33rd JSSX*; 2018 Oct 1-5; Kanazawa; Japan; p-183.

Poulikova K., **Vyhlidalova B.**, Bartonkova I., Dvorak, Z.: Antagonists effects of carvones at human AhR. *International Meeting on 22nd MDO and 33rd JSSX*; 2018 Oct 1-5; Kanazawa; Japan; p-182.

Vyhlidalova B., Krasulova K., Poulikova K., Bartonkova I., Dvorak Z.: Dual effects of methylated indoles on CYP1A1 in human hepatocytes. *12th International ISSX meeting*; 2019 July 28-31; Portland; Oregon; p-20.

Certificate of Elsevier Language Editing Services

ELSEVIER

The following article was edited by Elsevier Language Editing Services:

**"Endogenous and xenobiotic indoles as
modulators of AhR and PXR signaling pathways"**

Authored by:

Mgr. Barbora Vyhlidalova

Date: 01-Jul-2022
Serial number: LEPHD-1256-63963981C6B3
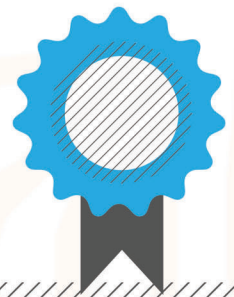
APPENDIX I.

Vyhlidalova B., Poulikova K., Bartonkova I., Krasulova K., Vanco J., Travnicek Z., Mani S., Dvorak Z. (2019): Mono-methylindoles induce CYP1A genes and inhibit CYP1A1 enzyme activity in human hepatocytes and HepaRG cells. *Toxicol Lett,* 313: 66-76. **[IF$_{2019}$ 3.569]**
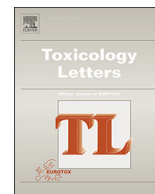
Mono-methylindoles induce CYP1A genes and inhibit CYP1A1 enzyme activity in human hepatocytes and HepaRG cells

Barbora Vyhlídalová[a], Karolína Poulíková[a], Iveta Bartoňková[a], Kristýna Krasulová[a,b], Jan Vančo[b], Zdeněk Trávníček[b], Sridhar Mani[c], Zdeněk Dvořák[a,b,*]

[a] Department of Cell Biology and Genetics, Faculty of Science, Palacky University, Slechtitelu 27, 783 71, Olomouc, Czech Republic
[b] Regional Centre of Advanced Technologies and Materials, Faculty of Science, Palacky University, Slechtitelu 27, 783 71, Olomouc, Czech Republic
[c] Department of Genetics and Department of Medicine, Albert Einstein College of Medicine, Bronx, NY, 10461, USA

GRAPHICAL ABSTRACT
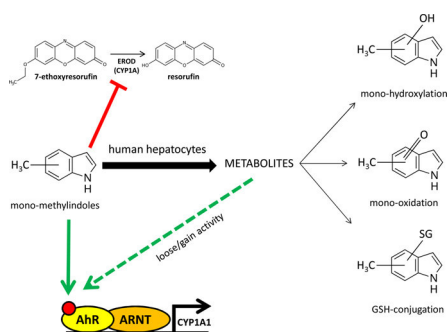
ARTICLE INFO

ABSTRACT

Mono-methylindoles (MMI) were described as agonists and/or antagonists of the human aryl hydrocarbon receptor (AhR). Here, we investigated the effects of MMI on AhR-CYP1A pathway in human hepatocytes and HepaRG cells derived from human progenitor hepatic cells. All MMI, except of 2-methylindole, strongly induced CYP1A1 and CYP1A2 mRNAs in HepaRG cells. Induction of CYP1A genes was absent in AhR-knock-out HepaRG cells. Consistently, CYP1A1 and CYP1A2 mRNAs and proteins were induced by all MMIs (except 2-methylindole), in human hepatocytes. The enzyme activity of CYP1A1 was inhibited by MMIs in human hepatocytes and LS180 colon cancer cells in a concentration-dependent manner (IC$_{50}$ values from 1.2 μM to 23.8 μM and from 3.4 μM to 11.4 μM, respectively). Inhibition of CYP1A1 activity by MMI in human liver microsomes was much weaker as compared to that in intact cells. Incubation of parental MMI with human hepatocytes either diminished (4-methylindole, 6-methylindole) or enhanced (7-methylindole) their agonist effects on AhR in AZ-AHR reporter cells. In conclusion, overall effects of MMI on AhR-CYP1A pathway in human cells comprise the induction of CYP1A genes through AhR, the inhibition of CYP1A catalytic activity and possibly the metabolic transformation causing loss or gain of AhR agonist activity of parental compounds.

1. Introduction

Aryl hydrocarbon receptor (AhR) is a central regulator of many physiologic and pathophysiologic processes and is a fundamental receptor involved in responses to xenobiotics and microbial products (Roager and Licht, 2018). At the molecular level, AhR acts as a ligand-activated transcriptional factor that binds response elements in DNA in the form of heterodimer with ARNT (AhR nuclear translocator), which is referred to as canonical signaling. Indeed, there are non-canonical (atypical) pathways described for AhR and those comprise some functions that include ARNT-independent effects (Wilson et al., 2013). Regardless, a major and unique AhR transcriptional target gene is CYP1A1 and a primary target used to assess AhR function (Hankinson, 2016; Mescher and Haarmann-Stemmann, 2018). CYP1A is also involved in the metabolism of many xenobiotics, but also in biotransformation of microbial tryptophan catabolite 3-methylindole (Lanza and Yost, 2001).

Ligands of AhR comprise wide spectrum of structurally unrelated compounds, including anthropogenic xenobiotics (e.g. polychlorinated biphenyls, polychlorinated dioxins), natural xenobiotics (e.g. flavonoids, anthocyanidins), endogenous intermediates (e.g. eicosanoids, tetrapyrroles, kynurenine) and compounds produced by intestinal microbiota (e.g. tryptophan catabolites), by pulmonary pathogens (e.g. pyocyanin) or UV irradiation in skin (indolocarbazoles) (Stejskalova et al., 2011). Different AhR ligands cause differential physiological and cellular effects, which is a general phenomenon related to ligand-receptor interaction and selective receptor-effector coupling. It is recognized that endogenous ligands of AhR have desirable biological effects while xenobiotic ligands of AhR do the opposite. Given the complex roles of AhR in human physiology and patho-physiology, the therapeutic (Roman et al., 2018) and chemopreventive targeting of AhR (Mescher and Haarmann-Stemmann, 2018) are emerging issues. A virtual black-box remains to decipher the roles for intestinal microbiome-produced AhR ligands, which may be considered both xenobiotics and endobiotics, and may have dual effects on human health. Indeed, AhR has been reported to participate in regulation of intestinal innate and mucosal immunity and that AhR activity can be modulated via intestinal indole-based microbiota-produced metabolites (Schiering et al., 2017). Several compounds, having an indole core in their structure, are AhR ligands. Besides xenobiotics, they are food-born substances, including those produced by the intestinal microbiota. The examples are diindolylmethane (Chen et al., 1998), indole-3-carbinol (Chen et al., 1996), indole-3-aldehyde (Rothhammer et al., 2016), skatole (3-methylindole) (Rasmussen et al., 2016) or indole itself, which is human AhR specific ligand (Hubbard et al., 2015). We have recently described series of methyl- and methoxy-indoles as novel ligands of AhR, acting in a context-dependent manner as full agonists, partial agonists or antagonists (Stepankova et al., 2018). In the context of methylation of simple indoles, structure-function would be crucial to know for developing skatole-like mimics as potential lead or drug-like AhR ligands, e.g. for use in the therapy of inflammatory bowel disease.

Here we report a follow-up study, with focus on the effects of simple mono-methylindoles (MMI) on AhR activation dependence in cell lines and the expression and catalytic activity of CYP1A1 in human hepatic and LS180 colon cancer in vitro models.

2. Materials and methods

2.1. Chemicals and reagents

4-Me-indole (97% purity as determined by supplier) was obtained from Energy Chemical (Shanghai, China). All other mono-methylated indoles (purity from 97% to 99% as determined by supplier), foetal bovine serum, hygromycin B, dimethylsulfoxide (DMSO) were purchased from Sigma Aldrich (Prague, Czech Republic). Reporter lysis buffer was purchased from Promega (Hercules, CA, USA) and 2,3,7,8-tetrachlorodibenzo-p-dioxin (TCDD) was from Ultra Scientific (North Kingstown, RI, USA). All other chemicals used in this research were of the highest quality commercially available.

2.2. Cell lines

Stably transfected reporter gene AZ-AHR cell line was described previously (Novotna et al., 2011). Human Caucasian colon adenocarcinoma cell line LS180 was purchased from European Collection of Cell Cultures (ECACC No. 87021202). Both AZ-AHR and LS180 cells were cultured in Dulbecco's modified Eagle's medium (DMEM) supplemented with 10% foetal bovine serum, 4 mM L-glutamine, 1% non-essential amino acids and 1 mM sodium pyruvate.

AHR knock-out (AHR-KO) and control 5 F Clone HepaRG cells were obtained from Sigma Aldrich (Prague, Czech Republic). The cells were cultured using ISOM medium as recommended by manufacturer.

Primary human hepatocyte cultures used in this study were of two origins: (i) Short-term primary human hepatocytes in monolayer batch Hep200565 (female, 21 years, Caucasian), Hep200570 (male, 64 years, unknown ethnicity), Hep200571 (male, 77 years, unknown ethnicity) and Hep220993 (female, 76 years, Caucasian) were purchased from Biopredic International (Rennes, France). (ii) Primary human hepatocytes from multiorgan donor LH75 (female, 78 years, Caucasian) were prepared at Faculty of Medicine, Palacky University Olomouc. Liver tissue was obtained from Faculty Hospital Olomouc, Czech Republic, and the tissue acquisition protocol followed the requirements issued by "Ethical Committee of the Faculty Hospital Olomouc, Czech Republic" and Transplantation law #285/2002 Coll. Primary human hepatocyte cultures were maintained in serum-free cultivation medium.

2.3. Reporter gene assay in AZ-AHR cells

AZ-AHR cells were seeded in 96-well plates and allowed to attach and stabilize for 24 h. Thereafter, AZ-AHR cells were incubated for 24 h with culture media aspired from human hepatocytes cultures, which were before that incubated for 0 h and 24 h with vehicle (DMSO; 0.1% v/v), 2,3,7,8-tetrachlorodibenzo-p-dioxin (TCDD; 5 nM), and test MMI (200 µM). Then, cells were lysed and luciferase activity was measured using Tecan Infinite M200 plate luminometer (Schoeller Instruments, Czech Republic). Experiments were performed in triplicates and data are expressed as fold induction over negative control (DMSO; 0.1% v/v).

2.4. mRNA isolation and quantitative reverse transcriptase polymerase chain reaction

Total RNA was isolated using TRI Reagent® (Sigma Aldrich, Prague, Czech Republic). The concentration and purity of total RNA was determined spectrophotometrically. 1000 ng of total RNA was used for cDNA synthesis using M-MuLV reverse transcriptase (New England Biolabs, Ipswich, MA, USA). The reverse transcription was performed in 42 °C for 60 min using Random Primers 6 (New England Biolabs, Ipswich, MA, USA) and diluted in ratio 1:4 by PCR grade water. The quantitative reverse transcriptase polymerase chain reaction (qRT-PCR) was performed on the Lightcycler 480 II using the LightCycler ® 480 Probes Master (Roche Diagnostic Corporation, Prague, Czech Republic). The levels of *CYP1A1, CYP1A2* and *GAPDH* mRNAs were determined using the Universal Probe Library probes (UPL; Roche Diagnostic Corporation, Prague, Czech Republic) in combination with specific primers as described previously (Kubesova et al., 2016). The following protocol was used: an activation step at 95 °C for 10 min was followed by 45 cycles of PCR (denaturation at 95 °C for 10 s; annealing with elongation at 60 °C for 30 s). All measurements were performed in triplicates and the gene expression was normalized to *glyceraldehyde-3-phosphate dehydrogenase* (*GAPDH*) as a house-keeping gene. Data were processed using delta-delta Ct method and expressed as fold induction

Induction of CYP1A1 and CYP1A2 mRNA by mono-methylindoles in HepaRG cells
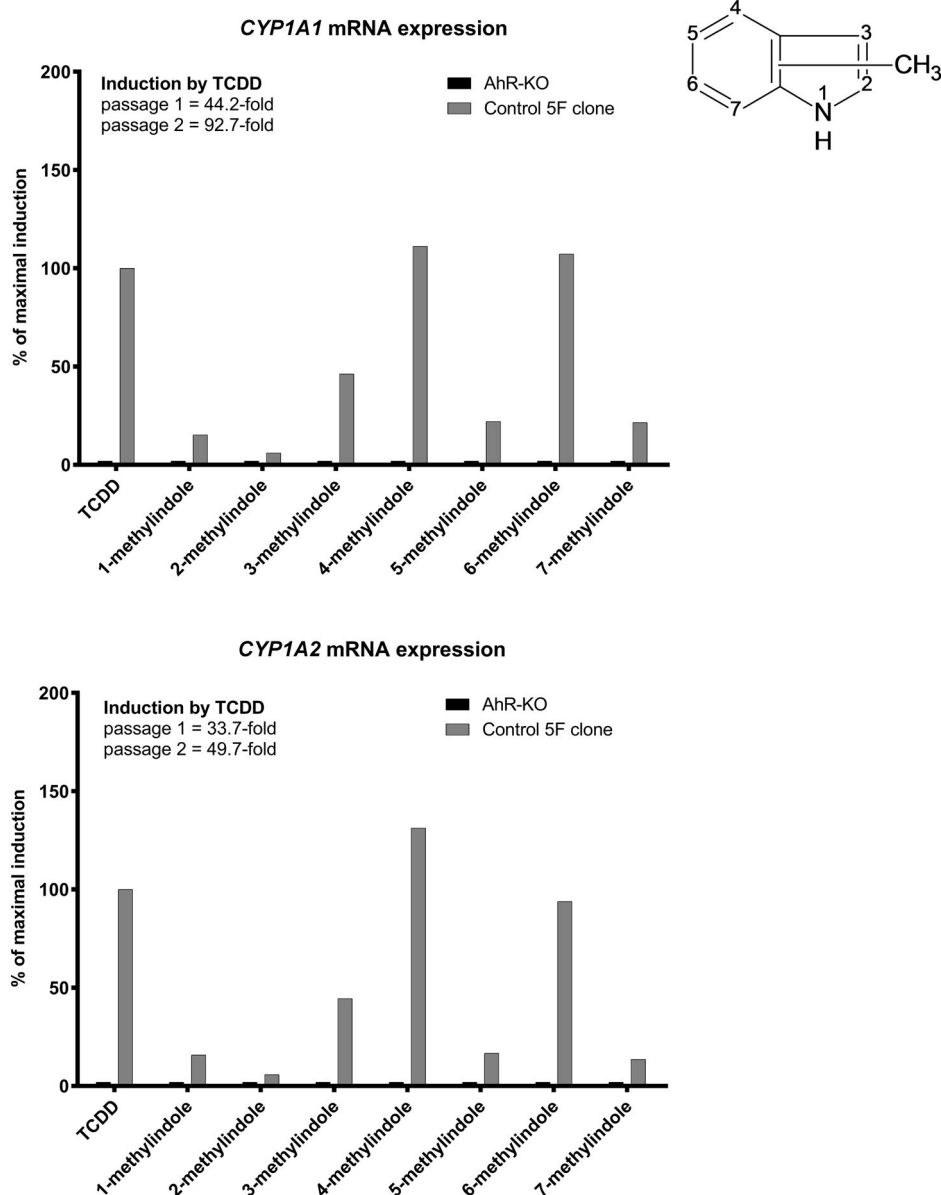
CYP1A1 mRNA expression

Induction by TCDD
passage 1 = 44.2-fold
passage 2 = 92.7-fold

- ■ AhR-KO
- ■ Control 5F clone

y-axis: % of maximal induction

x-axis: TCDD, 1-methylindole, 2-methylindole, 3-methylindole, 4-methylindole, 5-methylindole, 6-methylindole, 7-methylindole

CYP1A2 mRNA expression

Induction by TCDD
passage 1 = 33.7-fold
passage 2 = 49.7-fold

- ■ AhR-KO
- ■ Control 5F clone

y-axis: % of maximal induction

x-axis: TCDD, 1-methylindole, 2-methylindole, 3-methylindole, 4-methylindole, 5-methylindole, 6-methylindole, 7-methylindole

Fig. 1. Effects of MMI on the expression of *CYP1A1* and *CYP1A2* mRNAs in HepaRG cells. AhR knock-out (AHR-KO) and control 5 F Clone of HepaRG cells were incubated for 24 h with the vehicle (DMSO; 0.1% v/v), dioxin (TCDD; 5 nM) and mono-methylindoles (MMI; 200 μM). The expression of *CYP1A1* and *CYP1A2* mRNAs was determined by RT-PCR in two consecutive cell passages (n = 2) and the data were normalized to *GAPDH* mRNA level. RT-PCR analyses were carried out in triplicates (technical replicates).

over negative control (DMSO).

2.5. Simple western blotting by Sally Sue™

Total protein extracts were prepared using non-denaturing ice-cold lysis buffer (150 mM

NaCl; 10 mM Tris pH 7.2; 0.1% (w/v) SDS; 1% (v/v) Triton X-100; anti-phosphatase cocktail; anti-protease cocktail; 1% (v/v) sodium deoxycholate; 5 mM EDTA). The concentration of proteins was determined using Bradford reagent.

All reagents, capillaries and 384-well plates used for the simple western by Sally Sue™ were purchased from ProteinSimple (San Jose, CA, USA) and handled according to the manufacturer's instructions. CYP1A1 (mouse monoclonal, sc-393979, A-9, dilution 1:100) and CYP1A2 (mouse monoclonal, sc-53614, 3B8C1, dilution 1:1000)

primary antibodies were purchased from Santa Cruz Biotechnology Inc. (Santa Cruz, CA, USA). β-actin (mouse monoclonal; 3700S, 8H10D10, dilution 1:1000) primary antibody was obtained from Cell Signalling Technology (Denvers, Massachusetts, USA). Target proteins were detected by conjugation of specific primary antibodies with horseradish-conjugated secondary antibody followed by reaction with chemiluminescent substrate. Data were analysed using the Compass Software version 2.6.5.0 by ProteinSimple. For the purposes of quantification, signals were normalized to β-actin as a loading control and expressed as fold induction over negative control (DMSO). Note: The presented data are not recorded gels but intensity bands generated by ProteinSimple software from automated capillary electrophoresis analyses.

Induction of CYP1A1 and CYP1A2 mRNA by mono-methylindoles in human hepatocytes

Human hepatocytes culture LH75

Human hepatocytes culture HEP200565

Human hepatocytes culture HEP200570
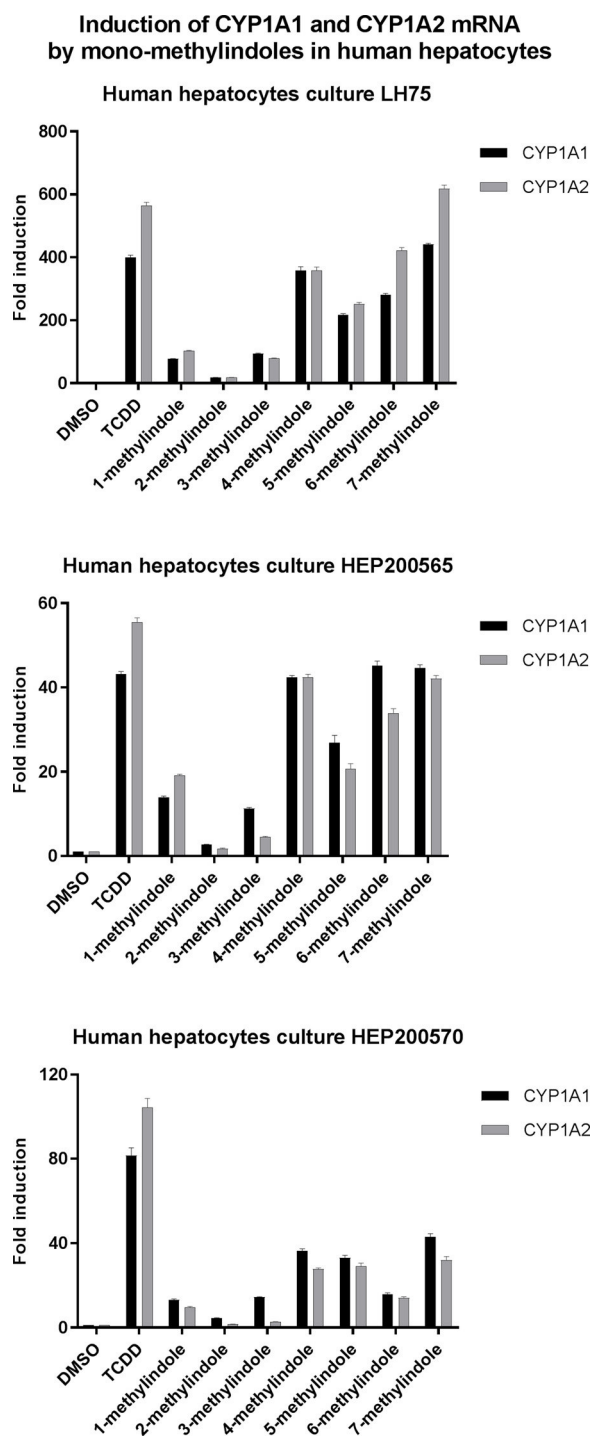
Fig. 2. Effects of MMI on the expression of *CYP1A1* and *CYP1A2* mRNAs in primary human hepatocytes. Primary human hepatocytes cultures, obtained from three liver tissue donors (n = 3) (LH75, HEP200565, HEP200570) were incubated for 24 h with the vehicle (DMSO; 0.1% v/v), dioxin (TCDD; 5 nM) and mono-methylindoles (MMI; 200 μM). The expression of *CYP1A1* and *CYP1A2* mRNAs was determined by RT-PCR and the data were normalized to *GAPDH* mRNA level. Data in each hepatocytes culture are expressed as the means ± SD from triplicate RT-PCR measurements (technical replicates).

2.6. CYP1A1 enzyme activity in human liver microsomes

XTreme 200 Pooled Human liver microsomes were obtained from XenoTech (Lenexa, KS, USA). The CYP1A1 enzyme activity was determined using P450-Glo™ CYP1A1 (Luciferin-CEE) Assay system from

Promega (Hercules, CA, USA). The reaction was performed using 96-well white plates and the luminescence signal was recorded by Tecan Infinite M200 Pro plate reader (Schoeller Instruments, Prague, Czech Republic). The amount of produced luminescence is directly proportional to CYP1A1 activity. Reaction mixtures were buffered with 100 mM K_2PO_4 (pH 7.4) and contained test compound, human liver microsomes (HLM, 1 mg/ml), specific enzyme substrate (Luciferin-CEE) and NADPH regenerating system. Tested MMI were assayed in concentrations between 0.1 μM and 200 μM. Each reaction was performed in duplicates at 37 °C, and two independent measurements were performed for each replicate. Inhibition of CYP1A1 catalytic activity was evaluated by plotting remaining percentage of activity against concentration of tested compound.

2.7. Single concentration inactivation assay in human liver microsomes

A single concentration of MMI (200 μM) and vehicle (DMSO) was pre-incubated for 30 min at 37 °C, with HLM (in amount 10-fold higher than required for the assay; 10 mg/mL) containing NADPH regenerating system. Thereafter, an aliquot from pre-incubation was incubated for additional 30 min in the buffer containing Luciferin-CEE. In parallel, a single concentration (200 μM) of MMI was pre-incubated in the absence of NADPH regenerating system, which was added as late as into the secondary incubation. The percentage of inhibition, expressing time-dependent inhibition, observed following the pre-incubation was calculated using the equation below, where R is response of the metabolite (Atkinson et al., 2005):

$$\% \ TDI = 100 \ * \ (1 \ - \ (R_{tested + NADPH}/R_{vehicle + NADPH})/(R_{tested-NADPH}/R_{vehicle-NADPH}))$$

2.8. CYP1A1 enzyme activity in LS180 cells and primary human hepatocytes

The P450-Glo™ CYP1A1 cell-based assay from Promega (Hercules, CA, USA) was used to determine CYP1A1 catalytic activity in cultured adherent cells. The amount of produced luminescence was directly proportional to CYP1A1 activity. Experiments were performed in two layouts: (i) Assessing CYP1A1 induction and inhibition by MMI: Cells were incubated for 24 h with MMI in concentrations ranging from 0.1 μM to 200 μM, vehicle (DMSO; 0.1% v/v) and TCDD (5 nM). Thereafter, enzyme substrate luciferin-CEE was applied for additional 3 h; (ii) Assessing inhibition of TCDD-induced CYP1A1 by MMI: Cells were incubated for 24 h with TCDD (5 nM). Thereafter, enzyme substrate luciferin-CEE together with MMI was applied for additional 3 h.

Two independent experiments were performed, and in each, incubations were in duplicates. Net luminescence signals were calculated by subtracting background luminescence values (no-cell control) from treated and untreated values. Induction of CYP1A1 catalytic activity was evaluated by plotting fold induction against MMI concentrations.

2.9. Metabolism of mono-methylindoles in human hepatocytes by liquid chromatography / mass spectrometry (LC/MS)

Three cultures of primary human hepatocytes (LH75, Hep200565, Hep200570) were incubated for 24 h with MMI in 200 μM concentration. Thereafter, culture media were aspired and used for reporter gene assay in AZ-AHR cells (*vide supra*) and for LC/MS analyses. Briefly, a slightly modified method of previously reported one (Zhang et al., 2014) was used for separation of metabolites using the UHPLC Dionex UltiMate 3000 (Thermo Fisher Scientific) coupled with the LCQ Fleet™ Ion Trap Mass Spectrometer (Thermo) using the electrospray ionization in positive ionization mode. The mobile phase consisted of water supplemented with 0.1% trifluoroacetic acid (TFA) and acetonitrile supplemented with 0.1% of TFA. During the 18 min analysis, the mobile

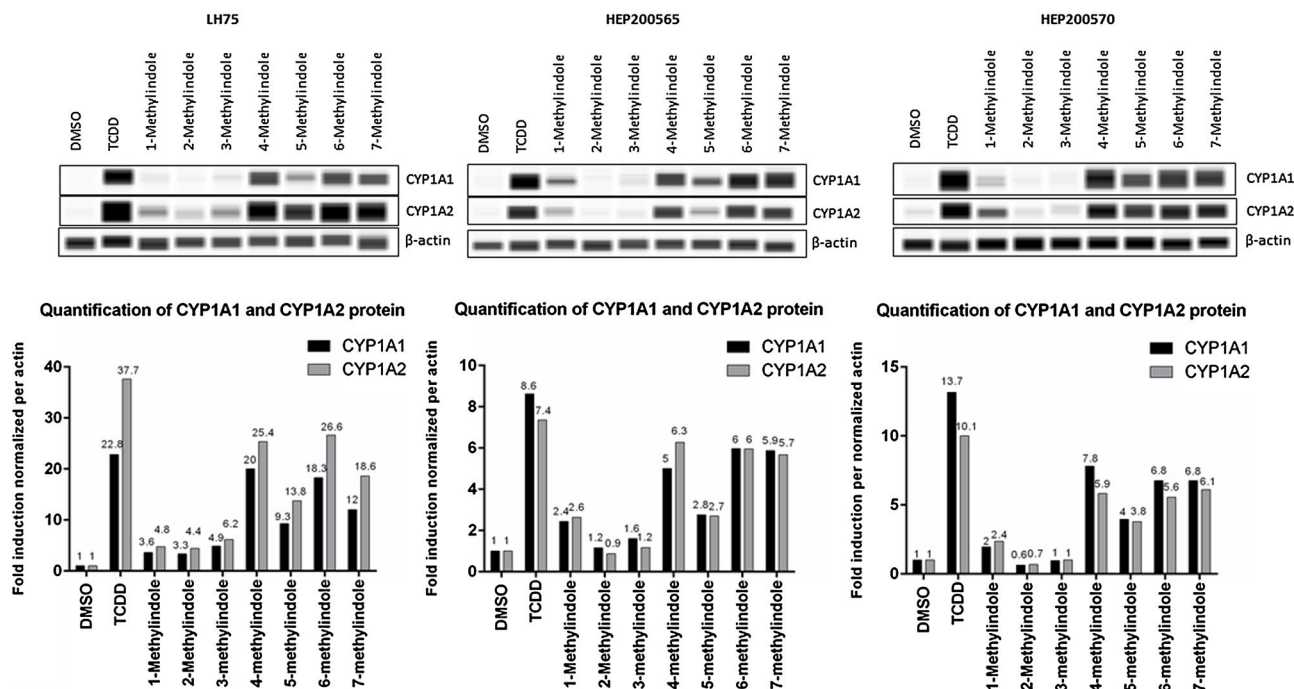**Induction of CYP1A1 and CYP1A2 proteins by mono-methylindoles in human hepatocytes**

Fig. 3. Effects of MMI on the expression of CYP1A1 and CYP1A2 proteins in primary human hepatocytes. Primary human hepatocytes from three donors (n = 3) (cultures LH75, HEP200565, HEP200570) were incubated for 24 h with the vehicle (DMSO; 0.1% v/v), dioxin (TCDD; 5 nM) and mono-methylindoles (MMI; 200 μM). The levels of CYP1A1 and CYP1A2 proteins were determined by quantitative automated western-blot analyzer SallySue. *Upper panels*: Records of CYP1A1, CYP1A2 and β-actin proteins from SallySue software: *Lower panels*: Bar graphs show quantified CYP1A1 and CYP1A2 proteins, normalized to β-actin levels. Note: The presented data are not recorded gels but intensity bands generated by ProteinSimple software from automated capillary electrophoresis analyses.

Induction of CYP1A1 catalytic activity in human hepatocytes after 24h treatment
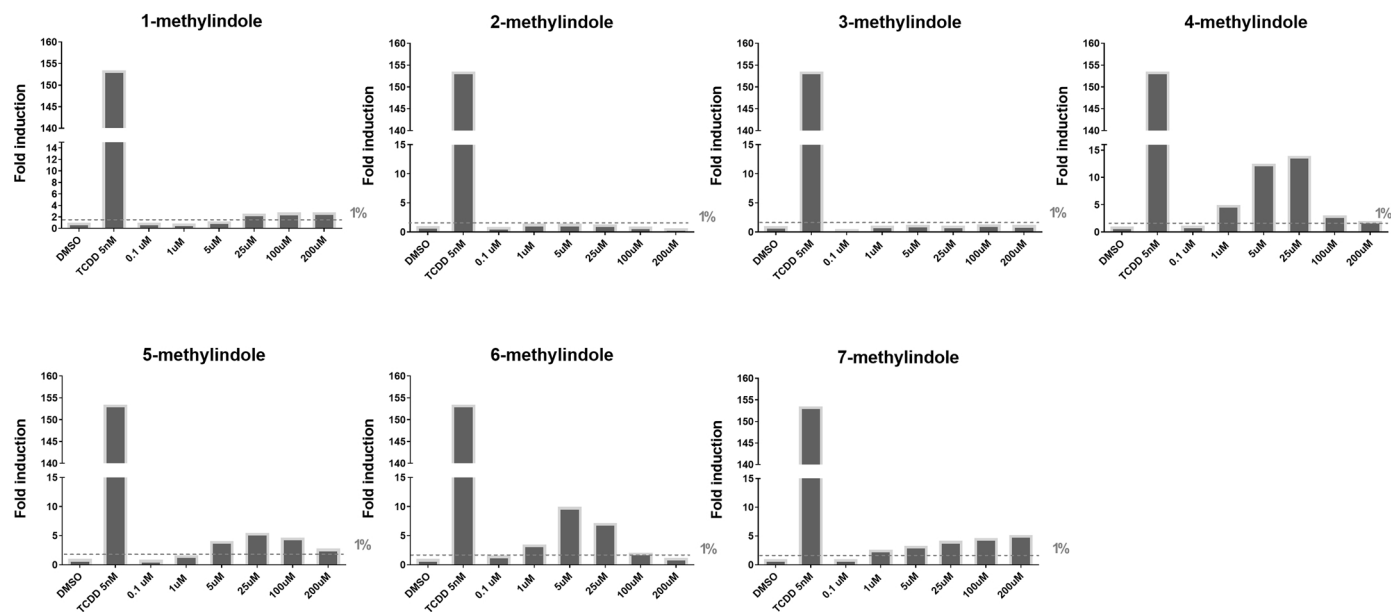
Fig. 4. Induction of CYP1A1 catalytic activity in primary human hepatocytes by mono-methylindoles. Primary human hepatocytes from two donors (n = 2) (cultures Hep200571 and Hep220993) were incubated with mono-methylindoles (0.1 μM, 1 μM, 5 μM, 25 μM, 100 μM, 200 μM), TCDD (5 nM) and vehicle (DMSO; 0.1% v/v) for 24 h. Specific CYP1A1 substrate luciferin-CEE was then applied to the cells for additional 3 h. Net luminescence signals were calculated by subtracting background luminescence values (no-cell control) from treated and untreated values. Induction of CYP1A1 catalytic activity was evaluated by plotting fold induction against MMI concentrations. Incubations were performed in two parallel wells (technical duplicates). Bar graph shows data from culture Hep220993.

Inhibition of CYP1A1 catalytic activity in human hepatocytes

	IC50 [μM]	
	Hep 200591	Hep 220993
1-methylindole	3.50	23.80
2-methylindole	1.41	7.62
3-methylindole	1.67	9.86
4-methylindole	1.40	5.31
5-methylindole	1.48	3.70
6-methylindole	1.22	4.88
7-methylindole	1.34	5.22
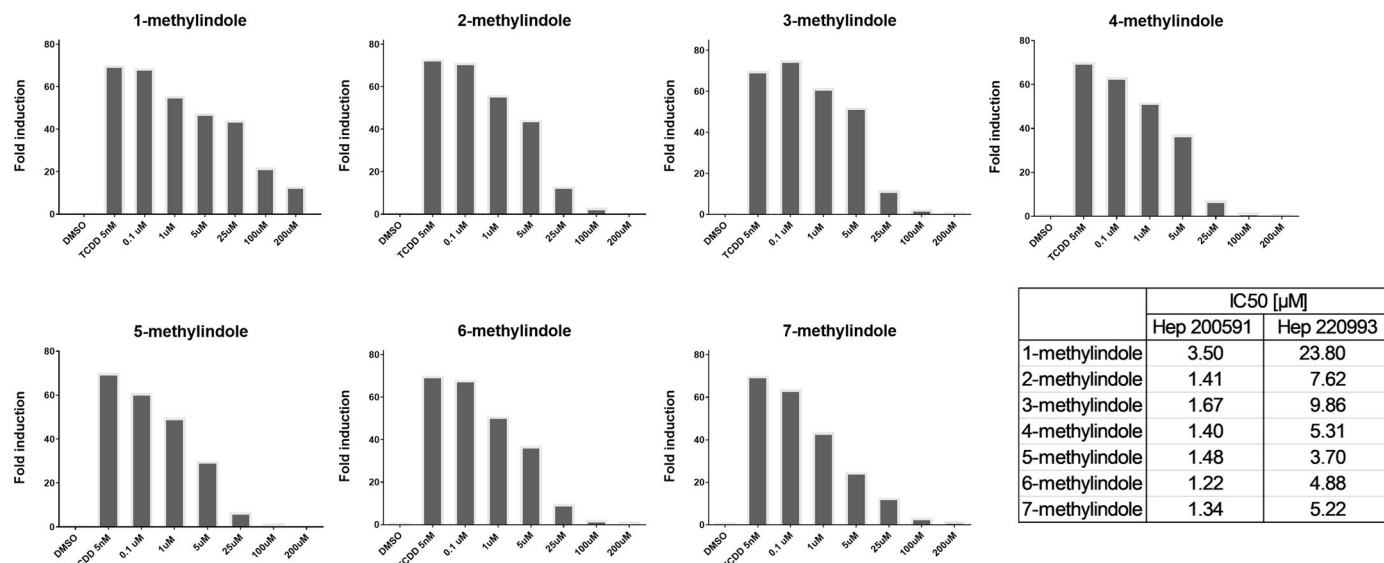
Fig. 5. Inhibition of CYP1A1 catalytic activity in primary human hepatocytes by mono-methylindoles. Primary human hepatocytes from two donors (n = 2) (cultures Hep200571 and Hep220993) were pre-incubated with 5 nM TCDD for 24 h. Thereafter, mono-methylindoles (0.1 μM, 1 μM, 5 μM, 25 μM, 100 μM, 200 μM) in the mixture with specific CYP1A1 substrate luciferin-CEE were applied to the cells for 3 h. Incubations were performed in two parallel wells (technical duplicates). Bar graph shows data from culture Hep220993. The values of IC_{50} were calculated using data from both cultures and inserted in the figure (bottom right).

Induction of CYP1A1 catalytic activity in LS180 cells after 24h treatment
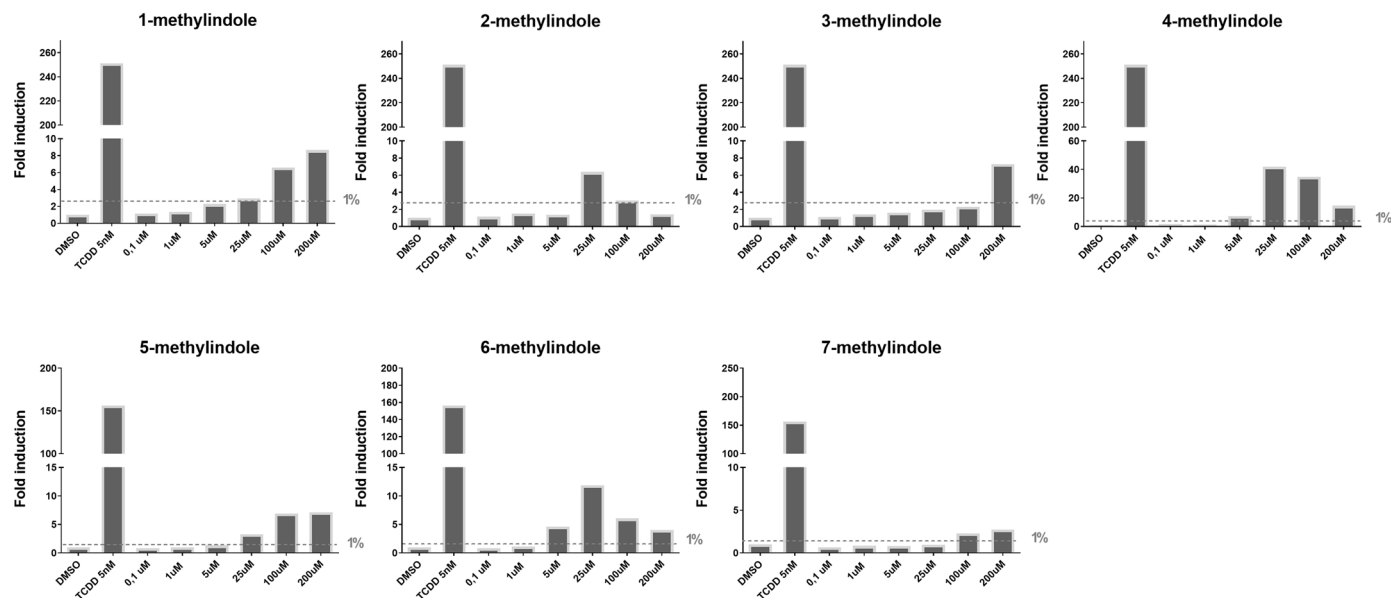
Fig. 6. Induction of CYP1A1 catalytic activity in LS180 cells by mono-methylindoles. Intestinal LS180 cells were plated and stabilized for 24 h. Thereafter, cells were incubated with mono-methylindoles (0.1 μM, 1 μM, 5 μM, 25 μM, 100 μM, 200 μM), TCDD (5 nM) and vehicle (DMSO; 0.1% v/v) for 24 h. Specific CYP1A1 substrate luciferin-CEE was then applied to the cells for additional 3 h. Net luminescence signals were calculated by subtracting background luminescence values (no-cell control) from treated and untreated values. Induction of CYP1A1 catalytic activity was evaluated by plotting fold induction against MMI concentrations. Two independent experiments were performed, and in each, incubations were in duplicates.

phase gradient was used starting with 95% of water for 1 min, followed by the linear gradient to 15 min down to 5% of water, followed by the rapid linear gradient to 18 min reconstituting the starting 95% of water. The stable mobile phase flow of 0.5 mL/min was applied at the reverse-phase chromatographic column Agilent Poroshell 120 EC-C18, 4.6 × 50 mm, 2.7 μm particle size. The PDA detector was set to the detection wavelengths of 254 ± 4 nm, 210 ± 4 nm, 225 ± 4 nm (used for quantification of residual levels of MMI) and 350 ± 4 nm and the MS analyser was set to detect the mass range of 50–2000 m/z. The sample volume applied to the column was 10 μl in all cases. All samples were analysed in three parallel determinations and the LC/MS data were analysed using the Thermo Excalibur 2.2 Qual Browser (Thermo).

Inhibition of CYP1A1 catalytic activity in LS180 cells

	IC$_{50}$ [μM] (n=2)
1-methylindole	11.44 ± 1.40
2-methylindole	5.71 ± 0.93
3-methylindole	7.56 ± 0.92
4-methylindole	4.63 ± 1.88
5-methylindole	4.82 ± 0.99
6-methylindole	3.39 ± 0.75
7-methylindole	10.44 ± 0.95
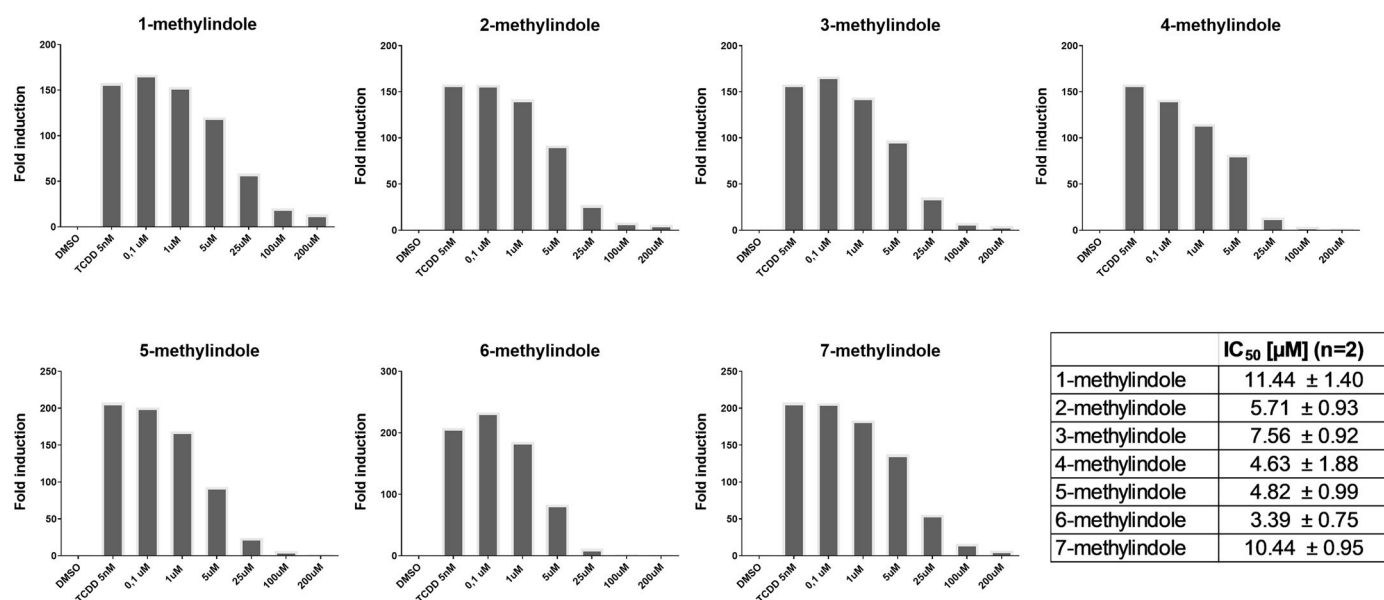
Fig. 7. Inhibition of CYP1A1 catalytic activity in LS180 cells by mono-methylindoles. Intestinal LS180 cells were plated and stabilized for 24 h, prior to the incubation with 5 nM TCDD for additional 24 h. Thereafter, mono-methylindoles (0.1 μM, 1 μM, 5 μM, 25 μM, 100 μM, 200 μM) in the mixture with specific CYP1A1 substrate luciferin-CEE were applied to the cells for 3 h. Two independent experiments (biological replicates) were performed, and in each, incubations were in duplicates (technical replicates). The values of IC$_{50}$ were calculated and inserted in the figure (bottom right).

2.10. Statistics

In order to determine significantly different results over negative control (vehicle; DMSO; 0.1%), one-way analysis of variance (ANOVA) followed by Dunnett's test was applied. The result was considered significant if the p-value was lower than 0.05. Prior to the ANOVA, the normality of data was checked using the Shapiro-Wilk normality test. The IC$_{50}$ calculations were determined using the nonlinear regression fitting by least-square method. The D'Agostino-Pearson omnibus normality test was applied and strict convergence criteria were selected to verify the normality of the data. The R-squared value was checked in all of the calculations and did not drop below 0.7. All the calculations were performed using GraphPad Prism version 8.0 for Windows (GraphPad Software, La Jolla, CA).

3. Results

3.1. Mono-methylindoles induce CYP1A1 and CYP1A2 mRNAs in HepaRG cell by AhR-dependent mechanism

In the first series of experiments, we examined the effects of MMI on the expression of *CYP1A1* and *CYP1A2* mRNAs, which are prototypical AhR-dependent genes (Fig. 1). We used progenitor hepatic cells HepaRG that are highly competent for induction studies of xenobiotic-metabolizing genes. Control clone (5 F) and AhR knock-out variant of HepaRG cells (AhR-KO) were incubated for 24 h with vehicle (DMSO; 0.1%), model CYP1A inducer dioxin (TCDD; 5 nM) and test MMI (200 μM). The expression of *CYP1A* genes was determined by the means of RT-PCR. In two consecutive passages of 5 F-HepaRG cells, dioxin strongly induced CYP1A1 (44-fold and 93-fold) and CYP1A2 (34-fold and 50-fold) mRNA. Derivatives 4-methylindole and 6-methyl indole induced *CYP1A* genes with efficacy similar to that of TCDD (~100%). Modest but variable levels of *CYP1A* induction was achieved by 1-methylindole (~15%), 3-methyl indole (~50%), 5-methylindole (~20%) and 7-methylindole (~20%), while 2-methylindole was nearly inactive. MMI did not induce CYP1A1 mRNA in AhR-KO-HepaRG cells (Fig. 1).

3.2. Mono-methylindoles induce CYP1A1 and CYP1A2 mRNAs and proteins in primary human hepatocytes

We also examined the effects of MMI on the expression of CYP1A1 and CYP1A2 mRNAs and proteins in primary human hepatocytes cultures, obtained from three different donors of liver tissue (Figs. 2 and 3). Human hepatocytes were incubated for 24 h with vehicle (DMSO; 0.1%), dioxin (TCDD; 5 nM) and MMI (200 μM). The expression of *CYP1A* genes was determined by the means of RT-PCR. The levels of CYP1A1 and CYP1A2 proteins were determined by quantitative automated western-blot analyzer SallySue. Dioxin strongly induced CYP1A1 and CYP1A2 mRNAs and proteins in all three human hepatocytes cultures. The effects of MMI were highly consistent between individual human hepatocytes cultures and the changes in the expression of *CYP1A1* and *CYP1A2* mRNAs were followed by the same trend at the levels of CYP1A1 and CYP1A2 proteins. Strong inducers of CYP1A1 and CYP1A2 were MMI methylated at positions 4, 5, 6 and 7. Modest induction of CYP1A was achieved by 1-methylindole and 3-methylindole, while 2-methylindole had no effect (Figs. 2 and 3). The effects of MMI on *CYP1A* expression in human hepatocytes are in accordance with those observed in HepaRG cells. The exception was 7-methylindole, which was modest *CYP1A* inducer in HepaRG cells (Fig. 1) and in LS180 intestinal cells (Stepankova et al., 2018), but strong inducer in all human hepatocytes cultures (Fig. 2). Such a behavior indicates possible metabolic enhancement of 7-methylindole AhR-activity by human hepatocytes.

Note: The presented data of CYP1A1, CYP1A2 and β-actin proteins are not recorded gels but intensity bands generated by ProteinSimple software from automated capillary electrophoresis analyses.

3.3. Effects of mono-methylindoles on CYP1A1 catalytic activity in cultured human hepatocytes and LS180 cells

Since prototypical functional endpoint of AhR-dependent gene induction is the expression of CYP1A1 enzyme, we assayed the effects of MMI on CYP1A1 catalytic activity in cell cultures, using primary human
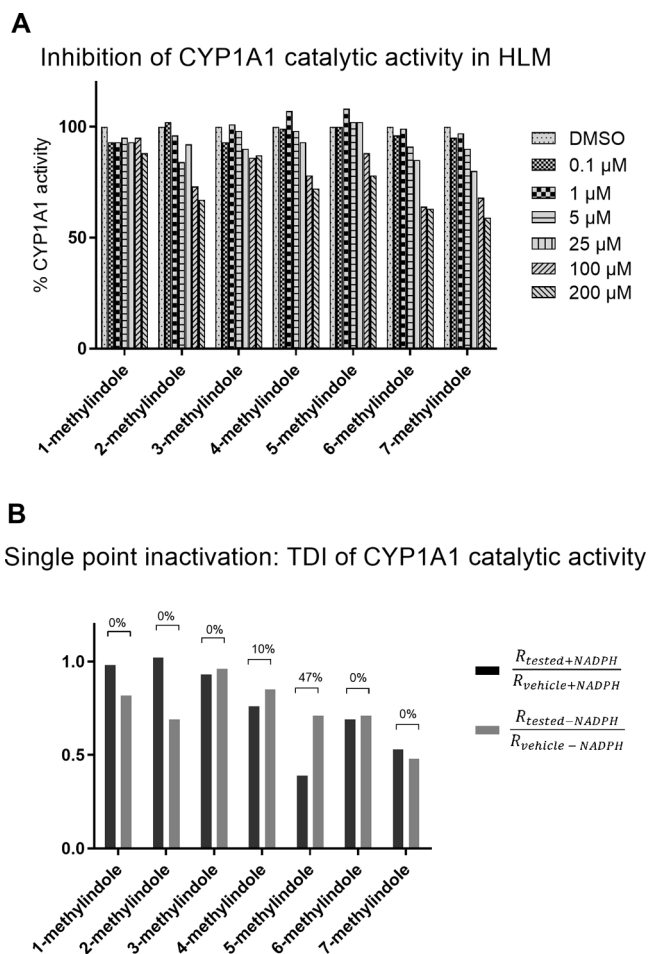
A

Inhibition of CYP1A1 catalytic activity in HLM

B

Single point inactivation: TDI of CYP1A1 catalytic activity

Fig. 8. Effects of mono-methylindoles on catalytic activity of CYP1A1 in human liver microsomes. Inhibition of CYP1A1 activity by MMI in HLM was assessed using specific enzyme substrate Luciferin-CEE. Two independent experiments were performed, with measurements in duplicates. **_Panel A_**: MMI were used in concentrations 0.1 μM, 1 μM, 5 μM, 25 μM, 100 μM and 200 μM. Inhibition of enzyme activity was expressed as the mean ± SD and bar graph shows *per* cents of remaining activity relative to the control (100%, without MMI). **_Panel B_**: Single point inactivation assay, using 200 μM concentration of MMI. Bar graph shows the percentage of inhibition, expressing time-dependent inhibition (TDI) (for details see Materials and Methods).

hepatocytes and intestinal LS180 cells. Importantly, measuring CYP1A1 catalytic activity comprises the information about the amount (induction or degradation) and catalytic activity (inhibition) of CYP1A1 enzyme. Therefore, experiments were performed in two layouts: (i) Assessing CYP1A1 induction and inhibition: Cells were incubated for 24 h with MMI (0.1 μM - 200 μM); thereafter, enzyme substrate luciferin-CEE was applied for additional 3 h (Fig. 4; Fig. 6); (ii) Assessing inhibition of TCDD-induced CYP1A1: Cells were incubated for 24 h with TCDD (5 nM). Thereafter, enzyme substrate luciferin-CEE together with MMI (0.1 μM - 200 μM) was applied for additional 3 h (Fig. 5; Fig. 7). The induction of CYP1A1 enzyme activity by TCDD in human hepatocytes cultures Hep200571 and Hep220993 was 11-fold and 153-fold, respectively. No induction was observed in human hepatocytes incubated with 2-methylindole and 3-methylindole. Concentration-dependent induction of CYP1A1 activity was attained by 1-methylindole and 7-methylindole, but the relative efficacy was very weak (~2%) as compared to TCDD. Inverse U-shaped, concentration-dependent profiles of CYP1A1 induction, peaking between 5 μM and 25 μM, were observed for 4-methylindole, 5-methylindole and 6-methylindole (Fig. 4). Catalytic activity of CYP1A1 was concentration-dependently inhibited by all tested MMI, in human hepatocytes pre-incubated for

24 h with TCDD, with IC_{50} values ranging from 1.2 μM to 23.8 μM (Fig. 5).

The induction of CYP1A1 catalytic activity in LS180 cells by TCDD ranged from 150-fold to 250-fold as compared to vehicle-treated cells. All tested MMI induced CYP1A1 catalytic activity in LS180 cells, yielding distinct concentration-response profiles. Concentration-dependent pattern was observed for 1-methylindole, 3-methylindole, 5-methylindole and 7-methylindole. In contrast, inverse U-shape profiles were observed for 2-methylindole, 4-methylindole and 6-methylindole, peaking at 25 μM concentration. Maximal relative efficacies of MMI ranged from 2% to 25%, as compared to 5 nM TCDD (Fig. 6). All tested MMI inhibited concentration-dependently CYP1A1 catalytic activity in TCDD-pre-incubated LS180 cells, with IC_{50} values ranging from 3.4 μM to 11.4 μM (Fig. 7).

3.4. Enzyme kinetic of CYP1A1 in human liver microsomes by mono-methylindoles

Inhibition of CYP1A1 activity by MMI in HLM was assessed using specific enzyme substrate Luciferin-CEE. Tested MMI were used in concentrations 0.1 μM, 1 μM, 5 μM, 25 μM, 100 μM and 200 μM. With exception of 1-methylindole, all MMI caused concentration-dependent inhibition of CYP1A1 activity. However, these effects were rather moderate and IC_{50} values were not reached even at 200 μM concentrations of MMI (Fig. 8A). We also performed a *single concentration inactivation assay*, using 200 μM concentration of MMI. This assay allows uncovering time-dependent inhibition (TDI) of CYP1A1, which refers to a change in potency during an *in vitro* incubation. We observed TDI for 4-methylindole (10%) and 5-methylindole (47%) (Fig. 8B). Potential mechanisms may include the formation of inhibitory metabolites or mechanism-based inhibition.

3.5. Agonist activity of mono-methylindoles at AhR is altered after pre-incubation with human hepatocytes

Indoles undergo cytochrome P450-mediated oxidative metabolic transformation, as documented in literature (Gillam et al., 2000) or in our microsomal time-dependent inhibition assay (Fig. 8). Therefore, we collected culture media from human hepatocytes incubated for 0 h and 24 h with MMI, and we subjected these samples to reporter gene assay in AZ-AHR cells to find out, whether biotransformation alters AhR agonist activity of parental MMI. Firstly, we proved that the application of ISOM culture medium from human hepatocytes does not influence the responsivity of AZ-AHR cells to AhR agonists as compared to common DMEM medium (Fig. 9D). Pre-incubation of 4-methylindole and 6-methylindole with three different human hepatocytes cultures (LH75, Hep200565, Hep200570) led to drastic diminution of AhR-agonist activity of these two derivatives. In lesser extent, AhR-agonist activity of 3-methylindole also dropped. In contrast, 7-methylindole, which is weak agonist of AhR, gained strong AhR-agonist activity after the incubation with human hepatocytes (Fig. 9). These data reveal that hepatic cells transform MMI into metabolites with altered AhR-agonist activities.

3.6. Metabolism of mono-methylindoles in primary human hepatocytes

In final series of experiments, we performed liquid chromatography / mass spectrometry (LC/MS) analyzes of culture media from three human hepatocytes cultures incubated with MMI. The concentration of parental MMI in culture media drastically dropped after incubation with human hepatocytes; in the samples treated with 1-methylindole, no residual MMI was detected after 24 h. In case of the samples treated with other MMI, the residual concentrations of MMI were in the range of 6.3–35.9 % of the initial 200 μM concentration and apparent differences were observed between the three cultures of used hepatocytes (Fig. 10A). The causes for such a decrease of MMI in media may

AhR dependent luciferase induction in AZ-AHR cells by metabolites of mono-methylindoles from Human Hepatocytes
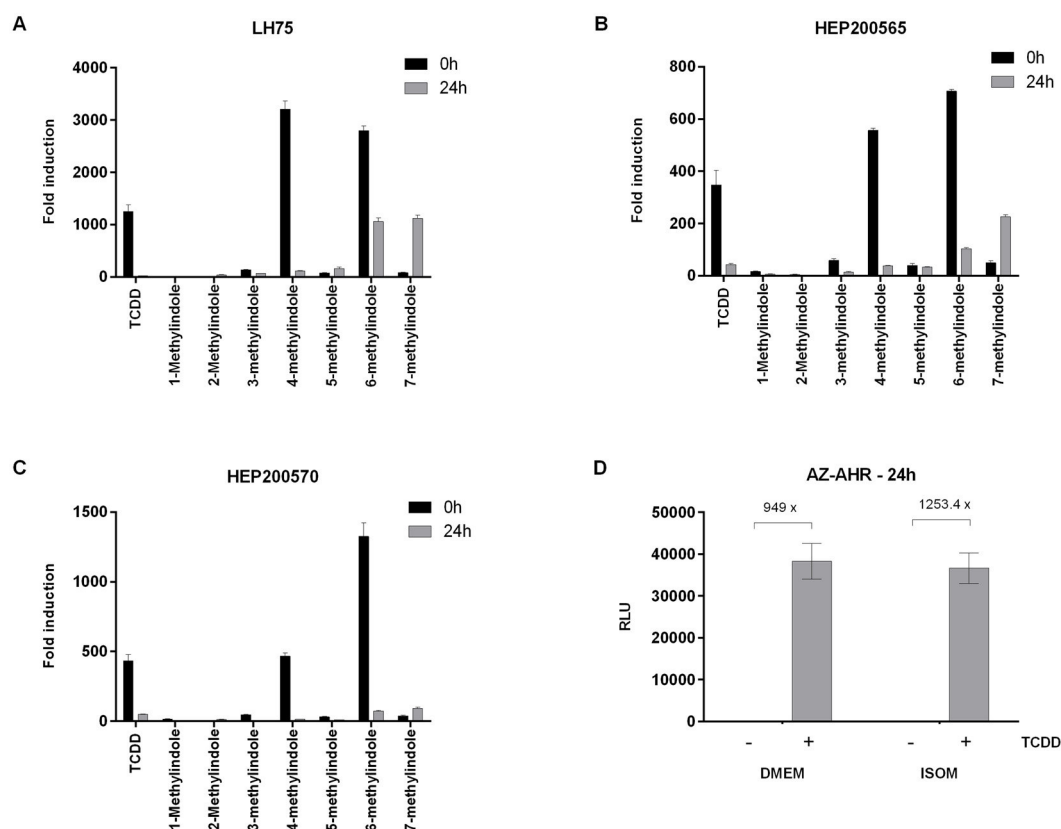

Fig. 9. Agonist activities of MMI metabolites at AhR in reporter gene assay. Primary human hepatocytes cultures (LH75, Hep200565, Hep200570) were incubated for 0 h and 24 h with mono-methylindoles (200 μM). Thereafter, culture medium from hepatocytes cultures was collected and applied to AZ-AHR cells for 24 h (***Panels A, B, C***). AZ-AHR cells were lysed and luciferase activity was measured. Data are expressed as a fold induction of luciferase activity over vehicle-treated cells and they are the mean ± SD from triplicates. ***Panel D***: Responsivity of AZ-AHR to TCDD (24 h; 5 nM) in DMEM and ISOM culture media.

comprise metabolic transformation, but also active uptake by human hepatocytes, degradation in media or non-specific binding. We also aimed to identify the classes of putative MMI metabolites, employing the means of selective molecular mass search, based on the previously published metabolic studies (Zhang et al., 2014; Lanza et al., 1999). In our specific case, we were able to identify two major types of metabolites in the cell culture media after 24 h of incubation. The first set of mass-ionization peaks identified represents the various derivatives of mono-oxidated MMI, such as hydroxylated or monomethyl-oxindole derivatives, which were detected in the region of t_R = 7.0–7.5 min and were represented by the molecular peak at 148.10 m/z in the mass spectrum (Fig. 10D and E), corresponding to the mono-protonated species. In this region, we observed substantial differences between the chromatograms obtained for specific MMI. The most substantial differences were observed between the chromatograms obtained for 2-methylindole and 7-methylindole (see the highlighted region in Fig. 10B), while the peak at t_R = 7.16 min was observed in the chromatogram for 7-methylindole only. The second set of mass-ionization peaks identified comprised GSH-conjugated MMI derivatives, observed at t_R ≈ 9.70 min, 11.15 min, and 11.60 min (Fig. 10C), represented by the molecular peak at 437.13 m/z in the mass spectra, corresponding to the [GS–MMI + H]$^+$ species.

4. Discussion

Compounds with an indole ring in their structure, including xenobiotics, endogenous compounds or microbial products, have been demonstrated as ligands of human AhR (Hubbard et al., 2015). A wide array of indole-based AhR-active substances is produced by intestinal microbiota from dietary precursors, such as glucobrassicin, and from essential amino acid tryptophan that originates mainly from cleavage of dietary proteins. For instance, skatole (3-methylindole), which is produced by decarboxylation of indole-3-acetate by human intestinal microbiome (Roager and Licht, 2018), was recently described as a partial agonist of human AhR (Rasmussen et al., 2016). As a prelude to further discovery of such indole derivatives, we have systematically investigated the entire series of mono-methylated indoles as ligands for AhR-CYP1A activation and antagonism. The effects overall of MMI on AhR-CYP1A pathway in human cells comprise the induction of CYP1A genes through AhR, the inhibition of CYP1A catalytic activity and possibly the metabolic transformation causing loss or gain of AhR agonist activity of parental compounds.

The relative efficacy of individual MMI at AhR differed substantially. For example, 4-methylindole and 6-methylindole were approx. 25 times more efficacious AhR agonists as compared to 3-methylindole (skatole), while 2-methylindole was nearly inactive at AhR (Stepankova et al., 2018). Given the fact that very subtle change in chemical structure of MMI, such as a shift in methyl moiety at indole ring, results in dramatic impact on MMI activity at AhR, we performed current follow-up study. Firstly, we show that MMI induce *CYP1A1* and *CYP1A2* genes in human hepatic progenitor cells HepaRG, by AhR-dependent mechanism, which is supported by the loss of *CYP1A* induction in AhR knock-out HepaRG cells. MMI also induced *CYP1A1* and *CYP1A2* mRNAs and proteins in primary cultures of human hepatocytes. Relative efficacies of MMI in HepaRG cells and human hepatocytes were similar to those observed previously for *CYP1A1* in intestinal
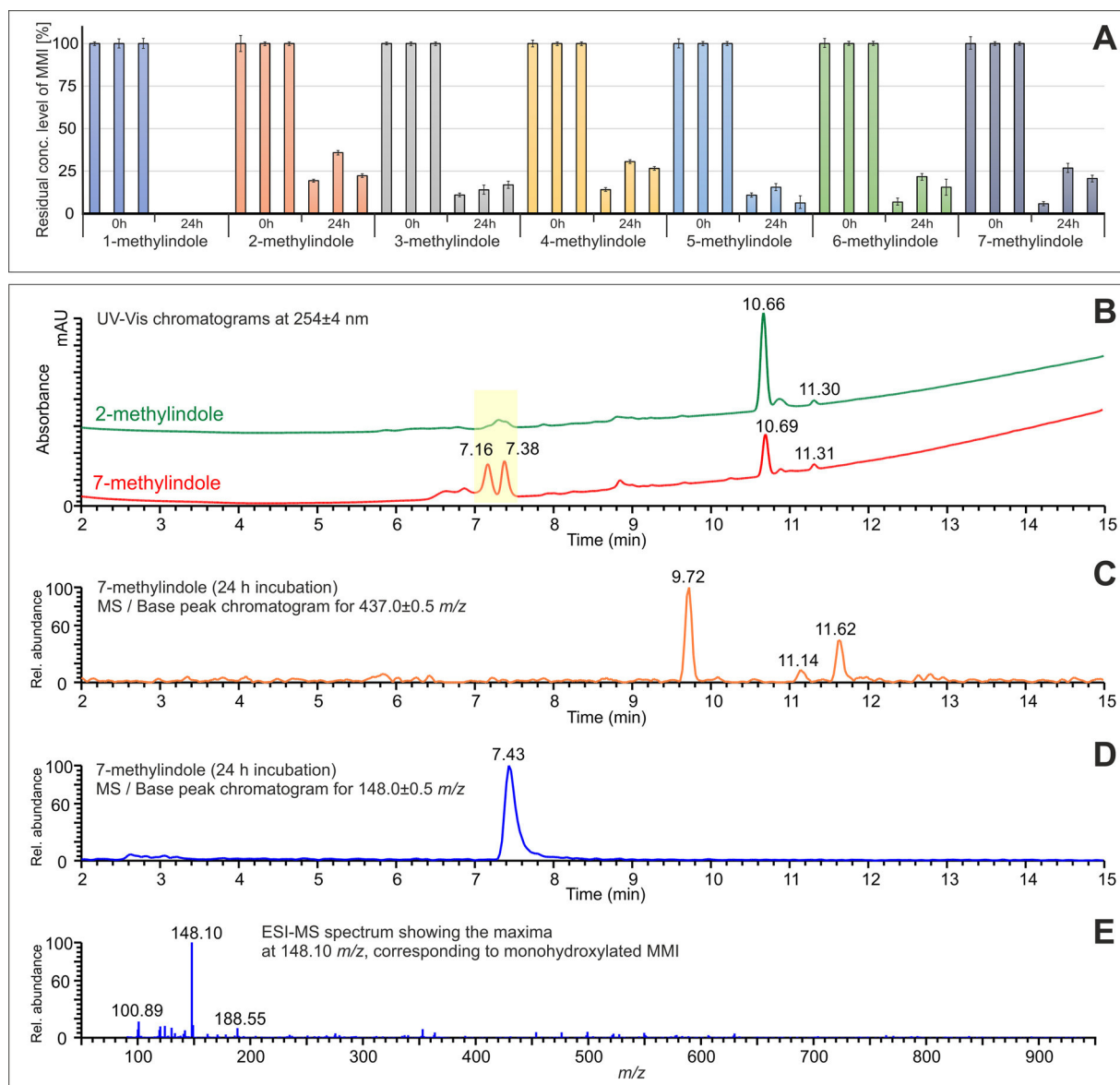
Fig. 10. Liquid Chromatography / Mass Spectrometry analyzes of mono-methylindoles metabolites. *Panel A:* The quantitative evaluation of residual MMI levels in culture media after 24 h incubation with human hepatocytes (cultures LH75, Hep200565, Hep200570); *Panel B:* The comparison of UV/Vis chromatograms for the samples of 2-methylindole and 7-methylindole showing the significant differences in the region of mono-oxidated metabolites (highlighted in yellow); *Panel C:* The base-peak chromatogram for the mass range of $437.0 \pm 0.5 \, m/z$ showing the GSH-conjugated metabolites of 7-methylindole at tR = 9.72 min, 11.14 min, and 11.62 min; *Panel D:* The base-peak chromatogram for the mass range of $148.0 \pm 0.5 \, m/z$ showing the broad peak of mono-oxidated metabolites of 7-methylindole at tR = 7.43 min; *Panel E:* Mass spectrum, corresponding to the mono-oxidated species of 7-methylindole with the maxima at 148.10 m/z, *i.e.* $[MMI+H]^+$ species.

cancer cells LS180 (Stepankova et al., 2018), with one exception. While 7-methylindole was weak inducer of *CYP1A1* in LS180 and HepaRG, it was very strong inducer of *CYP1A* genes in three cultures of human hepatocytes. Since primary human hepatocytes are fully equipped with xenobiotic-metabolizing apparatus, the plausible explanation for strong gain of capability to induce CYP1A genes by 7-methylindole might be its metabolic conversion to highly AhR-active product. We observed substantially increased activation of AhR in transgenic reporter gene cells AZ-AHR by culture media from human hepatocytes incubated 24 h with 7-methylindole as compared to media containing 7-methylindole without pre-incubation, which corroborates the hypothesis about metabolic activation of 7-methylindole. In contrast to gain of AhR activity of 7-methylindole, we observed loss of AhR agonist activity of 4-methylindole after incubation with human hepatocytes. Drastic drop of MMI concentrations in culture media after 24 h incubation with human hepatocytes indicates either metabolic degradation or active cellular

uptake of parental MMI. By the means of LC/MS analyses, we observed in the cell culture media the formation of different derivatives of mono-oxidated MMI (mono-hydroxylated MMI or mono-methyl-oxindole derivatives) and GSH-conjugates of MMI. Significant differences were observed in the amount and types of mono-oxidated metabolites in the samples. Conjugation with large polar molecule of glutathione and/or the introduction of hydroxyl group in indole skeleton could compromise AhR agonist activity of MMI, the latter being observed also by other authors (Heath-Pagliuso et al., 1998). Speculatively, this could be a case of AhR agonist activity loss for 4-methylindole. On the other hand, formation of mono-methyl-oxindoles might lead to the formation of condensed products, analogical to indigo and indirubin, which are prominent AhR agonists. This could be the reason for gain of AhR agonist activity by 7-methylindole. Collectively, distinct metabolic signatures for individual MMI might result in no change, loss or gain of AhR agonist activity.

The activators of AhR and inducers of CYP1A genes are often the inhibitors of CYP1A enzymes. Indeed, this was also the case of MMI, which inhibited catalytic activity of CYP1A1 in cultured LS180 cells and human hepatocytes. Interestingly, the inhibition of CYP1A1 by MMI in human liver microsomes was much weaker as compared to hepatocytes or LS180 cells, suggesting formation of inhibitory metabolites in the cells. Another explanation could be a formation of metabolites with altered inhibitory capacity against CYP1A1, following the incubation with human hepatocytes (Figs. 4 and 5) and LS180 cells (Figs. 6 and 7). Hence, the measurements of CYP1A1 catalytic activity in cell cultures comprise mixed effects of parental MMIs and their metabolites. In addition, *single concentration inactivation assay* revealed time-dependent inhibition of CYP1A1 by 4-methylindole and 5-methylindole. Importantly, the overall effects of MMIs on CYP1A1 enzyme activity in cells cultured for 24 h (Figs. 4 and 6) comprise both inhibition of catalytic activity and increase of CYP1A1 amount by the gene induction, which may yield atypical dose-response profiles. Indeed, the sum effects of 4-methylindole and 6-methylindole in human hepatocytes and LS180 cells involve concentration-dependent increase on CYP1A1 amount (induction) and concentration-dependent inhibition of CYP1A1 activity, which results in inverse U-shaped profiles.

Overall, the effects of MMI on AhR-CYP1A signaling pathway involve agonist/antagonist effects at AhR and consequent changes in the expression of *CYP1A* genes, inhibition of CYP1A1 catalytic activity and the combined action of parental compounds and their metabolites. The data presented here might represent a cornerstone for development of highly efficacious AhR-active skatole-like scaffolds with potentially therapeutic use in inflammatory bowel disease.

Authors contributions

Participated in research design: Zdeněk Dvořák, Sridhar Mani
Conducted experiments: Iveta Bartoňková, Barbora Vyhlídalová, Kristýna Krasulová, Karolína Poulíková, Jan Vančo, Zdeněk Trávníček
Contributed new reagents and analytic tools: Zdeněk Dvořák, Zdeněk Trávníček
Performed data analysis: Iveta Bartoňková, Barbora Vyhlídalová, Kristýna Krasulová, Karolína Poulíková, Jan Vančo, Zdeněk Dvořák
Wrote or contributed to the writing of the manuscript: Zdeněk Dvořák, Sridhar Mani

Funding

Declaration of Competing Interest

The authors declare that they have no known competing financial interests or personal relationships that could have appeared to influence the work reported in this paper.

The authors declare the following financial interests/personal relationships which may be considered as potential competing interests:

Data availability statement

All data generated or analyzed during this study are included in this published article.

Transparency document

The Transparency document associated with this article can be found in the online version.

References

Roager, H.M., Licht, T.R., 2018. Microbial tryptophan catabolites in health and disease. Nat. Commun. 9 (1), 3294.

Wilson, S.R., Joshi, A.D., Elferink, C.J., 2013. The tumor suppressor Kruppel-like factor 6 is a novel aryl hydrocarbon receptor DNA binding partner. J. Pharmacol. Exp. Ther. 345 (3), 419–429.

Hankinson, O., 2016. The role of AHR-inducible cytochrome P450s in metabolism of polyunsaturated fatty acids. Drug Metab. Rev. 48 (3), 342–350.

Mescher, M., Haarmann-Stemmann, T., 2018. Modulation of CYP1A1 metabolism: from adverse health effects to chemoprevention and therapeutic options. Pharmacol. Ther. 187, 71–87.

Lanza, D.L., Yost, G.S., 2001. Selective dehydrogenation/oxygenation of 3-methylindole by cytochrome p450 enzymes. Drug Metab. Dispos. 29 (7), 950–953.

Stejskalova, L., Dvorak, Z., Pavek, P., 2011. Endogenous and exogenous ligands of aryl hydrocarbon receptor: current state of art. Curr. Drug Metab. 12 (2), 198–212.

Roman, A.C., et al., 2018. The aryl hydrocarbon receptor in the crossroad of signalling networks with therapeutic value. Pharmacol. Ther. 185, 50–63.

Schiering, C., et al., 2017. Feedback control of AHR signalling regulates intestinal immunity. Nature 542 (7640), 242–245.

Chen, I., et al., 1998. Aryl hydrocarbon receptor-mediated antiestrogenic and antitumorigenic activity of diindolylmethane. Carcinogenesis 19 (9), 1631–1639.

Chen, I., Safe, S., Bjeldanes, L., 1996. Indole-3-carbinol and diindolylmethane as aryl hydrocarbon (Ah) receptor agonists and antagonists in T47D human breast cancer cells. Biochem. Pharmacol. 51 (8), 1069–1076.

Rothhammer, V., et al., 2016. Type I interferons and microbial metabolites of tryptophan modulate astrocyte activity and central nervous system inflammation via the aryl hydrocarbon receptor. Nat. Med. 22 (6), 586–597.

Rasmussen, M.K., et al., 2016. Skatole (3-Methylindole) is a partial aryl hydrocarbon receptor agonist and induces CYP1A1/2 and CYP1B1 expression in primary human hepatocytes. PLoS One 11 (5) e0154629.

Hubbard, T.D., et al., 2015. Adaptation of the human aryl hydrocarbon receptor to sense microbiota-derived indoles. Sci. Rep. 5 12689.

Stepankova, M., et al., 2018. Methylindoles and methoxyindoles are agonists and antagonists of human aryl hydrocarbon receptor. Mol. Pharmacol. 93 (6), 631–644.

Novotna, A., Pavek, P., Dvorak, Z., 2011. Novel stably transfected gene reporter human hepatoma cell line for assessment of aryl hydrocarbon receptor transcriptional activity: construction and characterization. Environ. Sci. Technol. 45 (23), 10133–10139.

Kubesova, K., Travnicek, Z., Dvorak, Z., 2016. Pleiotropic effects of gold(I) mixed-ligand complexes of 9-deazahypoxanthine on transcriptional activity of receptors for steroid hormones, nuclear receptors and xenoreceptors in human hepatocytes and cell lines. Eur. J. Med. Chem. 121, 530–540.

Atkinson, A., Kenny, J.R., Grime, K., 2005. Automated assessment of time-dependent inhibition of human cytochrome P450 enzymes using liquid chromatography-tandem mass spectrometry analysis. Drug Metab. Dispos. 33 (11), 1637–1647.

Zhang, C.H., et al., 2014. For a series of methylindole analogs, reactive metabolite formation is a poor predictor of intrinsic cytotoxicity in human hepatocytes. Toxicol. Res. 3 (3), 184–190.

Gillam, E.M., et al., 2000. Oxidation of indole by cytochrome P450 enzymes. Biochemistry 39 (45), 13817–13824.

Lanza, D.L., et al., 1999. Specific dehydrogenation of 3-methylindole and epoxidation of naphthalene by recombinant human CYP2F1 expressed in lymphoblastoid cells. Drug Metab. Dispos. 27 (7), 798–803.

Heath-Pagliuso, S., et al., 1998. Activation of the Ah receptor by tryptophan and tryptophan metabolites. Biochemistry 37 (33), 11508–11515.

APPENDIX II.

Vyhlidalova B., Bartonkova I., Jiskrova E., Li H., Mani S., Dvorak, Z. (2020): Differential activation of human pregnane X receptor PXR by isomeric mono-methylated indoles in intestinal and hepatic in vitro models. *Toxicol Lett,* 324: 104-110. **[IF$_{2020}$ 4.374]**
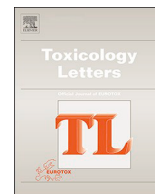
Differential activation of human pregnane X receptor PXR by isomeric mono-methylated indoles in intestinal and hepatic *in vitro* models

Barbora Vyhlídalová[a], Iveta Bartoňková[a], Eva Jiskrová[a], Hao Li[b], Sridhar Mani[b], Zdeněk Dvořák[a],*

[a] *Department of Cell Biology and Genetics, Faculty of Science, Palacky University, Slechtitelu 27, 783 71 Olomouc, Czech Republic*
[b] *Department of Genetics and Department of Medicine, Albert Einstein College of Medicine, Bronx, NY 10461, USA*

ARTICLE INFO

ABSTRACT

Dietary and microbial indoles can act as ligands and activators of pregnane X receptor (PXR), with implications in human intestinal health. In the current study, we examined the effects of simple mono-methylated indoles (MMIs) on the activity and function of PXR, using a series of human hepatic and intestinal cell models. Indoles 1-MMI and 2-MMI strongly induced CYP3A4 and MDR1 mRNAs in human intestinal adenocarcinoma cells LS180, but not in primary human hepatocytes. The levels of CYP3A4 mRNA were increased by 1-MMI and 2-MMI in wild type, but not in PXR-knock-out human hepatic progenitor HepaRG cells, implying the involvement of PXR in CYP3A4 induction by MMIs. Utilizing reporter gene assay, we observed dose-dependent activation of PXR by all MMIs, and their efficacies and potencies were comparable. Tested MMIs also displayed moderate antagonist effects on PXR, revealing about partial agonist effects of these compounds. As demonstrated using the Chromatin immunoprecipitation assay (ChIP),1-MMI increased PXR occupancy of the CYP3A4 promoter. Time-Resolved Fluorescence Resonance Energy Transfer revealed that MMIs are weak ligands of human PXR. Collectively, we show that MMIs are ligands and partial agonists of human PXR, which induce PXR-regulated genes in human intestinal cells.

1. Introduction

The pregnane X receptor (PXR) is a nuclear receptor, which transcriptionally regulates drug-metabolizing enzymes and drug transporters, the most important representatives being cytochrome P450 CYP3A4 and multidrug resistance 1 (MDR1), respectively. Besides its role as a xenosensor, PXR plays multiple physiological roles such as regulating carbohydrate and lipid metabolism, controlling cell proliferation and cell migration, inflammatory response, apoptosis, and DNA damage (Oladimeji and Chen, 2018). A variety of structurally diverse xenobiotics activates PXR, including drugs (antibiotics, azole antifungals, calcium channel blockers) (Drocourt et al., 2001; Svecova et al., 2008; Yasuda et al., 2008), environmental pollutants (phthalates, bis-phenols) (Wyde et al., 2005), naturally occurring compounds (Carazo et al., 2019) or herbal products and dietary supplements (Staudinger et al., 2006). Endogenous activators of PXR comprise steroids (Kliewer et al., 1998), bile acids (Staudinger et al., 2001), vitamin E (Cho et al., 2009), and vitamin K (Tabb et al., 2003). In recent years, there has been an emerging interest in elucidating the physiological and pathophysiological roles of intestinal microbial metabolites as potential ligands of nuclear receptors (Kim, 2018). For instance, microbial-derived vitamin K2 and lithocholic acid activate PXR and drive maturation of P450 enzymes postpartum, thereby, are critical regulators of liver development (Avior et al., 2015). A prominent class of biologically active compounds, produced by human intestinal microbiota, are catabolites of tryptophan, which have been demonstrated as ligands for aryl hydrocarbon receptor (AhR) (Roager and Licht, 2018). In addition to microbial indoles, a variety of xenobiotic and dietary indoles are ligands for AhR (Hubbard et al., 2015; Jin et al., 2014; Rasmussen et al., 2016; Stepankova et al., 2018). Since the majority of AhR ligands are also ligands for PXR (cca 88 % overlap for dual activators: PubChem Bioassay ID 434939, it is reasonable to assume that indoles might also be PXR ligands. Indeed, we showed that diindolylmethane, a digestion product of indole-3-carbinol from cruciferous vegetables, is a ligand and activator of PXR that induces CYP3A4 and MDR1 genes Pondugula et al., 2015). We have also demonstrated that microbial-derived indole-3-propionic acid is a ligand of PXR *in vivo*, which regulates intestinal barrier function (Venkatesh et al., 2014).

Reporter gene assay LS180 + wt-PXR + pCYP3A4-luc / 24 h

Agonist effects
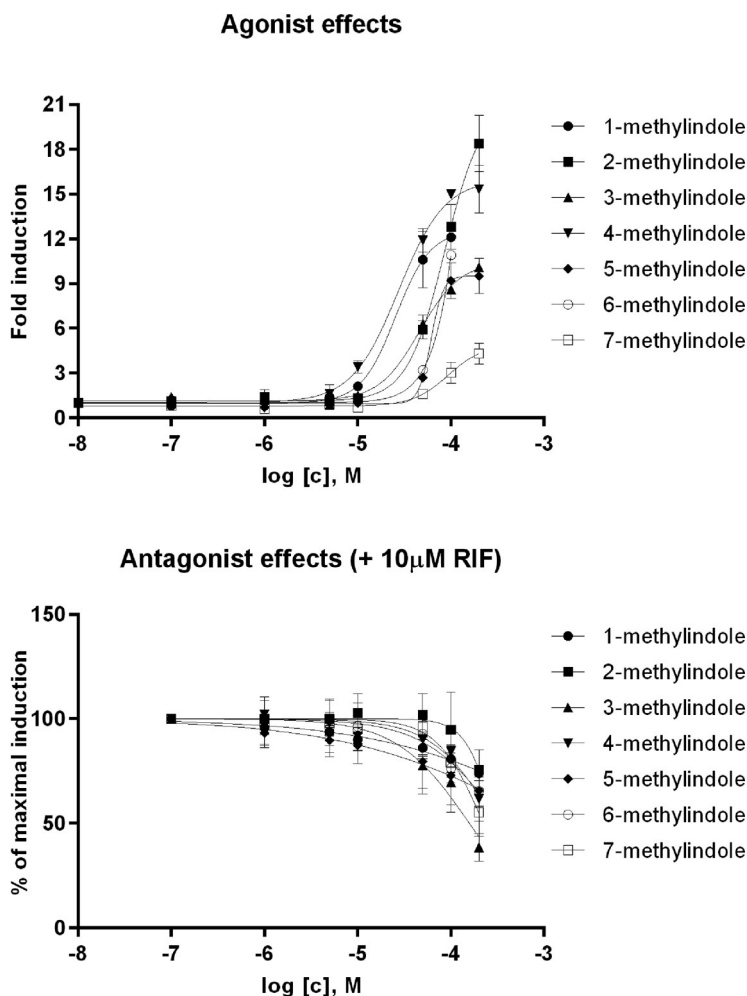

Antagonist effects (+ 10μM RIF)

Fig. 1. Effects of mono-methylated indoles on transcriptional activity of pregnane X receptor (PXR) in reporter gene assay. Cell line LS180 was transiently co-transfected with *p3A4-luc* reporter plasmid and PXR vector and incubated for 24 h with vehicle (DMSO, 0.1 % v/v) and /or tested compounds in concentrations ranging from 10 nM to 200 μM. Incubations were in the presence (antagonist mode) or in the absence (agonist mode) of PXR ligand rifampicin (RIF, 10 μM). Experiments were performed in three consecutive cell passages. Each treatment was carried out in four technical replicates (culture wells). Representative experiments from one cell passage are shown in the plots. **_Upper panel:_** Agonist mode. Data are expressed as a fold induction over a negative control. **_Middle panel:_** Antagonist mode. Data are expressed as a percentage of maximal induction attained by 10 μM rifampicin. **_Lower panel:_** The table shows EC_{50}, IC_{50}, and relative efficacy values. Relative efficacies (%) were obtained by dividing the maximal induction attained by tested compound by the induction attained by 10 μM rifampicin. Relative efficacies are expressed as a mean ± SD from three independent experiments.

	EC_{50} [μM] (n = 3)	Relative efficacy [%]	IC_{50} [μM] (n = 3)
1-methylindole	22.1 ± 1.0	67.4 ± 22.7	> 200
2-methylindole	73.6 ± 2.3	97.0 ± 17.7	> 200
3-methylindole	48.3 ± 7.5	46.6 ± 4.0	153.63 ± 39.17
4-methylindole	23.8 ± 1.9	111.4 ± 7.2	> 200
5-methylindole	66.8 ± 10.7	49.1 ± 9.2	> 200
6-methylindole	45.1 ± 10.6	70.4 ± 17.9	> 200
7-methylindole	75.7 ± 7.0	34.1 ± 8.6	> 200

Recently, we described a series of methoxylated and methylated indoles as agonists and antagonists of AhR (Stepankova et al., 2018; Vyhlidalova et al., 2019). In the current study, we investigated the effects of mono-methylated indole isomers on the PXR signaling pathway in intestinal and hepatic cell models. We show that indole methylated at position 1 and 2 are ligands and activators of PXR, which induce CYP3A4 and MDR1 genes.

2. Materials and methods

2.1. Chemicals and reagents

Mono-methylated indoles (purity at the range from 97 % to 99 %),

except for 4-Me-indole, charcoal-stripped fetal bovine serum, dimethylsulfoxide (DMSO) and rifampicin (RIF) were obtained from Sigma Aldrich (Prague, Czech Republic). 4-Me-indole (97 % purity) was purchased from Energy Chemical (Shanghai, China). FuGENE® HD Transfection reagent and reporter lysis buffer were purchased from Promega (Hercules, CA, USA). All other chemicals were of the highest quality commercially available.

2.2. Cell lines

Human Caucasian colon adenocarcinoma cell lines LS180 and LS174 T were purchased from the European Collection of Cell Cultures ECACC No. 87021202 and American Type Culture Collection ATCC,
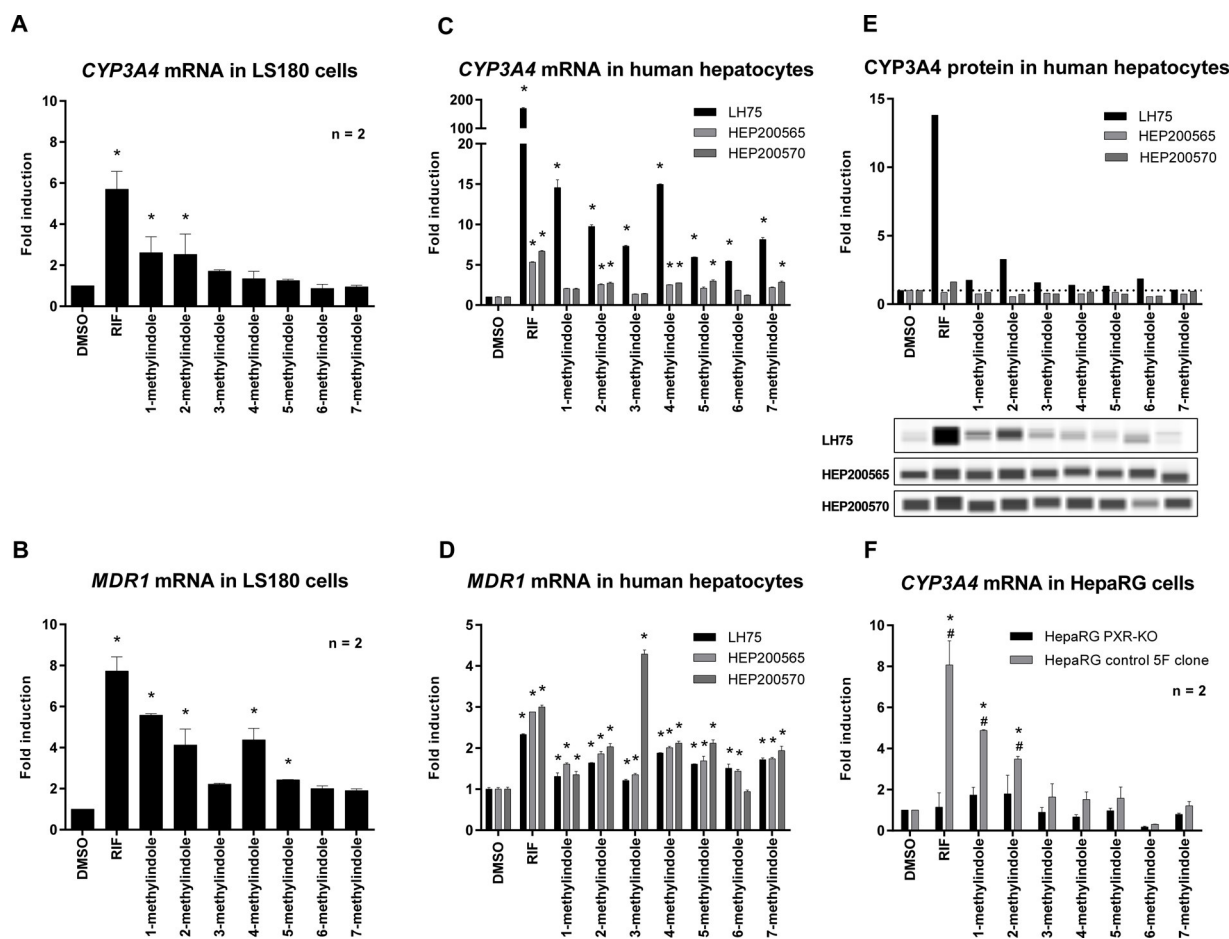
Fig. 2. Effects of mono-methylated indoles on the expression of CYP3A4 and MDR1 genes in human hepatic and intestinal cells. Cultured cells were incubated for 24 h with the vehicle (DMSO; 0.1 % v/v), rifampicin (RIF; 10 μM) and/or mono-methylated indoles (MMI; 200 μM). The levels of *CYP3A4* and *MDR1* mRNA were determined by RT-PCR and the data were normalized *perGAPDH* mRNA level. Each measurement was done in triplicates (technical replicates). * = value significantly different from negative control (p < 0.05). # = value significantly different from control 5 F clone (p < 0.05). Graphs show a mean ± SD and are expressed as a fold induction over negative control. Levels of CYP3A4 protein were normalized *per* β-actin levels (quantitation by SallySue software) and the data were expressed as a fold induction over negative control. **_PANEL (A), (B):_** Incubations were performed in two consecutive passages of LS180 cells transiently transfected with PXR vector. **_PANEL (C), (D), (E):_** Primary human hepatocytes from three different donors, (LH75, HEP200565, HEP200570). **_PANEL (F):_** Incubations were performed in two consecutive passages of HepaRG (control clone and PXR-KO) cells.

respectively. Cells were maintained in Dulbecco's modified Eagle's medium DMEM supplemented with 10 % charcoal-stripped fetal bovine serum, four mM L-glutamine, 1 % non-essential amino acids, one mM sodium pyruvate 100 U/mL streptomycin and 100 μg/mL penicillin.

Short-term primary human hepatocytes in monolayer batch Hep200565 (female, 21 years, Caucasian) and Hep200570 (male, 64 years, unknown ethnicity) were purchased from Biopredic International (Rennes, France). The activity of phase I (CYP1A2 – phenacetin-*O*-deethylase; CYP2B6 – bupropion hydroxylase; CYP2C19 – S-mephenytoin hydroxylase; CYP2D6 – dextromethorphan-*O*-demethylase; CYP3A4/5 – midazolam-1′-hydroxylase) and phase II (UGT1A1,1A6, 1A9, 2B15 – paracetamol glucuronidation; SULT1A1, 1A3/4, 1E1 – paracetamol sulphation) enzymes was determined and provided by Biopredic International. Primary human hepatocyte culture from multiorgan donor LH75 (female, 78 years, Caucasian) was prepared at the Faculty of Medicine, Palacky University Olomouc. The tissue acquisition protocol complied with the regulation issued by "Ethical Committee of the Faculty Hospital Olomouc, Czech Republic" and with Transplantation law #285/2002 Coll. Primary human hepatocyte cultures were cultured confluent 2 D monolayer in serum-free ISOM medium (Isom et al., 1985), as described elsewhere (Pichard et al., 1990).

PXR knock-out (PXR-KO) and control 5 F Clone HepaRG hepatic progenitor cells were purchased from Sigma Aldrich (Prague, Czech Republic) and cultured according to the manufacturer's instructions.

All cell lines were incubated at 37 °C and 5 % CO₂ in a humidified incubator.

2.3. Reporter gene assay

A chimera p3A4-luc reporter construct containing the basal promoter (-362/+53) with proximal PXR response element, and distal xenobiotic responsive enhancer module (-7836/-7208) of the CYP3A4 gene 5′-flanking region inserted into the pGL4.10 reporter vector was described elsewhere (Pavek et al., 2010). The expression vector for human PXR, pSG5-PXR, was kindly provided by Dr. S. Kliewer - University of Texas, Dallas, TX. LS180 cells were transiently transfected with pSG5-PXR and p3A4-luc by lipofection (FuGENE® HD Transfection reagent). Transfected cells were seeded in 96-well plates and allowed to stabilize for 24 h. After that, cells were treated for 24 h with monomethylated indoles and vehicle (DMSO, 0.1 % v/v) in the presence or absence of rifampicin (RIF, 10 μM). Cells were lysed, and luciferase activity was measured with using a Tecan Infinite M200 Pro Plate Reader (Schoeller Instruments, Czech Republic). Experiments were performed in three consecutive cell passages, and the analyses in each passage were performed in quadruplicates (technical replicates). The
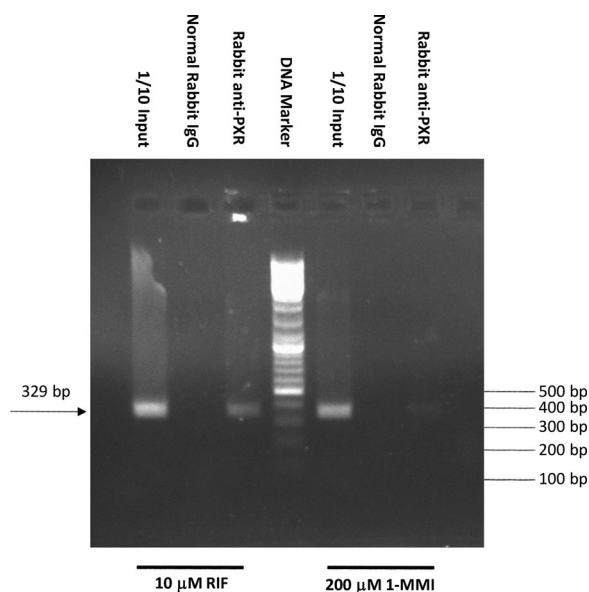
Fig. 3. Binding of PXR in CYP3A4 Promoter by ChIP Assay. LS174 T cells were transfected with pSG5-PXR vector were incubated for 24 h with vehicle (DMSO), 10 μM Rifampicin (RIF) and 200 μM 1-methylindole (1-MMI). Chromatin Immunoprecipitation (ChIP) was performed according to Methods and Protocols. The purified chromatin (anti-PXR) was subjected to PCR reaction using CYP3A4 promoter primers and PCR products were resolved on 1.5 % agarose gel.

values of IC_{50} and EC_{50} were calculated by GraphPad Prism 6 Software (GraphPad Software, San Diego, CA).

2.4. mRNA isolation, reverse transcription and qRT-PCR

The total RNA was isolated by TRI Reagent® (Sigma Aldrich, Prague, Czech Republic). The concentration and purity of isolated RNA were measured by NanoDrop™ Lite spectrophotometer by Thermo Fisher Scientific (Waltham, MA, USA). 1000 ng of total RNA was used for cDNA synthesis using M-MuLV reverse transcriptase (New England Biolabs, Ipswich, MA, USA) at 42 °C for 60 min in the presence of Random Primers 6 (New England Biolabs, Ipswich, MA, USA). The quantitative reverse transcriptase-polymerase chain reaction (qRT-PCR) was performed on Light Cycler 480 II apparatus using the LightCycler® 480 Probes Master (Roche Diagnostic Corporation, Prague, Czech Republic). The levels of *GAPDH*, *CYP3A4* and *MDR1* mRNAs were determined using Universal Probes Library (UPL; Roche Diagnostic Corporation, Prague, Czech Republic) probes and primers, as described elsewhere (Bartonkova and Dvorak, 2018). The protocol was as follows: an activation step at 95 °C for 10 min was followed by 45 cycles of PCR (denaturation at 95 °C for 10 s; annealing with elongation at 60 °C for 30 s). All measurements were carried out in triplicates. *Glyceraldehyde-3-phosphate dehydrogenase* (*GAPDH*), which is a house-keeping gene, was used for the normalization of gene expression. Data were processed by the delta-delta method.

2.5. Simple western blotting by Sally Sue™

Detection of CYP3A4 and β-actin proteins from primary human hepatocytes was performed by automated capillary electrophoresis Sally Sue™ Simple Western System (ProteinSimple™; San Jose CA, USA) using the Compass Software version 2.6.5.0 (ProteinSimple™). Total protein extracts were prepared using non-denaturizing ice-cold lysis buffer (150 mM NaCl; 50 mM HEPES; 5 mM EDTA; 1% (v/v) Triton X-100; anti-protease cocktail, anti-phosphatase cocktail). Bradford reagent was used for a determination of protein concentration. Primary

antibodies anti-CYP3A4 (mouse monoclonal, sc-53850, HL3, dilution from 1:5000 to 1:20000, Santa Cruz Biotechnology, Santa Cruz, CA, USA) and β-actin (mouse monoclonal, 3700S, dilution 1:1000, Cell Signalling Technology, Denvers, Massachusetts, USA) were used. Detection was done by a horseradish-conjugated secondary antibody using a chemiluminescent substrate. Signals were normalized per β-actin as a loading control and expressed as fold induction over negative control.

2.6. Chromatin immunoprecipitation assay ChIP

LS174 cells were transiently transfected with pSG5-PXR, plated in 150-mm cell culture dishes and grown to confluence about 10^7 cells. Cells were incubated for 24 h with the vehicle, rifampicin (10 μM), and 1-MMI (200 μM). Chromatin Immunoprecipitation (ChIP) was performed using our previous protocol (Nelson et al., 2006; Wang et al., 2011). Rabbit anti-PXR (sc-25381), normal rabbit IgG (sc-2027), and protein A-Agarose (sc-2001) were from Santa Cruz Biotechnology (CA, USA). PCR was performed with CYP3A4 primers located in the CYP3A4 promotor (from -280 to +50). The primers were: 5′-AGAGACAAGGG CAAGAGAGAG-3′ and 5′-CTCTTTGCTGGGCTAGTGCA-3′. Positive PCR yields a 329 bp band.

2.7. Time-resolved fluorescence resonance energy transfer TR-FRET

The LanthaScreen® TR-FRET PXR (SXR) Competitive Binding Assay Kit (Thermo Fischer Scientific, Waltham, MA, USA) was used to determine the binding of mono-methylated indoles at PXR. The experiments were performed in a volume of 20 μl in 384-well black plates with concentrations of mono-methylated indoles ranging from 0.1 μM to 400 μM. Vehicle (DMSO) and SR12813 (100 μM) were used as a negative and positive control, respectively. The incubation time of the reaction mixture was 1 h in the dark at room temperature. Afterward, applying the excitation filter 340 nm, the fluorescent signals were measured at 495 nm and 520 nm on Tecan Infinite F200 Pro Plate Reader (Schoeller Instruments, Czech Republic). The TR-FRET ratio was calculated by dividing the emission signal at 520 nm by that at 495 nm. Binding assays were done in three independent experiments, and IC_{50} values were calculated using GraphPad Prism 6 software (GraphPad Software, San Diego, CA) applying standard curve interpolation (sigmoidal, 4 PL, variable slope). Each curve of tested mono-methylated indole was classified according to the concentration-response-curve (CRC) classification system (Shukla et al., 2009).

2.8. Statistics

One-way analysis of variance (ANOVA) with Dunnett´s multiple comparison test was used for comparison of two groups. The result was considered significant if the p-value < 0.05. The normality of the data was tested using the Shapiro-Wilk normality test. All calculation were done using GraphPad Prism version 6.0 for Windows (GraphPad Software, La Jolla, CA).

3. Results

3.1. Effects of mono-methylated indoles on transcriptional activity of pregnane X receptor (PXR) in LS180 cells

In the first series of experiments, we examined the effects of mono-methylated indoles on basal and ligand-inducible transcriptional activity of human PXR, by means of reporter gene assay. For this purpose, LS180 cells transiently transfected with human PXR expression vector and pCYP3A4-luc reporter plasmid (for details see Materials and Methods), were incubated for 24 h with vehicle (DMSO; 0.1 % V/V) and tested MMIs in concentration range from 10 nM to 200 μM, in the absence (agonist mode) or presence (antagonist mode) of rifampicin (RIF;
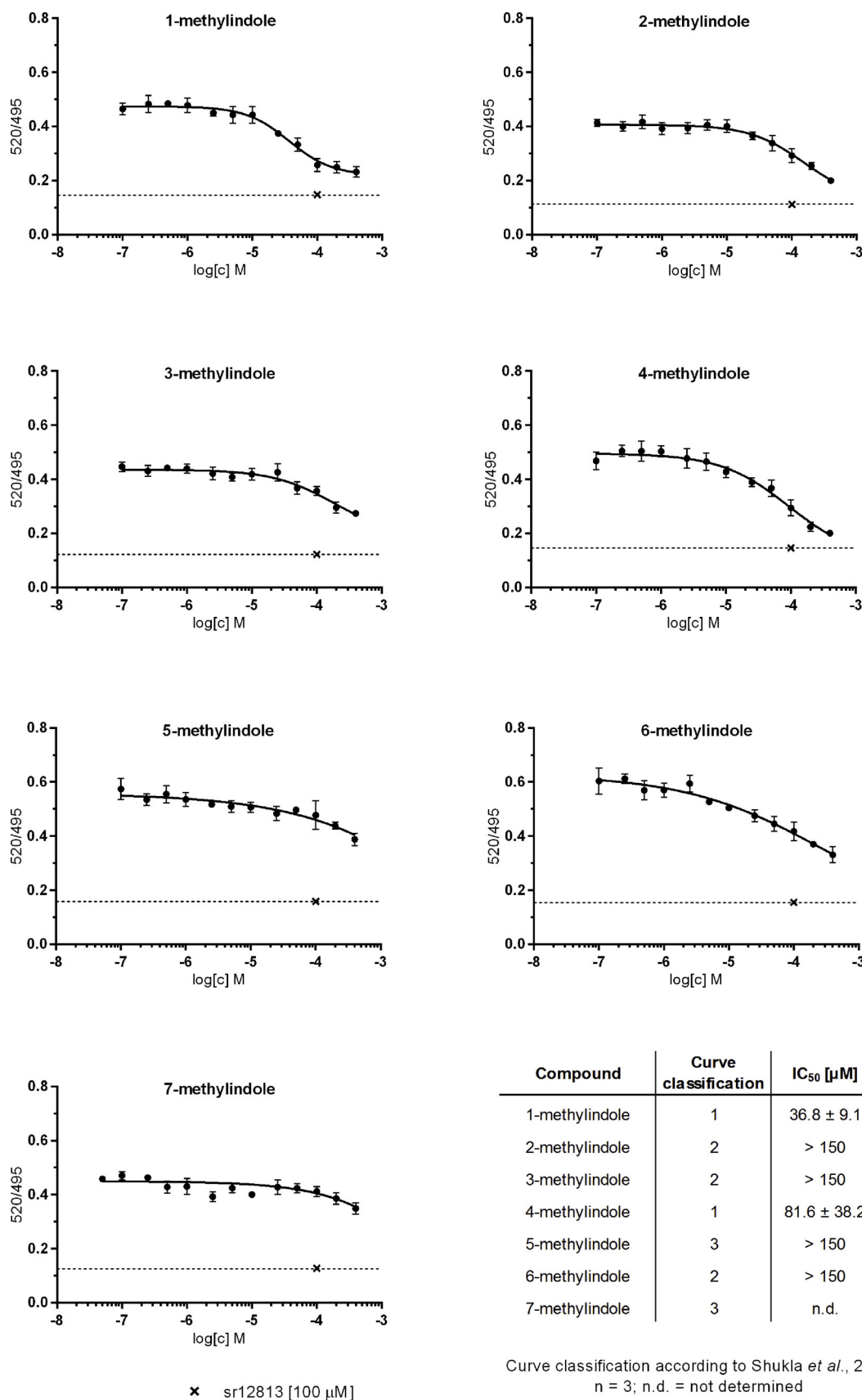
Fig. 4. Binding of mono-methylated indoles at PXR – TR-FRET assay. TR-FRET ratios 520/495 nm is plotted against concentration of compound(s). Half-maximal inhibitory concentrations IC_{50} were obtained from interpolated standard curves (sigmoidal, variable slope), and are shown in table together with curve classification. Experiments were performed three times ($n = 3$) and the representative plots are shown. The presented data are mean ± SE from quadruplicates (technical replicates). Positive control SR12813 (100 μM) is depicted as a single point at the dashed line inserted in each plot.

Compound	Curve classification	IC_{50} [μM]
1-methylindole	1	36.8 ± 9.1
2-methylindole	2	> 150
3-methylindole	2	> 150
4-methylindole	1	81.6 ± 38.2
5-methylindole	3	> 150
6-methylindole	2	> 150
7-methylindole	3	n.d.

Curve classification according to Shukla *et al.*, 2009
n = 3; n.d. = not determined

✕   sr12813 [100 μM]

10 μM). Induction of luciferase activity by RIF, as compared to vehicle-treated cells, ranged from 13-fold to 24-fold in three consecutive cell passages. All MMIs elicited dose-dependent activation of PXR, and their potencies were comparable, with EC_{50} values ranging from 22.1 μM to 75.7 μM. Relative efficacies of MMIs, as compared to 10 μM RIF, ranged from 34 % to 111 % (Fig. 1). Tested MMIs also displayed moderate dose-dependent antagonist effects on RIF-mediated activation of PXR, but IC_{50} was reached only for 3-MMI (153.63 ± 39.17 μM) (Fig. 1). Taken together, the data above reveal about partial agonist effects of MMIs at PXR.

3.2. Effects of mono-methylated indoles on the expression of CYP3A4 and MDR1 in human hepatic and intestinal cells

We investigated whether mono-methylated indoles induce CYP3A4 and MDR1, which are typical PXR-regulated genes, in human hepatic and intestinal cells. Rifampicin, a model ligand and activator of PXR, induced CYP3A4 and MDR1 mRNAs approx. 6-fold and 8-fold, respectively, in human colon adenocarcinoma cell line LS180 transiently transfected with PXR vector. 1-MMI and 2-MMI achieved significant induction of CYP3A4 (cca 2-fold) and MDR1 (cca 5-fold) mRNAs. Besides, MDR1, but not CYP3A4, was induced by 4-MMI (4-fold) and 5-MMI (2-fold) (Fig. 2A,B). In primary human hepatocytes cultures from three different liver donors, rifampicin significantly induced CYP3A4 and MDR1 mRNAs. The effects of MMIs on PXR-regulated genes in human hepatocytes displayed inter-individual patterns depending on particular liver tissue donors. The effects were overall negative, with the exception of weak CYP3A4 mRNA induction by 1-MMI, 2-MMI, and 4-MMI (borderline induction > 5% of that by RIF) in culture LH75 (Fig. 2C,D). Similarly, the level of CYP3A4 protein was increased only by 2-MMI in hepatocytes culture LH79 (Fig. 2E). Noteworthy, unlike in cell lines, human hepatocytes are fully metabolically active; thereby, the gene induction comprises the effects of both maternal compounds and their metabolites. This behavior is consistent with our previous observations elsewhere (Vyhlidalova et al., 2019). We also used wild type (control 5 F clone) and PXR-knock out (PXR-KO) variant of human hepatic progenitor HepaRG cells to delineate the role of PXR in CYP3A4/MDR1 induction by MMIs. Rifampicin induced CYP3A4 mRNA in 5 F-HepaRG (8-fold), but not in PXR-KO-HepaRG cells. Significant induction of CYP3A4 mRNA was observed for 1-MMI (5-fold) and 2-MMI (4-fold) only in wild type 5 F-HepaRG cells (Fig. 2F), which is consistent with CYP3A4 induction pattern observed in LS180 cells (Fig. 2A). Additionally, these data confirm that CYP3A4 induction by 1-MMI and 2-MMI is PXR-dependent.

3.3. Binding of PXR in CYP3A4 gene promotor

The capability of MMIs to transform PXR in its DNA-binding form was assessed by chromatin immune precipitation assay (ChIP). Intestinal LS174 T cells, transfected with PXR vector, were incubated for 24 h with the vehicle, RIF (10 μM), and 1-MMI (200 μM), which was selected as lead, PXR-active MMI. The promotor of the CYP3A4 gene was slightly enriched with PXR in cells incubated with 1-MMI (Fig. 3). These data reveal that the induction of CYP3A4 by MMIs involves increased binding of PXR in CYP3A4 promotor.

3.4. Binding of mono-methylated indoles at PXR

Cell-free, competitive ligand-binding assay (Time-Resolved Fluorescence Resonance Energy Transfer; TR-FRET) was used to assess the binding of mono-methylated indoles to the ligand-binding domain (LBD) of PXR. With the exception of 7-MMI, all test compounds caused the dose-dependent displacement of the fluorescent ligand from PXR-LBD (Fig. 4). Typical, class-I (Shukla et al., 2009) full-length sigmoid curve, was recorded for 1-MMI ($IC_{50} = 36.8 ± 9.1$ μM) and 4-MMI ($IC_{50} = 81.6 ± 38.2$ μM). These data imply that MMIs are weak ligands

of PXR.

4. Discussion

In the current study, we show that mono-methylated indole isomers differentially affect the PXR-CYP3A4 signaling pathway in human hepatic and intestinal cells. While indole methylated at position 3 (3-MMI) is a microbial catabolite formed from dietary tryptophan in intestines (often referred to as skatole) (Roager and Licht, 2018), the other MMIs isomers are xenobiotics. Across all assays employed in this paper, we identified 1-MMI as the most PXR-active derivative. This lead MMI induced PXR-regulated gene CYP3A4 in intestinal LS180 cells and in hepatic progenitor cells HepaRG, but not in primary human hepatocytes. The induction of CYP3A4 was nullified in PXR-knock-out HepaRG cells, which testifies to the involvement of PXR in the process. Direct interaction of 1-MMI with ligand-binding domain of PXR was demonstrated by TR-FRET assay ($IC_{50} \sim 37$ μM). Increased binding of PXR in the promotor of CYP3A4 was confirmed by ChIP assay. The inconsistency between CYP3A4 expression in cell lines and primary human hepatocytes probably stems from the sophisticated metabolic equipment of human hepatocytes as compared to cell lines. Indeed, in the recent study, we observed both loss and gain of MMI effects at AhR in human hepatocytes, which was ascribed to the metabolic transformation of parental compounds (Vyhlidalova et al., 2019). Reporter gene assay revealed that 1-MMI is a partial agonist of PXR. Whereas 1-MMI dose-dependently activated PXR ($EC_{50} \sim 22$ μM; relative efficacy ~ 67 %), it also caused a weak dose-dependent inhibition of rifampicin-mediated PXR activity ($IC_{50} > 200$ μM). From a therapeutic point of view, the lack of CYP3A4 induction by MMIs in human hepatocytes would predestine these compounds as intestinal-selective PXR modulators, having no systemic effects. Also, fecal concentrations of skatol (3-methyl indole) in humans reached up to 750 μM, which supports the use of high MMI concentrations *in vitro* in the current study, still having *in vivo* relevance (Gao et al., 2018).

The Janus-faced nature of PXR activation by xenobiotics (drugs) is a challenge of current pharmacotherapy. On the one hand, PXR activation results in the induction of drug-metabolizing genes, thereby being a cause for drug-drug interactions and the reason for rejection of a drug candidate in the early phase of testing. Also, dysregulation of lipid and carbohydrate metabolism occurs as a side-effect of PXR-active drugs. On the other hand, there is an increasing body of evidence that therapeutic targeting PXR might be an effective strategy in the treatment of intestinal inflammatory diseases. In this context, the potential repositioning of PXR-active drugs is considered a vital approach in the therapy of intestinal pathologies. Concerning the indole moiety as a pharmacophore in targeting PXR, we have recently identified dietary (Pondugula et al., 2015) and microbial (Venkatesh et al., 2014) indoles that activate PXR. Also, many approved and widely used drugs, such as anti-migraine triptans, beta-blockers pindolol, and bucindolol, or alpha-blocker indoramin, have indole moiety in their structure.

An important aspect of therapeutic targeting of PXR is the fact that many xenobiotics are dual activators of PXR and AhR. Moreover, there exists a mutual functional cross-talk between AhR and PXR (Rasmussen et al., 2017). Therefore, differential therapeutic outcomes are expected for PXR-selective *versus* dual AhR/PXR activators. It is not yet established whether dual targeting AhR/PXR improves or deteriorates net PXR biological effects under general or specific conditions, however. Recently, we described a series of methoxylated and methylated indoles as agonists and antagonists of AhR (Stepankova et al., 2018; Vyhlidalova et al., 2019). We identified 4-MMI, 5-MMI, and 6-MMI as powerful AhR agonists, while 2-MMI had vigorous antagonist activity at AhR. Interestingly, skatole, the only non-xenobiotic isomer, was demonstrated as AhR partial agonist by Rasmussen group (Rasmussen et al., 2016) and confirmed in our study (Stepankova et al., 2018). The lead PXR-active 1-MMI resulting from the current study displayed only negligible AhR activity, which allows considering 1-MMI as selective

PXR activator.

Overall, the data presented here may pave the avenue in designing new indole-based therapeutic scaffolds aimed for the treatment of PXR-responsive pathologies such as inflammatory pathologies of the gastrointestinal tract.

Authors contributions

Participated in research design: Zdeněk Dvořák, Sridhar Mani

Conducted experiments: Barbora Vyhlídalová, Eva Jiskrová, Iveta Bartoňková, Hao Li

Contributed new reagents and analytic tools: Zdeněk Dvořák, Sridhar Mani

Performed data analysis: Barbora Vyhlídalová, Eva Jiskrová, Iveta Bartoňková, Zdeněk Dvořák, Hao Li

Wrote or contributed to the writing of the manuscript: Zdeněk Dvořák, Barbora Vyhlídalová, Sridhar Mani

Funding

Data availability statement

All data generated or analyzed during this study are included in this published article.

Transparency document

The Transparency document associated with this article can be found in the online version.

Declaration of Competing Interest

The authors declare that they have no conflict of interest.

References

Avior, Y., Levy, G., Zimerman, M., Kitsberg, D., Schwartz, R., Sadeh, R., Moussaieff, A., Cohen, M., Itskovitz-Eldor, J., Nahmias, Y., 2015. Microbial-derived lithocholic acid and vitamin K2 drive the metabolic maturation of pluripotent stem cells-derived and fetal hepatocytes. Hepatology 62, 265–278.

Bartonkova, I., Dvorak, Z., 2018. Essential oils of culinary herbs and spices activate PXR and induce CYP3A4 in human intestinal and hepatic in vitro models. Toxicol. Lett. 296, 1–9.

Carazo, A., Mladenka, P., Pavek, P., 2019. Marine ligands of the pregnane X receptor (PXR): an overview. Mar. Drugs 17.

Cho, J.Y., Kang, D.W., Ma, X., Ahn, S.H., Krausz, K.W., Luecke, H., Idle, J.R., Gonzalez, F.J., 2009. Metabolomics reveals a novel vitamin E metabolite and attenuated vitamin E metabolism upon PXR activation. J. Lipid Res. 50, 924–937.

Drocourt, L., Pascussi, J.M., Assenat, E., Fabre, J.M., Maurel, P., Vilarem, M.J., 2001. Calcium channel modulators of the dihydropyridine family are human pregnane X receptor activators and inducers of CYP3A, CYP2B, and CYP2C in human hepatocytes. Drug Metab. Dispos. 29, 1325–1331.

Gao, J., Xu, K., Liu, H., Liu, G., Bai, M., Peng, C., Li, T., Yin, Y., 2018. Impact of the gut microbiota on intestinal immunity mediated by tryptophan metabolism. Front. Cell. Infect. Microbiol. 8, 13.

Hubbard, T.D., Murray, I.A., Bisson, W.H., Lahoti, T.S., Gowda, K., Amin, S.G., Patterson, A.D., Perdew, G.H., 2015. Adaptation of the human aryl hydrocarbon receptor to sense microbiota-derived indoles. Sci. Rep. 5, 12689.

Isom, H.C., Secott, T., Georgoff, I., Woodworth, C., Mummaw, J., 1985. Maintenance of differentiated rat hepatocytes in primary culture. Proc. Natl. Acad. Sci. U.S.A. 82, 3252–3256.

Jin, U.H., Lee, S.O., Sridharan, G., Lee, K., Davidson, L.A., Jayaraman, A., Chapkin, R.S., Alaniz, R., Safe, S., 2014. Microbiome-derived tryptophan metabolites and their aryl hydrocarbon receptor-dependent agonist and antagonist activities. Mol. Pharmacol. 85, 777–788.

Kim, C.H., 2018. Immune regulation by microbiome metabolites. Immunology 154, 220–229.

Kliewer, S.A., Moore, J.T., Wade, L., Staudinger, J.L., Watson, M.A., Jones, S.A., McKee, D.D., Oliver, B.B., Willson, T.M., Zetterstrom, R.H., Perlmann, T., Lehmann, J.M., 1998. An orphan nuclear receptor activated by pregnanes defines a novel steroid signaling pathway. Cell 92, 73–82.

Nelson, J.D., Denisenko, O., Sova, P., Bomsztyk, K., 2006. Fast chromatin immunoprecipitation assay. Nucleic Acids Res. 34, e2.

Oladimeji, P.O., Chen, T., 2018. PXR: more than just a master xenobiotic receptor. Mol. Pharmacol. 93, 119–127.

Pavek, P., Pospechova, K., Svecova, L., Syrova, Z., Stejskalova, L., Blazkova, J., Dvorak, Z., Blahos, J., 2010. Intestinal cell-specific vitamin D receptor (VDR)-mediated transcriptional regulation of CYP3A4 gene. Biochem. Pharmacol. 79, 277–287.

Pichard, L., Fabre, I., Fabre, G., Domergue, J., Saint Aubert, B., Mourad, G., Maurel, P., 1990. Cyclosporin A drug interactions. Screening for inducers and inhibitors of cytochrome P-450 (cyclosporin A oxidase) in primary cultures of human hepatocytes and in liver microsomes. Drug Metab. Dispos. 18, 595–606.

Pondugula, S.R., Flannery, P.C., Abbott, K.L., Coleman, E.S., Mani, S., Samuel, T., Xie, W., 2015. Diindolylmethane, a naturally occurring compound, induces CYP3A4 and MDR1 gene expression by activating human PXR. Toxicol. Lett. 232, 580–589.

Rasmussen, M.K., Balaguer, P., Ekstrand, B., Daujat-Chavanieu, M., Gerbal-Chaloin, S., 2016. Skatole (3-Methylindole) Is a Partial Aryl Hydrocarbon Receptor Agonist and Induces CYP1A1/2 and CYP1B1 Expression in Primary Human Hepatocytes. PLoS One 11, e0154629.

Rasmussen, M.K., Daujat-Chavanieu, M., Gerbal-Chaloin, S., 2017. Activation of the aryl hydrocarbon receptor decreases rifampicin-induced CYP3A4 expression in primary human hepatocytes and HepaRG. Toxicol. Lett. 277, 1–8.

Roager, H.M., Licht, T.R., 2018. Microbial tryptophan catabolites in health and disease. Nat. Commun. 9, 3294.

Shukla, S.J., Nguyen, D.T., Macarthur, R., Simeonov, A., Frazee, W.J., Hallis, T.M., Marks, B.D., Singh, U., Eliason, H.C., Printen, J., Austin, C.P., Inglese, J., Auld, D.S., 2009. Identification of pregnane X receptor ligands using time-resolved fluorescence resonance energy transfer and quantitative high-throughput screening. Assay Drug Dev. Technol. 7, 143–169.

Staudinger, J.L., Goodwin, B., Jones, S.A., Hawkins-Brown, D., MacKenzie, K.I., LaTour, A., Liu, Y., Klaassen, C.D., Brown, K.K., Reinhard, J., Willson, T.M., Koller, B.H., Kliewer, S.A., 2001. The nuclear receptor PXR is a lithocholic acid sensor that protects against liver toxicity. Proc. Natl. Acad. Sci. U.S.A. 98, 3369–3374.

Staudinger, J.L., Ding, X., Lichti, K., 2006. Pregnane X receptor and natural products: beyond drug-drug interactions. Expert Opin. Drug Metab. Toxicol. 2, 847–857.

Stepankova, M., Bartonkova, I., Jiskrova, E., Vrzal, R., Mani, S., Kortagere, S., Dvorak, Z., 2018. Methylindoles and methoxyindoles are agonists and antagonists of human aryl hydrocarbon receptor. Mol. Pharmacol. 93, 631–644.

Svecova, L., Vrzal, R., Burysek, L., Anzenbacherova, E., Cerveny, L., Grim, J., Trejtnar, F., Kunes, J., Pour, M., Staud, F., Anzenbacher, P., Dvorak, Z., Pavek, P., 2008. Azole antimycotics differentially affect rifampicin-induced pregnane X receptor-mediated CYP3A4 gene expression. Drug Metab. Dispos. 36, 339–348.

Tabb, M.M., Sun, A., Zhou, C., Grun, F., Errandi, J., Romero, K., Pham, H., Inoue, S., Mallick, S., Lin, M., Forman, B.M., Blumberg, B., 2003. Vitamin K2 regulation of bone homeostasis is mediated by the steroid and xenobiotic receptor SXR. J. Biol. Chem. 278, 43919–43927.

Venkatesh, M., Mukherjee, S., Wang, H., Li, H., Sun, K., Benechet, A.P., Qiu, Z., Maher, L., Redinbo, M.R., Phillips, R.S., Fleet, J.C., Kortagere, S., Mukherjee, P., Fasano, A., Le Ven, J., Nicholson, J.K., Dumas, M.E., Khanna, K.M., Mani, S., 2014. Symbiotic bacterial metabolites regulate gastrointestinal barrier function via the xenobiotic sensor PXR and Toll-like receptor 4. Immunity 41, 296–310.

Vyhlidalova, B., Poulikova, K., Bartonkova, I., Krasulova, K., Vanco, J., Travnicek, Z., Mani, S., Dvorak, Z., 2019. Mono-methylindoles induce CYP1A genes and inhibit CYP1A1 enzyme activity in human hepatocytes and HepaRG cells. Toxicol. Lett. 313, 66–76.

Wang, H., Venkatesh, M., Li, H., Goetz, R., Mukherjee, S., Biswas, A., Zhu, L., Kaubisch, A., Wang, L., Pullman, J., Whitney, K., Kuro-o, M., Roig, A.I., Shay, J.W., Mohammadi, M., Mani, S., 2011. Pregnane X receptor activation induces FGF19-dependent tumor aggressiveness in humans and mice. J. Clin. Invest. 121, 3220–3232.

Wyde, M.E., Kirwan, S.E., Zhang, F., Laughter, A., Hoffman, H.B., Bartolucci-Page, E., Gaido, K.W., Yan, B., You, L., 2005. Di-n-butyl phthalate activates constitutive androstane receptor and pregnane X receptor and enhances the expression of steroid-metabolizing enzymes in the liver of rat fetuses. Toxicol. Sci. 86, 281–290.

Yasuda, K., Ranade, A., Venkataramanan, R., Strom, S., Chupka, J., Ekins, S., Schuetz, E., Bachmann, K., 2008. A comprehensive in vitro and in silico analysis of antibiotics that activate pregnane X receptor and induce CYP3A4 in liver and intestine. Drug Metab. Dispos. 36, 1689–1697.

APPENDIX III.

Vyhlidalova B., Krasulova K., Pecinkova P., Marcalikova A., Vrzal R., Zemankova L., Vanco J., Travnicek Z., Vondracek J., Karasova M., Mani S., Dvorak, Z. (2020): Gut Microbial Catabolites of Tryptophan Are Ligands and Agonists of the Aryl Hydrocarbon Receptor: A Detailed Characterization. *Int. J. Mol. Sci*, 21(7): 2614. **[IF$_{2020}$ 5.924]**

Article

Gut Microbial Catabolites of Tryptophan Are Ligands and Agonists of the Aryl Hydrocarbon Receptor: A Detailed Characterization

Barbora Vyhlídalová [1,†], **Kristýna Krasulová** [1,†], **Petra Pečinková** [1], **Adéla Marcalíková** [1], **Radim Vrzal** [1], **Lenka Zemánková** [1], **Jan Vančo** [2], **Zdeněk Trávníček** [2], **Jan Vondráček** [3], **Martina Karasová** [3], **Sridhar Mani** [4,*] and **Zdeněk Dvořák** [1,*]

[1] Department of Cell Biology and Genetics, Faculty of Science, Palacky University, Slechtitelu 27, 783 71 Olomouc, Czech Republic; vyhlidalovabara@gmail.com (B.V.); kkrasulova@seznam.cz (K.K.); petra.pecinkova@upol.cz (P.P.); Marcalikova.Adela@seznam.cz (A.M.); radim.vrzal@email.cz (R.V.); lenka.zemankova@upol.cz (L.Z.)

[2] Division of Biologically Active Complexes and Molecular Magnets, Regional Centre of Advanced Technologies and Materials, Faculty of Science, Palacký University, Šlechtitelů 27, 783 71 Olomouc, Czech Republic; jan.vanco@upol.cz (J.V.); zdenek.travnicek@upol.cz (Z.T.)

[3] Department of Cytokinetics, Institute of Biophysics of the Czech Academy of Sciences, Královopolská 135, 61265 Brno, Czech Republic; vondracek@ibp.cz (J.V.); karasova@ibp.cz (M.K.)

[4] Department of Genetics and Department of Medicine, Albert Einstein College of Medicine, Bronx, NY 10461, USA

*   Correspondence: sridhar.mani@einstein.yu.edu (S.M.); moulin@email.cz (Z.D.); Tel.: +001-718-430-2871 (S.M.); +420-58-5634903 (Z.D.)

†   These authors contributed equally to this work.

check for updates

Abstract: We examined the effects of gut microbial catabolites of tryptophan on the aryl hydrocarbon receptor (AhR). Using a reporter gene assay, we show that all studied catabolites are low-potency agonists of human AhR. The efficacy of catabolites differed substantially, comprising agonists with no or low (i3-propionate, i3-acetate, i3-lactate, i3-aldehyde), medium (i3-ethanol, i3-acrylate, skatole, tryptamine), and high (indole, i3-acetamide, i3-pyruvate) efficacies. We displayed ligand-selective antagonist activities by i3-pyruvate, i3-aldehyde, indole, skatole, and tryptamine. Ligand binding assay identified low affinity (skatole, i3-pyruvate, and i3-acetamide) and very low affinity (i3-acrylate, i3-ethanol, indole) ligands of the murine AhR. Indole, skatole, tryptamine, i3-pyruvate, i3-acrylate, and i3-acetamide induced *CYP1A1* mRNA in intestinal LS180 and HT-29 cells, but not in the AhR-knockout HT-29 variant. We observed a similar CYP1A1 induction pattern in primary human hepatocytes. The most AhR-active catabolites (indole, skatole, tryptamine, i3-pyruvate, i3-acrylate, i3-acetamide) elicited nuclear translocation of the AhR, followed by a formation of AhR-ARNT heterodimer and enhanced binding of the AhR to the CYP1A1 gene promoter. Collectively, we comprehensively characterized the interactions of gut microbial tryptophan catabolites with the AhR, which may expand the current understanding of their potential roles in intestinal health and disease.

Keywords: aryl hydrocarbon receptor; tryptophan; indoles; microbiome

1. Introduction

The microbial community of the human gastrointestinal tract plays a vital role in the maintenance of gut health and host nutrition. The colonic bacteria also contribute to the regulation of functions of distant organs, including the brain, liver, immune system, and pancreas. The intestinal microbiome

has also been linked to the etiology of inflammatory bowel disease, obesity, diabetes, or cardiovascular diseases [1]. Intestinal bacterial metabolites comprise a wide range of compounds; however, three major classes of compounds seem to play a significant role in intestinal physiology: short-chain fatty acids, secondary bile acids, and tryptophan catabolites. A plethora of microbial intestinal catabolites of tryptophan (MICT), including indole (IND), tryptamine (TA), skatole (3MI), indole-3-pyruvate (IPY), indole-3-lactate (ILA), indole-3-acrylate (IAC), indole-3-propionate (IPA), indole-3-acetamide (IAD), indole-3-acetate (IAA), indole-3-ethanol (IET), indole-3-aldehyde (IA), and indole-3-acetaldehyde, have been identified so far [2]. In recent years, it also became evident that a principal molecular target for indole-based compounds is the aryl hydrocarbon receptor (AhR). This receptor is a ligand-inducible transcription factor that resides in the cell cytosol in its resting state. Upon ligand binding, AhR translocates into the nucleus, where it heterodimerizes with AhR nuclear translocator (ARNT), and the AhR/ARNT heterodimer binds to the dioxin responsive elements within enhancer and promoter regions of the AhR target genes. The AhR plays multiple roles in the regulation of immune responses, xenoprotection, bone remodeling, carcinogenesis, cell regeneration, organ development, metabolic diseases, and neurophysiology [3–7]. The AhR ligands can be both xenobiotics and endogenous compounds [8–10]. A variety of indole-based compounds have been documented to act as AhR ligands, including indirubin and indigo [11], bilirubin, biliverdin and hemin [12], diindolylmethane [13] and other di-indole derivatives [14], indole-3-carbinol [15], indoxyl-3-sulfate [16,17], ultraviolet photoproducts of tryptophan [18], including 6-formylindolo[3 ,2-b]carbazole (FICZ) [19], marine brominated indoles [20], and several MICTs (TA, IAA [21], IA [17], IND [22], or 3MI [23,24]). Indoles may act as human AhR-selective agonists, but also as AhR antagonists in a context-specific manner [22,25].

Several isolated reports dealt with the biological effects of MICT via the AhR. Tryptophan microbial catabolite IA has been found to engage the AhR and to balance mucosal reactivity via interleukin-22 [26]. Lamas et al. have shown that deficiency in the microbial production of microbial tryptophan product IAA leads to increased susceptibility to colitis, involving the AhR-dependent pathways [27]. Therefore, it is of particular interest to know how individual MICT influence AhR signaling.

The intestinal concentrations of MICTs are mostly unknown. The most studied ones include the fecal levels of indole, where its concentrations have been reported to range from 250 up to 2500 µM [2,25,27,28]. The fecal concentrations of 3MI spanned from 40 to 750 µM in healthy subjects and patients with intestinal pathologies, respectively [29]. The concentration of IAA in fecal samples of healthy adults can approach five (5) µM [27]. We have found indole levels ranging from 40 to 130 µM in colonoscopy aspirates from 36 healthy and colitis human subjects, which suggests that the intestinal indole levels could be lower than those in feces. In the same cohort, we found IPA levels to be about 0.5 µM (unpublished observations, Mani Lab).

In the current study, we investigated in detail the effects of MICT on the AhR-CYP1A signaling pathway. We tested MICT at concentrations up to 200 µM (1 mM for indole) given their abundance in intestines. We found that MICT is low-affinity ligands of AhR, which act as low-potency and high-efficacy agonists of AhR. MICT induced nuclear translocation of AhR, the heterodimerization of AhR with ARNT, the binding of AhR to CYP1A1 promoter, and the induction of CYP1A1, in the AhR-dependent manner, in both hepatic and intestinal cells. The most efficacious MICT included IND, 3MI, TA, IPY, IAC, and IAD, whereas IAA, IPA, ILA, and IA were inactive.

2. Results

2.1. Tryptophan in the CULTURE Medium Does not Influence AhR Activity

We aimed to evaluate the biological activities of tryptophan metabolites. Since conventional cell culture media and fetal bovine serum contain Trp, which may impact the background AhR-mediated activity [30], we first validated the appropriateness of Trp-containing media for such a study. Using HPLC, we determined Trp concentration in cultures of AZ-AHR, LS174T, and HaCaT cells throughout 24 h. The initial concentration of Trp in culture medium containing 10% serum was approx. 75 µM,

and it slowly linearly decreased, down to approx. 60 µM after 24 h of incubation, regardless of the cell-type being used (Supplementary Figure S2A). Therefore, we considered Trp concentration in cell cultures to be stable over the time of incubation. Trp did not activate AhR up to 100 µM concentration in AZ-AHR cell cultures when using Trp-free/serum-free medium, whereas both TCDD and IND induced luciferase activity by 10000-fold and 500-fold, respectively (Supplementary Figure S2B). We compared the activation of AhR by TDCC and IND in AZ-AHR cells cultured in conventional, Trp-free, serum-free, and Trp-free/serum-free media. We concluded that the presence of Trp in the culture medium would not interfere with MICT testing under standard cell culture conditions (Supplementary Figure S2C). Moreover, Trp did not displace ^{3}H-TCDD from binding at the murine AhR (data not shown).

2.2. MICTs Exhibit Full and Partial Agonist Effects on AhR in the AZ-AHR Reporter Cell Line

In the first series of experiments, we evaluated the agonistic and antagonistic effects of MICT on the AhR activation. All compounds were tested at concentrations of up to 200 µM, except for IAC (the maximum concentration was 100 µM due to solubility limitations) and IND (10 mM, given its known high intestinal concentrations). All MICTs activated the AhR in a dose-dependent manner; however, we did not reach the plateau, and their relative efficacies differed substantially. The effectively inactive agonists were IPA, IAA, ILA, and IA ($\approx$8-fold induction). 3MI, TA, IET, and IAC (fold inductions from 40-fold to 100-fold) displayed a medium efficacy agonism. In contrast, the most efficacious agonists included IND, IPY, and IAD (fold inductions from 200-fold to 600-fold). The relative potencies of MICT were rather low, with their EC_{50} ranging from 42 to 103 µM. A notable exception was IND, with $EC_{50} \approx 1.5$ mM (Figure 1; upper panels). The antagonistic effects of MICT were evaluated against typical full agonists of the AhR, comprising TCDD, BaP, and FICZ, which were applied at fixed concentrations corresponding to their EC_{80}. IA, IND, and TA displayed a dose-dependent antagonistic effect against all used agonists. In contrast, we observed no antagonistic effects against any of the full agonists to be exhibited by IET, IAC, ILA, IAA, and IPA. A ligand-selective antagonism was observed for 3MI, which dose-dependently inhibited the AhR activation by TCDD and BaP, but not by FICZ. Interestingly, IAD and IPY had dual effects on ligand-activated AhR. These two compounds antagonized TCDD, but potentiated the agonistic effects of BaP and FICZ (Figure 1; lower panels).
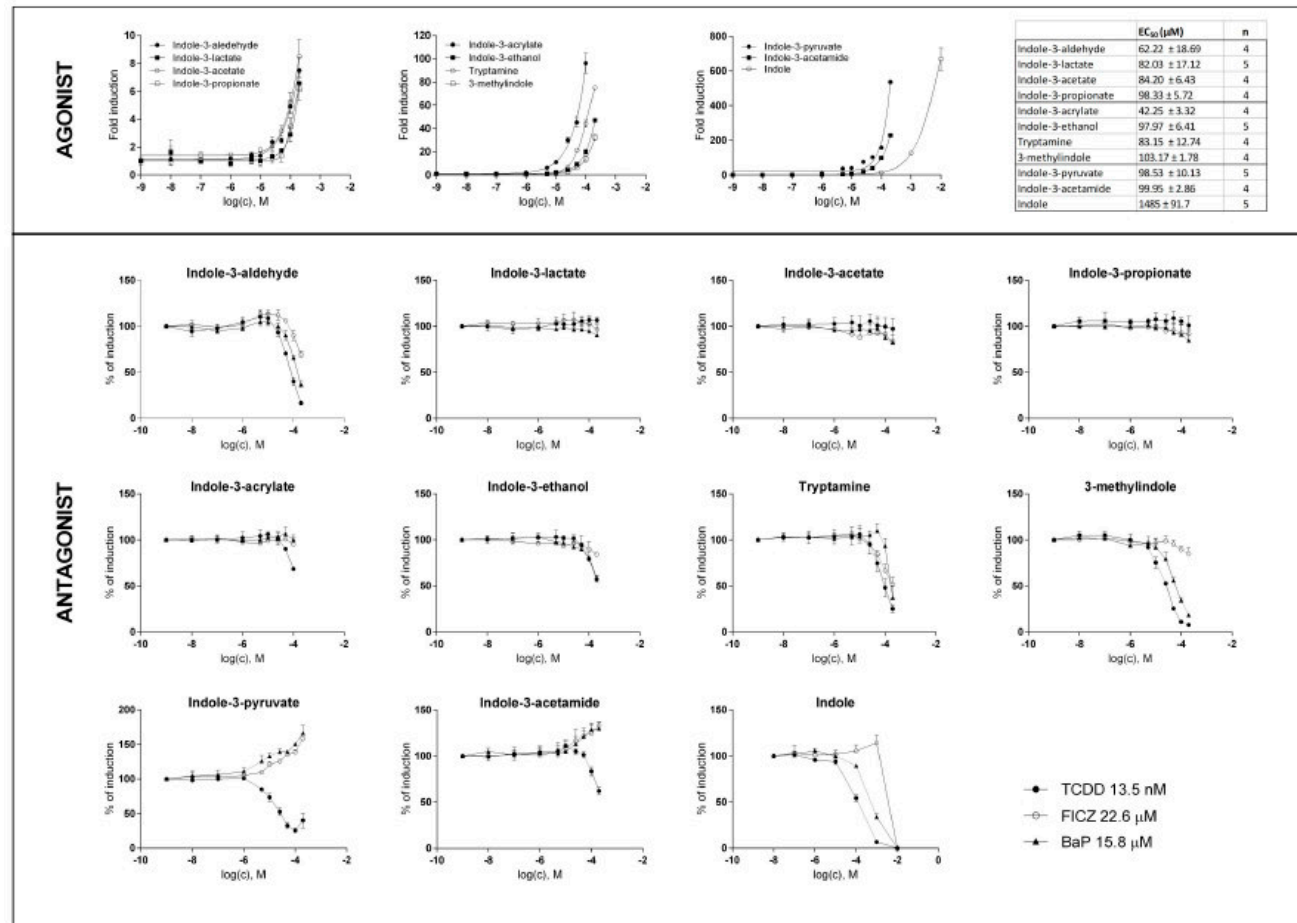
Figure 1. Effects of MICT on the AhR transcriptional activity in the reporter gene assay. AZ-AHR cells were incubated for 24 h with vehicle (DMSO; 0.1% v/v) and increasing concentrations of MICT, in the absence (agonist analyses) or the presence (antagonist analyses) of TCDD (13.5 nM), BaP (15.8 μM) and FICZ (22.6 μM). Following the treatments, we lysed cells, and luciferase activity was measured. Experiments were performed at least in four consecutive cell passages. Incubations were performed in quadruplicates (technical replicates). In agonist analyses, the data from a representative experiment, expressed as a fold induction of luciferase activity over control cells, are shown. In antagonist analyses, the data are a percentage of maximal induction, and they are the mean ± SD. The inserted table shows the number of cell passages and calculated EC$_{50}$ for each test compound.

2.3. MICT Is Orthosteric Ligands of the AhR

The ability of MICT to bind the AhR was then evaluated by competitive radio-ligand binding assay, using cytosols from mouse hepatoma cells Hepa1c1c7. High-affinity AhR ligand FICZ actively displaced [^{3}H]-TCDD from binding at AhR (IC$_{50}$ ≈ 2 nM). Among tested MICT, we identified low-affinity AhR ligands including 3MI (IC$_{50}$ 72 μM), IPY (IC$_{50}$ 55 μM) and IAD (IC$_{50}$ 44 μM), and very low-affinity ligands comprising IAC (IC$_{50}$ 710 μM), IET (IC$_{50}$ 1540 μM) and IND (IC$_{50}$ 1130 μM) (Figure 2). Figure 3 shows a comprehensive chart and "heat map," summarizing AhR binding affinities of individual MICT, as well as their respective agonistic and antagonistic effects towards the AhR.
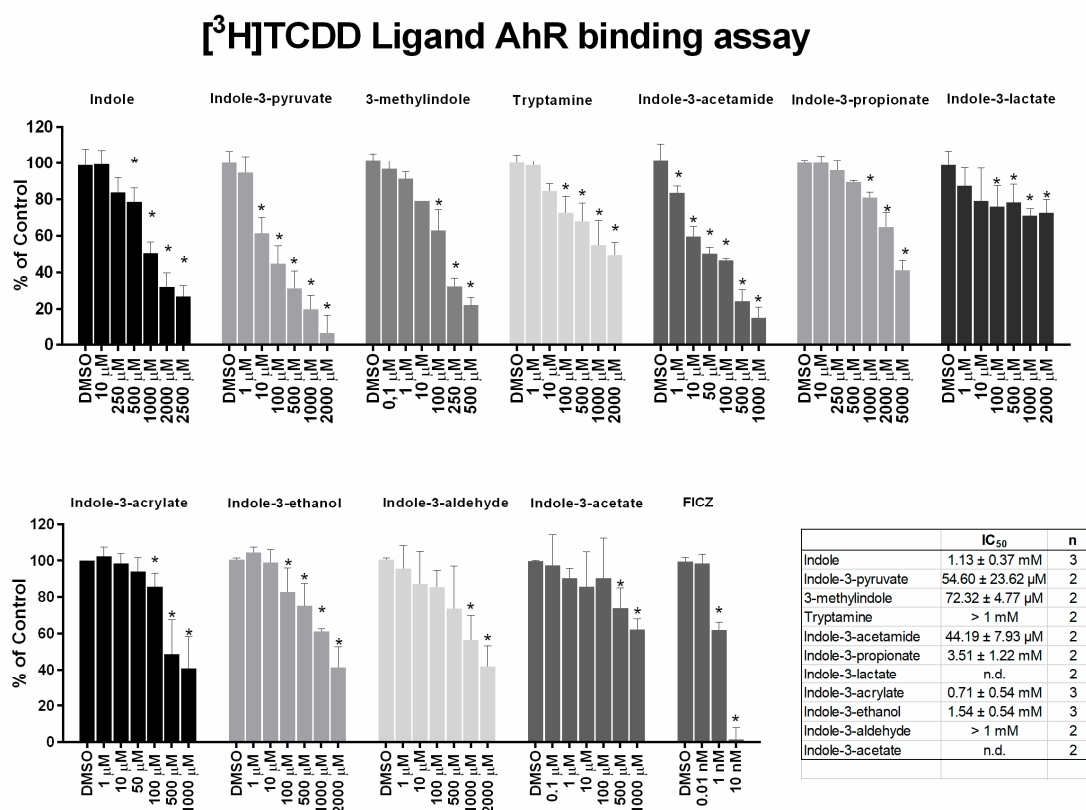
Figure 2. Competitive radio-ligand binding assay. Cytosols from Hepa1c1c7 cells were incubated with vehicle (negative control; 0.1% *V/V*), FICZ (positive control; 0.01 nM – 10 nM), TCDF (non-specific binding; 200 nM) and increasing doses of MICT in the presence of 2 nM [^{3}H]-TCDD. The specific binding of [^{3}H]-TCDD was determined as a difference between total and non-specific (200 nM; TCDF) reactions (value for vehicle DMSO; 0.1% *V/V* = corresponds to *specific binding of [^{3}H]-TCDD = 100%*). At least two independent experiments were performed and the incubations were done in triplicates in each experiment (technical replicates). The error bars represent the mean ± SD. * = significantly different from the vehicle (*p* < 0.05). The inserted table shows the number of repeats and IC$_{50}$ values for each MICT.
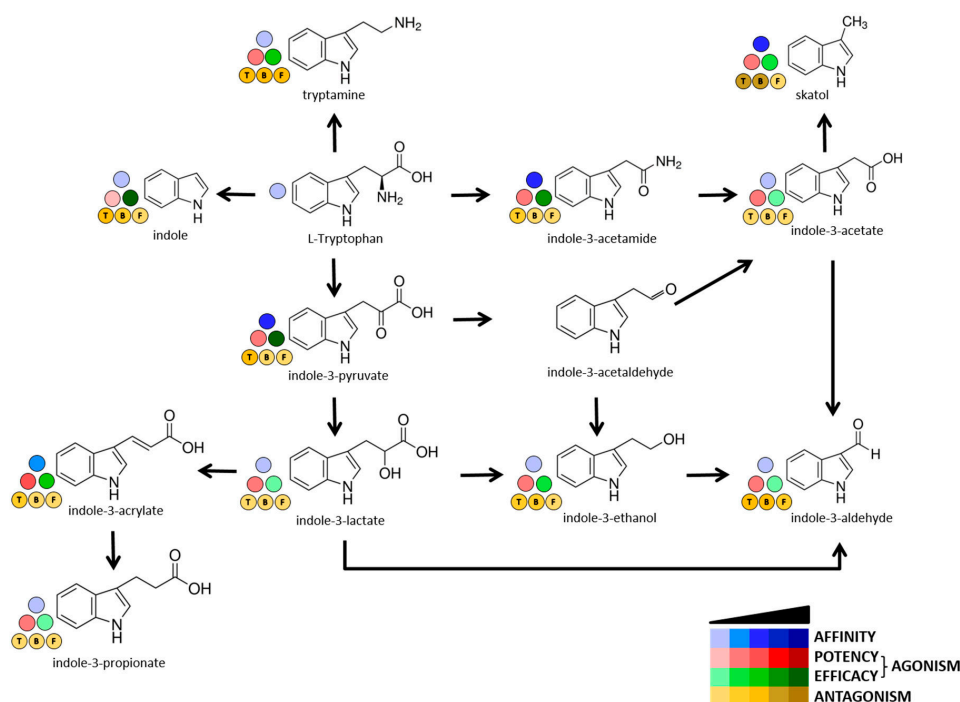
Figure 3. Quantitative characterization of interactions between MICT and AhR. A scheme depicts intestinal microbial catabolism of tryptophan, and the source data come from Figures 1 and 2. The Blue scale refers to the affinity of MICT (ligand binding). The Red & Green scales quantify the relative agonist effects of MICT; Red ≈ potency (EC_{50}), Green ≈ efficacy (E_{MAX}). The Brown scale quantifies the relative antagonist effects (IC_{50}) of MICT against three different agonists used at EC_{80} concentration and designated as "T" = TCDD, "B" = BaP, "F" = FICZ.

2.4. MICT as Inducers of the AhR Target Gene CYP1A1

Since MICT acted as ligands and full/partial agonists of the AhR, we next examined their effects on the induction of expression of CYP1A1, a prototypical AhR target gene. We incubated intestinal and hepatic cells with MICT for 24 h and *measured CYP1A1* mRNA levels by qRT-PCR. We observed a strong induction of *CYP1A1* mRNA in intestinal LS180 cells by IND, IPY, 3MI, TA, IAC, and IAD (Figure 4A), which was largely consistent with the reporter gene assay data (except for IET). The antagonistic effects were observed primarily in the case of IND, 3MI, IPY, and IA, and to a lesser extent, also exhibited by IAA, IPA, ILA, and IAC, in LS180 cells co-incubated with TCDD (Figure 4B). This profile was only partially consistent with the reporter gene assay results, which could be due to the cell-type specific effects. A strong induction of *CYP1A1* mRNA was observed for IPY, IAC, and IAD, while IND, 3MI, and TA acted as weaker inducers in colon HT-29 cells. The qualitative profiles of *CYP1A1* mRNA induction in both intestinal cell models were identical. Moreover, CYP1A1 induction by TCDD and MICT was nullified in the AhR knock-out HT-29 variant (Figure 4C), which corroborates the involvement of AhR in MICT-dependent CYP1A1 induction. Finally, IND, IPY, 3MI, IAC, and IAD, but not TA, induced *CYP1A1* mRNA in primary cultures of human hepatocytes obtained from three different donors (Figure 4D). The lack of induction by TA could be, in part, related to its extensive hepatic metabolism.

INDUCTION OF *CYP1A1* mRNA IN INTESTINAL (LS180 / HT-29) CELLS AND HUMAN HEPATOCYTES
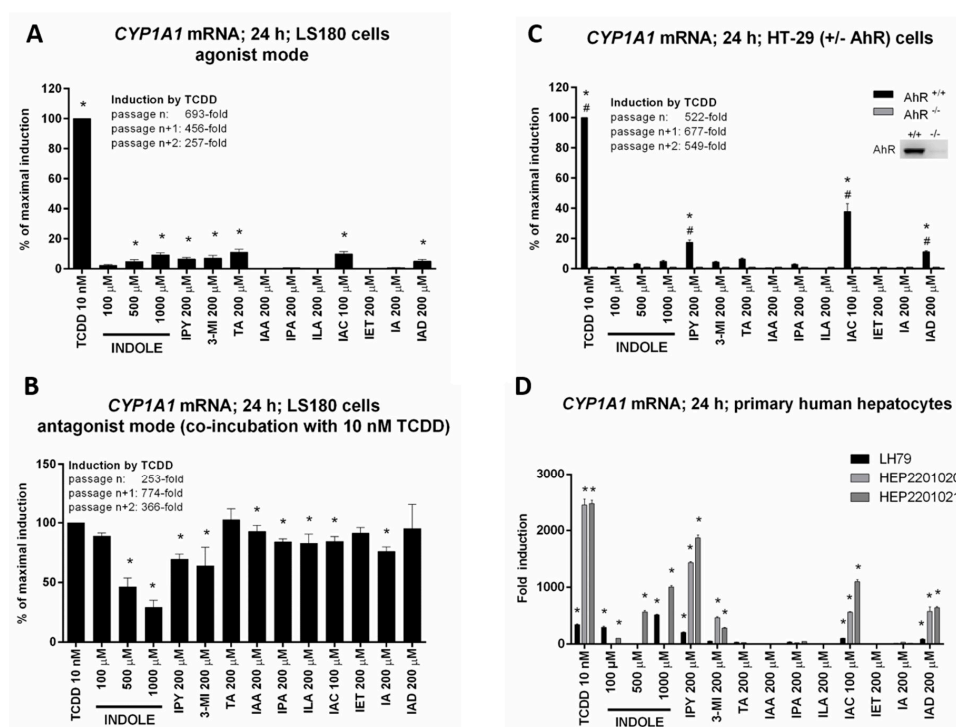
Figure 4. Effects of MICT on the induction of *CYP1A1* mRNA in human hepatic and intestinal cells. Cultured cells were incubated for 24 h with the vehicle (DMSO; 0.1% *v/v*) and tested MICT in the presence or absence of TCDD (10 nM). RT-PCR determined the level of *CYP1A1* mRNA, and the data were normalized per *GAPDH* mRNA level. Each measurement was done in triplicates (technical replicates). * = a value significantly different from the negative control ($p < 0.05$). (**A,B**) Experiments in three consecutive passages of human colon adenocarcinoma cell line LS180 in the absence (**A**) and the presence (**B**) of 10 nM TCDD. The bar graphs show the percentage of maximal induction attained by TCDD and are expressed as the mean ± SD. (**C**) Experiments in three consecutive passages of wild-type (AhR$^{+/+}$) and AhR-knockout (AhR$^{-/-}$) HT-29 cells. The bar graph shows a percentage of maximal induction achieved by TCDD. The data are expressed as the mean ± SD. # = a value significantly different from HT-29 wild-type (AhR$^{+/+}$) ($p < 0.05$). Insert Western Blot shows confirmation of AhR knock-out. (**D**) Primary human hepatocytes from three different donors (LH79, Hep2201020, and Hep2201021). The bar graph shows a fold induction of *CYP1A1* mRNA over vehicle-incubated cells.

2.5. The Lead MICT Trigger Nuclear Translocation of the AhR and the Formation of AhR-ARNT Heterodimer and Its Binging to the CYP1A1 Promoter

Lead AhR-active MICT, including IND, IPY, 3MI, IAC, IAD, and TA, were subjected to a series of assays for their ability to trigger molecular functions of AhR in LS180 cells. An early cellular event, following ligand binding, is the nuclear translocation of the AhR, where it forms a heterodimer with ARNT, which in turn binds DRE motifs in its target gene promoters. All tested lead MICT triggered a massive nuclear translocation of AhR, which was of a similar intensity to that that elicited by TCDD, as revealed by immune-fluorescence detection (Figure 5; Supplementary Table S1). Consequently, protein co-immune-precipitation assay confirmed that IND, IPY, 3MI, IAC, IAD, and TA induce a formation of AhR-ARNT heterodimer (Figure 6). Finally, the binding of the AhR to the promoter of the CYP1A1 gene was correspondingly enhanced by all lead MICT as by TCDD, as revealed by the results of the ChIP assay (Figure 7).
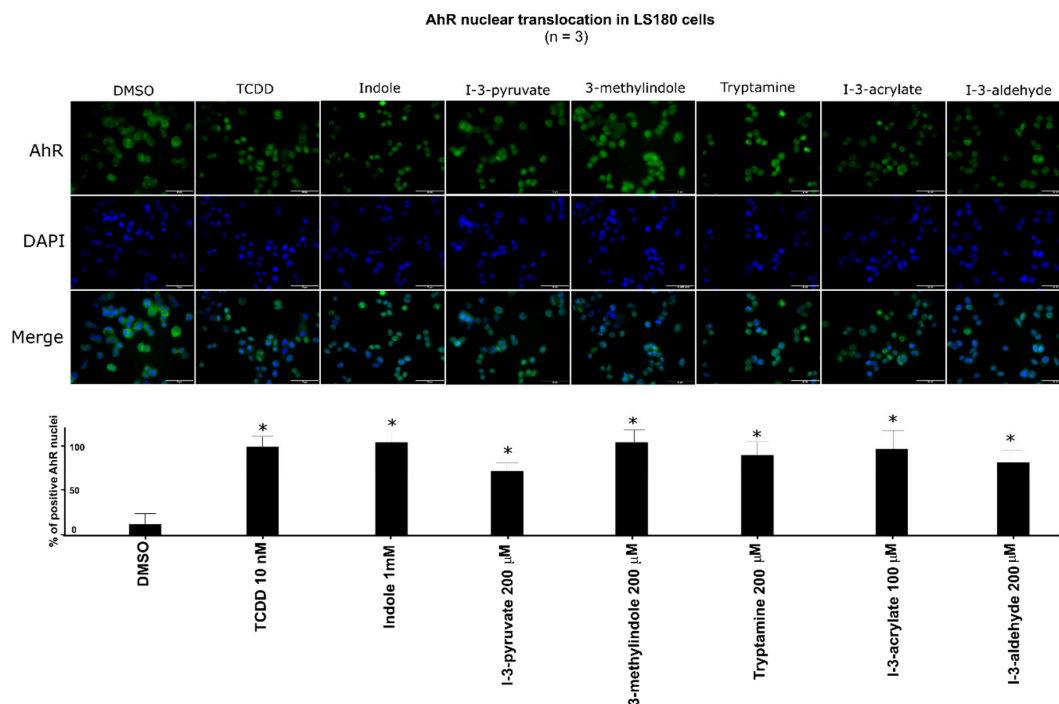
Figure 5. Effect of MICT on nuclear translocation of the AhR. LS180 cells were incubated for 90 min with vehicle (DMSO; 0.1% *V/V*), TCDD (10 nM), and test MICT. The experiments were performed in three consecutive cell passages with all tested compounds in duplication. Fluorescence images depict sub-cellular localization of AhR (upper panels) and nuclear staining by DAPI (lower panels). Representative micrographs are shown. The bar graph shows the percentage of AhR positive nuclei (mean ± SD; *n* = 3) relative to TCDD-treated cells (also ref. Supplementary Table S1). * = a value significantly different from negative control ($p < 0.05$).
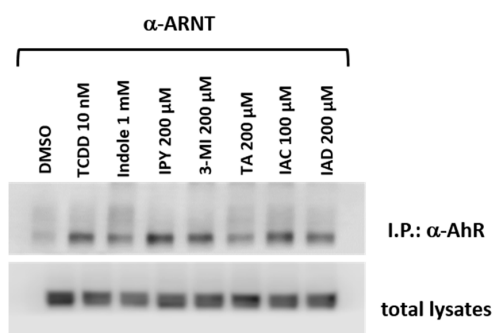
Figure 6. MICTs induce a formation of the AhR-ARNT heterodimer. Intestinal LS180 cells were incubated with TCDD, tested MICT, and vehicle (DMSO; 0.1% *V/V*) for 90 min. Protein co-immunoprecipitation of ARNT was carried out, as described in the Methods section. The representative immunoblots of immuno-precipitated protein eluates and total cell lysates are shown. The experiments were performed in two consecutive cell passages.
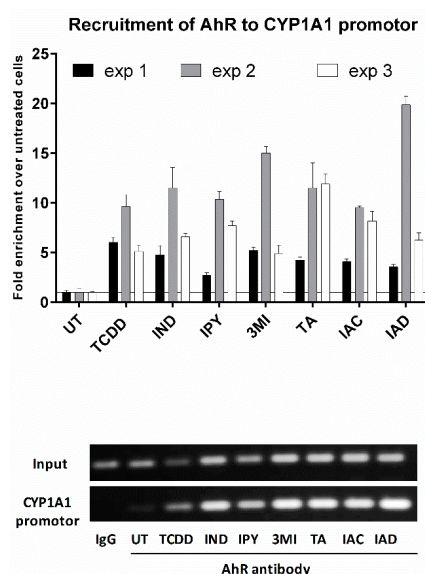
Figure 7. MICT elicit the binding of the AhR to *CYP1A1* promoter, as determined by the chromatin immunoprecipitation assay (ChIP). LS180 cells were incubated with vehicle, TCDD, and tested compounds, as described in Materials and Methods, and were then subjected to ChIP analysis. Bar graphs show binding of the AhR to CYP1A1 promoter as quantified by RT-PCR. The entire protocol was carried out in three consecutive cell passages. The data are expressed as a fold enrichment to vehicle-treated cells and show the mean ± SD from duplicates (technical replicates). DNA fragments amplified by PCR were resolved on 2% agarose gel (representative record from "exp 2" is shown).

3. Discussion

In the current paper, we demonstrate that the microbial catabolite of tryptophan acts, to a different extent, as ligands and agonists of AhR. These actions of tryptophan catabolites are mainly supported by our observations that MICT: (i) displace [^{3}H]-TCDD from the AhR in the ligand-binding assay; (ii) activate AhR in reporter gene assays; (iii) induce AhR target gene expression; (iv) trigger the nuclear translocation of AhR; (v) induce the formation of AhR-ARNT heterodimer; (vi) enhance the binding of the AhR to *CYP1A1* promoter. A resume of the obtained data is shown in Table 1.

Indeed, investigators have previously shown that several compounds formed in vivo and in vitro from Trp act as ligands and activators of AhR. These include photo-reactive Trp catabolites formed in the skin after irradiation by UV light [19], endogenous Trp metabolites [28], or microbial metabolites produced in the skin [31] or intestines [2,23]. Several (individual) Trp metabolites were studied in vitro for their AhR-mediated activities, but also in vivo, thus unveiling their potential physiological and pathological roles dependent on the AhR activation [17,26,27,31]. Nevertheless, a comprehensive study, describing the complex effects of the entire human or microbial Trp metabolome on the AhR has not been conducted so far. Our study is the first one to comprehensively describe the effects of all known human microbial intestinal catabolites of Trp on the AhR activity and functions.

We mainly focused on a comparative overview of effects occurring at the biologically relevant concentrations of MICT. For instance, Lamas et al. reported average fecal concentrations of IAA in healthy human subjects (*n* = 32) to be about five (5) μM, and a similar concentration of IAA (1 μM) has been found in mouse feces. However, they have observed a significant activation of the AhR (15-fold) by IAA only at concentrations exceeding 1000× those in vivo (approx. 5000 μM) [27]. Jin et al. reported IAA concentrations in mouse cecum and feces to range between 20 μM and 30 μM. They observed a very low induction of *CYP1A1* mRNA by 100 μM IAA (≈ 5-fold) in Caco-2 and MDA-MB-231 cells (but not in MDA-MB-468 cells); this induction was more robust (between 10-fold and 35-fold) with IAA in concentrations exceeding 500 μM [25]. Heath-Pagliuso et al. have also described the activation of mouse and guinea pig AhR by IAA, but only at a two (2)-mM concentration [21]. In the present study,

we describe negligible activation of AhR (Figure 1) and no induction of *CYP1A1* mRNA in LS180 cells, HT-29 cells, and primary human hepatocytes (Figure 4) by 200 μM IAA. Overall, given the observable intestinal and fecal concentrations of IAA in human (≈5 μM), and the AhR-active concentrations of IAA in vitro (100–5000 μM), the potential AhR-mediated biological effects of IAA in vivo would be somewhat limited. Similarly, we found a negligible activation of AhR and no induction of *CYP1A1* mRNA by 200 μM IPA, which is consistent with data published by Hubbard et al. [22], who described no AhR activation by ten (10) μM IPA in HepG2 cells. Since the levels of IPA in colonoscopy aspirates from 36 healthy and colitis subjects can approach ≈0.5 μM (unpublished observations, Mani Lab), the biological effects of IPA mediated by the AhR could be negligible. The relevance of IND intestinal concentrations is critical for the assessment of its AhR-dependent effects in humans. The fecal levels of IND in human subjects range between 250 and 2500 μM [2,25,27,28]; however, its concentrations in colonoscopy aspirates ranged only from 40 to 130 μM (unpublished observations, Mani Lab). Similarly, fecal IND concentrations in mice were about 700 μM, while those in the cecum were about 300 μM. In the same study, there was a moderate induction of *CYP1A1* mRNA in various human cells at 500–1000 μM concentration of IND [25], which is consistent with data presented in our current study (Figures 1 and 4). Interestingly, the activation of AhR and the induction of *CYP1A1* mRNA was achieved in HepG2 cells by 100 μM IND, but incubation time in this study was only four (4) h [22]. This observation corroborates our findings in the recent studies, where we observed a higher relative efficacy of methylindoles at AhR after four (4) h of incubation as compared to 24 h [24,32]. Fecal concentrations of 3MI vary substantially between healthy subjects (≈40 μM) and in patients with intestinal pathologies (≤750 μM) [29]. The activation of the AhR and induction of CYP1A1 by 3MI at concentrations occurring in intestines in vivo is reported here and in several other studies [22–24,32], which suggests that the AhR activation could contribute to known physiological and pathophysiological roles of 3MI in gut tissue. The intestinal concentration of TA in humans is largely unknown. Jin et al. found ten (10) and 15 μM TA levels in mouse feces and cecum, respectively, and observed *CYP1A1* mRNA induction by 50 μM TA in Caco-2 and MDA-MB-486/231 cells [25], which seems consistent with our findings in AZ-AHR, LS180 or HT-29 cells. Conflicting results exist for IA. We observed a weak affinity to the mouse AhR (IC_{50} > 1000 μM), as well as a very low efficacy (6-fold induction) and low potency (EC_{50} = 62 μM) towards the human AhR. Moreover, IA exhibited a weak antagonistic effect on the human AhR, when activated by TCDD, BaP, and FICZ (IC_{50} ≈ 100–200 μM). Previously, Zelante et al. reported a vigorous agonist activity of IA in mouse H1L1.1c2 reporter cells [26]. Yu et al. have demonstrated that IA attenuates inflammation in patients with atopic dermatitis through the AhR; however, direct evidence for IA effects on AhR has not been presented in that study [31].

The entire intestinal microbial metabolic pathway of Trp comprises twelve catabolites [2], of which we studied eleven compounds in detail. While the activity of several MICTs at AhR was reported (vide supra), five derivatives, including IAD, ILA, IPY, IAC, and IET, have not been previously evaluated. Importantly, except for the ILA, these MICTs appear to be the strongest AhR agonists and ligands within the Trp microbial catabolic pathway, which suggests the existence of underexplored chemical space in therapeutic targeting AhR, using microbial catabolites and their mimics. Interestingly, we have just recently described indole microbial metabolites-based mimics as selective ligands of human pregnane X receptor (PXR), with anti-inflammatory activity in vitro and in vivo [33]. AhR has also been implicated in the control of inflammation within the intestine; in particular, within its immune cell compartment [34]. Thus, more information about the impact of MICT (or their derivatives) on intestinal health is needed.

Table 1. Summary of MICT effects on the AhR–CYP1A1 pathway.

Compound	Affinity (IC_{50})	Potency (EC_{50})	Efficacy (E_{MAX})	Antagonism (IC_{50})	Gene Expression	AhR Cell Functions (Translocation; Heterodimerization; DNA-Binding)
Indole	very low	very low	high	yes–all ligands	strong inducer	highly active–all parameters
Skatole	low	low	medium	ligand selective	strong inducer	highly active–all parameters
Tryptamine	no	low	medium	yes–all ligands	strong inducer	highly active–all parameters
I3-acetamide	low	low	high	none	strong inducer	highly active–all parameters
I3-acetate	no	low	low	none	inactive	not tested
I3-acrylate	very low	low	medium	none	strong inducer	highly active–all parameters
I3-aldehyde	no	low	low	yes–all ligands	inactive	not tested
I3-ethanol	very low	low	medium	ligand selective	inactive	not tested
I3-lactate	no	low	low	none	inactive	not tested
I3-propionate	no	low	low	none	inactive	not tested
I3-pyruvate	low	low	high	ligand selective	strong inducer	highly active–all parameters

Finally, an intriguing future challenge is to investigate the mixed (combined) effects of MICT on the AhR in both mechanistic and translational studies. Since MICTs occur within intestines as complex mixtures, an understanding of their cumulative impact on the AhR might be a clue for the therapeutic targeting of AhR. Indeed, we have previously observed synergistic effects of several methylated and methoxylated indoles on the AhR in vitro [24]. Future studies should also address not only the combined effects of MICT themselves but their interactions with other classes of important intestinal microbial metabolites, including short-chain fatty acids and bile acids.

4. Materials and Methods

4.1. Chemicals and Reagents

Indole-3-aldehyde (97% purity), indole-3-ethanole (97% purity), benzo[a]pyrene (BaP; B1760, Lot SLBS0038V, purity 99%), 6-formylindolo[3,2-b]carbazole (FICZ; SML1489, Lot 0000026018, purity 99.5%), dimethylsulfoxide (DMSO), Triton X-100, bovine serum albumin, and hygromycin B were obtained from Sigma-Aldrich (Prague, Czech Republic). All other MICTs (purity ≥ 98% as determined by supplier) and anti-AhR (Alexa fluor 488) (SC-133088) antibody were purchased from Santa Cruz Biotechnology (Santa Cruz, CA, USA). 2,3,7,8-tetrachlorodibenzo-*p*-dioxin (TCDD) was from Ultra Scientific (RI, USA). 2,3,7,8-tetrachlorodibenzofuran (TCDF) was from Ambinter (Orleáns, France). Luciferase lysis buffer was from Promega (Madison, CA, USA). DAPI (4′,6-diamino-2-phenylindole) was from Serva (Heidelberg, Germany). [³H]-TCDD (purity 98.6%; ART 1642, Lot 181018) was purchased from American Radiolabeled Chemicals. Bio-Gel® HTP Hydroxyapatite (1300420, Lot 64079675) was obtained from Bio-Rad Laboratories. All other chemicals were of the highest purity commercially available.

4.2. Cell Cultures

The stably transfected reporter gene AZ-AHR cell line was described previously [35]. Human Caucasian colon adenocarcinoma cell line LS180 (ECACC No. 87021202) and mouse hepatoma Hepa1c1c7 (ECACC No. 95090613) were purchased from the European Collection of Cell Cultures and cultured as recommended by the supplier.

CRISPR/Cas9 knockout of the AhR in HT-29 cells: A CRISPR/Cas9 expression vector with GFP, pSpCas9(BB)-2A-GFP (PX458) (#48138; Addgene, Cambridge, MA, USA) was used for integration of the gRNA complementary to exon 2 of the AHR gene. 4×10^5 cells were seeded in a 6-well plate and transfected (at 60–70% confluence) with a mixture of vector DNA and Lipofectamine™ 3000 (Life Technologies) according to the manufacturer's instructions. The transfected cells positive for GFP signal were sorted using BD Aria II Sorp (Becton Dickinson, Franklin Lakes, NJ, USA), in a single cell suspension into a 96-well plate. DNA isolation was performed by a QIAamp DNA Mini Kit (Qiagen, Hilden, Germany) according to the manufacturer's instructions. The function of the CRISPR/Cas9 system was verified by the SURVEYOR mutation detection kit (Integrated DNA Technologies, Leuven, Belgium) according to the manufacturer's instructions. The positive clones were checked for AhR expression by Western Blotting. PCR amplification products were purified using the QIAquick PCR Purification Kit (Qiagen) and integrated into a plasmid vector (pGEM_T Easy Vector Systems, Promega), and E.coli DHP α (MAX Efficiency DH5a Competent Cells, Thermo Fisher; Waltham, MA, USA) were transformed according to manufacturer's instructions, DNA was isolated, and deletions in the AhR gene sequences were verified by sequencing (Mix2seq, Eurofins Genomic, Luxembourg). Supplementary Figure S1 shows the sequencing data of the HT-29 AhR KO clone E4 variant.

Primary human hepatocyte cultures were from two sources: (i) long-term human hepatocytes in monolayer batch Hep2201020 (male, 75 years, Caucasian) and Hep2201021 (male, 66 years, Caucasian) were purchased from Biopredic International (Rennes, France); (ii) primary human hepatocytes from multiorgan donor LH79 (male, 60 years, Caucasian) were prepared at Palacky University Olomouc. Liver tissue was obtained from Faculty Hospital Olomouc, and the tissue acquisition protocol followed the requirements issued by the "Ethical Committee of the Faculty Hospital Olomouc, Czech Republic" and Transplantation law #285/2002 Coll.

4.3. Reporter Gene Assay in the AZ-AHR Cells

AZ-AHR cells were incubated for 24 h with vehicle (DMSO; 0.1% *v/v*) and increasing concentrations of tested MICT in the presence or absence of TCDD (13.5 nM), FICZ (22.6 µM), or BaP (15.8 µM). Then, cells were lysed, and luciferase activity was measured using the Tecan Infinite M200 plate luminometer (Schoeller Instruments, Czech Republic). The experiments were performed in at least four consecutive cell passages, and the treatments were in quadruplicates (technical replicates). The values of half-maximal effective concentration (EC_{50}) for each MICT, and half-maximal inhibitory concentration (IC_{50}—where appropriate) were calculated.

4.4. mRNA Isolation and Quantitative Real-Time Reverse Transcriptase-Polymerase Chain Reaction (qRT-PCR)

Total RNA was isolated using TRI Reagent® (Sigma Aldrich, Prague, Czech Republic). cDNA was synthesized using M-MuLV reverse transcriptase (New England Biolabs, Ipswich, MA, USA). The reverse transcription was performed at 42 °C for 60 min using Random Primers 6 (New England Biolabs, Ipswich, MA, USA) and diluted in a 1:4 ratio by PCR-grade water. The quantitative reverse transcriptase-polymerase chain reaction (qRT-PCR) was performed on the Lightcycler 480 II using the LightCycler ® 480 Probes Master (Roche Diagnostic Corporation, Prague, Czech Republic). The levels of *CYP1A1* and *GAPDH* mRNAs were determined using the Universal Probe Library probes (UPL; Roche Diagnostic Corporation, Prague, Czech Republic) in combination with specific primers, using a protocol described elsewhere [36]. All measurements were performed in triplicates, and the gene expression was normalized to *glyceraldehyde-3-phosphate dehydrogenase (GAPDH)* as a house-keeping

gene. The data were processed using the delta-delta Ct method and expressed as a fold induction over the negative control (DMSO) or as a percentage of the positive control (maximal induction by TCDD).

4.5. Competitive Radio-Ligand AhR Binding Assay

Ligand binding assay was performed using cytosolic protein extracts from murine Hepa1c1c7 cells as described [37]. Briefly, aliquots of protein (2 mg/mL) were incubated at the room temperature for two (2) h with 2 nM [^{3}H]-TCDD in the presence of DMSO (vehicle control), FICZ (positive control), 200 nM TCDF (non-specific binding) or increasing concentration of MICT. After the incubation, the hydroxyapatite slurry was added to the samples and the suspension was incubated on ice and washed three times with HEGT buffer. The hydroxyapatite pellet was re-suspended in scintillation cocktail, and radioactivity was determined in a liquid scintillation counter. The specific binding of [^{3}H]-TCDD was determined by subtracting the radioactivity of non-specific reaction (TCDF) from total radioactivity. The values of IC$_{50}$ were calculated where appropriate.

4.6. Immunofluorescence Detection of the Nuclear Translocation of the AhR

LS180 cells (60,000 cells/well) were plated on 8-well chambered slides (94.6140.802, Sarstedt, Nümbrecht, Germany) and allowed to grow overnight. Then, the cells were incubated with DMSO (0.1% *V/V*), TCDD (10 nM), IND (1000 μM), IPY (200 μM), 3MI (200 μM), TA (200 μM), IAC (100 μM), and IAD (200 μM). The staining procedure was described in detail elsewhere [24]. The images were captured using an IX73 fluorescence microscope (Olympus, Tokyo, Japan). The immunofluorescence signal intensity (of the AhR antibody) in the nucleus was evaluated visually. For percentage calculation, approximately 500 cells from at least four randomly selected fields of view in each specimen were used.

4.7. Chromatin Immunoprecipitation Assay (ChIP)—the Detection of the Binding of the AhR to CYP1A1 Promoter

LS180 cells (4 million) were seeded in a 60-mm dish in Dulbecco's modified Eagle's medium (D6546; Sigma Aldrich). The following day, the cells were incubated with DMSO (0.1% *V/V*), TCDD (10 nM), IND (1000 μM), IPY (200 μM), 3MI (200 μM), TA (200 μM), IAC (100 μM), and IAD (200 μM) for 90 min at 37 °C. ChIP assay was performed as we described in detail elsewhere [24].

4.8. Protein Co-Immunoprecipitation—the Detection of the Formation of the AhR-ARNT Heterodimer

Intestinal LS180 cells were incubated with TCDD, tested MICT, and vehicle (DMSO; 0.1% *V/V*) for 90 min at 37 °C. The Pierce™ Co-Immunoprecipitation Kit (Thermo Fisher Scientific) with covalently coupled AhR antibody (mouse monoclonal, sc-133088, A-3, Santa Cruz Biotechnology) was used. Eluted protein complexes and total parental lysates were resolved on SDS-PAGE gels followed by Western Blot analysis and immuno-detection with ARNT-1 antibody (mouse monoclonal, sc-17812, G-3, Santa Cruz Biotechnology). Chemiluminescent detection was performed using horseradish peroxidase-conjugated anti-mouse secondary antibody (7076S, Cell Signaling Technology) and WesternSure$^®$ PREMIUM Chemiluminescent Substrate (LI-COR Biotechnology) by C-DiGit$^®$ Blot Scanner (LI-COR Biotechnology).

4.9. Determination of the Levels of Tryptophan in Cell Culture Media by High-Performance Liquid Chromatography (HPLC)

The levels of tryptophan were determined in the samples of culture media isolated from the growing cells in 2-h intervals from 0 h to 24 h. A simple gradient HPLC method using an Agilent 1260 Infinity system (consisting of a quaternary gradient pump, autosampler, column thermostat, and diode array detector (DAD)) was used. The starting mobile phase mix consisted of 90% of 0.2% trifluoroacetic acid (TFA) and 10% of acetonitrile (MeCN), and, during the run, a linear gradient was applied for up to 15 min, increasing the percentage of MeCN to 90%. A post time of 5 min was applied to achieve the proper starting conditions for the next run. The stable mobile phase flow of 0.5 mL/min was applied at the reverse phase chromatographic column Agilent Poroshell 120 EC-C18, 4.6 × 50 mm,

2.7 μm particle size. The DAD detector was set to detect the following wavelengths: 290 ± 4 nm (A), 254 ± 4 nm (B), 210 ± 4 nm (C), and 275 ± 4 nm (D) (used for the quantification of the tryptophan levels) with a reference range of wavelengths of 820 ± 100 nm. The sample volume applied to the column was ten (10) μL in all cases. The external calibration in the concentration range of 0.7–112.0 μM was used, giving a straight calibration curve with R2 = 0.9999. The peak of tryptophan was identified at t_R = 5.0 ± 0.1 min, and in all determinations was completely resolved from other peaks in the chromatogram. The individual determinations were done in duplicate, and the concentration levels were expressed as mean values ± sample standard deviations.

4.10. Human Studies

The colonoscopy aspirate or fecal collection study was collected under Institutional Review Board (IRB)-approved studies for aspirate or fecal collections (#2015-4465; #2009-446; #2007-554). The patients eligible for colonoscopy were enrolled sequentially after they provided study consent (#2015-4465; audited by the IRB on 24 April 2019). All patients were screened and evaluated by a single gastroenterologist and Inflammatory Bowel Disease specialist (DL). Patients were enrolled if they had a diagnosis of inflammatory bowel disease (Crohn's disease or Ulcerative colitis) or were undergoing routine screening colonoscopy for colorectal polyps/cancer screening or required a colonoscopy as part of their medical management of any gastrointestinal disorder as clinically indicated. IBD and control tissue pathology were obtained under a separate protocol (CCI#2007-554).

4.11. Statistical Analyses

In order to determine significantly different results over the negative control (vehicle; DMSO; 0.1%), one-way analysis of variance (ANOVA), followed by Dunnett's test, was applied. The result was considered significant if the p-value was lower than 0.05. All the calculations (including IC_{50} and EC_{50}) were performed using GraphPad Prism version 8.0 for Windows (GraphPad Software, La Jolla, CA, USA).

5. Conclusions

A number of recent studies have indicated that the impact of MICTs on the AhR activity contributes to the control of intestinal homeostasis in both health and disease conditions. In this study, we provide a comprehensive quantitative characterization of the effects of microbial Trp metabolome on the human AhR, using a series of intestinal and liver cell models. We particularly focused on the effects of MICTs, which would occur at their biologically relevant concentrations, based both on literary evidence and our own results of analyses of colonoscopy aspirates. Our data suggest that all of the studied MICTs may act as low potency agonists of the AhR; however, their action on the AhR may differ substantially, as they can, in turn, behave as full agonists, partial agonists, or even ligand-selective antagonists of the human AhR. However, for some compounds, these effects may occur well beyond their intestinal levels. The activity of MICT in the AhR reporter gene assay mostly corresponded with their binding to the receptor, induction of its nuclear translocation, and binding to DNA within the CYP1A1 regulatory regions, as well as CYP1A1 transcription. Importantly, for the first time, we show that IAD, IPY, IAC, and IET, four MICTs that have not been previously evaluated, appear to be among the strongest AhR ligands within the microbial Trp metabolic pathway. Given the proposed role(s) of the AhR in the control of the gut immune system or intestinal inflammation, it will be important to address the role(s) of these MICT both individually or as complete mixtures in future mechanistic and translational studies addressing gut health.

Abbreviations

AhR	Aryl Hydrocarbon Receptor
ARNT	Aryl hydrocarbon receptor nuclear translocator
BaP	benzo[a]pyrene
FICZ	6-formylindolo[3,2-b]carbazole
IAA	indole-3-acetate
IAC	indole-3-acrylate
IAD	indole-3-acetamide
IET	indole-3-ethanol
ILA	indole-3-lactate
IND	indole
IPA	indole-3-propionate
IPY	indole-3-pyruvate
3MI	skatole
MICT	microbial intestinal catabolites of tryptophan
PXR	Pregnane X Receptor
TA	Tryptamine
TCDD	2,3,7,8-tetrachlorodibenzo-*p*-dioxin

References

1. Sivaprakasam, S.; Bhutia, Y.D.; Ramachandran, S.; Ganapathy, V. Cell-Surface and Nuclear receptors in the colon as targets for bacterial metabolites and its relevance to colon health. *Nutrients* **2017**, *9*, 856. [CrossRef] [PubMed]

2. Roager, H.M.; Licht, T.R. Microbial tryptophan catabolites in health and disease. *Nat. Commun.* **2018**, *9*, 3294. [CrossRef] [PubMed]

3. Gutierrez-Vazquez, C.; Quintana, F.J. Regulation of the immune response by the aryl hydrocarbon receptor. *Immunity* **2018**, *48*, 19–33. [CrossRef] [PubMed]

4. Bock, K.W. Human and rodent aryl hydrocarbon receptor (AHR): From mediator of dioxin toxicity to physiologic AHR functions and therapeutic options. *Biol. Chem.* **2017**, *398*, 455–464. [CrossRef] [PubMed]

5. Venkatesh, M.; Mukherjee, S.; Wang, H.; Li, H.; Sun, K.; Benechet, A.P.; Qiu, Z.; Maher, L.; Redinbo, M.R.; Phillips, R.S.; et al. Symbiotic bacterial metabolites regulate gastrointestinal barrier function via the xenobiotic sensor PXR and Toll-like receptor 4. *Immunity* **2014**, *41*, 296–310. [CrossRef]

6. Qiu, Z.; Cervantes, J.L.; Cicek, B.B.; Mukherjee, S.; Venkatesh, M.; Maher, L.A.; Salazar, J.C.; Mani, S.; Khanna, K.M. Pregnane X receptor regulates pathogen-induced inflammation and host defense against an intracellular bacterial infection through toll-like receptor 4. *Sci. Rep.* **2016**, *6*, 31936. [CrossRef]

7. Hakkola, J.; Rysa, J.; Hukkanen, J. Regulation of hepatic energy metabolism by the nuclear receptor PXR. *Biochim. Biophys. Acta* **2016**, *1859*, 1072–1082. [CrossRef]

8. Stejskalova, L.; Dvorak, Z.; Pavek, P. Endogenous and exogenous ligands of aryl hydrocarbon receptor: Current state of art. *Curr. Drug Metab.* **2011**, *12*, 198–212. [CrossRef]

9. Denison, M.S.; Nagy, S.R. Activation of the aryl hydrocarbon receptor by structurally diverse exogenous and endogenous chemicals. *Annu. Rev. Pharmacol. Toxicol.* **2003**, *43*, 309–334. [CrossRef]

10. Abel, J.; Haarmann-Stemmann, T. An introduction to the molecular basics of aryl hydrocarbon receptor biology. *Biol. Chem.* **2010**, *391*, 1235–1248. [CrossRef]

11. Adachi, J.; Mori, Y.; Matsui, S.; Takigami, H.; Fujino, J.; Kitagawa, H.; Miller, C.A., III; Kato, T.; Saeki, K.; Matsuda, T. Indirubin and indigo are potent aryl hydrocarbon receptor ligands present in human urine. *J. Biol. Chem.* **2001**, *276*, 31475–31478. [CrossRef] [PubMed]

12. Sinal, C.J.; Bend, J.R. Aryl hydrocarbon receptor-dependent induction of cyp1a1 by bilirubin in mouse hepatoma hepa 1c1c7 cells. *Mol. Pharmacol.* **1997**, *52*, 590–599. [CrossRef] [PubMed]

13. Chen, I.; McDougal, A.; Wang, F.; Safe, S. Aryl hydrocarbon receptor-mediated antiestrogenic and antitumorigenic activity of diindolylmethane. *Carcinogenesis* **1998**, *19*, 1631–1639. [CrossRef] [PubMed]

14. Chowdhury, G.; Dostalek, M.; Hsu, E.L.; Nguyen, L.P.; Stec, D.F.; Bradfield, C.A.; Guengerich, F.P. Structural identification of Diindole agonists of the aryl hydrocarbon receptor derived from degradation of indole-3-pyruvic acid. *Chem. Res. Toxicol.* **2009**, *22*, 1905–1912. [CrossRef]

15. Chen, I.; Safe, S.; Bjeldanes, L. Indole-3-carbinol and diindolylmethane as aryl hydrocarbon (Ah) receptor agonists and antagonists in T47D human breast cancer cells. *Biochem. Pharmacol.* **1996**, *51*, 1069–1076. [CrossRef]

16. Schroeder, J.C.; Dinatale, B.C.; Murray, I.A.; Flaveny, C.A.; Liu, Q.; Laurenzana, E.M.; Lin, J.M.; Strom, S.C.; Omiecinski, C.J.; Amin, S.; et al. The uremic toxin 3-indoxyl sulfate is a potent endogenous agonist for the human aryl hydrocarbon receptor. *Biochemistry* **2010**, *49*, 393–400. [CrossRef]

17. Rothhammer, V.; Mascanfroni, I.D.; Bunse, L.; Takenaka, M.C.; Kenison, J.E.; Mayo, L.; Chao, C.C.; Patel, B.; Yan, R.; Blain, M.; et al. Type I interferons and microbial metabolites of tryptophan modulate astrocyte activity and central nervous system inflammation via the aryl hydrocarbon receptor. *Nat. Med.* **2016**, *22*, 586–597. [CrossRef]

18. Helferich, W.G.; Denison, M.S. Ultraviolet photoproducts of tryptophan can act as dioxin agonists. *Mol. Pharmacol.* **1991**, *40*, 674–678.

19. Bergander, L.; Wahlstrom, N.; Alsberg, T.; Bergman, J.; Rannug, A.; Rannug, U. Characterization of in vitro metabolites of the aryl hydrocarbon receptor ligand 6-formylindolo[3,2-b]carbazole by liquid chromatography-mass spectrometry and NMR. *Drug Metab. Dispos. Biol. Fate Chem.* **2003**, *31*, 233–241. [CrossRef]

20. DeGroot, D.E.; Franks, D.G.; Higa, T.; Tanaka, J.; Hahn, M.E.; Denison, M.S. Naturally occurring marine brominated indoles are aryl hydrocarbon receptor ligands/agonists. *Chem. Res. Toxicol.* **2015**, *28*, 1176–1185. [CrossRef]

21. Heath-Pagliuso, S.; Rogers, W.J.; Tullis, K.; Seidel, S.D.; Cenijn, P.H.; Brouwer, A.; Denison, M.S. Activation of the Ah receptor by tryptophan and tryptophan metabolites. *Biochemistry* **1998**, *37*, 11508–11515. [CrossRef] [PubMed]

22. Hubbard, T.D.; Murray, I.A.; Bisson, W.H.; Lahoti, T.S.; Gowda, K.; Amin, S.G.; Patterson, A.D.; Perdew, G.H. Adaptation of the human aryl hydrocarbon receptor to sense microbiota-derived indoles. *Sci. Rep.* **2015**, *5*, 12689. [CrossRef]

23. Rasmussen, M.K.; Balaguer, P.; Ekstrand, B.; Daujat-Chavanieu, M.; Gerbal-Chaloin, S. Skatole (3-Methylindole) is a partial Aryl hydrocarbon receptor agonist and induces CYP1A1/2 and CYP1B1 expression in primary human hepatocytes. *PLoS ONE* **2016**, *11*, e0154629. [CrossRef] [PubMed]

24. Stepankova, M.; Bartonkova, I.; Jiskrova, E.; Vrzal, R.; Mani, S.; Kortagere, S.; Dvorak, Z. Methylindoles and methoxyindoles are agonists and antagonists of human Aryl hydrocarbon receptor. *Mol. Pharmacol.* **2018**, *93*, 631–644. [CrossRef]

25. Jin, U.H.; Lee, S.O.; Sridharan, G.; Lee, K.; Davidson, L.A.; Jayaraman, A.; Chapkin, R.S.; Alaniz, R.; Safe, S. Microbiome-derived tryptophan metabolites and their aryl hydrocarbon receptor-dependent agonist and antagonist activities. *Mol. Pharmacol.* **2014**, *85*, 777–788. [CrossRef] [PubMed]

26. Zelante, T.; Iannitti, R.G.; Cunha, C.; De Luca, A.; Giovannini, G.; Pieraccini, G.; Zecchi, R.; D'Angelo, C.; Massi-Benedetti, C.; Fallarino, F.; et al. Tryptophan catabolites from microbiota engage aryl hydrocarbon receptor and balance mucosal reactivity via interleukin-22. *Immunity* **2013**, *39*, 372–385. [CrossRef] [PubMed]

27. Lamas, B.; Richard, M.L.; Leducq, V.; Pham, H.P.; Michel, M.L.; Da Costa, G.; Bridonneau, C.; Jegou, S.; Hoffmann, T.W.; Natividad, J.M.; et al. CARD9 impacts colitis by altering gut microbiota metabolism of tryptophan into aryl hydrocarbon receptor ligands. *Nat. Med.* **2016**, *22*, 598–605. [CrossRef]

28. Hubbard, T.D.; Murray, I.A.; Perdew, G.H. Indole and tryptophan metabolism: Endogenous and dietary routes to Ah receptor activation. *Drug Metab. Dispos. Biol. Fate Chem.* **2015**, *43*, 1522–1535. [CrossRef]

29. Gao, J.; Xu, K.; Liu, H.; Liu, G.; Bai, M.; Peng, C.; Li, T.; Yin, Y. Impact of the gut microbiota on intestinal immunity mediated by tryptophan metabolism. *Front. Cell. Infect. Microbiol.* **2018**, *8*, 13. [CrossRef]

30. Oberg, M.; Bergander, L.; Hakansson, H.; Rannug, U.; Rannug, A. Identification of the tryptophan photoproduct 6-formylindolo[3,2-b]carbazole, in cell culture medium, as a factor that controls the background aryl hydrocarbon receptor activity. *Toxicol. Sci. Off. J. Soc. Toxicol.* **2005**, *85*, 935–943. [CrossRef]

31. Yu, J.; Luo, Y.; Zhu, Z.; Zhou, Y.; Sun, L.; Gao, J.; Sun, J.; Wang, G.; Yao, X.; Li, W. A tryptophan metabolite of the skin microbiota attenuates inflammation in patients with atopic dermatitis through the aryl hydrocarbon receptor. *J. Allergy Clin. Immunol.* **2019**, *143*, 2108–2119.e12. [CrossRef] [PubMed]

32. Vyhlidalova, B.; Poulikova, K.; Bartonkova, I.; Krasulova, K.; Vanco, J.; Travnicek, Z.; Mani, S.; Dvorak, Z. Mono-methylindoles induce CYP1A genes and inhibit CYP1A1 enzyme activity in human hepatocytes and HepaRG cells. *Toxicol. Lett.* **2019**, *313*, 66–76. [CrossRef] [PubMed]

33. Dvorak, Z.; Kopp, F.; Costello, C.M.; Kemp, J.S.; Li, H.; Vrzalova, A.; Stepankova, M.; Bartonkova, I.; Jiskrova, E.; Poulikova, K.; et al. Targeting the pregnane X receptor using microbial metabolite mimicry. *EMBO Mol. Med.* **2020**, e11621. [CrossRef]

34. Metidji, A.; Omenetti, S.; Crotta, S.; Li, Y.; Nye, E.; Ross, E.; Li, V.; Maradana, M.R.; Schiering, C.; Stockinger, B. The environmental sensor AHR protects from inflammatory damage by maintaining intestinal stem cell homeostasis and barrier integrity. *Immunity* **2018**, *49*, 353–362.e5. [CrossRef] [PubMed]

35. Novotna, A.; Pavek, P.; Dvorak, Z. Novel stably transfected gene reporter human hepatoma cell line for assessment of aryl hydrocarbon receptor transcriptional activity: Construction and characterization. *Environ. Sci. Technol.* **2011**, *45*, 10133–10139. [CrossRef] [PubMed]

36. Kubesova, K.; Travnicek, Z.; Dvorak, Z. Pleiotropic effects of gold(I) mixed-ligand complexes of 9-deazahypoxanthine on transcriptional activity of receptors for steroid hormones, nuclear receptors and xenoreceptors in human hepatocytes and cell lines. *Eur. J. Med. Chem.* **2016**, *121*, 530–540. [CrossRef]

37. Denison, M.S.; Rogers, J.M.; Rushing, S.R.; Jones, C.L.; Tetangco, S.C.; Heath-Pagliuso, S. Analysis of the aryl hydrocarbon receptor (AhR) signal transduction pathway. *Curr. Protoc. Toxicol.* **2002**, *11*. [CrossRef]

APPENDIX IV.

Illes P., Krasulova K., **Vyhlidalova B.**, Poulikova K., Marcalikova A., Pecinkova P., Sirotova N., Vrzal R., Mani S., Dvorak, Z. (2020): Indole microbial intestinal metabolites expand the repertoire of ligands and agonists of the human pregnane X receptor. *Toxicol Lett,* 334: 87-93. **[IF$_{2020}$ 4.374]**
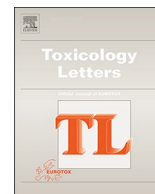
Indole microbial intestinal metabolites expand the repertoire of ligands and agonists of the human pregnane X receptor

Peter Illés[a], Kristýna Krasulová[a], Barbora Vyhlídalová[a], Karolína Poulíková[a], Adéla Marcalíková[a], Petra Pečinková[a], Natália Sirotová[a], Radim Vrzal[a], Sridhar Mani[b,**], Zdeněk Dvořák[a,*]

[a] *Department of Cell Biology and Genetics, Faculty of Science, Palacký University, Šlechtitelů 27, 783 71 Olomouc, Czech Republic*
[b] *Department of Genetics and Department of Medicine, Albert Einstein College of Medicine, Bronx, NY 10461, USA*

GRAPHICAL ABSTRACT
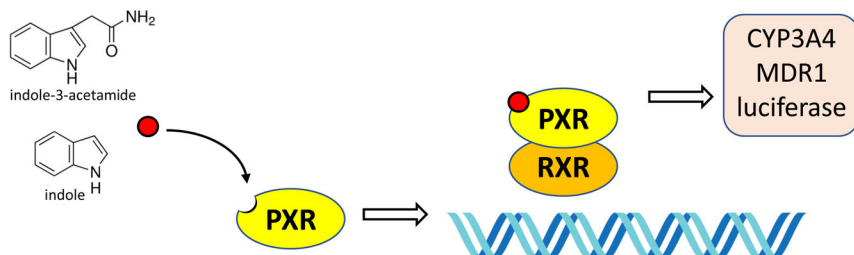
ARTICLE INFO

ABSTRACT

The interplays between the metabolic products of intestinal microbiota and the host signaling through xenobiotic receptors, including pregnane X receptor (PXR), are of growing interest, in the context of intestinal health and disease. A distinct class of microbial catabolites is formed from dietary tryptophan, having the indole scaffold in their core structure, which is a biologically active entity. In the current study, we examined a series of ten tryptophan microbial catabolites for their interactions with PXR signaling. Utilizing a reporter gene assay, we identified indole (IND) and indole-3-acetamide (IAD) as PXR agonists. IND and IAD induced PXR-regulated genes CYP3A4 and MDR1 in human intestinal cancer cells. Using time-resolved fluorescence resonance energy transfer, we show that IND (IC$_{50}$ 292 μM) and IAD (IC$_{50}$ 10 μM) are orthosteric ligands of PXR. Binding of PXR in its DNA response elements was enhanced by IND and IAD, as revealed by chromatin immunoprecipitation assay. We demonstrate that tryptophan microbial intestinal metabolites IND and IAD are ligands and agonists of human PXR. These findings are of particular importance in understanding the roles of microbial catabolites in human physiology and pathophysiology. Furthermore, these results are seminal in expanding potential drug repertoire through microbial metabolic mimicry.

1. Introduction

The pregnane X receptor (PXR) is a member of the nuclear receptors family (NR1I2), which is transcriptionally active in the form of a heterodimer with the retinoid X receptors. PXR is an orphan nuclear receptor activated by naturally occurring steroids such as pregnenolone and progesterone and synthetic glucocorticoids and anti-glucocorticoids (Kliewer et al., 1998). Xenobiotics induce cytochrome P450 CYP3A4 expression and do this *via* PXR activation. These actions are thought to be a cause of pharmacokinetic drug interactions (Lehmann et al., 1998). Since then, PXR has been considered a xenosensor that is a culprit of drug interactions caused by xenobiotics at the transcriptional level, and the activation of which is undesired (Sinz, 2013). With the discovery of endogenous ligands, such as bile acids and their precursors (Goodwin et al., 2003; Staudinger et al., 2001), estrogens (Mnif et al., 2007), or vitamin K2 (Tabb et al., 2003), the PXR was "*de-orphanized*," and its physiological and pathophysiological importance emerged. PXR is involved in the control of various physiological processes and the intermediary metabolism of lipids, glucose (Moreau et al., 2008), and bile acids (Kliewer and Willson, 2002). Given a substantial involvement of the PXR in the onset, progress and prognosis of diseases such as cancer (Chai et al., 2020), diabetes (Hukkanen et al., 2014), metabolic syndrome (Tovar-Palacio et al., 2012), cardiovascular pathologies (Pulakazhi Venu et al., 2019; Zhang et al., 2019), inflammatory bowel disease (Cheng et al., 2012), acute kidney injury (Yu et al., 2020) and neurological pathologies (Langmade et al., 2006; Jain et al., 2014), therapeutic targeting of the PXR are of particular interest (Chai et al., 2019).

During the past two decades, there has been a cumulating body of evidence that the PXR is a target for the human microbiota's metabolic products. For instance, microbial-derived lithocholic acid and vitamin K2 were shown to drive the PXR-dependent metabolic maturation of pluripotent stem cells-derived and fetal hepatocytes (Avior et al., 2015). We have demonstrated that intestinal microbial-specific indoles regulate intestinal barrier function through the PXR. Indole 3-propionic acid (IPA) regulated mucosal integrity in mice *via* a pathway that involves luminal sensing and signaling by Toll-Like Receptor 4. Also, combinations of indole (IND) and IPA or indole-3-acetic acid (IAA) activated the human PXR, while isolated effects of IPA and IAA on the human PXR were negligible (Venkatesh et al., 2014). In a recent follow-up study, we described PXR-mediated intestinal anti-inflammatory effects of newly designed compounds, which structurally mimicked microbial indole-based catabolites (Dvorak et al., 2020). Endothelium-dependent vasodilatation was influenced through the PXR activated by circulating IPA generated by intestinal microbiota (Pulakazhi Venu et al., 2019). Gut microbiota-derived IPA was found protective against acute radiation syndrome *via* PXR / acyl-CoA-binding protein signaling pathways (Xiao et al., 2020). We reported that skatole (3-methyl-indole), which is intestinal microbial catabolite of tryptophan, is a very low-affinity ligand ($IC_{50} > 150$ μM) and a partial agonist ($EC_{50} \approx 48$ μM / $IC_{50} \approx 154$ μM) of human PXR (Vyhlidalova et al., 2020a).

In the current study, we have examined the effects of known intestinal microbial metabolites of tryptophan (10 compounds; for structure, see Fig. 1) on the activity and functions of the human PXR. We found that indole-3-acetamide (IAD) and IND are ligands and agonists of the human PXR, which induce PXR-regulated genes in the intestinal cells, while the remaining derivatives are PXR-inactive.

2. Materials and methods

2.1. Chemicals and reagents

Indole-3-aldehyde (97 % purity), indole-3-ethanol (97 % purity), dimethylsulfoxide (DMSO), rifampicin (RIF), Triton X-100, bovine serum albumin, hygromycin B and TRI Reagent® were obtained from Sigma-Aldrich (Prague, Czech Republic). All other MICT (purity ≥ 98

%) were purchased from Santa Cruz Biotechnology (Santa Cruz, CA, USA). FuGENE® HD Transfection reagent and luciferase lysis buffer were from Promega (Madison, CA, USA). Universal Probes Library (UPL) probes were purchased from Roche Diagnostics Corporation (Prague, Czech Republic). M-MuLV reverse transcriptase was from New England Biolabs (Ipswich, MA, USA). All other chemicals were of the highest purity commercially available.

2.2. Cell cultures

Human Caucasian colon adenocarcinoma cell line LS180 (ECACC No. 87,021,202) was purchased from the European Collection of Cell Cultures and cultured as recommended by the supplier. LS174 T cells (ATCC: CL-188; 7 000 3535) (Synthego Corporation, Redwood City, CA, USA) were the parental cells used to generate PXR knockout variant LS174 T PXR-KO, using CRISPR Cas9 technology, as we described and validated recently (Dvorak et al., 2020).

Primary long-term human hepatocyte cultures in monolayer, batch Hep2201020 (male, 75 years, Caucasian) and Hep2201021 (male, 66 years, Caucasian), were purchased from Biopredic International (Rennes, France). Primary human hepatocytes culture LH79 (male, 60 years, Caucasian) was prepared at Palacky University Olomouc. Liver tissue was obtained from a multiorgan donor in Faculty Hospital Olomouc. The tissue acquisition protocol followed the requirements issued by the "Ethical Committee of the Faculty Hospital Olomouc, Czech Republic" and Transplantation law #285/2002 Coll.

2.3. Reporter gene assay

Intestinal LS180 cells were transiently transfected with human PXR expression vector pSG5-hPXR (kindly provided by Dr. S. Kliewer, University of Texas, Dallas, TX) and p3A4-Luc reporter construct by lipofection (FuGENE® HD Transfection reagent) (Vyhlidalova et al., 2020a). Cells were incubated for 24 h with tested compounds, vehicle (DMSO, 0.1 % v/v) or rifampicin (RIF, ten μM). Following cell lysis, luciferase activity was measured using a Tecan Infinite M200 Pro Plate Reader (Schoeller Instruments, Czech Republic). Experiments were performed in at least three consecutive cell passages, and the analyses in each passage were performed in quadruplicates (technical replicates).

2.4. mRNA isolation and quantitative real-time reverse transcriptase-polymerase chain reaction (qRT-PCR)

LS180 cells transiently transfected with pSG5-hPXR expression vector using FuGENE® HD Transfection reagent (Vyhlidalova et al., 2020a), untransfected LS174 T and LS174 T PXR-KO cells and human hepatocytes were treated for 24 h with examined compounds, vehicle (DMSO, 0.1 % v/v) or rifampicin (RIF, ten μM). According to the manufacturer's instructions, the total RNA was isolated by TRI Reagent®, and the cDNA was synthesized using M-MuLV reverse transcriptase. The qRT-PCR was performed in a LightCycler 480II apparatus (Roche Diagnostics Corporation, Prague, Czech Republic), and the levels of *CYP3A4*, *MDR1*, and *GAPDH* mRNAs were determined using UPL probes as described elsewhere (Bartonkova and Dvorak, 2018). The gene expression levels of *CYP3A4* and *MDR1* were normalized to the housekeeping gene *glyceraldehyde-3-phosphate dehydrogenase* (*GAPDH*). Measurements were performed in triplicates (technical replicates), and the data were processed using the delta − delta method. Experiments were performed in three consecutive cell passages.

2.5. Time resolved-fluorescence resonance energy transfer (TR-FRET)

The LanthaScreen® TR-FRET PXR (SXR) Competitive Binding Assay Kit (Thermo Fischer Scientific, Waltham, MA, USA) was used to determine the binding of indole and indole-3-acetamide at PXR, according
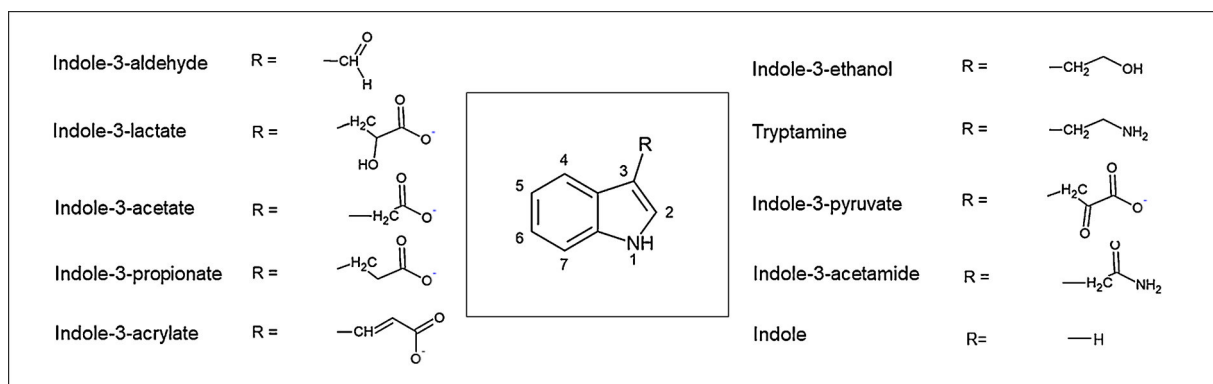
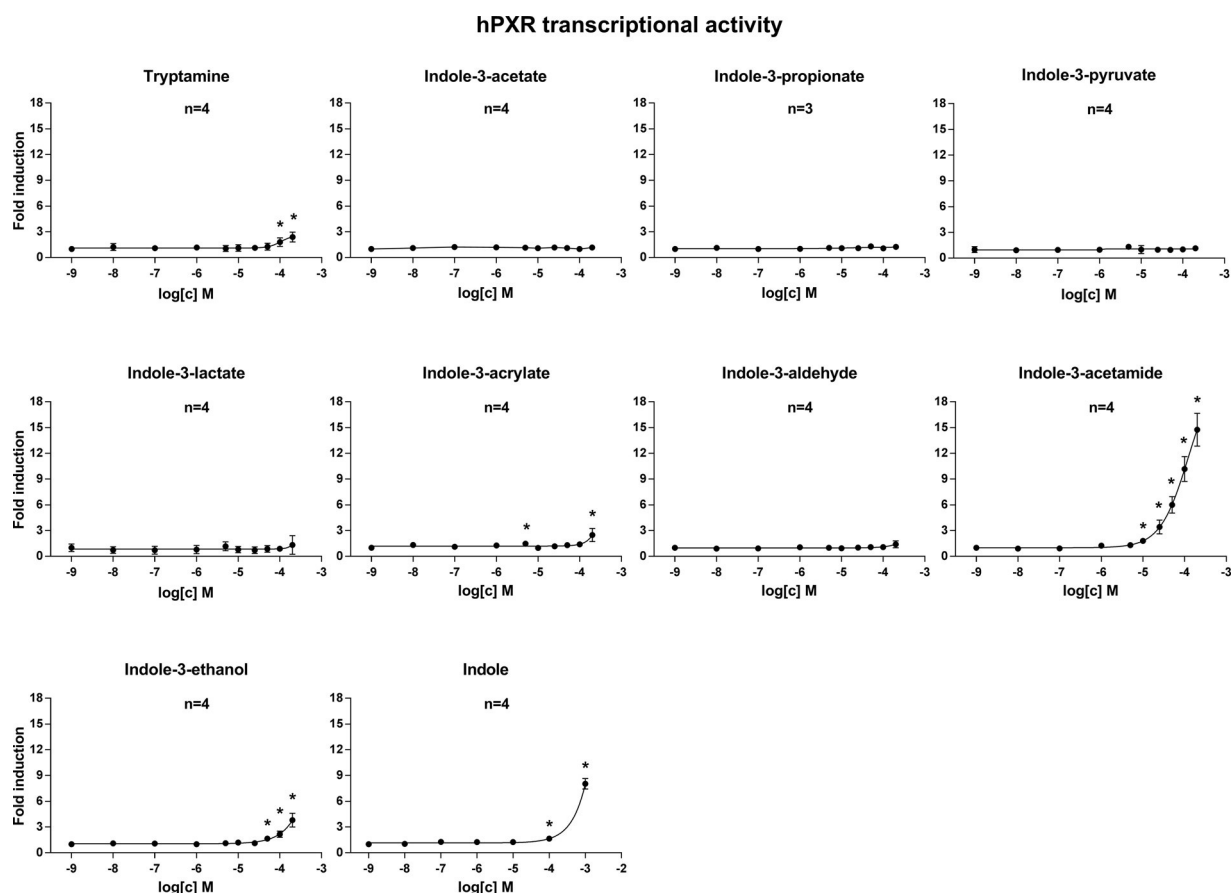**Fig. 1.** Chemical structures of tryptophan microbial catabolites.

Fig. 2. Activation of the PXR by tryptophan catabolites - reporter gene assay. LS180 cells transiently transfected with the pSG5-hPXR expression plasmid and the p3A4-luc reporter plasmid were incubated for 24 h with increasing concentrations of tryptophan catabolites. After treatment, the cells were lysed, and luciferase activity was measured; the analyses were performed in quadruplicates (technical replicates). The data represent the means ± SD from at least three consecutive cell passages (biological replicates). They are expressed as fold induction of luciferase activity over the luciferase activity of the cells treated with the lowest concentration of a particular compound (1 nM). An asterisk (*) indicates a significant difference (P < 0.05) in comparison to the cells exposed to the lowest concentration of the examined compound.

to the procedure, which was described elsewhere (Vyhlidalova et al., 2020a). Binding assays were done in quadruplicates (technical replicates), in at least three independent experiments (biological replicates), and IC_{50} values were calculated.

2.6. Chromatin immunoprecipitation assay (ChIP) - detection of the PXR binding to MDR1 promotor

The polyclonal population of LS174 T (3 million; RM12-PXR) cells with stably transfected pReceiver-M12 expression plasmid containing

PXR1 (NM_003889) gene in ORF under permanent geneticin selection pressure was seeded in a 60-mm dish in Dulbecco's modified Eagle's medium (D6546; Sigma Aldrich) containing 5 % of FBS and 5% of FBS-CS for two days. Then, the cells were incubated in DMEM with 10 % FBS-CS only containing DMSO, rifampicin (RIF; 10 μM), IAD (200 μM), IND (1000 μM) for 20 h at 37 °C. ChIP procedure was performed as we described elsewhere (Stepankova et al., 2018), with following modifications: a) 5 μL of anti-PXR antibody (Perseus Proteomics, PH-H4417−00) was used against 30 μg of digested chromatin; b) primers used for the amplification of MDR1 promoter DNA were as follows:

forward: 5′-GAGTGAACGTTACCTCATT GAAC-3′; reverse: 5′−CCGAA ATGGCTTTTGAATTG-3′ (Kameyama et al., 2016). Then, the fold enrichment method was applied and in parallel, an amplicon of 156 bp length corresponding to this region was detected by agarose gel electrophoresis.

2.7. Statistical analyses

The Student's *t*-test determined statistically significant differences in the results over the negative or positive control. The differences were considered significant at $p < 0.05$. IC_{50} values and curve fittings were calculated using GraphPad Prism 7 software (GraphPad

Software, La Jolla, CA, USA).

3. Results

3.1. Indole and indole-3-acetamide activate the human PXR

The capability of microbial intestinal tryptophan metabolites to activate human PXR was evaluated in human intestinal LS180 cells transiently co-transfected with hPXR vector and pCYP3A4-luc reporter plasmids. Cells were incubated for 24 h with tested compounds, vehicle (DMSO; 0.1 % v/v/), and rifampicin (RIF; 10 μM), a model PXR activator. None of the compounds tested was cytotoxic to LS180 cells, as revealed by the MTT test (data not shown). Dose-dependent activation of the PXR was observed for IAD, which increased luciferase activity approx. 15-fold in 200 μM concentration. However, a plateau was not reached, and EC_{50} was not calculated. IND activated PXR only in the highest concentration (1 mM). The relative efficacies of both IAD and IND in the highest applied concentrations were comparable with that of 10 μM RIF. Very weak but significant PXR activation was achieved by tryptamine (TA) and indole-3-ethanol (IET). Remaining tested catabolites did not activate the PXR (Fig. 2).

3.2. Indole and indole-3-acetamide induce CYP3A4 and MDR1 through the PXR

Tryptophan microbial catabolites were incubated for 24 h in primary human hepatocytes and human intestinal cells LS174 T, and the expression of PXR-target genes was measured using RT-PCR. Both IND and IAD induced CYP3A4 and MDR1 mRNAs in LS174 T cells, whereas other tryptophan metabolites were inactive. Relative efficacies of IND / IAD, as compared to 10 μM RIF, were ≈10 % and ≈40 % for CYP3A4 and MDR1, respectively (Fig. 3A). Weak induction (≈8% relative efficacy) of CYP3A4 mRNA by IND and IAD was observed only in primary human hepatocytes culture LH79, but not in cultures HEP2201020 and HEP2201021, (Fig. 3B). Expression of MDR1 in human hepatocytes was not evaluated, because of this gene in poorly inducible in hepatic cells. These data reveal about globally negative effects of IND and IAD on PXR-target genes expression in primary human hepatocytes. We performed a comparative analysis of CYP3A4 and MDR1 mRNAs transcription patters in wild-type LS174 T cells, PXR-knockout LS174 T cells, and LS180 cells transiently transfected with wt-PXR vector. Both CYP3A4 and MDR1 mRNAs were induced by RIF, IND, and IAD in wild-type LS174 T cells (Fig. 3C), consistent with data in all-compounds screen (Fig. 3A). These effects were nullified in the PXR-knockout variant of LS174 T cells, revealing about the PXR-dependent induction of CYP3A4 and MDR1 by IND and IAD. Using LS180 cells over-expressing transiently the human PXR, we observed an induction of MDR1 mRNA by RIF (8-fold), IND (2-fold), and IAD (5-fold), whereas the induction of CYP3A4 mRNA was only weak (2-fold for RIF) (Fig. 3C).

3.3. Indole and indole-3-acetamide are ligands of the human PXR

Competitive ligand binding assay, based on the principle of time-resolved fluorescence resonance energy transfer (TR-FRET), was used to assess the binding of IAD and IND in the ligand-binding domain of the human PXR. Both IND (IC_{50} 292 μM) and IAD (IC_{50} 10 μM) dose-dependently displaced fluorescent PXR ligand Fluormone™ from binding to the PXR (Fig. 4). This implies that both compounds are orthosteric ligands of the human PXR that directly bind to the receptor.

3.4. Indole and indole-3-acetamide enhance binding of the PXR in the MDR1 promotor

In a final series of experiments, we examined the capability of IAD and IND to enhance the binding of the PXR in the promotor of MDR1, using chromatin immune-precipitation ChIP assay. The incubation of LS174 T intestinal cells stably over-expressing PXR (RM12-PXR clone) with both IAD and IND resulted in the enrichment of the MDR1 promotor with the PXR (Fig. 5). These observations are consistent with findings that IAD and IND bind to the PXR, activate PXR, and induce PXR-dependent genes.

4. Discussion

In the current paper, we demonstrate that tryptophan microbial catabolites indole and indole-3-acetamide are the ligands and agonists of human PXR that induce PXR-dependent genes in the intestinal cells. These findings extend current limited knowledge on the interactions between human intestinal microbiota products and the PXR. To date, most efforts were focused on the effects of IPA, not only locally in the intestines (Venkatesh et al., 2014), but also on systemic ones (Pulakazhi Venu et al., 2019; Xiao et al., 2020). In our pioneer work, we observed that intestinal anti-inflammatory effects of IPA *via* the PXR were only faint, but strongly augmented when combined with IND (Venkatesh et al., 2014). The phenomenon of the PXR activation by combined indoles was further elaborated in our recent study, where we designed high-affinity ligands ($IC_{50} < 1$ μM) and potent and efficacious PXR-selective agonists with anti-inflammatory activity, exploiting indoles-based hybrid structure scaffolds (Dvorak et al., 2020). Whereas the majority of *in vitro* studies is carried out with the individual compounds, the real situation *in vivo* in the gastro-intestinal tract is determined by the simultaneous presence of multiple metabolites. Indeed, besides tryptophan metabolites, there are present short and medium chain fatty acids, bile acids and many other substances that may act on the PXR either directly (orthosteric, allosteric) or indirectly through other factors.

Twelve metabolites formed from dietary tryptophan by human intestinal microbiota were identified (Roager and Licht, 2018). However, only IPA, IND, and 3-methylindole (skatole) were studied for their PXR activity (Pulakazhi Venu et al., 2019; Venkatesh et al., 2014; Xiao et al., 2020; Vyhlidalova et al., 2020a). In contrast, the effects of microbial tryptophan metabolites on another xenosensor, human aryl hydrocarbon receptor (AhR), were extensively studied (Stepankova et al., 2018; Heath-Pagliuso et al., 1998; Hubbard et al., 2015; Rasmussen et al., 2016; Rothhammer et al., 2016). Recently, we demonstrated that the entire metabolic array stemming from parental tryptophan are the ligands and activators of the AhR, differing in their pharmacology parameters (Vyhlidalova et al., 2020b).

Interestingly, many compounds are dual activators of the AhR and the PXR. For instance, 2.281 AhR-active compounds identified by a large-screen panel (PubChem Bioassay ID 2796), were counter-screened for the PXR activity (PubChem Bioassay ID 434,939), yielding 2.017 positive hits, *i.e.*, having 88 % overlap of AhR and PXR activators. Also, there is a mutual negative cross-talk between the AhR and the PXR signaling pathways (Rasmussen et al., 2017). Taken together, dual activation of AhR/PXR and cross-talk between these two receptors might explain why we observed PXR activation by IPA in HEK293 cells that lack the AhR (Venkatesh et al., 2014), but not in intestinal LS180 cells that harbor fully functional endogenous AhR.

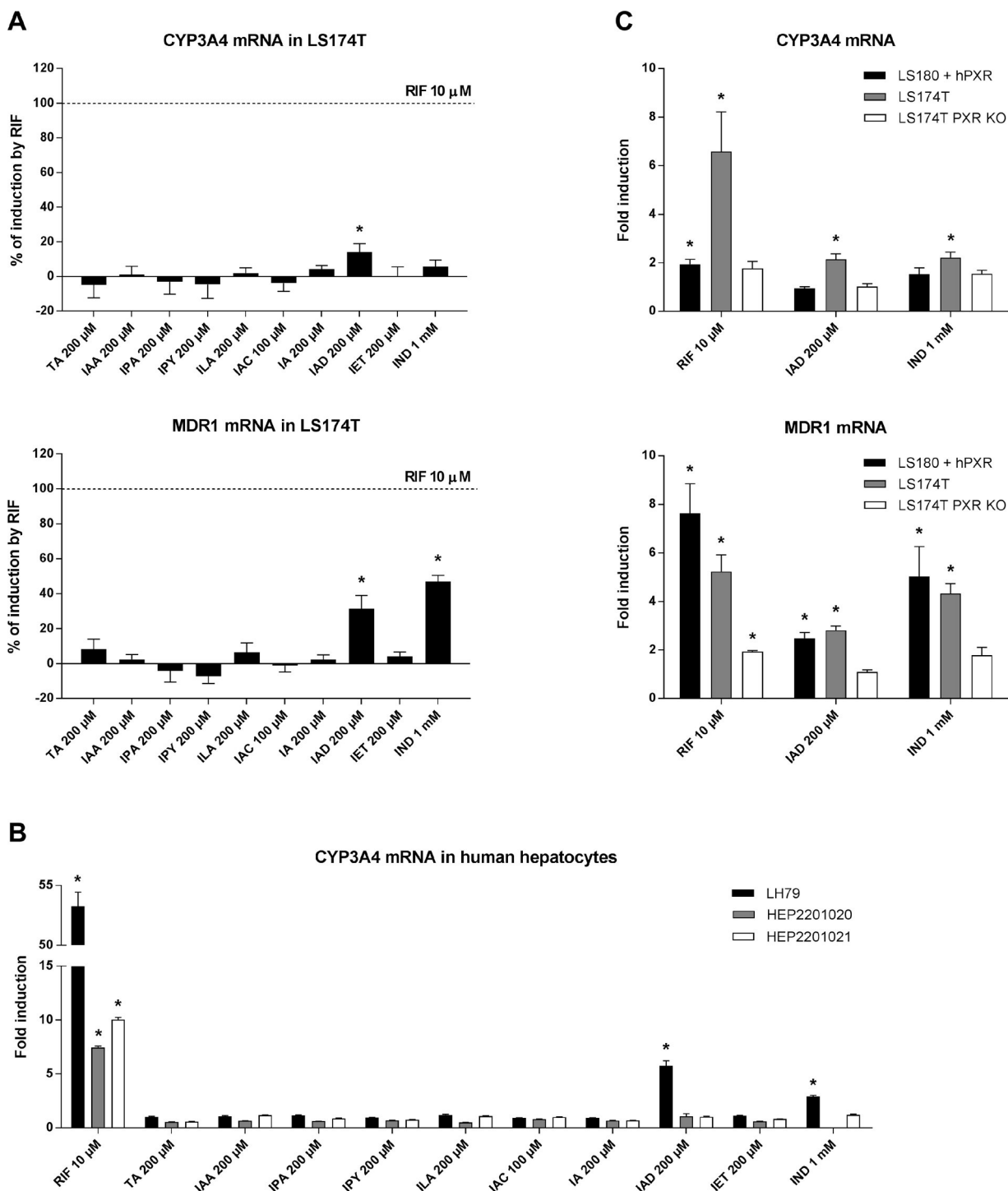In the present study, we identified IND as a low-affinity (IC_{50} 292

Fig. 3. Induction of gene expression of *CYP3A4* and *MDR1* by tryptophan catabolites. A) LS174 T cells were treated with tryptophan catabolites, vehicle (DMSO; 0.1 % v/v) or rifampicin (RIF; 10 μM) for 24 h. The levels of *CYP3A4* and *MDR1* were determined by qRT-PCR and are expressed as a % of induction by RIF (10 μM). The data represent the means ± SD from three consecutive cell passages. B) Human hepatocytes were exposed to tryptophan catabolites, vehicle (DMSO; 0.1 % v/v) or rifampicin (RIF; 10 μM). After 24 h, qRT-PCR was performed, and the level of *CYP3A4* mRNA was determined. The data for each hepatocyte culture are expressed as a fold induction ± SD over the vehicle-treated cells (DMSO; 0.1 % v/v). C) LS180 cells transiently transfected with pSG5-hPXR expression plasmid, LS174 T cells and LS174 T PXR-KO cells were exposed to indole-3-acetamide (IAD; 200 μM), indole (IND; 1 mM), vehicle (DMSO; 0.1 % v/v) or rifampicin (RIF; 10 μM) for 24 h. The levels of *CYP3A4* and *MDR1* were determined by qRT-PCR and are expressed as fold induction over the vehicle-treated cells (DMSO; 0.1 % v/v). The data represent the means ± SD from three consecutive cell passages. An asterisk (*) in all graphs indicates a significant difference ($P < 0.05$) in comparison to the vehicle-treated cells.

μM) orthosteric ligand of the human PXR, which displayed low-potency and high-efficacy agonist effects on the PXR. Fecal concentrations of IND were reported to span from 250 μM to 2500 μM (Roager and Licht, 2018; Jin et al., 2014; Lamas et al., 2016), which is sufficient to activate

intestinal PXR. We also show that IAD is a medium-affinity (IC$_{50}$ 10 μM) ligand of the PXR; however, intestinal or fecal concentrations of IAD are unknown. Altered cecal levels of IAD were reported in mice suffering from metabolic disorders induced by excess alcohol consumption, but

hPXR ligand binding

IND: IC$_{50}$ = 292.33 ± 69.72 μM (n = 4)

IAD: IC$_{50}$ = 10.10 ± 2.32 μM (n = 3)
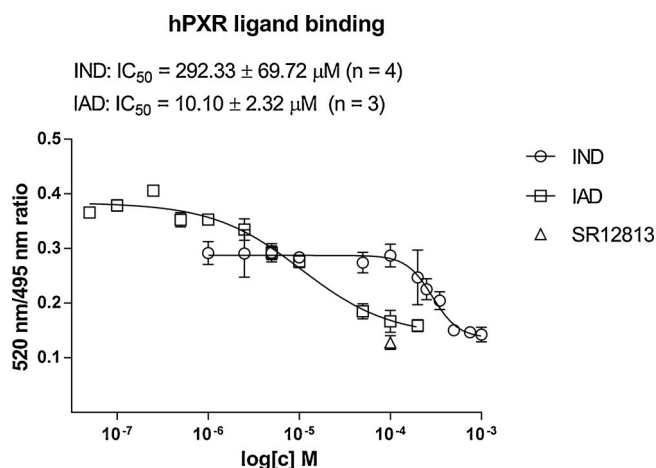
Fig. 4. PXR Ligand Competition by indole and indole-3-acetamide. TR-FRET ratios 520/495 nm were plotted against concentrations of tested compounds. Half-maximal inhibitory concentrations IC$_{50}$ were calculated and are inserted in the plot. Experiments were performed at least three times (*n* = 3), and the representative plots are shown. The presented data are mean ± SE from quadruplicates (technical replicates). Positive control SR12813 (100 μM) is depicted as a single point (triangle symbol).
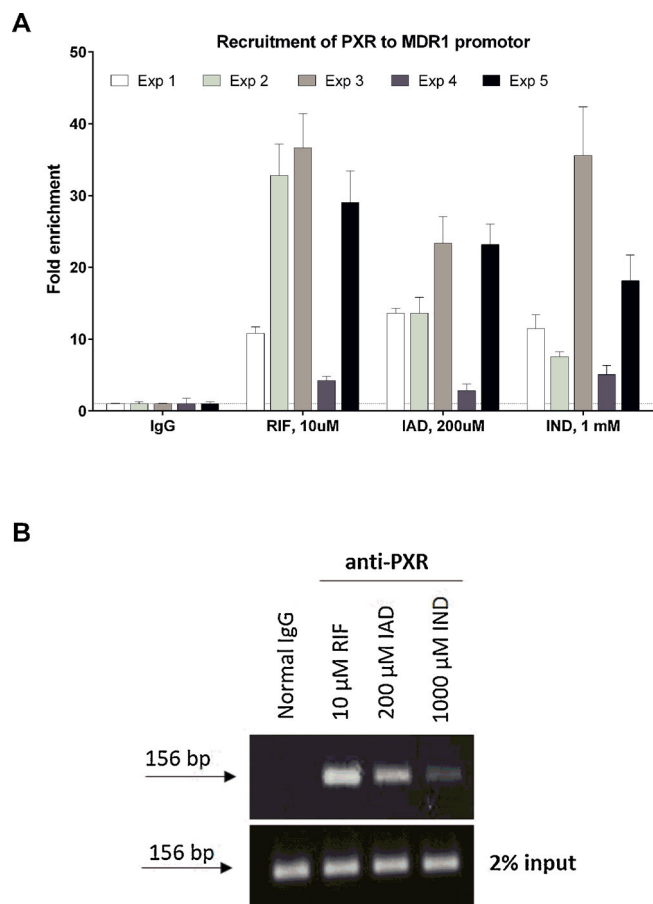
Fig. 5. Chromatin immunoprecipitation: ChIP (PXR–MDR1). RM12-PXR cells were incubated with vehicle (DMSO; 0.1 % v/v), rifampicin (RIF; 10 μM), IAD (200 μM) and IND (1000 μM) for 20 h. Then, cells were subjected to ChIP analysis using anti-PXR antibody and RT-PCR amplification of MDR1 promotor primers. A) Bar graphs show enrichment of MDR1 promotor with PXR as the fold increase in signal relative to the background signal, *i.e.* normal (mock) IgG. Experiments were performed in five consecutive cell passages. B) Representative DNA fragments amplified by PCR analysed on a 2% agarose gel are shown.

the concentrations of IAD were not presented in this study (Liu et al., 2019). Interestingly, a series of viral polymerase inhibitors were assayed in a PXR counter-screen panel. The presence of indole-*N*-acetamide moiety was identified as a culprit of PXR off-target effects (Harper et al., 2005). Hence, it seems that the introduction of acetamide moiety in IND at positions 1 or 3 results in increased PXR activity of these derivatives as compared to IND. Also, mono-methylation of IND at any position yielded PXR agonists with increased potency over IND (Vyhlidalova et al., 2020a). On the other hand, IND, IAD and mono-methylindoles are the ligands and agonists of the AhR (Stepankova et al., 2018; Vyhlidalova et al., 2020b, 2019). Since proper activation of both the AhR and the PXR by indole-based microbial catabolites was demonstrated beneficial for the intestinal health, it is disputable, whether to design microbial metabolic mimicry that is AhR-selective, PXR-selective or AhR/PXR-dual agonists. For instance, in our series of PXR-selective agonists, synthesized based on a rational design approach, the essential PXR-active entity was 1-(phenylsulfonyl)-indol-2-yl scaffold. The new introduction of the unsubstituted indol-2-yl group led to the acquisition of the AhR activity and the AhR/PXR-dual agonists. Moreover, the removal of phenyl sulfonyl substituent resulted in AhR-superactive compounds (Dvorak et al., 2020). Chen et al. employed a rational drug design approach to obtain potent AhR-agonist indole-based drugs lead to inflammatory bowel disease therapy, which displayed physiochemical drug-likeness properties, desirable pharmacokinetic profiles, and low toxicity. The most potent AhR agonists (EC$_{50}$ in nanomolar range) were 6-(indole-3-carbonyl)picolinonitrile and (indol-3-yl)(6-(trifluoromethyl)pyridin-2-yl)methanone, which are structurally simple, 3-mono-substituted indoles (Chen et al., 2020).

Our studies add to the expanding list of indole metabolites that have activity as ligands for PXR. A complete structure-activity relationship of these metabolites could pave the way for defining minimal structural motifs of indoles required for PXR activation. The implication of these findings is several. First, approaches similar to Chen et al. would allow for minimalist changes in indole metabolite structures to expand for more potent and drug-like chemicals. Second, metabolite scaffolds mimicked in this manner could be less toxic to the host when compared to an at-random selection of PXR activating xenobiotics chosen from a chemical library. Third, multitargeting of indole metabolism in bacteria coupled with host PXR activation could prevent intestinal inflammation in conditions such as antibiotic-associated hemorrhagic colitis (von Tesmar et al., 2018). Finally, this opens up approaches for dual targeting of PXR/AhR for purposes of anti-inflammatory therapy.

Authors contributions

Participated in research design: ZD, SM, PI
Conducted experiments: BV, KP, KK, PP, RV, PI, NS, AM
Contributed new reagents and analytic tools: ZD
Performed data analysis: BV, KP, KK, PP, RV, PI, NS, ZD, AM
Wrote or contributed to the writing of the manuscript: ZD, SM, PI

Funding

Declaration of Competing Interest

The authors declare that they have no known competing financial interests or personal relationships that could have appeared to influence the work reported in this paper.

References

Avior, Y., Levy, G., Zimerman, M., Kitsberg, D., Schwartz, R., Sadeh, R., Moussaieff, A., Cohen, M., Itskovitz-Eldor, J., Nahmias, Y., 2015. Microbial-derived lithocholic acid, and vitamin K2 drive the metabolic maturation of pluripotent stem cells-derived and fetal hepatocytes. Hepatology 62, 265–278.

Bartonkova, I., Dvorak, Z., 2018. Essential oils of culinary herbs and spices activate PXR and induce CYP3A4 in human intestinal and hepatic in vitro models. Toxicol. Lett. 296, 1–9.

Chai, S.C., Lin, W., Li, Y., Chen, T., 2019. Drug discovery technologies identify and characterize modulators of the pregnant X receptor and the constitutive androstane receptor. Drug Discov. Today 24, 906–915.

Chai, S.C., Wright, W.C., Chen, T., 2020. Strategies for developing pregnane X receptor antagonists: implications from metabolism to cancer. Med. Res. Rev. 40, 1061–1083.

Chen, J., Haller, C.A., Jernigan, F.E., Koerner, S.K., Wong, D.J., Wang, Y., Cheong, J.E., Kosaraju, R., Kwan, J., Park, D.D., Thomas, B., Bhasin, S., De La Rosa, R.C., Premji, A.M., Liu, L., Park, E., Moss, A.C., Emili, A., Bhasin, M., Sun, L., Chaikof, E.L., 2020. Modulation of lymphocyte-mediated tissue repair by rational design of heterocyclic aryl hydrocarbon receptor agonists. Sci. Adv. 6 eaay8230.

Cheng, J., Shah, Y.M., Gonzalez, F.J., 2012. Pregnane X receptor as a target for the treatment of inflammatory bowel disorders. Trends Pharmacol. Sci. 33, 323–330.

Dvorak, Z., Kopp, F., Costello, C.M., Kemp, J.S., Li, H., Vrzalova, A., Stepankova, M., Bartonkova, I., Jiskrova, E., Poulikova, K., Vyhlidalova, B., Nordstrom, L.U., Karunaratne, C.V., Ranhotra, H.S., Mun, K.S., Naren, A.P., Murray, I.A., Perdew, G.H., Brtko, J., Toporova, L., Schon, A., Wallace, W.G., Walton, W.G., Redinbo, M.R., Sun, K., Beck, A., Kortagere, S., Neary, M.C., Chandran, A., Vishveshwara, S., Cavalluzzi, M.M., Lentini, G., Cui, J.Y., Gu, H., March, J.C., Chatterjee, S., Matson, A., Wright, D., Flannigan, K.L., Hirota, S.A., Sartor, R.B., Mani, S., 2020. Targeting the pregnane X receptor using microbial metabolite mimicry. EMBO Mol. Med. 12, e11621.

Goodwin, B., Gauthier, K.C., Umetani, M., Watson, M.A., Lochansky, M.I., Collins, J.L., Leitersdorf, E., Mangelsdorf, D.J., Kliewer, S.A., Repa, J.J., 2003. Identification of bile acid precursors as endogenous ligands for the nuclear xenobiotic pregnane X receptor. Proc Natl Acad Sci U S A 100, 223–228.

Harper, S., Avolio, S., Pacini, B., Di Filippo, M., Altamura, S., Tomei, L., Paonessa, G., Di Marco, S., Carfi, A., Giuliano, C., Padron, J., Bonelli, F., Migliaccio, G., De Francesco, R., Laufer, R., Rowley, M., Narjes, F., 2005. Potent inhibitors of subgenomic hepatitis C virus RNA replication through optimization of indole-N-acetamide allosteric inhibitors of the viral NS5B polymerase. J. Med. Chem. 48, 4547–4557.

Heath-Pagliuso, S., Rogers, W.J., Tullis, K., Seidel, S.D., Cenijn, P.H., Brouwer, A., Denison, M.S., 1998. Activation of the Ah receptor by tryptophan and tryptophan metabolites. Biochemistry 37, 11508–11515.

Hubbard, T.D., Murray, I.A., Bisson, W.H., Lahoti, T.S., Gowda, K., Amin, S.G., Patterson, A.D., Perdew, G.H., 2015. Adaptation of the human aryl hydrocarbon receptor to sense microbiota-derived indoles. Sci. Rep. 5, 12689.

Hukkanen, J., Hakkola, J., Rysa, J., 2014. Pregnane X receptor (PXR)–a contributor to the diabetes epidemic? Drug Metabol. Drug Interact. 29, 3–15.

Jain, S., Rathod, V., Prajapati, R., Nandekar, P.P., Sangamwar, A.T., 2014. Pregnane X Receptor, and P-glycoprotein: a connexion for Alzheimer's disease management. Mol. Divers. 18, 895–909.

Jin, U.H., Lee, S.O., Sridharan, G., Lee, K., Davidson, L.A., Jayaraman, A., Chapkin, R.S., Alaniz, R., Safe, S., 2014. Microbiome-derived tryptophan metabolites and their aryl hydrocarbon receptor-dependent agonist and antagonist activities. Mol. Pharmacol. 85, 777–788.

Kameyama, N., Kobayashi, K., Shimizu, S., Yamasaki, Y., Endo, M., Hashimoto, M., Furihata, T., Chiba, K., 2016. Involvement of ESE-3, epithelial-specific ETS factor family member 3, in transactivation of the ABCB1 gene via pregnane X receptor in intestine-derived LS180 cells but not in liver-derived HepG2 cells. Drug Metab. Pharmacokinet. 31, 340–348.

Kliewer, S.A., Willson, T.M., 2002. Regulation of xenobiotic, and bile acid metabolism by the nuclear pregnane X receptor. J. Lipid Res. 43, 359–364.

Kliewer, S.A., Moore, J.T., Wade, L., Staudinger, J.L., Watson, M.A., Jones, S.A., McKee, D.D., Oliver, B.B., Willson, T.M., Zetterstrom, R.H., Perlmann, T., Lehmann, J.M., 1998. An orphan nuclear receptor activated by pregnanes defines a novel steroid signaling pathway. Cell 92, 73–82.

Lamas, B., Richard, M.L., Leducq, V., Pham, H.P., Michel, M.L., Da Costa, G., Bridonneau, C., Jegou, S., Hoffmann, T.W., Natividad, J.M., Brot, L., Taleb, S., Couturier-Maillard, A., Nion-Larmurier, I., Merabtene, F., Seksik, P., Bourrier, A., Cosnes, J., Ryffel, B., Beaugerie, L., Launay, J.M., Langella, P., Xavier, R.J., Sokol, H., 2016. CARD9 impacts colitis by altering gut microbiota metabolism of tryptophan into aryl hydrocarbon receptor ligands. Nat. Med. 22, 598–605.

Langmade, S.J., Gale, S.E., Frolov, A., Mohri, I., Suzuki, K., Mellon, S.H., Walkley, S.U., Covey, D.F., Schaffer, J.E., Ory, D.S., 2006. Pregnane X receptor (PXR) activation: a mechanism for neuroprotection in a mouse model of Niemann-Pick C disease. Proc. Natl. Acad. Sci. U. S. A. 103, 13807–13812.

Lehmann, J.M., McKee, D.D., Watson, M.A., Willson, T.M., Moore, J.T., Kliewer, S.A.,

1998. The human orphan nuclear receptor PXR is activated by compounds that regulate CYP3A4 gene expression and cause drug interactions. J. Clin. Invest. 102, 1016–1023.

Liu, X., Zhao, K., Yang, X., Zhao, Y., 2019. Gut microbiota, and metabolome response of Decaisnea insignis seed oil on metabolism disorder induced by excess alcohol consumption. J. Agric. Food Chem. 67, 10667–10677.

Mnif, W., Pascussi, J.M., Pillon, A., Escande, A., Bartegi, A., Nicolas, J.C., Cavailles, V., Duchesne, M.J., Balaguer, P., 2007. Estrogens and antiestrogens activate hPXR. Toxicol. Lett. 170, 19–29.

Moreau, A., Vilarem, M.J., Maurel, P., Pascussi, J.M., 2008. Xenoreceptors CAR and PXR activation and consequences on lipid metabolism, glucose homeostasis, and inflammatory response. Mol. Pharm. 5, 35–41.

Pulakazhi Venu, V.K., Saifeddine, M., Mihara, K., Tsai, Y.C., Nieves, K., Alston, L., Mani, S., McCoy, K.D., Hollenberg, M.D., Hirota, S.A., 2019. The pregnane X receptor and its microbiota-derived ligand indole 3-propionic acid regulate endothelium-dependent vasodilation. Am. J. Physiol. Endocrinol. Metab. 317, E350–E361.

Rasmussen, M.K., Balaguer, P., Ekstrand, B., Daujat-Chavanieu, M., Gerbal-Chaloin, S., 2016. Skatole (3-Methylindole) is a partial aryl hydrocarbon receptor agonist and induces CYP1A1/2 and CYP1B1 expression in primary human hepatocytes. PLoS One 11, e0154629.

Rasmussen, M.K., Daujat-Chavanieu, M., Gerbal-Chaloin, S., 2017. Activation of the aryl hydrocarbon receptor decreases rifampicin-induced CYP3A4 expression in primary human hepatocytes and HepaRG. Toxicol. Lett. 277, 1–8.

Roager, H.M., Licht, T.R., 2018. Microbial tryptophan catabolites in health and disease. Nat. Commun. 9, 3294.

Rothhammer, V., Mascanfroni, I.D., Bunse, L., Takenaka, M.C., Kenison, J.E., Mayo, L., Chao, C.C., Patel, B., Yan, R., Blain, M., Alvarez, J.I., Kebir, H., Anandasabapathy, N., Izquierdo, G., Jung, S., Obholzer, N., Pochet, N., Clish, C.B., Prinz, M., Prat, A., Antel, J., Quintana, F.J., 2016. Type I interferons, and microbial metabolites of tryptophan modulate astrocyte activity and central nervous system inflammation via the aryl hydrocarbon receptor. Nat. Med. 22, 586–597.

Sinz, M.W., 2013. Evaluation of pregnane X receptor (PXR)-mediated CYP3A4 drug-drug interactions in drug development. Drug Metab. Rev. 45, 3–14.

Staudinger, J.L., Goodwin, B., Jones, S.A., Hawkins-Brown, D., MacKenzie, K.I., LaTour, A., Liu, Y., Klaassen, C.D., Brown, K.K., Reinhard, J., Willson, T.M., Koller, B.H., Kliewer, S.A., 2001. The nuclear receptor PXR is a lithocholic acid sensor that protects against liver toxicity. Proc Natl Acad Sci U S A 98, 3369–3374.

Stepankova, M., Bartonkova, I., Jiskrova, E., Vrzal, R., Mani, S., Kortagere, S., Dvorak, Z., 2018. Methylindoles, and methoxyindoles are agonists and antagonists of human aryl hydrocarbon receptor. Mol. Pharmacol. 93, 631–644.

Tabb, M.M., Sun, A., Zhou, C., Grun, F., Errandi, J., Romero, K., Pham, H., Inoue, S., Mallick, S., Lin, M., Forman, B.M., Blumberg, B., 2003. Vitamin K2 regulation of bone homeostasis is mediated by the steroid and xenobiotic receptor SXR. J. Biol. Chem. 278, 43919–43927.

Tovar-Palacio, C., Torres, N., Diaz-Villasenor, A., Tovar, A.R., 2012. The role of nuclear receptors in the kidney in obesity and metabolic syndrome. Genes Nutr. 7, 483–498.

Venkatesh, M., Mukherjee, S., Wang, H., Li, H., Sun, K., Benechet, A.P., Qiu, Z., Maher, L., Redinbo, M.R., Phillips, R.S., Fleet, J.C., Kortagere, S., Mukherjee, P., Fasano, A., Le Ven, J., Nicholson, J.K., Dumas, M.E., Khanna, K.M., Mani, S., 2014. Symbiotic bacterial metabolites regulate gastrointestinal barrier function via the xenobiotic sensor PXR and Toll-like receptor 4. Immunity 41, 296–310.

von Tesmar, A., Hoffmann, M., Abou Fayad, A., Huttel, S., Schmitt, V., Herrmann, J., Muller, R., 2018. Biosynthesis of the Klebsiella oxytoca pathogenicity factor tilivalline: heterologous expression, in vitro biosynthesis, and inhibitor development. ACS Chem. Biol. 13, 812–819.

Vyhlidalova, B., Poulikova, K., Bartonkova, I., Krasulova, K., Vanco, J., Travnicek, Z., Mani, S., Dvorak, Z., 2019. Mono-methylindoles induce CYP1A genes and inhibit CYP1A1 enzyme activity in human hepatocytes and HepaRG cells. Toxicol. Lett. 313, 66–76.

Vyhlidalova, B., Bartonkova, I., Jiskrova, E., Li, H., Mani, S., Dvorak, Z., 2020a. Differential activation of human pregnane X receptor PXR by isomeric mono-methylated indoles in intestinal and hepatic in vitro models. Toxicol. Lett. 324, 104–110.

Vyhlidalova, B., Krasulova, K., Pecinkova, P., Marcalikova, A., Vrzal, R., Zemankova, L., Vanco, J., Travnicek, Z., Vondracek, J., Karasova, M., Mani, S., Dvorak, Z., 2020b. Gut microbial catabolites of tryptophan are ligands and agonists of the aryl hydrocarbon receptor: a detailed characterization. Int. J. Mol. Sci. 21.

Xiao, H.W., Cui, M., Li, Y., Dong, J.L., Zhang, S.Q., Zhu, C.C., Jiang, M., Zhu, T., Wang, B., Wang, H.C., Fan, S.J., 2020. Gut microbiota-derived indole 3-propionic acid protects against radiation toxicity via retaining acyl-CoA-binding protein. Microbiome 8, 69.

Yu, X., Xu, M., Meng, X., Li, S., Liu, Q., Bai, M., You, R., Huang, S., Yang, L., Zhang, Y., Jia, Z., Zhang, A., 2020. Nuclear receptor PXR targets AKR1B7 to protect mitochondrial metabolism and renal function in AKI. Sci. Transl. Med. 12.

Zhang, M., Zhang, Z., Xie, X., Yao, Q., Liu, J., Lai, B., Xiao, L., Wang, N., 2019. Xenobiotic pregnane X receptor promotes neointimal formation in balloon-injured rat carotid arteries. J. Cell. Physiol. 234, 4342–4351.

PALACKÝ UNIVERSITY OLOMOUC

Faculty of Science

Department of Cell Biology and Genetics

ENDOGENOUS AND XENOBIOTIC INDOLES AS MODULATORS OF THE AHR AND PXR SIGNALLING PATHWAYS

Ph.D. Thesis Summary

P1527 Biology

Mgr. Barbora Vyhlídalová

Olomouc 2022

The Ph.D. thesis is based on my research carried out within framework of Ph.D. study program P1527 Biology at the Department of Cell Biology and Genetics, Faculty of Science, Palacký University Olomouc, in the period September 2017-August 2022.

Ph.D. candidate: Mgr. Barbora Vyhlídalová

                  Department of Cell Biology and Genetics

                  Faculty of Science, Palacký University Olomouc

                  Šlechtitelů 27, 783 71 Olomouc, Czech Republic

Supervisor: Prof. RNDr. Zdeněk Dvořák, DrSc. et Ph.D.

                  Department of Cell Biology and Genetics

                  Faculty of Science, Palacký University Olomouc

                  Šlechtitelů 27, 783 71 Olomouc, Czech Republic

Opponents:

The summary of the Ph.D. thesis has been sent out on …………………………….
The oral defense takes place at the Faculty of Science, Palacký University Olomouc, …………………………………………………………………………...
The Ph.D. thesis is available at the library of biological science, Faculty of Science, Palacký University Olomouc, Šlechtitelů 27, 783 71 Olomouc, Czech Republic.

Acknowledgement

Summary

The human microbiome produces diverse metabolites that affect human health. A distinct class of microbial catabolites is formed from dietary tryptophan, some of which have already been described as ligands of the aryl hydrocarbon receptor (AhR) and the pregnane X receptor (PXR). Both receptors act as sensors for endogenous and exogenous compounds, and thus regulate gene expression of drug-metabolizing enzymes. In addition, both AhR and PXR play pivotal roles in various physiological and pathophysiological processes. For this reason, these receptors are important therapeutic targets for existing and novel compounds. However, not all microbial tryptophan catabolites have been systematically studied in relation to AhR and PXR, which would be significant to general intestinal health. Tryptophan catabolites contain indole in their structure, which is considered a biologically active component. Thus, endogenous and xenobiotic indole derivatives have been the subject of many studies and may have both beneficial and deleterious biological effects through these receptors.

In the present thesis, I have investigated the effects of tryptophan catabolites and mono-methylated indoles on the activities of AhR and PXR and the subsequent molecular events involved in these signalling pathways. Appropriate human and mouse intestinal and hepatic *in vitro* cell models were used for the study. Our findings showed that mono-methylated indoles are ligands and partial agonists of human PXR that induce PXR-regulated genes in human intestinal cells. Mono-methylated indoles display dual effects on the AhR-CYP1A signalling pathway in human intestinal and liver cells. On the one hand, they are AhR-dependent inducers of CYP1A genes, and on the other hand, they are inhibitors of CYP1A1 catalytic activity. In addition, this study demonstrated that the tryptophan catabolites are low-potency agonists of AhR, and their effects on AhR may differ substantially, as they may behave as full agonists, partial agonists, or even ligand-selective antagonists of human AhR. The findings of this study, for the first time, showed that indole-3-acetamide, indole-3-pyruvate, indole-3-acrylate, and indole-3-ethanol were among the strongest AhR ligands within the microbial tryptophan pathway and that indole and indole-3-acetamide are ligands and agonists of human PXR. In conclusion, this study

comprehensively characterised the interactions of gut microbial tryptophan catabolites and synthetic mono-methylated indoles with AhR and PXR, which may expand the current understanding of their potential roles inhuman intestinal health and disease. Furthermore, these findings would expand the potential drug repertoire through the concept of indole-based mimicry.

Souhrn

Lidský mikrobiom produkuje rozmanité metabolity, které ovlivňují lidské zdraví. Jedna skupina mikrobiálních katabolitů je tvořena z tryptofanu přijatého v potravě, z nichž některé již byly popsány jako ligandy aryl uhlovodíkového receptoru (AhR) a pregnanového X receptoru (PXR). Oba receptory působí jako xenoreceptory endogenních i exogenních sloučenin a regulují tak genovou expresi enzymů metabolizujících léčiva. Kromě toho AhR i PXR hrají významnou roli v různých fyziologických a patofyziologických procesech. Z tohoto důvodu jsou tyto receptory významným terapeutickým cílem pro stávající i nové látky. Doposud však nebyly systematicky studovány všechny známé tryptofanové katabolity ve vztahu k AhR a PXR, což by byl jedinečný a přímo aplikovatelný přístup ke střevnímu zdraví všeobecně. Tryptofanové katabolity obsahují ve své struktuře indol, který je považován za biologicky aktivní část. Předmětem mnoha studií jsou tedy endogenní I xenobiotické deriváty indolu, které mohou mít prostřednictvím těchto receptorů, jak příznivé, tak negativní biologické účinky.

V předkládané disertační práci jsem se zabývala studiem účinků tryptofanových katabolitů a mono-methylovaných indolů na aktivitu AhR a PXR receptoru a následné molekulární děje účastnící se těchto signálních drah. Pro studium byly použity vhodné *in vitro* modely lidských a myších, střevních a jaterních buněk. Naše zjištění ukázala, že mono-methylované indoly jsou ligandy a parciální agonisté lidského PXR, které indukují PXR cílové geny v lidských střevních buňkách. Zároveň mono-methylované indoly mají dvojí účinek na AhR-CYP1A signální dráhu v lidských střevních a jaterních buňkách. Jednak indukují expresi CYP1A genů prostřednictvím AhR, ale na druhé straně jsou inhibitory CYP1A1 katalytické aktivity. Dále jsme prokázali, že tryptofanové katabolity jsou AhR agonisté s nízkou účinností, avšak jejich působení na AhR se může podstatně lišit, protože se mohou chovat jako úplní agonisté, částeční agonisté nebo dokonce ligandově selektivní antagonisté lidského AhR. Výsledky této studie poprvé ukázaly, že indol-3-acetamid, indol-3-pyruvát, indol-3-akrylát a indol-3-etanol patří mezi nejsilnější ligandy AhR v rámci mikrobiální tryptofanové dráhy a že indol a indol-3-acetamid jsou ligandy a agonisté lidského PXR. Závěrem lze říci, že tato studie komplexně charakterizovala interakce střevních mikrobiálních katabolitů tryptofanu a syntetických mono-

methylovaných indolů s AhR a PXR, což může rozšířit současné chápání o jejich potencionálních rolích v lidském střevním zdraví a onemocněních. Navíc tato zjištění jsou zásadní pro rozšíření potencionálního repertoáru léčiv prostřednictvím konceptu mimikry na bázi indolů.

CONTENT

1 AIMS

The main goal of this study was to evaluate the effects of microbial intestinal catabolites of tryptophan (MICTs) and mono-methylated indoles (MMIs) on the AhR and PXR signalling pathways. The objectives of the study were to investigate the *in vitro* effects of the test compounds on:

1) The transcriptional activities of AhR and PXR in human cancer cell lines

2) The expression of AhR and PXR target genes in human cancer cell lines, immortalised hepatic progenitor cell lines, and primary human hepatocytes

3) The molecular functions of AhR and PXR, including nuclear translocation, heterodimerisation, and DNA binding

2 INTRODUCTION

The gastrointestinal microbiota plays an important role in the maintenance of gut health and host nutrition. In addition, microbes have been extensively studied due to their ability to affect the functions of distant organs and send signal across the gut-brain and gut-liver axes. The imbalance of the normal intestinal microbiome has been linked to dysbiosis and the etiology of several diseases, such as inflammatory bowel disease (IBD), diabetes, atopy, and obesity (Bull et Plummer, 2014; Wishart, 2019).

Among a wide range of intestinal microbial metabolites, indoles have been found to be involved in the crosstalk between several organs and host physiology. Most indole-based molecules exert biological functions through receptor-mediated signal transduction pathways, including the aryl hydrocarbon receptor (AhR) and the pregnane X receptor (PXR) that are expressed in various cell types within the gut (epithelial cells, fibroblasts, and immune cells) (Kumar et al., 2021). A variety of xenobiotic and dietary indoles, in addition to microbial indoles, have been described as ligands of AhR and PXR.

AhR and PXR have become promising targets for the treatment of different diseases, such as immune disorders, inflammatory diseases, and specific tumours. The identification of ligands with defined health-promoting effects and/or pharmaceutical properties for AhR and PXR is a key strategy for the development of new drugs targeting these receptors (Mulero-Navarro et

Fernandez-Salguero, 2016). Our group recently described PXR-mediated intestinal anti-inflammatory effects of newly designed compounds that structurally mimick microbial indole-based catabolites (Dvorak et al., 2020). A number of reports suggests that dietary and microbial indoles exhibit both agonist and antagonist activities for AhR and/or the PXR and may modulate gastrointestinal immune cells, increase barrier function, and inhibit intestinal inflammation (Hubbard et al., 2015a; Venkatesh et al., 2014; Zelante et al., 2013).

AhR and PXR are xenobiotic receptors that act as transcription factors for the regulation of their target genes. PXR is a member of the nuclear receptor family, whereas AhR belongs to the basic-helix-loop-helix-Period/ARNT/Single minded (bHLH-PAS) family, but both show functional analogy. These receptors are well-described regulators of drug-metabolizing enzymes and the transcriptional activities of drug transporters, which include members of the cytochrome P450 family. Although the CYP genes are primarily induced by xenobiotics, they are also induced by endobiotics (Larigot et al., 2018). Besides their roles as xenosensors, both AhR and PXR are involved in various cellular and biological processes, such as immune responses, carcinogenesis, cell migration, metabolic diseases, and DNA damage (Bock, 2017; Gutierrez-Vazquez et Quintana, 2018; Hakkola et al., 2016; Chai et al., 2020; Kolluri et al., 2017; Qiu et al., 2016). Different ligands may have varying physiological and cellular effects. It is generally known that the sustained activation of these receptors by endogenous ligands is essential for proper cell function; however, exogenous ligands have deleterious effects on human health (Stejskalova et al., 2011). These ligand-specific biologic responses are caused by the interaction of AhR and PXR with other transcription factors and the direct recruitment of distinct coactivators, leading to the expression of different target genes (e.g. CYPs and pro-inflammatory or anti-inflammatory cytokines) (Gutierrez-Vazquez et Quintana, 2018; Poulain-Godefroy et al., 2020). Microbiota-derived compounds may be considered pseudo-endogenous ligands and may have dual effects on human health (Murray et Perdew, 2020). AhR is involved in the regulation of intestinal innate and mucosal immunity and its activity can be modulated by intestinal indole-based microbiota-derived metabolites (Schiering et al., 2017). Therefore, it is necessary to know and investigate the metabolic fate and effects of these compounds in organisms. This knowledge

should be crucial for the development of new indole-based compounds as potential drugs for different diseases, such as IBD.

3 TEST COMPOUNDS

3.1 Microbial intestinal catabolites of tryptophan (MICTs)

Tryptophan formed from nutrient digestion may serve as a substrate for enzymes in the gut microbiota. Direct bacterial transformation of tryptophan leads to the production of various catabolites, which includes indole (IND), tryptamine (TA), 3-methylindole (3-MMI; skatole), indole-3-acrylate (IAC), indole-3-lactate (ILA), indole-3-pyruvate (IPY), indole-3-propionate (IPA), indole-3-acetate (IAA), indole-3-ethanol (IET), indole-3-acetamide (IAD), indole-3-aldehyde (IA), and indole-3-acetaldehyde (IAL) (Roager et Licht, 2018). Some of these microbial indole derivatives have already been identified as AhR and PXR ligands, through which they affect intestinal barrier integrity and immune response (Lamas et al., 2016; Venkatesh et al., 2014; Zelante et al., 2013). All MICTs, except IAL, were analysed in this work, and their effects on AhR and the PXR signalling pathways were determined. Structurally, these indole derivatives are aromatic bicyclic molecules that are composed of benzene fused to a pyrrole ring carrying different substituents at position 3.

Tryptophan is transformed by many Gram-positive and Gram-negative bacteria species, such as *Escherichia coli*, *Vibrio cholera*, *Bacteroides*, and *Clostridium,* into indole. The conversion to indole is induced by the enzymatic activity of tryptophanase (TnaA). Although indole has been known for > 100 years, the exploration of its detailed biological functions has only begun recently (Roager et Licht, 2018). Indole is the main tryptophan metabolite; it is an intracellular signalling molecule involved in the regulation of a number of biological processes (e.g. regulation of bacterial sporulation and virulence, bacterial motility, biofilm formation, and antibiotics resistance) (Li et Young, 2013). It has been reported that indole activates AhR, resulting in increased production of interleukin-22 (IL-22). IL-22 is a protein that controls the secretion of antimicrobial peptides and protects against pathogenic infections (Levy et al., 2017). The intestinal concentrations of MICTs are mostly unknown. Relatively high levels of indole (0.25–6 mM) have been detected in the faecal samples

of healthy adults (Dong et al., 2020; Dvorak et al., 2020; Hubbard et al., 2015b; Jin et al., 2014; Lamas et al., 2016; Roager et Licht, 2018). Different bacterial species generate various MICTs through different metabolic pathways. For instance, *Peptostreptococcus* metabolises tryptophan to IPA and IAC, while *Clostridium sporogenes* triggers tryptophan conversion into TA, ILA, and IPA (Roager et Licht, 2018).

Tryptophan decarboxylation induced by tryptophan decarboxylase enzyme leads to the production of tryptamine, which is another regulator of intestinal motility and immune functions (Williams et al., 2014; Wlodarska et al., 2015). Tryptamine is able to inhibit IDO1 enzyme, which subsequently influences immune surveillance (Tourino et al., 2013). In addition, TA acts as a ligand for AhR, and through AhR, it regulates intestinal immunity in DSS-induced colitis in mice by suppressing the expression of pro-infllammatory cytokines (Islam et al., 2017). TA is also responsible for serotonin release from enteroendocrine cells (Takaki et al., 1985).

A part of tryptophan may be metabolised to other indole derivatives by gut microbiota. The effects of indole derivatives on intestinal homeostasis have also been reported. Some *Clostridium*, *Bacteroides*, *Peptostreptococcus*, and *E. coli* spp convert tryptophan to tryptamine and indole-3-pyruvate, which are then metabolised to ILA, IAC, IPA, and IAA. Similarly, *Lactobacillus* are capable of converting tryptophan into IA and ILA in the presence of aromatic amino acid aminotransferase and an indolelactate dehydrogenase (Gao et al., 2018; Roager et Licht, 2018). Recent studies have shown that IPA can decrease intestinal permeability through the regulation of junctional proteins and maintain intestinal homeostasis through suppressed expression of cytokines, including TNF-α and IL-6, and these are mediated by the PXR and Toll-like receptor 4 (TLR4) pathway (Venkatesh et al., 2014). Furthermore, commensal *Lactobacilli* is able to produce IA from tryptophan. IA conduces to increased production of IL-22 through AhR in intestinal immune cells. Thus, it provides resistance against *Candida albicans* colonization and mucosal protection against inflammation (Zelante et al., 2013). IA also triggers AhR-dependent IL-10 expression in the intestine and subsequent expansion of goblet cells, thereby strengthening the intestinal barrier through mucus production (Powell et al., 2020). It has been reported that the concentration of IAA in the faecal samples of healthy individuals is 5 µM (Lamas

et al., 2016), while the concentrations of other indole derivatives (e.g. IPA, TA, ILA, IA) in the human gut have not yet been determined.

Finally, 3-methylindole (skatole) is an intestinal microbiota-derived metabolite of tryptophan (Jensen et al., 1995), which is synthesised from IAA by *Bacteroides* and *Clostridium* in the presence of indoleacetate decarboxylase. 3-MMI has been extensively studied due to its typical faecal odour and the occurrence of this odour in pork (Roager et Licht, 2018). Skatole formation is a two-step process mediated by at least two different bacterial species. This possibly explains the high variable intestinal concentration of 3 MMI. The concentration of IAA, the precursor of skatole, is another rate-limiting factor (Gao et al., 2018). Skatole exerts bacteriostatic effects on Gram-negative enterobacteria, such as *Salmonella*, *Shigella*, and *Escherichia*. Therefore, it may affect the composition of intestinal microbiota (Yokoyama et Carlson, 1979). Apart from this function, skatole can activate human AhR in a dose-dependent manner, but can only exhibit modest activation of mouse AhR. Such skatole-mediated activation of human AhR within the GI tract may regulate intestinal homeostasis (Hubbard et al., 2015a).
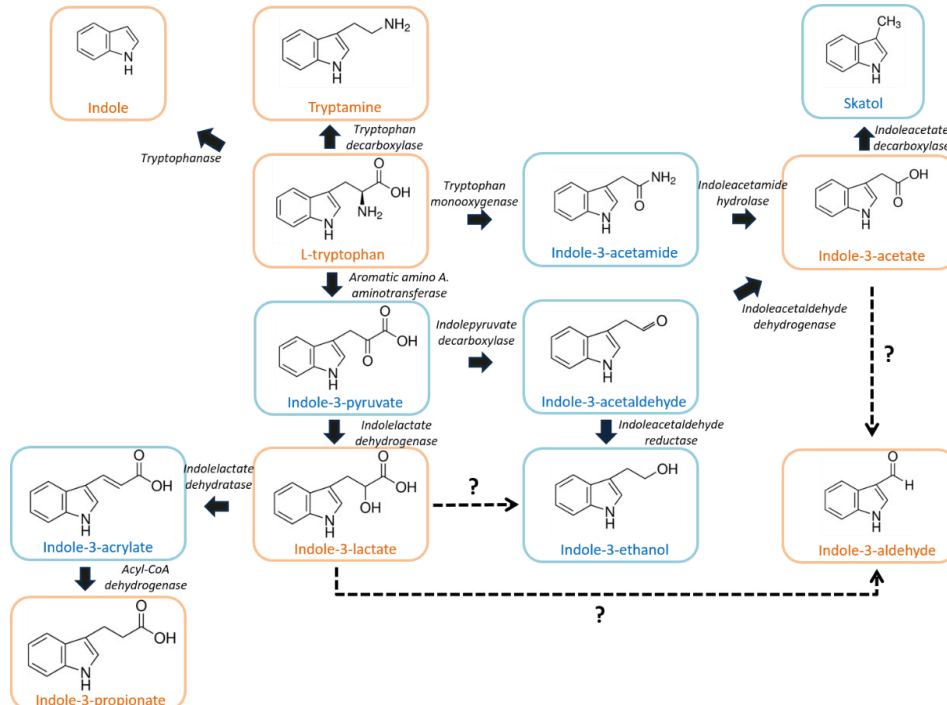

Figure 1: Microbial generation of tryptophan catabolites in the human gut. Overview of the different ways microbes degrade tryptophan in the human gut. The metabolites framed in orange colour represent the most commonly detected tryptophan catabolites in the human gut. Dashed lines represent pathways where no enzymes have been identified. Adopted from (Roager et Licht, 2018).

3.2 **Mono-methylated indoles (MMIs)**

This section is on the effects of seven MMI isomers on the AhR and PXR signalling pathways. Several studies monitored the biological processes of some MMIs connected to these signalling pathways. However, for most MMIs, these mechanisms remain unknown. MMIs differ from each other in the position of attached methyl group on the indole core. While 3-MMI is a microbial catabolite formed from dietary tryptophan in intestines (described above), the other MMIs isomers are xenobiotics. Rasmussen et al. demonstrated that 3-MMI is a partial agonist of human AhR and an inducer of CYP1A1, CYP1A2, and CYP1B1 genes in HepG2 cell line and primary human hepatocytes, which was later confirmed also by other researchers (Rasmussen et al., 2016; Stepankova et al., 2018). The same authors also showed that indole-3-carbinol (skatole metabolite) is a more potent inducer of human AhR than skatole (Rasmussen et al., 2016). Skatole also induces the expression of CYP1A1 mRNA and protein in primary normal bronchial epithelial cells at physiologically relevant concentrations (Weems et Yost, 2010). Using a reporter gene assay, Hubbard el al. showed that 3-MMI, but not 1-MMI or 2-MMI activates AhR. However, experiments were carried out with only up to 10 μM concentrations of MMI (Hubbard et al., 2015a). 3-MMI, as well as xenobiotic 2-MMI, induced ethoxy-resorufin-O-deethylase activity in Zebrafish (Brown et al., 2015) and Atlantic killifish embryos (Brown et al., 2016).

Apart from 3-methylindole, the metabolism of the other tested MMIs is unknown. Because many AhR ligands are also PXR ligands (approx. 88 % overlap for dual activators: PubChem Bioassay ID434939 and PubChem Bioassay ID2796), it is reasonable to assume that indoles might also be PXR ligands.
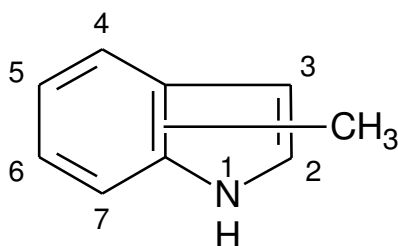

Figure 2: Chemical structure of mono-methylated indoles

4 MATERIALS AND METHODS

4.1 Biological materials

4.1.1 Cancer cell lines

The human Caucasian colon adenocarcinoma cell line LS180 (ECACC No. 87021202) and mouse hepatoma cell line Hepa-1c1c7 (ECACC No. 95090613) were purchased from the European Collection of Authenticated Cell Cultures (ECACC). Human Caucasian colon adenocarcinoma cell line LS174T (ATCC: CL-188; 7 000 3535) (Synthego Corporation, Redwood City, CA, USA) was used, as the parental cell line, to develop the PXR-knockout variant LS174T PXR-KO, utilizing CRISPR/Cas9 technology, as recently described (Dvorak et al., 2020). Human Caucasian colon adenocarcinoma cell lines HT-29 wild-type and AHR knock-out variant clone E4 were a generous gift from prof. RNDr. Jan Vondráček Ph.D. (IBP Brno, Czech Republic). The AHR knock-out variant, a clone E4 of HT-29 cell line, was generated using CRISPR/Cas9 as previously described (Vyhlidalova et al., 2020). Stably transfected reporter gene cell line AZ-AhR (Novotna et al., 2011) and the polyclonal population of LS174T (RM12-PXR) cells with stably transfected pReceiver-M12 expression plasmid (Illes et al., 2020) were developed in our laboratory. All the cell lines, except for Hepa-1c1c7, were maintained in Dulbecco´s modified Eagle´s medium (DMEM) supplemented with 10 % foetal bovine serum or 10 % charcoal-stripped foetal bovine serum, 2 mM L-glutamine, 1 % non-essential amino acids, 100 U/ml streptomycin, and 100 µg/ml penicillin. The Hepa-1c1c7 cell line was cultured in minimal essential medium without nucleosides (MEM) enriched with 10 % foetal bovine serum and 2 mM L-glutamine. All used cells were incubated at 37 °C and 5 % CO_2.

4.1.2 Primary and progenitor hepatic cell lines and immortalised keratinocytes

Human immortal keratinocyte cell line HaCaT was kindly donated by *P. Boukamp* (IUF Düsseldorf, Germany) and was cultured in DMEM as earlier described.

Three human hepatoma HepaRG™-derived cell lines (5F Clone control cells, AHR knock-out (AHR-KO) and PXR-knock-out (PXR-KO)) were obtained

from Sigma Aldrich (Prague, Czech Republic) and incubated according to the manufacturer's instructions.

Primary cultures of human hepatocytes were of dual origins: (i) cultures in a monolayer batch marked with "HEP" were purchased from Biopredic International (Rennes, France); (ii) cultures from multi-organ donors marked with "LH" were prepared at the Faculty of Medicine, Palacký University Olomouc. The liver tissues were obtained from the University Hospital Olomouc, Czech Republic, and the tissue acquisition protocol complied with the requirements/regulations issued by "Ethical Committee of the University Hospital Olomouc, Czech Republic" and with transplantation Law #285/2002 Coll. Primary human hepatocyte cultures were maintained in serum-free ISOM medium (Isom et al., 1985; Pichard-Garcia et al., 2002). The age and sex of each donor are mentioned below (Table 1). The cells were incubated at 37 °C with 5 % CO_2.

Table 1: Age and gender of donors of used primary human cultures

Batch number	Sex	Age
HEP200565	Female	21
HEP200570	Male	64
HEP200571	Male	77
HEP220993	Female	76
HEP2201020	Male	75
HEP2201021	Male	66
LH75	Female	75
LH79	Male	60

4.2 Compounds and reagents

DMEM, MEM, foetal bovine serum (FBS), charcoal-stripped foetal bovine serum (CS-FBS), non-essential amino-acids, L-glutamine, penicillin, streptomycin, dimethyl sulfoxide (DMSO, D8418), rifampicin (RIF, R3501, Lot 0000104692, purity ≥ 97 %), hygromycin B, TRI Reagent®, Triton™ X-100, D-luciferin, coenzyme A, adenosine triphosphate (ATP), bovine serum albumin, benzo[a]pyrene (BaP, B1760, Lot SLB0038V, purity 99 %), 6-formylindolo[3,2-b]carbazole (FICZ, SML1489, Lot 0000026018, purity 99.5 %), 1-methylindole (193984, Lot BGBC4251V, purity ≥ 97 %), 2-methylindole (M51407, Lot BCBF7494V, purity 98 %), 3-methylindole (M51458,

Lot STBK2264, purity 98 %), 5-methylindole (222410, Lot STBF3756V, purity 99 %), 6-methylindole (246328, Lot MKBJ2514V, purity 97 %), 7-methylindole (M51490, Lot MKBP5287V, purity 97 %), indole-3-aldehyde (129445, Lot STBH5988, purity 97 %) and indole-3-ethanol (T90301, Lot BCBW9114, purity 97 %) were purchased from Sigma Aldrich (Prague, Czech Republic). 4-methylindole (E020483, Lot AH160074, purity 98 %) was obtained from Energy Chemical (Shanghai, China). Tryptamine (SC-206065, Lot E0218, purity 99.9 %), indole-3-propionate (SC-255215, Lot E0218, purity ≥ 98 %), indole-3-acetamide, (SC-255213, Lot K0618, purity ≥ 98 %), indole-3-pyruvate (SC-218597, Lot K1218, purity ≥ 95 %), indole-3-acetate (SC-254494, Lot A2218, purity ≥ 99 %), indole-3-lactate (SC-489732, Lot B2321, purity 99.7 %), indole-3-acrylate (SC-272496, Lot K1618, purity 98.4 %), indole (SC-257606, Lot J0918, purity ≥ 98 %), primary mouse monoclonal antibodies against CYP1A1 (sc-393979, A-9), CYP1A2 (sc-53614, 3B8C1), CYP3A4 (sc-53850, HL3), ARNT-1 (sc-17812, G-3), AhR (sc-133088, A-3) and AhR labeled with Alexa fluor 488 (sc-133088 AF488, A-3), PXR rabbit polyclonal antibody (sc-25381, H-160), normal rabbit IgG (sc-2027) were acquired from Santa Cruz Biotechnology (Santa Cruz, CA, USA). Other primary antibodies against AhR (rabbit monoclonal; 83200S, D5S6H) and β-actin (mouse monoclonal; 3700S, 8H10D10) as well as anti-mouse secondary antibody conjugated to horseradish peroxidase (7076S) were purchased from Cell Signalling Technology (Danvers, MA, USA). An anti-PXR (mouse monoclonal; PP-H4417-00) antibody was obtained from Perseus Proteomics, Int. (Tokyo, Japan). WesternSure® PREMIUM Chemiluminescent Substrate was purchased from LI-COR Biotechnology (Lincoln, NE, USA), whereas reagents for Simple Western blotting by Sally Sue™, a goat anti-mouse secondary horseradish conjugated antibody, and antibody diluent were acquired from ProteinSimple (San Jose, CA, USA). Luciferase lysis buffer, FuGENE® HD Transfection Reagent, and P450-Glo™ CYP1A1 assay were purchased from Promega (Madison, WI, USA). M-MuLV Reverse Transcriptase and Random Primers 6 were acquired from New England Biolabs (Ipswith, MA, USA). UPL probes and oligonucleotide primers used in qPCR reactions were designed by Universal ProbeLibrary Assay Design Center and synthesised by Sigma Aldrich (Prague, Czech Republic), while LightCycler® 480 Probes Master was purchased from Roche Diagnostic

Corporation (Prague, Czech Republic). 2,3,7,8-tetrachlorodibenzo-p-dioxin (TCDD, RPE-029) was from Ultra Scientific (North Kingstown, RI, USA). 2,3,7,8-tetrachlorodibenzofuran (TCDF, Amb17620425, Lot 51207-31-9) was from Ambinter (Orleáns, France). DAPI (4',6-diamino-2-phenylindole) was from Serva (Heidelberg, Germany). [^{3}H]-TCDD (ART 1642, Lot 181018, purity 98.6 %) was purchased from American Radiolabeled Chemicals (St. Louis, MO, USA). Bio-Gel® HTP Hydroxyapatite (1300420, Lot 64079675) was obtained from Bio-Rad Laboratories (Hercules, CA, USA). LanthaScreen^{TM} TR-FRET PXR (SXR) Competitive Binding Assay Kit and Pierce^{TM} Co-Immunoprecipitation Kit were acquired from Thermo Fisher Scientific (Waltham, MA, USA). All other chemicals were of the highest quality commercially available.

4.3 Methods

4.3.1 Reporter gene assay

To investigate AhR transcriptional activity, stably transfected AZ-AhR cells were used (Novotna et al., 2011). LS180 cells, transiently transfected with human PXR expression vector pSG5-PXR, (kindly provided by Dr. S. Kliewer, University of Texas, Dallas, US) and a chimeric p3A4-luc reporter construct (Pavek et al., 2010) through lipofection (FuGENE® HD Transfection reagent), were used to study PXR transcriptional activity. The cells were seeded at a density of 25 × 10^3/well in 96-well plates and allowed to stabilise for 24 h. The cells were incubated for 24 h with tested compounds and/or vehicle (DMSO; 0.1 % v/v), in the presence (antagonist mode) or absence (agonist mode) of TCDD (13.5 nM), FICZ (22.6 μM), or BaP (15.8 μM) for AhR activity and RIF (10 μM) for PXR activity. In another experiment, the cells were incubated for 24 h with culture media aspired from human hepatocytes cultures that had been previously incubated for 0 h and 24 h with vehicle (DMSO; 0.1 % v/v), TCDD (5 nM), and mono-methylindoles (MMIs; 200 μM). This different approach of treating cells using collected culture media was applied to understand MMI metabolism (see chapter 5.1.4. and 5.1.5). Following cell lysis, luciferase activity was measured using a Tecan Infinite M200 Pro Plate Reader (Schoeller Instruments, Czech Republic).

4.3.2 mRNA isolation and quantitative reverse transcriptase polymerase chain reaction (qRT-PCR)

LS180 cells were used to explore mRNA expression levels of PXR target genes (CYP3A4 and MDR1). They were transiently transfected with a pSG5-hPXR expression vector through lipofection (FuGENE® HD Transfection reagent).

The cells were seeded in 12-well plates and stabilised for 24 h (48 h for primary human hepatocytes). Cultured cells were incubated for 24 h with vehicle (DMSO; 0.1 % v/v) or examined compounds in the presence (antagonist mode) or absence (agonist mode) of TCDD (5 nM or 10 nM) or RIF (10 µM), respectively. Total RNA was isolated by using TRI Reagent® according to the manufacturer's protocol. The concentration and quality of the RNA was determined with a NanoDrop™ Lite Spectrophotometer (Thermo Fisher Scientific, MA, USA). The isolated RNA (1000 ng) was used for cDNA synthesis using M-MuLV reverse transcriptase and Random Primers 6. The reverse transcription was carried out at 42 °C for 60 min, and the cDNA sample was diluted in ratio 1:4 with PCR-grade water. qRT-PCR was performed on LightCycler® 480 Instrument II (Roche Diagnostic Corporation, Prague, Czech Republic) using the LightCycler® Probes Master. The levels of all mRNAs were determined using the Universal Probes Library probes in combination with specific primers (Table 2). An activation step was conducted at 95 °C for 10 min, followed by 45 cycles of PCR (denaturation at 95 °C for 10 s; annealing with elongation at 60 °C for 30 s). All measurements were carried out in triplicates. The data were processed by the delta-delta C_t method and normalised to GAPDH as the housekeeping gene.

Table 2: Primer sequences with appropriate Universal Probes Library (UPL) numbers

Gene	Forward Primer (5′ → 3′)	Reverse Primer (5′ → 3′)	UPL no.
GAPDH	CTCTGCTCCTCCTGTTCGAC	ACGACCAAATCCGTTGACTC	60
CYP1A1	CCAGGCTCCAAGAGTCCA	AGGGATCTTGGAGGTGGCT	33
CYP1A2	ACAACCCTGCCAATCTCAAG	GGGAACAGACTGGGACAATG	34
CYP3A4	TGTGTTGGTGAGAAATCTGAGG	CTGTAGGCCCCAAAGACG	38
MDR1	CCTGGAGCGGTTCTACGA	TGAACATTCAGTCGCTTTATTTCT	147

4.3.3 Simple western blotting by Sally Sue^{TM}

The protein levels of CYP1A1, CYP1A2, CYP3A4, and β-actin in the total protein extracts prepared from primary human hepatocytes were determined. The cells were stabilised for 48 h before treatment, followed by incubation for 24 h with MMIs, TCDD (5 nM), RIF (10 µM), and/or vehicle (DMSO; 0.1 % v/v). After incubation, the cells were washed once in phosphate buffered saline (PBS) and centrifuged (4600 rpm/5 min/4 °C). Total protein extracts were prepared by resuspending the pellets in non-denaturizing ice cold lysis buffer (150 mM NaCl, 10 mM Tris (pH 7.2), 0.1 % (w/v), Triton X-100, anti-phosphatase cocktail, anti-protease cocktail, 1 % (v/v) sodium deoxycholate, and 5 mM EDTA). The suspension was vortexed and centiruged (13,200 rpm/ 15 min/4 °C). The supernatant was collected and the concentration of proteins was determined using Bradford reagent. Target proteins were detected by using automated capillary electrophoresis Sally Sue^{TM} Simple Western System (ProteinSimple^{TM}, San Jose CA, USA) and handled in accordance with the ProteinSimple manual. Primary antibodies for CYP1A1 (dilution 1:100), CYP1A2 (dilution 1:1000), CYP3A4 (dilution 1:5000 to 1:20000), and β-actin (dilution 1:1000) were used, and detection was performed using a horseradish conjugated secondary antibody on a chemiluminescent substrate. The data were analysed using Compass Software version 2.6.5.0 (ProteinSimple^{TM}). CYP signals were normalised to β-actin signal as a loading control and expressed as fold induction over negative control (DMSO).

4.3.4 Time resolved-fluorescence resonance energy transfer

The LanthaScreen^{TM} TR-FRET PXR (SXR) Competitive Binding Assay Kit (Thermo Fisher Scientific, Waltham, MA, USA) was used to determine the binding of MMIs, indole-3-acetamide, and indole at PXR. The experiments were performed in a volume of 20 µl in 384-well black plate with tested compounds prepared in serial dilution (from 11-points to 13-points), at concentrations ranging from 0.05 µM to 500 µM. Vehicle (DMSO) and SR12813 (100 µM) were used as negative and positive control, respectively. The plate was incubated for 1 h at room temperature in the dark. Subsequently, using the 340 nm excitation filter, the fluorescent signals were measured at 495 nm and 520 nm on the Tecan Infinite F200 Pro Plate Reader (Achoeller Instruments, Czech Republic).

For the TR-FRET ratio, the emission signal at 520 nm was divided by the emission signal at 495 nm. Binding assays were done in quadruplicates (technical replicates) in at least three independent experiments (biological replicates), and the IC_{50} values were calculated.

4.3.5 Chromatin immunoprecipitation assay

4.3.5.1 Detection of AhR binding to CYP1A1 promoter

LS180 cells were seeded in a 60-mm cell culture dish (4×10^6), and the following day, the cells were incubated with vehicle (DMSO; 0.1 % v/v), TCDD (10 nM), or the test compounds (indole 1000 µM, indole-3-acrylate 100 µM, others 200 µM) for 90 min at 37 °C. Chromatin immunoprecipitation assay (ChIP) procedure was performed in accordance with the manufacturer's protocol in the manual for the SimpleChIP Plus Enzymatic Chromatin IP Kit (Magnetic Beads; Cell Signalling Technology, Leiden, The Netherlands) and as previously described (Stepankova et al., 2018). Immunoprecipitation was achieved by the addition of 5 µl anti-AhR antibody (D5S6H, Cell Signalling Technology) to 25 µg of digested chromatin. The amplification of CYP1A1 promoter DNA was carried out with PCR using the following primers:

Forward 5'-AGCTAGGCCATGCCAAAT-3'
Reverse 5'-AAGGGTCTAGGTCTGCGTGT-3'

The data are expressed as the fold enrichment to vehicle-treated cells. The end point PCR product was separated using 2 % agarose gel electrophoresis.

4.3.5.2 Detection of PXR binding to MDR1 promoter

LS174T cells with stably transfected pReceiver-M12 expression plasmid (RM12-PXR) were seeded in a 60-mm cell culture dish (3 million) and allowed to stabilise. The following day, the cells were maintained in DMEM with 10 % CS-FBS containing vehicle (DMSO; 0.1% v/v), RIF (10 µM), indole-3-acetamide (IAD, 200 µM), and indole (IND, 1000 µM) for 20 h at 37 °C. ChIP assay was performed as previously described (Stepankova et al., 2018) with small modifications: a) 5 µl of anti-PXR antibody (PP-H4417-00, Perseus Proteomics Int.) was used against 30 µg of DNA; b) MDR1 promoter DNA was amplified by PCR using the following primers:

Forward 5'-GAGTGAACGTTACCTCATTGAAC-3'
Reverse 5'-CCGAAATGGCTTTTGAATTG-3'

The data were analysed as previously described, and the amplicon was electrophoresed on 2 % agarose gel after PCR.

4.3.5.3 Detection of PXR binding to CYP3A4 promoter

LS174T cells were transiently transfected with pSG5-PXR expression plasmid, plated in 150-mm cell culture dish, and grown to confluence. The cells were incubated with vehicle (DMSO; 0.1 % v/v), RIF (10 µM), and 1-MMI (200 µM) for 24 h at 37 °C. ChIP procedure was carried out as previously decribed (Dvorak et al., 2020) and 2 µg of anti-PXR antibody (SC-25381, H-160, Santa Cruz Biotechnology) was used for immunoprecipitation. Purified chromatin DNA was used to perform PCR amplification for CYP3A4 promoter DNA with the following primers:

Forward   5'-AGAGACAAGGGCAAGAGAG-3'

Reverse   5'-CTCTTTGCTGGGCTAGTGCA-3'

Next, the PCR products were resolved on 1.5 % agarose gel.

4.3.6 Protein Co-Immunoprecipitation

- **Detection of the formation of the AhR-ARNT heterodimer**

The formation of AhR-ARNT heterodimer was studied in cell lysates from intestinal LS180 cells, which were incubated with vehicle (DMSO; 0.1 % v/v), TCDD (10 nM), and the tested compounds-indole (IND, 1000 µM), indole-3-pyruvate (IPY, 200 µM), 3-methylindole (3-MMI, 200 µM), tryptamine (TA, 200 µM), indole-3-acrylate (IAC, 200 µM), and indole-3-acetamide (IAD, 200 µM) for 90 min at 37 °C. The Pierce™ Co-Immunoprecipitation Kit (Thermo Fisher Scientific, Waltham, MA, USA) and covalently coupled AhR antibody (mouse monoclonal, sc-133088, A-3, Santa Cruz Biotechnology) were used. Eluted protein complexes, in parallel with total parental lysates, were separated on 8 % SDS-PAGE gels, followed by western blot analysis and immuno-detection with ARNT-1 antibody (mouse monoclonal, sc-17812, G-3, Santa Cruz Biotechnology). Chemiluminescent detection was performed using horseradish peroxidase-conjugated anti-mouse secondary antibody (7076S, Cell Signalling Technology) and WesternSure® PREMIUM Chemiluminescent Substrate (LI-COR Biotechnology) by C-DiGit® Blot Scanner (LI-COR Biotechnology).

4.3.7 Competitive Radio-Ligand Binding Assay

The ligand binding assay was carried out using cytosolic protein extracts isolated from murine hepatoma Hepa1c1c7 cells as previously described (Denison et al., 2002). In brief, cytosolic protein (2 mg/ml) was incubated for 2 h at room temperature with 2 nM [^{3}H]-TCDD in the presence of vehicle (DMSO; negative control; 0.1% v/v), FICZ (positive control; 0.01 nM-10 nM), TCDF (non-specific binding; 200 nM), or increasing concentration of MICT. Next, the hydroxyapatite slurry was added to the samples and the suspension was kept on ice and washed three times with HEGT buffer. The hydroxyapatite pellet was resuspended in a scintillation cocktail, and radioactivity was determined using a liquid scintillation counter. The specific binding of [^{3}H]-TCDD was defined as the difference between total radioactivity and radioactivity of non-specific reaction (TCDF). Binding assays were performed in triplicates (technical replicates), in at least two independent experiments, and the IC$_{50}$ values were calculated where necessary.

4.3.8 High-performance liquid chromatography

High performance liquid chromatography (HPLC) was used to determine the levels of tryptophan in the samples of culture media isolated from the growing cells at 2 h intervals from 0 h to 24 h. A simple gradient HPLC method using an Agilent 1260 Infinity system (consisting of a quaternary gradient pump, autosampler, column thermostat, and diode array detector (DAD)) was used. The starting mobile phase mix consisted of 90 % of 0.2 % trifluoroacetic acid (TFA) and 10 % of acetonitrile (MeCN), and during the run, a linear gradient was applied up to 15 min, increasing the percentage of MeCN to 90 %. A post time of 5 min was applied to achieve the proper starting conditions for the next run. The stable mobile phase flow of 0.5 ml/min was applied at the reverse phase chromatographic column Agilent Poroshell 120 EC-C18, 4.6 × 50 mm, 2.7 μm particle size. The DAD detector was set to detect at the following wavelengths: 290 ± 4 nm (A), 254 ± 4 nm (B), 210 ± 4 nm (C), and 275 ± 4 nm (D, used for quantification of tryptophan levels) with a reference range of wavelengths of 820 ± 100 nm. The sample volume applied to the column was 10 μl in all the cases. An external calibration in the concentration range of 0.7 μM–112.0 μM was used, giving a straight calibration curve with R^2 = 0.9999. The peak

of tryptophan was identified at t_R = 5.0 ± 0.1 min, and it was completely resolved from other peaks in the chromatogram. The individual determinations were done in duplicate, and the concentration levels were expressed as mean values ± sample standard deviations.

4.3.9 Liquid chromatography/mass spectrometry

Liquid chromatography/mass spectrometry (LC/MS) analysis was used to determine MMI metabolites in the culture media samples. Three cultures of primary human hepatocytes (LH75, HEP200565, and HEP200570) were incubated with 200 µM MMIs for 24 h. Thereafter, culture media were aspired and used for reporter gene assay in AZ-AhR cells (*vide supra*) and for LC/MS analysis. Briefly, a previously described method (Zhang et al., 2014) with slight modification was used for the separation of the metabolites using the UHPLC Dionex UltiMate 3000 (Thermo Fisher Scientific) coupled with the LCQ Fleet™ Ion Trap Mass Spectrometer (Thermo) in a positive ionization mode. The mobile phase consisted of water supplemented with 0.1 % trifluoroacetic acid (TFA) and acetonitrile supplemented with 0.1 % of TFA. During the 18-min analysis, the mobile phase gradient comprised 95 % of water for 1 min, followed by the linear gradient to 15 min down to 5 % of water, followed by the rapid linear gradient to 18 min reconstituting the starting 95% of water. The stable mobile phase flow of 0.5 mL/min was applied at the reverse-phase chromatographic column Agilent Poroshell 120 EC-C18, 4.6 × 50 mm, 2.7 µm particle size. The PDA detector was set to the detection wavelengths of 254 ± 4 nm, 210 ± 4 nm, 225 ± 4 nm (used for quantification of residual levels of MMI), and 350 ± 4 nm, and the MS analyser was set to detect the mass range of 50-2000 m/z. The sample volume applied to the column was 10 µl in all the cases. All samples were analysed in three parallel determinations and the LC/MS data were analysed using the Thermo Excalibur 2.2 Qual Browser (Thermo).

4.3.10 Nuclear translocation of AhR

LS180 cells (60,000 cells/well) were plated on poly-D-lysine-coated 8-well chambered slides (94.6140.802, Sarstedt, Nümbrecht, Germany) and allowed to grow overnight. Next, the cells were incubated for 90 min with DMSO (0.1 % v/v), TCDD (10 nM), IND (1000 µM), 3-MMI (200 µM), TA (200 µM), IPY (200 µM), IAD (200 µM), and IAC (100 µM). The staining procedure has earlier been

described (Stepankova et al., 2018). The primary anti-AhR antibody used was Alexa Fluor 488 labelled mouse monoclonal (sc-133088, Santa Cruz Biotechnology, U.S.A.). The nuclei were stained with 4',6-diamino-2-phenylindole (DAPI), and the cells were enclosed by VectaShield® Antifade Mounting Medium (Vector Laboratories Inc., U.S.A.). The images were captured using an IX73 fluorescence microscope (Olympus, Tokyo, Japan). The immunofluorescence signal intensity (of the AhR antibody) in the nucleus was visually evaluated. To calculate the percentage number of cells, approximately 500 cells from at least four randomly selected fields of view in each specimen were used.

4.3.11 CYP1A1 enzyme activity

The P450-Glo^{TM} CYP1A1 cell-based assay was used to determine CYP1A1 catalytic activity in primary human hepatocytes and intestinal LS180 cells. The amount of luminescence produced was directly proportional to CYP1A1 activity. Experiments were carried out in two layouts: (i) Assessment of CYP1A1 induction and degradation by MMI: The cells were incubated with MMIs (0.1 μM–200 μM), vehicle (DMSO; 0.1 % v/v), and 5 nM TCDD for 24 h. Next, the enzyme substrate luciferin-CEE was added for additional 3 h; (ii) Assessment of the inhibition of TCDD-induced CYP1A1 by MMIs: The cells were pre-incubated with TCDD for 24 h, followed by the addition of enzyme substrate luciferin-CEE with MMIs for another 3 h. Each reaction was performed in duplicates, and two independent experiments were performed for each replicate. Net luminescence signals were determined by subtracting background luminescence values (no-cell control) from treated and untreated values. CYP1A1 catalytic activity was evaluated by plotting fold induction against MMI concentrations.

4.3.12 Statistical analysis

In order to determine significantly different results with respect to negative or positive control, one-way analysis of variance (ANOVA), followed by Dunnett's test, was applied. A p-value < 0.05 indicated statistical significance. The normality of the data was tested using the Shapiro-Wilk normality test. All calculations (including IC_{50} and EC_{50}) and curve fittings were performed using GraphPad Prism version 8.0 for Windows (GraphPad Software, La Jolla, CA, USA).

5 RESULTS AND DISCUSSION

In the present study, I systematically investigated the effects of the entire series of MMIs and 11 known human microbial intestinal tryptophan catabolites on the activities and functions of AhR and PXR. *In vitro* models of primary human hepatocytes, human hepatic progenitor cell lines, and cancer cell lines were used. The compounds were tested using various experimental approaches to determine the transcriptional activities of AhR and PXR, mRNA and protein expression levels of target genes, CYP1A1 catalytic activity, protein-protein interactions, DNA-protein interactions, and metabolism of the test compounds.

5.1 Effects of MMIs on the AhR signalling pathway

In the first part of the study, we demonstrated that MMIs induced CYP1A1 and CYP1A2 genes in HepaRG human hepatic progenitor cells through AhR-dependent mechanisms. MMIs also induced the mRNA and protein expression of CYP1A1 and CYP1A2 in the primary cultures of human hepatocytes. The relative efficacy of MMIs in HepaRG and primary human hepatocytes were similar to those detected previously for CYP1A1 in LS180 intestinal cancer cells (Stepankova et al., 2018), with one exception. Although 7-MMI was a weak inducer of CYP1A1 in LS180 and HepaRG cells, it was a very strong inducer of CYP1A genes in three cultures of human hepatocytes. Because primary human hepatocytes possess more sophisticated system for xenobiotic metabolism than cell lines, the plausible explanation for the strong increase in the ability to induce CYP1A genes by 7-MMI may be its metabolic conversion to a highly AhR-active product. The hypothesis of 7-MMI metabolic activation was supported by results demonstrating increased AhR activation in transgenic reporter gene AZ-AhR cells induced by culture media from human hepatocytes incubated 24 h with 7-MMI, compared with media containing 7-MMI without prior incubation. In contrast, we also observed loss of AhR agonist activity of 4-MMI after incubation with human hepatocytes. The dramatic decline in MMI concentrations in culture media after 24 h incubation with human hepatocytes indicated either metabolic degradation or active cellular uptake of parental MMI. Through LC/MS analysis, we observed the formation of various derivatives of mono-oxidated MMIs (mono-hydroxylated MMIs ormono-methyl-oxindole derivatives) and GSH-conjugates of MMIs in cell culture media. Significant

differences in the amounts and types of mono-oxidated metabolites were observed in the samples. Conjugation with a large polar glutathione molecule and/or introduction of hydroxyl groups into the indole skeleton could compromise AhR agonist activity of MMIs, which has also been observed by other authors (Heath-Pagliuso et al., 1998). Speculatively, this could be a reason for a loss of AhR agonist activity for 4-MMI. On the other hand, the formation of mono-methyl-oxindoles could lead to the formation of condensed products analogous to indigo and indirubin, which are potent AhR agonists (Adachi et al., 2001). This could be the reason for the acquisition of AhR agonist activity by 7-MMI. Collectively, distinct metabolic signatures for individual MMIs might result in no change, loss, or gain of AhR agonist activity. The activators of AhR and inducers of CYP1A genes are often the inhibitors of CYP1A enzymes. Indeed, the effects of MMIs on CYP1A1 enzyme activity in cultured LS180 cells and in primary human hepatocytes involved both the inhibition of catalytic activity and increase in CYP1A1 amount by induction, but with a different concentration-response pattern.

Figure 3: Effects of MMIs on the mRNA expression of CYP1A1 and CYP1A2 in HepaRG cells.
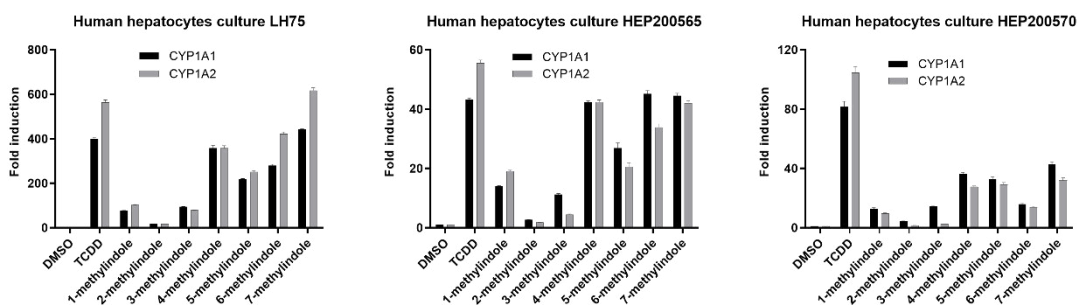
Figure 4: Effects of MMIs on the mRNA expression of CYP1A1 and CYP1A2 in primary human hepatocytes.
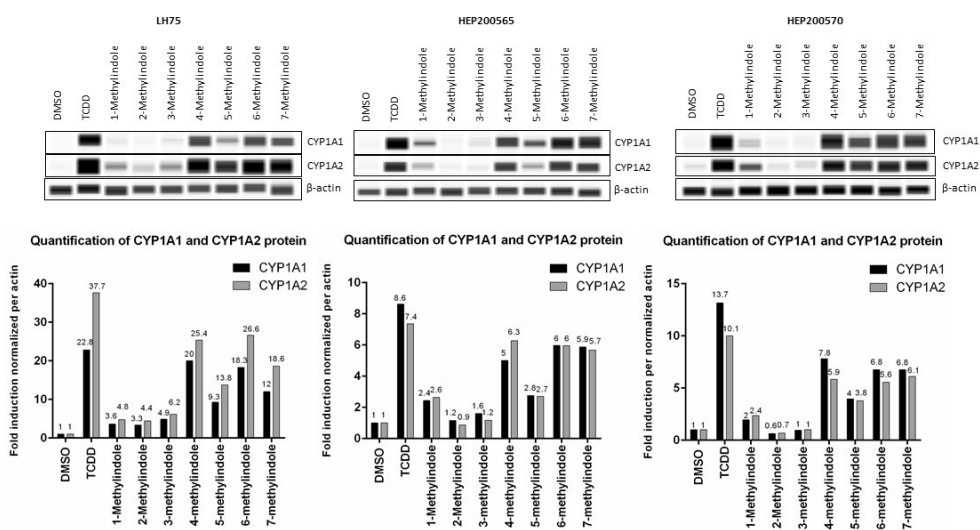
Figure 5: Effects of MMIs on the protein expression of CYP1A1 and CYP1A2 in primary human hepatocytes.
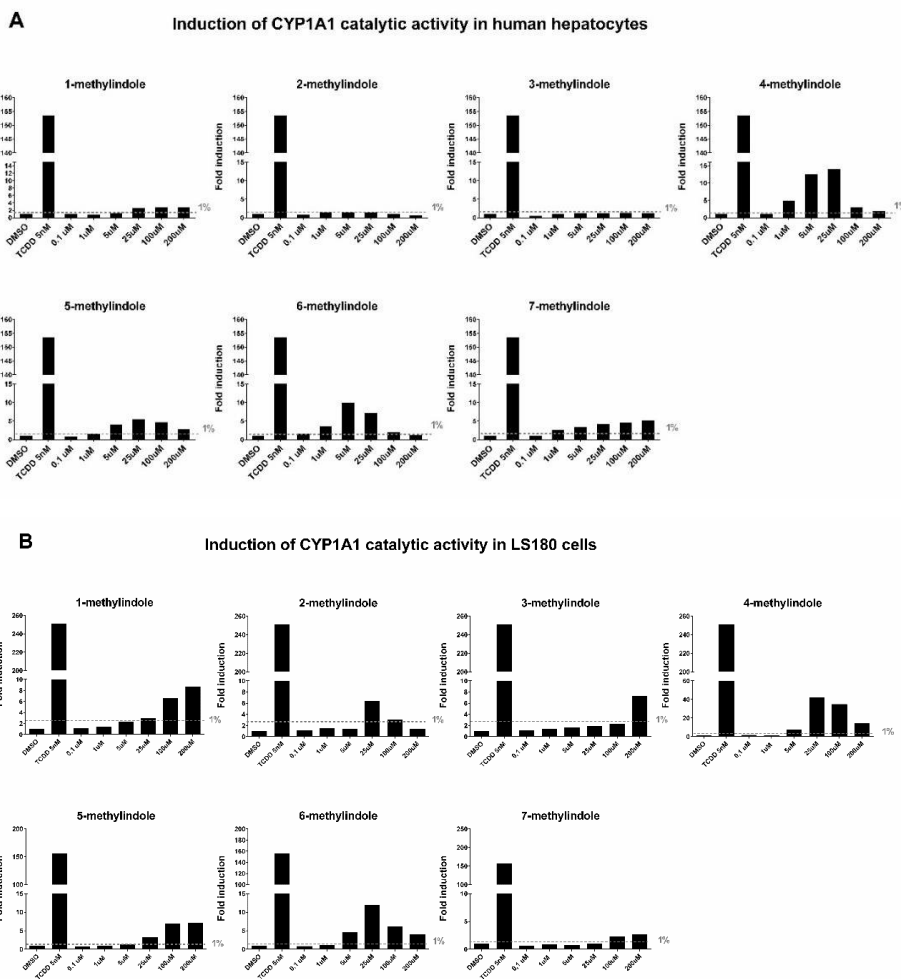

Figure 6: Effects of MMIs on the induction of the catalytic activity of CYP1A1 in primary human hepatocytes and LS180 cells.
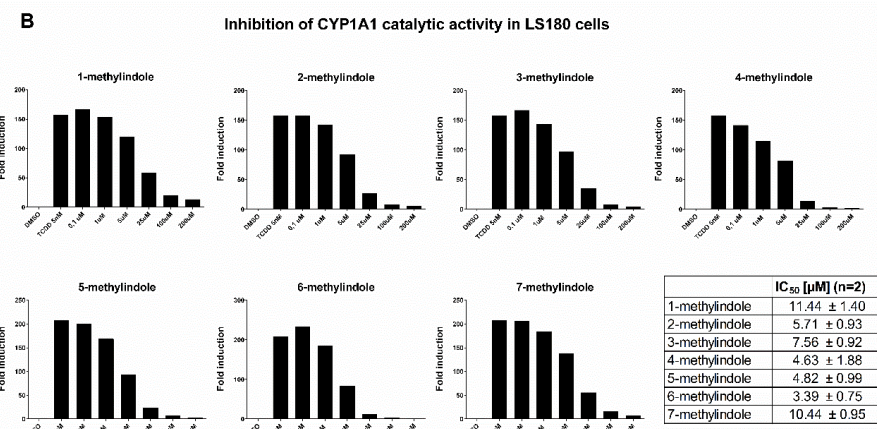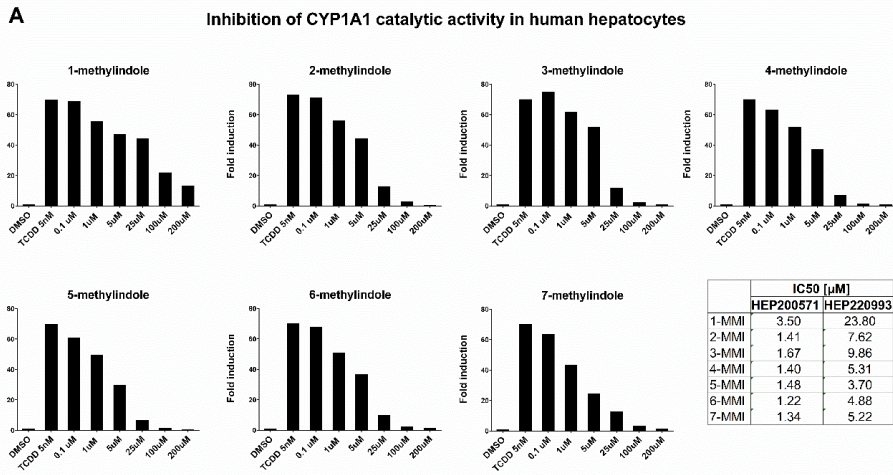
Figure 7: Inhibitory effects of MMIs on TCDD-induced catalytic activity of CYP1A1 in primary human hepatocytes and LS180 cells.
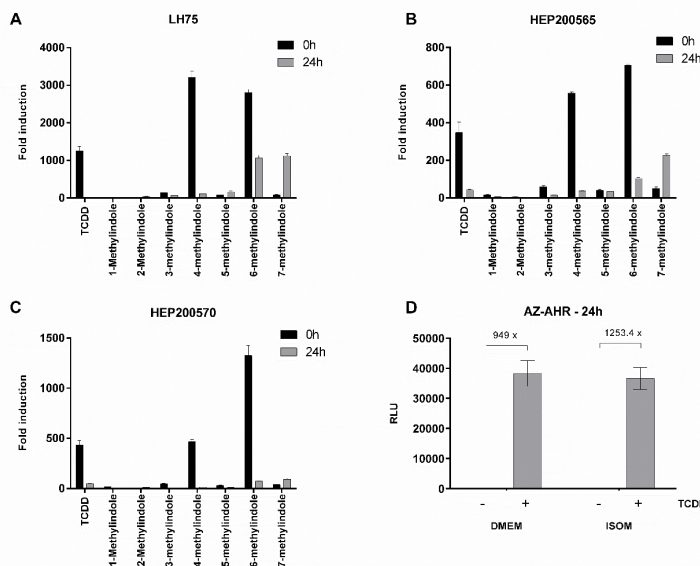
Figure 8: Effects of MMIs metabolites on transcriptional activation of AhR - reporter gene assay.

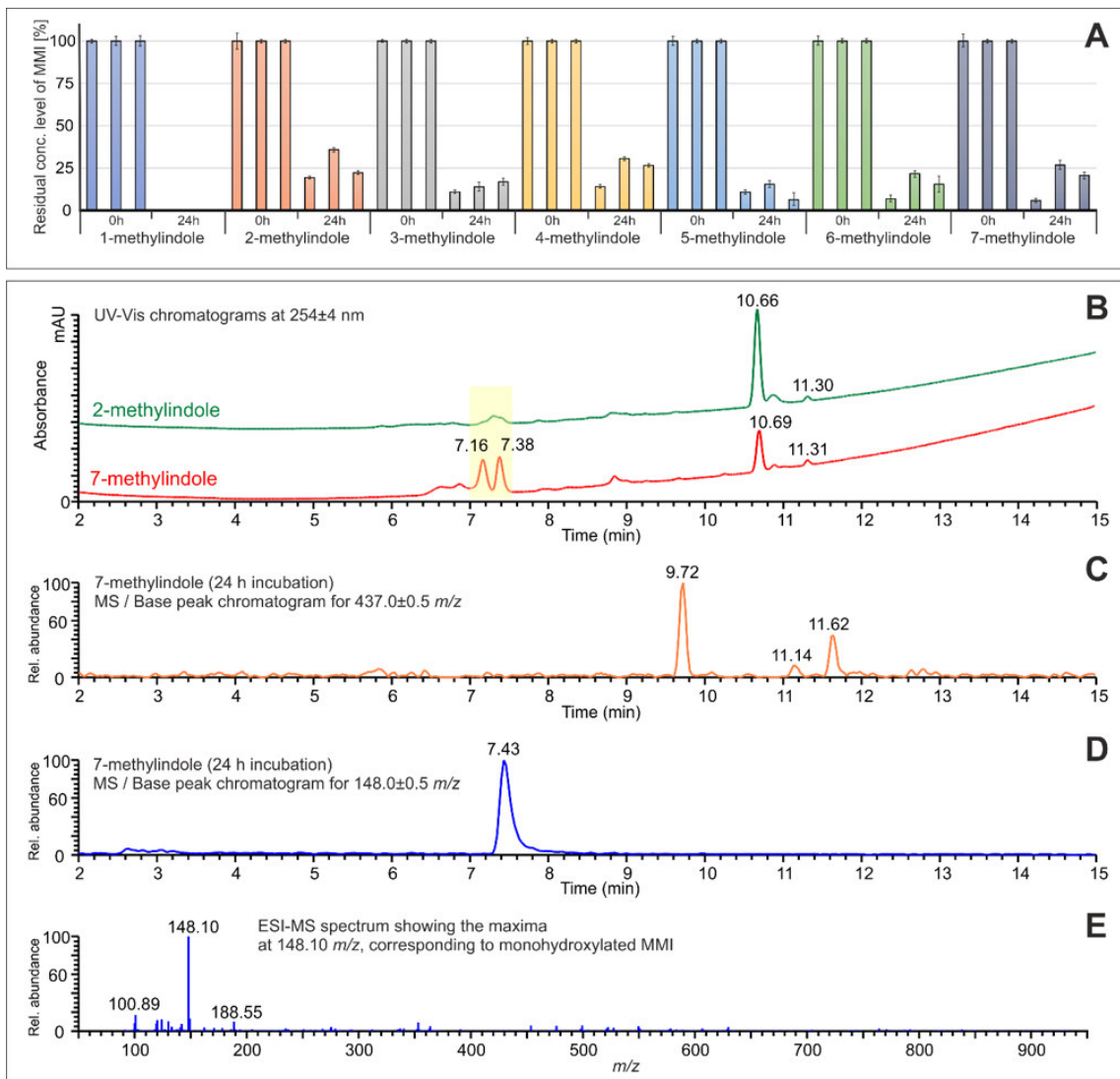# Liquid chromatography/mass spectrometry analyzes of MMI metabolites

Figure 9: Liquid Chromatography/Mass Spectrometry analysis of mono-methylindoles metabolites.

5.2 Effects of MMIs on the PXR signalling pathway

In the next part of the study, we showed differential effects on the PXR-CYP3A4 signalling pathway by MMIs in human hepatic and intestinal cells. We identified 1-MMI as the most PXR-active derivate across all performed assays and observed the induction of PXR-regulated CYP3A4 gene in intestinal LS180 cells and in hepatic progenitor cells HepaRG, but not in primary human hepatocytes. Direct interaction of PXR ligand-binding domain with 1-MMI was revealed using TR-FRET assay as well as ChIP assay, and the results showed 1-MMI-induced increase in PXR binding in the promoter of CYP3A4. The discrepancy in CYP3A4 expression in cell lines and primary human hepatocytes could be due to increased or decreased activities in metabolically competent human hepatocytes; similarly as in previous study (Vyhlidalova et al., 2019). 1-MMI is also a partial agonist of PXR as shown by the reporter gene assay. The absence of CYP3A4 induction by MMIs in primary human hepatocytes would predestine these compounds as intestinal-selective PXR modulators, having no systemic effects from a therapeutic standpoint.
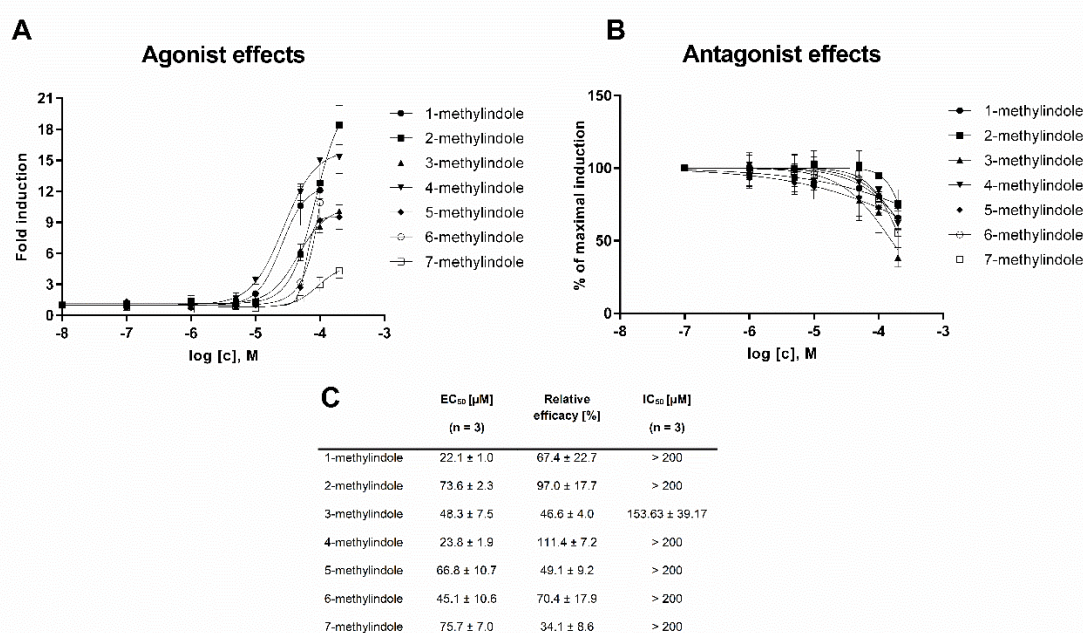

C	EC_{50} [μM] (n = 3)	Relative efficacy [%]	IC_{50} [μM] (n = 3)
1-methylindole	22.1 ± 1.0	67.4 ± 22.7	> 200
2-methylindole	73.6 ± 2.3	97.0 ± 17.7	> 200
3-methylindole	48.3 ± 7.5	46.6 ± 4.0	153.63 ± 39.17
4-methylindole	23.8 ± 1.9	111.4 ± 7.2	> 200
5-methylindole	66.8 ± 10.7	49.1 ± 9.2	> 200
6-methylindole	45.1 ± 10.6	70.4 ± 17.9	> 200
7-methylindole	75.7 ± 7.0	34.1 ± 8.6	> 200

Figure 10: Effects of MMIs on the transcriptional activity of PXR-reporter gene assay.
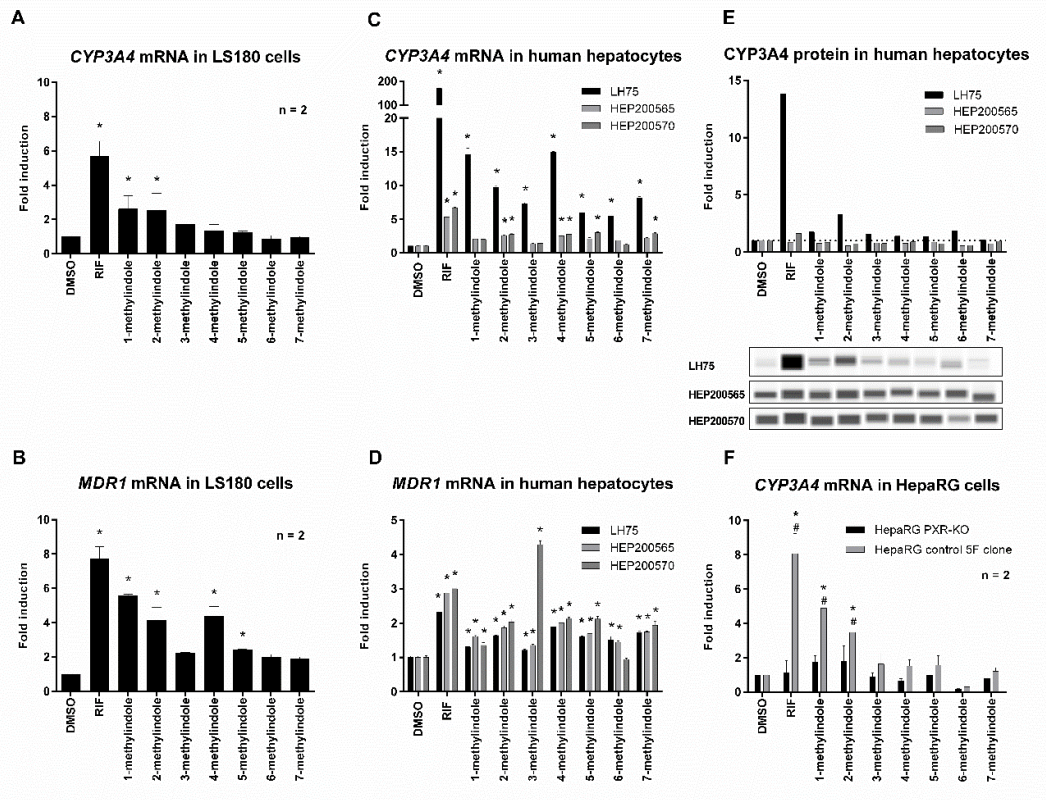
Figure 11: Effects of mono-methylated indoles on the expression of CYP3A4 and MDR1 genes in human hepatic and intestinal cells.
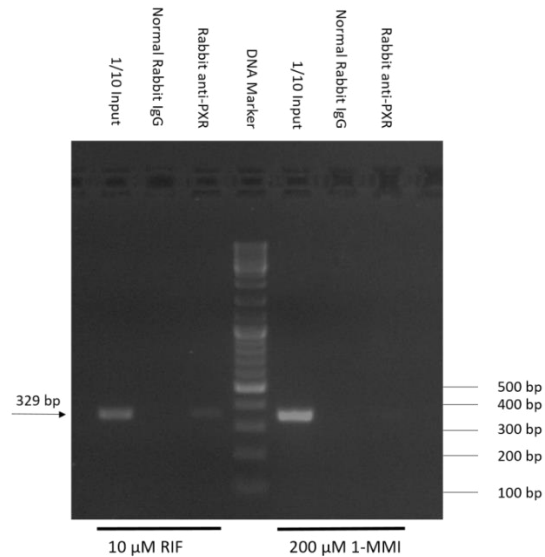

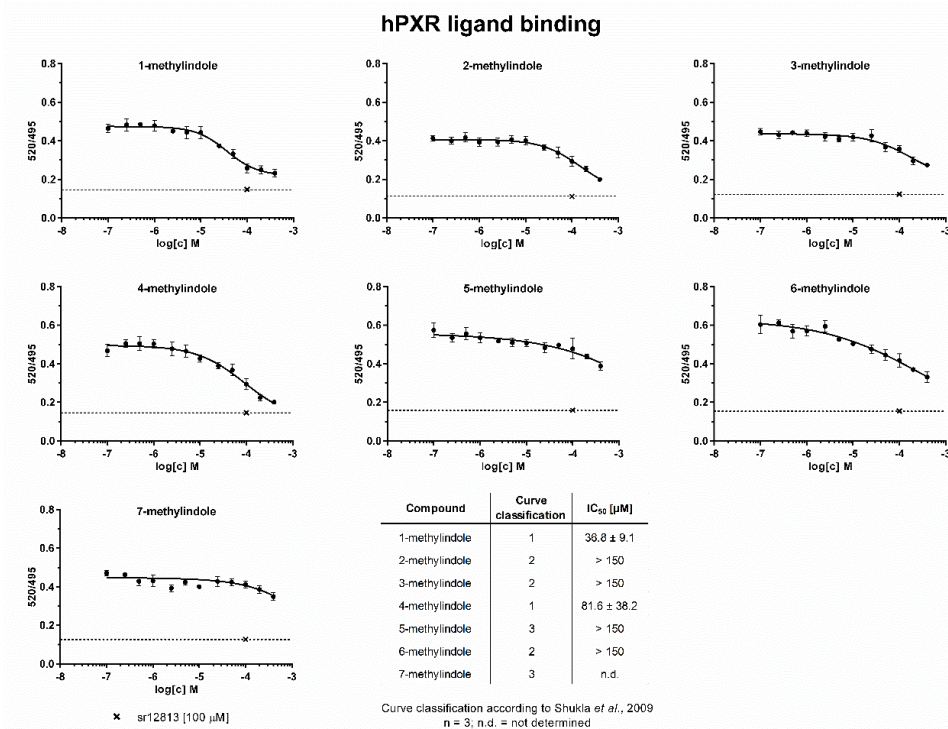**Figure 12: Effect of 1-MMI on the binding of PXR to DNA.**

hPXR ligand binding

Compound	Curve classification	IC_{50} [μM]
1-methylindole	1	36.8 ± 9.1
2-methylindole	2	> 150
3-methylindole	2	> 150
4-methylindole	1	81.6 ± 38.2
5-methylindole	3	> 150
6-methylindole	2	> 150
7-methylindole	3	n.d.

Curve classification according to Shukla *et al.*, 2009
n = 3; n.d. = not determined

Figure 13: Binding of MMIs at PXR-TR FRET assay.

5.3 Effects of microbial intestinal catabolites of tryptophan (MICTs) on the AhR signalling pathway

Next, we comprehensively described, for the first time, the effects of all known human MICTs on AhR activity and functions. We found that MICTs: (i) displaced [3H]-TCDD from the AhR in the ligand-binding assay; (ii) activated AhR in reporter gene assays; (iii) induced AhR target gene expression; (iv) triggered nuclear translocation of AhR; (v) induced the formation of AhR-ARNT heterodimer; and (vi) enhanced binding of AhR to CYP1A1 promoter. The results showed that MICTs act as ligands and agonists of AhR to different extent, as summarised in Table 3. We focused on the effects of MICTs occurring at biologically relevant concentrations after 24 h. Due to the concentrations used and the extensive metabolism of indole compounds, the plateau was not reached in the reporter gene assays and EC_{50} values were estimated. In the follow-up study, the effects of MICT were determined after 4 h and almost all MICTs reached a plateau (unpublished data). The relative efficacy was almost the same, compared with that of model AhR ligand TCDD; however, the EC_{50} values were significantly reduced after 4 h, compared with that observed

at 24 h. For example, the estimated EC_{50} for indole was 1485 ± 91.7 µM after 24 h, while EC_{50} for indole after 4 h was 37 ± 17 µM. Hubbard et al. observed dose-dependent indole-induced increase in AhR transcriptional activity with EC_{50} of 3 µM in HepG2 cells after 4 h (Hubbard et al., 2015a), which was relatively consistent with our findings from 30 experiments.

Table 3: Summary of MICT effects on the AhR-CYP1A1 pathway

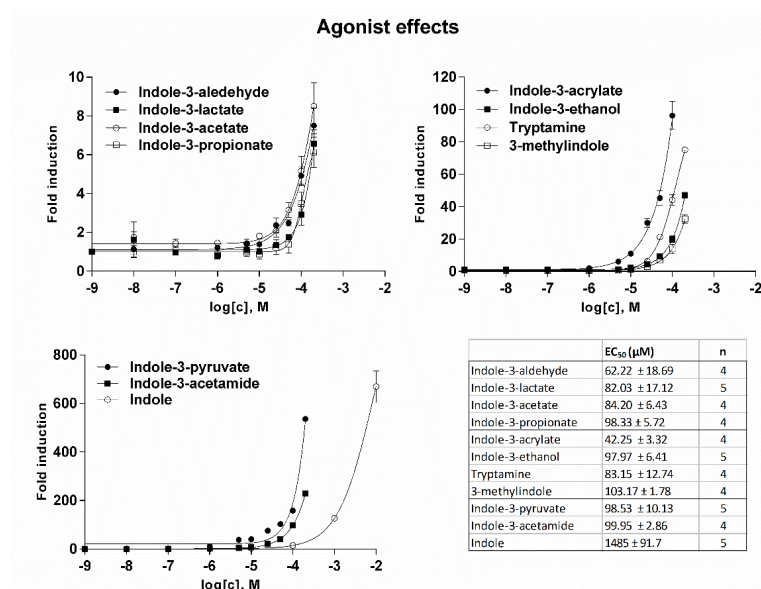| Compound	Affinity (IC_{50})	Potency (EC_{50})	Efficacy (E_{MAX})	Antagonism (IC_{50})	Gene expression	AhR cell functions (translocation; heterodimerisation; DNA-binding
Indole	very low	very low	high	yes – all ligands	strong inducer	highly active – all parameters
Skatole	low	low	medium	ligand selective	strong inducer	highly active – all parameters
Tryptamine	no	low	medium	yes – all ligands	strong inducer	highly active – all parameters
I3-acetamide	low	low	high	none	strong inducer	highly active – all parameters
I3-acetate	no	low	low	none	inactive	not tested
I3-acrylate	very low	low	medium	none	strong inducer	highly active – all parameters
I3-aldehyde	no	low	low	yes – all ligands	inactive	not tested
I3-ethanol	very low	low	medium	ligand selective	inactive	not tested
I3-lactate	no	low	low	none	inactive	not tested
I3-propionate	no	low	low	none	inactive	not tested
I3-pyruvate	low	low	high	ligand selective	strong inducer	highly active – all parameters

Figure 14: Effects of MICTs on the transcriptional activity of AhR (agonist mode)-reporter gene assay.
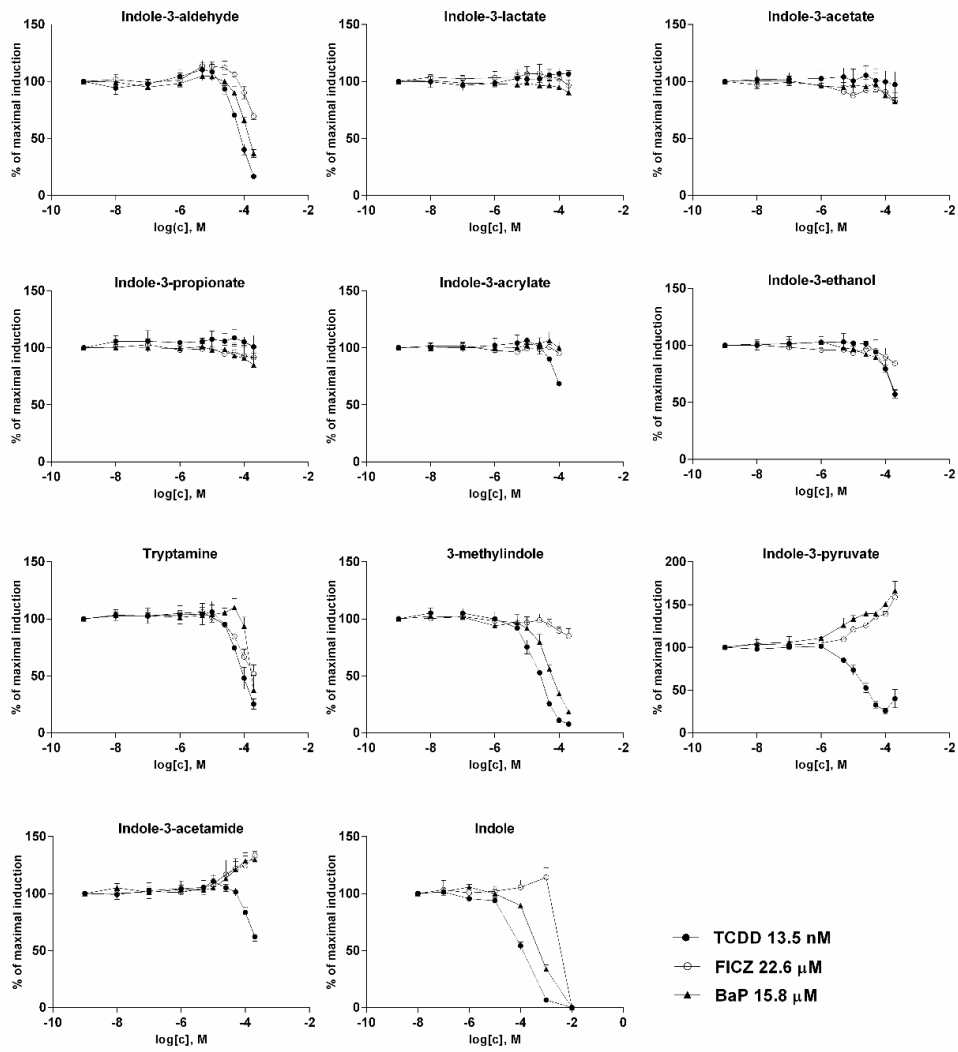
Antagonist effects

Figure 15: Effects of MICTs on the transcriptional activity of AhR (antagonist mode) - reporter gene assay.
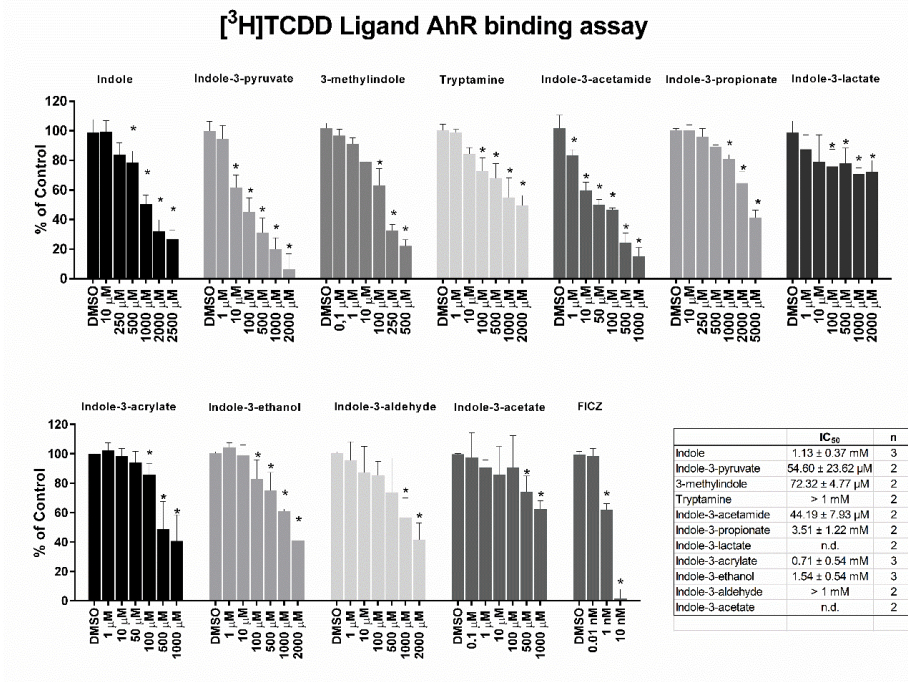
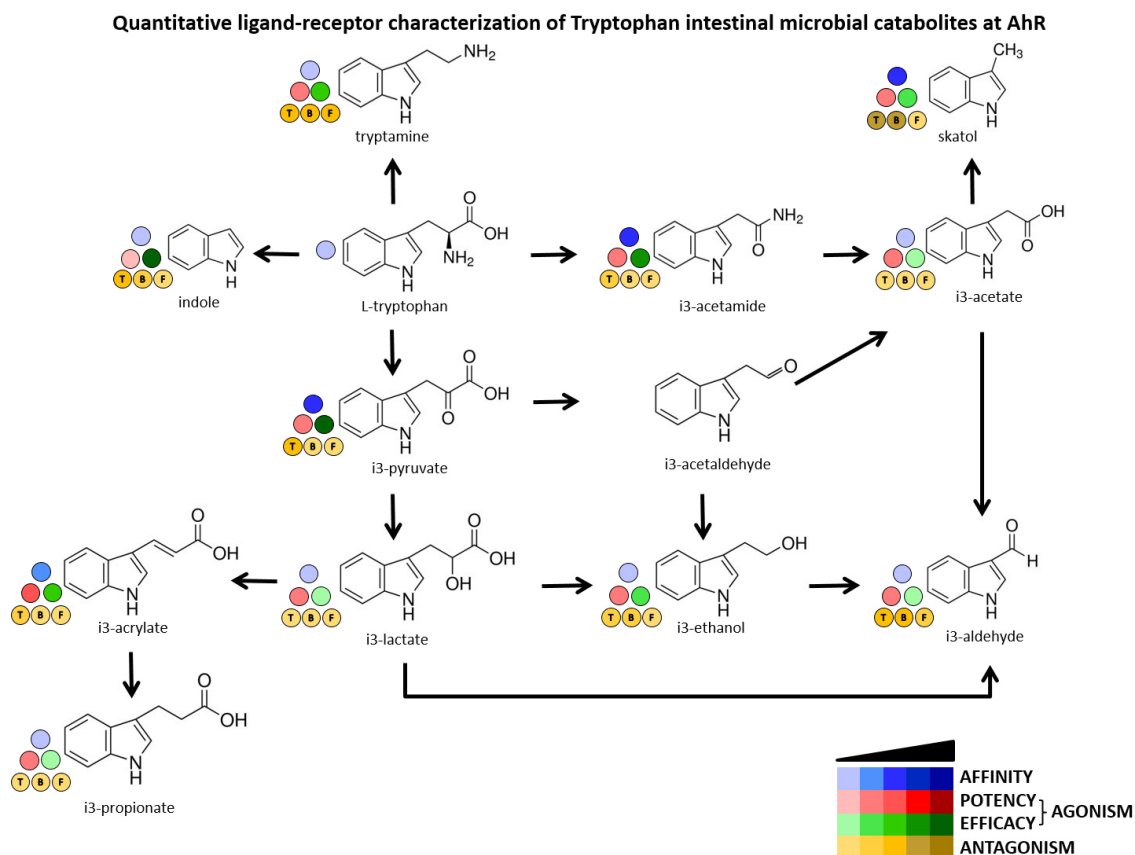**Figure 16: Binding of MICTs at AhR – competitive radio ligand binding assay.**

Figure 17: Quantitative characterisation of interactions between MICT and AhR.
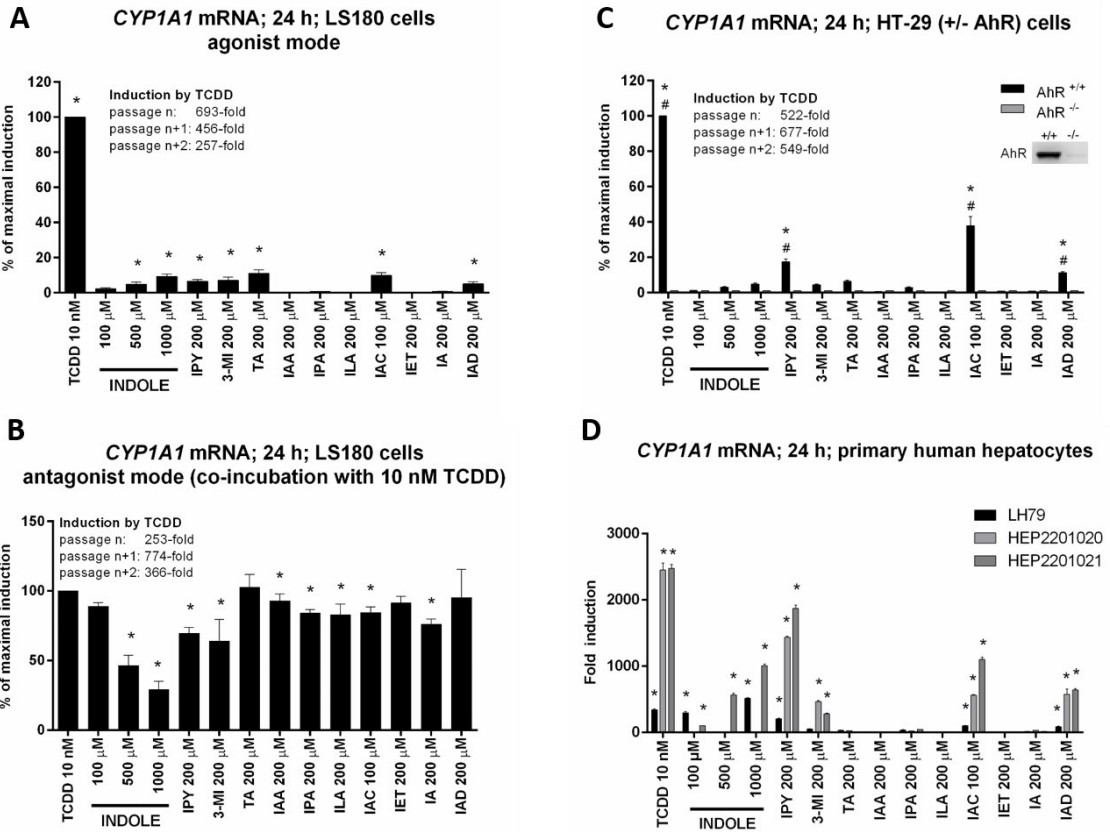
Figure 18: Effects of MICT on the expression of CYP1A1 mRNA in human hepatic and intestinal cells.
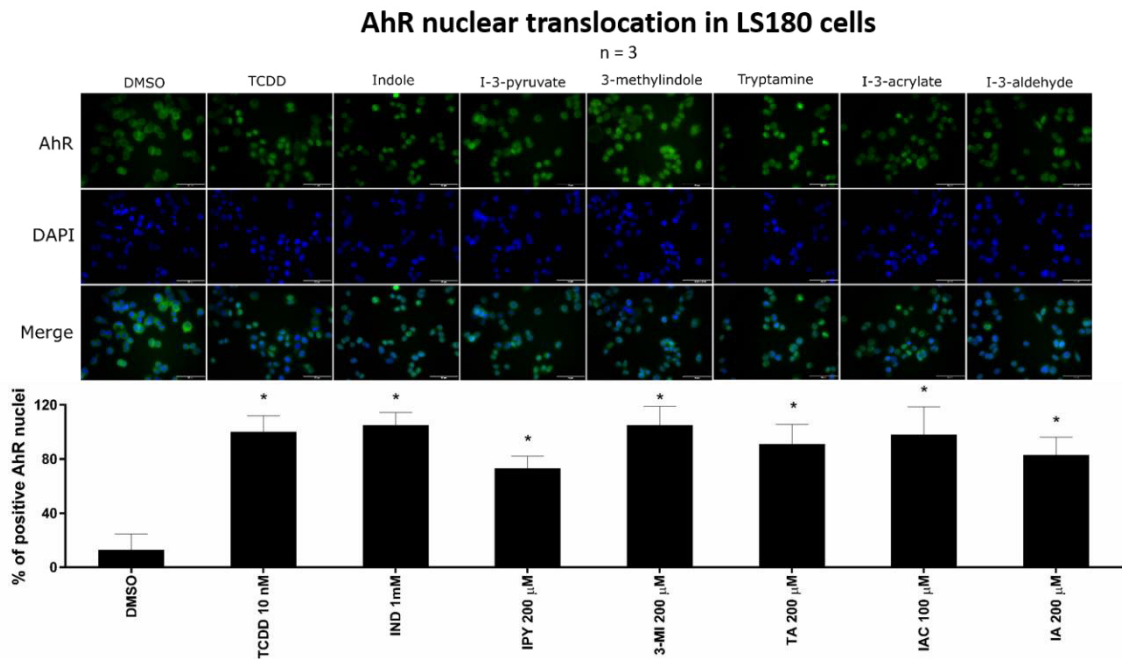

Figure 19: Effect of MICTs on the nuclear translocation of AhR.
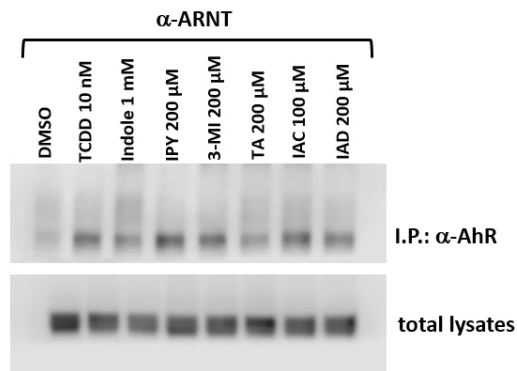
Protein co-immunoprecipitation AhR-ARNT

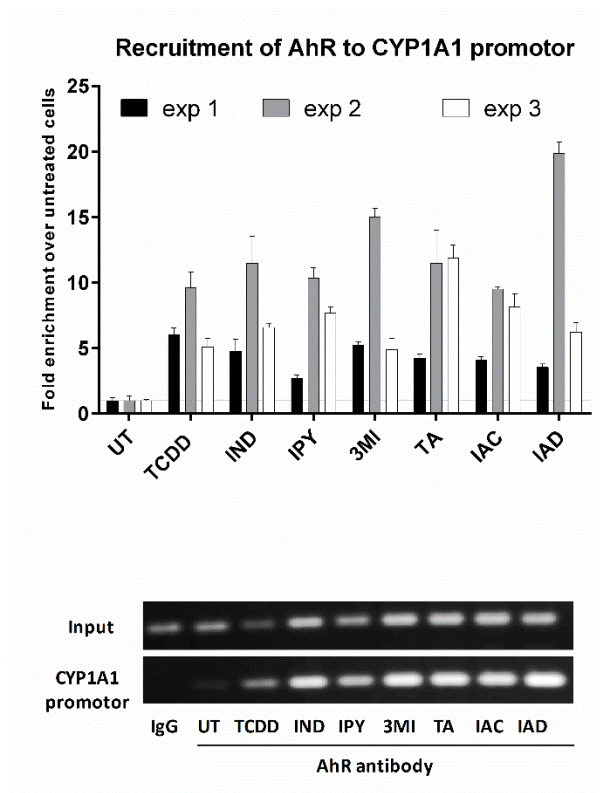**Figure 20: Effects of MICTs on the formation of the AhR-ARNT heterodimer.**

Figure 21: Effect of MICTs on AhR binding to DNA.

5.4 Effects of MICTs on the PXR signalling pathway

The last part of the study was focused on the effects of MICT on PXR activity and consecutive molecular events. We defined IND as a low-affinity (IC_{50} = 292 μM) ligand of the hPXR, which exhibited low-potency and high-efficacy agonist effects on PXR. IND concentration in faeces have been detected in the range of 250 μM to 6000 μM (Dvorak et al., 2020; Hubbard et al., 2015b; Jin et al., 2014; Lamas et al., 2016; Roager et Licht, 2018), which is sufficient to activate intestinal PXR. We also identified IAD as a medium-affinity (IC_{50} = 10 μM) ligand of PXR; however, intestinal or faecal concentrations of IAD are unknown. The other MICTs were inactive to PXR.
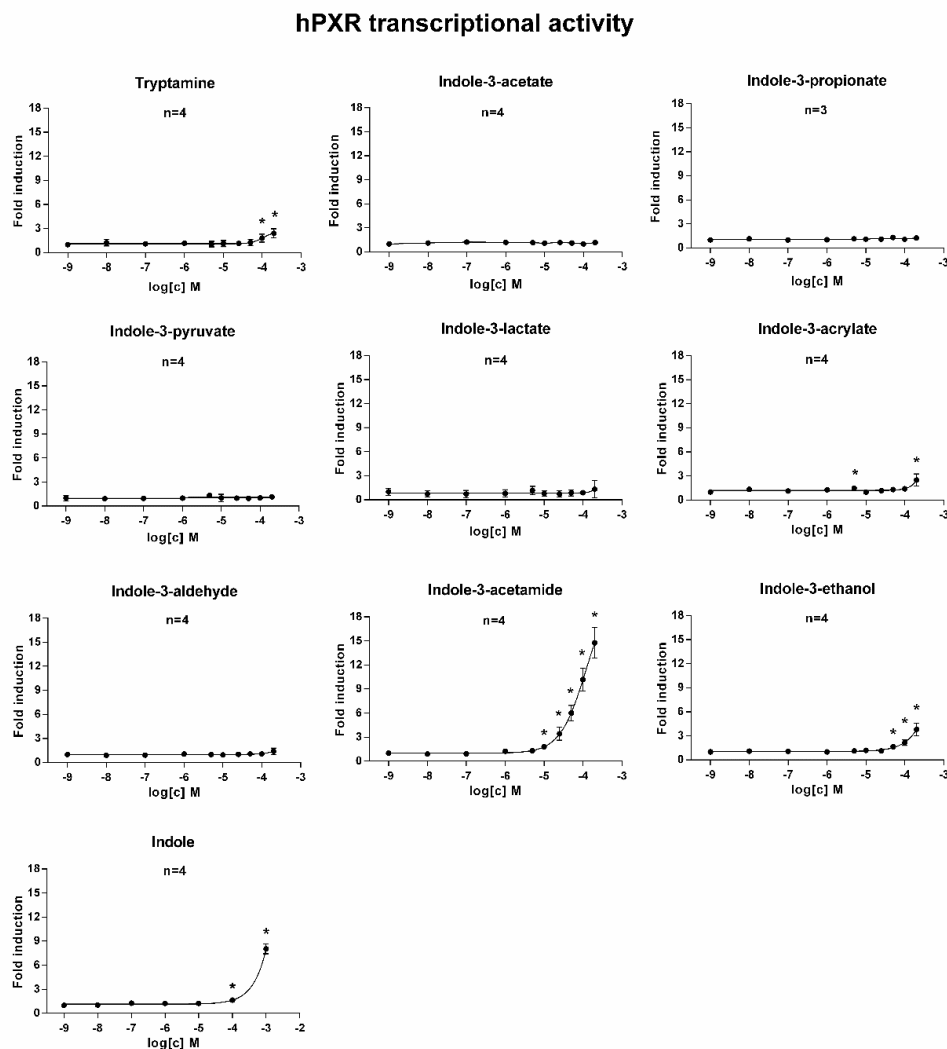

Figure 22: Effects of MICT on the transcriptional activity of PXR (agonist mode)–reporter gene assay.

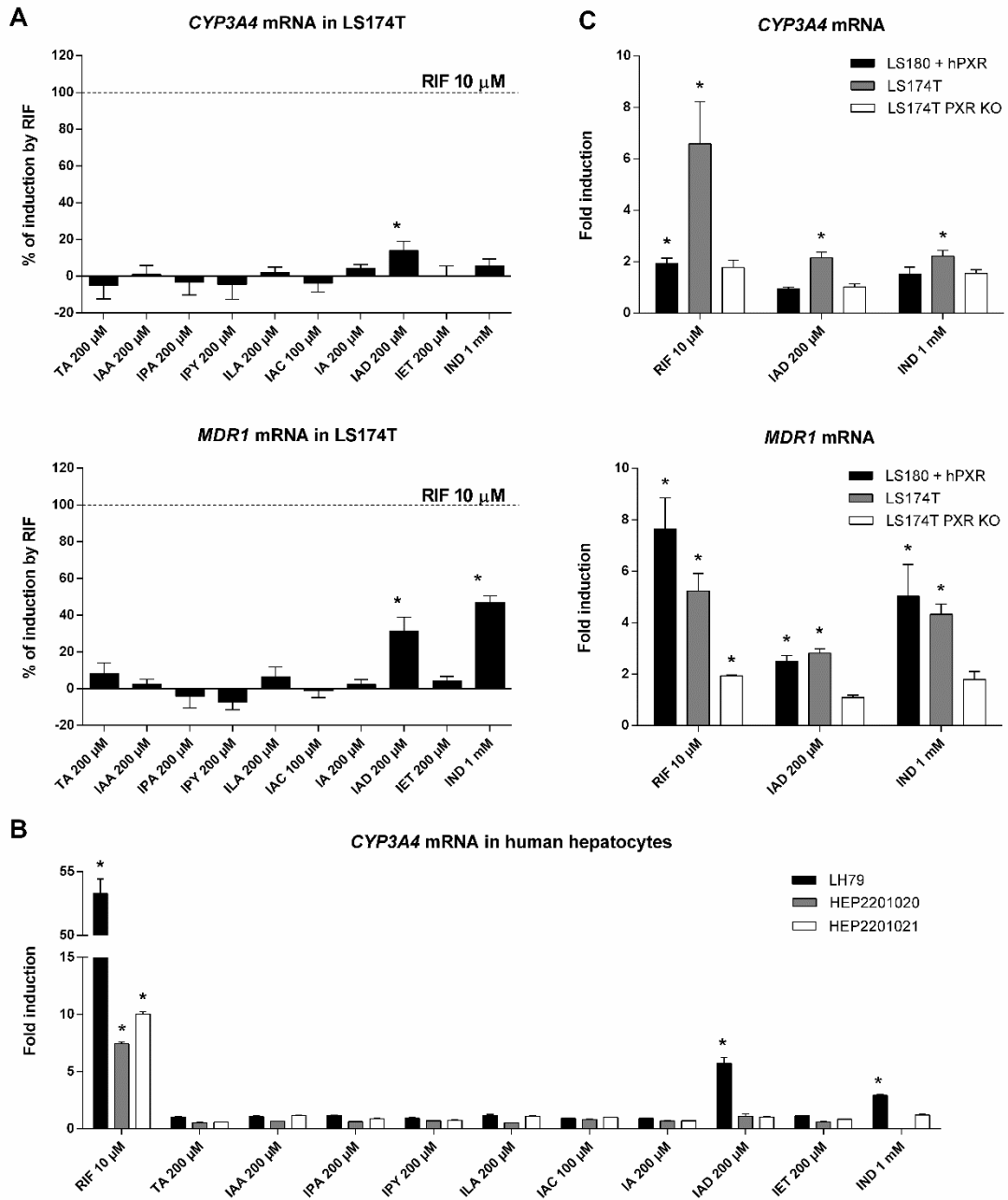**Figure 23: Effects of MICTs on the mRNA expression of CYP3A4 and MDR1 in human hepatic and intestinal cells.** Binding of IND and IAD to the ligand-binding domain of PXR

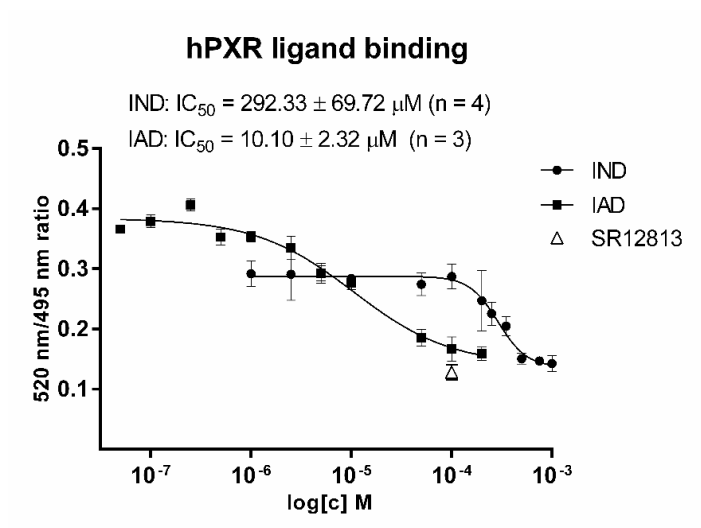## hPXR ligand binding

IND: $IC_{50} = 292.33 \pm 69.72$ μM (n = 4)

IAD: $IC_{50} = 10.10 \pm 2.32$ μM (n = 3)

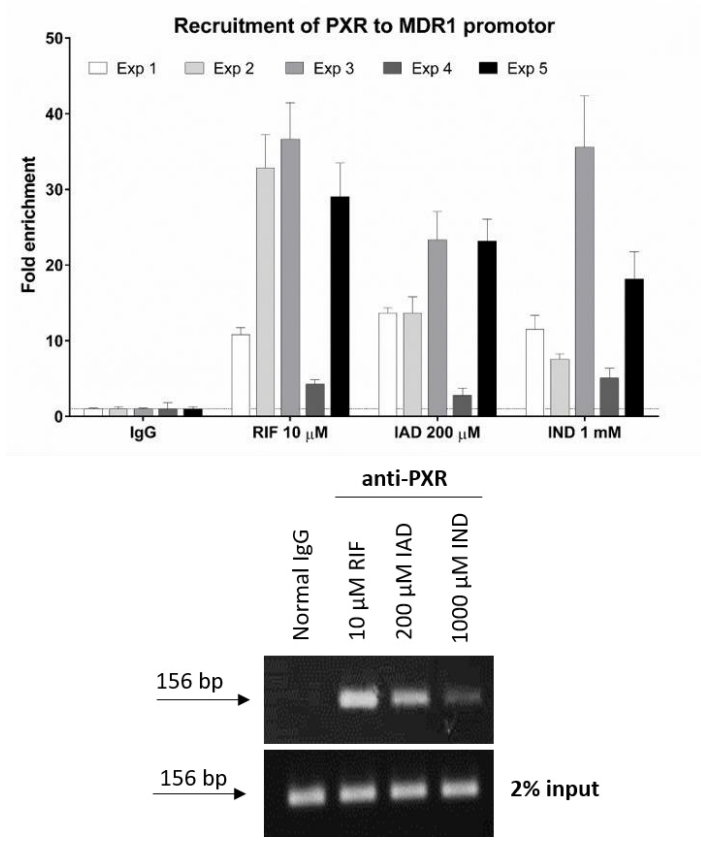**Figure 24: Binding of IND and IAD at PXR-TR FRET assay.**

Figure 25: Effect of MICTs on the binding of PXR to DNA.

Our findings suggest that small structural changes in the indole molecule lead to differential activation of AhR and PXR receptors; therefore, studying structure-activity relationship of compounds that are focused on specific target is essential for development new drugs. This study demonstrated that indole is identified as a dual activator of both receptor, but its 3-substituted metabolites bind to AhR and PXR with various affinity, potency and efficacy. Although mono-methyl substitution at any position of the indole ring increases PXR activity, we found that 3-substituted indoles with mono-carboxylic acids (acetate, acrylate, lactate, propionate, and pyruvate) as well as with aldehyde group are very weak or even inactive toward PXR. In contrast, all of these exhibited higher potency and efficacy to AHR than PXR. Interestingly, IPA does not activate human PXR in intestinal cells, but Venkatesh et al. demonstrated the agonistic effects of IPA in combination with indole in mice, which additionally had strong PXR-mediated anti-inflammatory effects (Venkatesh et al., 2014). Substitution with hydroxyethyl or hydroxyamine moieties exerted weak agonist effects on PXR, while acetamide moiety exerted strong PXR activation. Indole-3-acetamide also binds to AhR with similar affinity and potency to PXR, but PXR showed higher relative potency at the same metabolite concentration than AhR. However, we did not find any commonality between the structures of the studied indoles in relation to AhR activity, as was the case for PXR.

Overall, our studies expand the list of indole derivatives that can act as ligands for PXR and/or AhR. Our findings may pave way for the design of new indole-based therapeutic scaffolds for the treatment of different diseases, such as IBDs, in which both receptors are supposed to play an important role. However, the impact of MICTs (or their derivatives) on intestinal health requires further study, as they occur as complex mixtures within intestines and understanding their cumulative effects on AhR and PXR might be a clue for therapeutic targeting of these receptors.

6 CONCLUSION

The present thesis focused on the effects of 7 MMIs and 11 MICTs on the AhR and PXR signalling pathways. The major findings are:

(i) MMIs are agonists of AhR. The overall effects of MMIs on the AhR-CYP1A pathway in human cells involve the induction of CYP1A genes, the inhibition of CYP1A1 catalytic activity, and the combined action of parental compounds and their metabolites.

(ii) MMIs are partial agonists of PXR that induce PXR-regulated genes in intestinal cells, but not in primary human hepatocytes. The major PXR-active 1-MMI showed only negligible AhR activity, allowing 1-MMI to be considered as intestinal PXR-selective activator.

(iii) MICTs are low-potency agonists of AhR that induce CYP1A1 mRNA in intestinal cells and primary human hepatocytes as well as trigger all other molecular events of the AhR signalling pathway.

(iv) Indole and indole-3-acetamide are agonists of PXR and inducers of PXR-regulated genes in intestinal cells.

The data suggest that the position of the methylated group on the indole ring may be responsible for the preference of the compound for AhR/PXR binding. Furthermore, we found that indole and indole-3-acetamide are dual activators of AhR and PXR in intestinal cells, which could facilitate the understanding of the role of microbial catabolites in human physiology and pathophysiology.

7 REFERENCES

Adachi, J., Mori, Y., Matsui, S., Takigami, H., Fujino, J., Kitagawa, H., Miller, C.A., Kato, T., Saeki, K., Matsuda, T. (2001). Indirubin and indigo are potent aryl hydrocarbon receptor ligands present in human urine. *Journal of Biological Chemistry*, 276, 31475-31478.

Bock, K.W. (2017). Human and rodent aryl hydrocarbon receptor (AHR): from mediator of dioxin toxicity to physiologic AHR functions and therapeutic options. *Biol Chem*, 398, 455-464.

Brown, D.R., Clark, B.W., Garner, L.V., Di Giulio, R.T. (2015). Zebrafish cardiotoxicity: the effects of CYP1A inhibition and AHR2 knockdown following exposure to weak aryl hydrocarbon receptor agonists. *Environ Sci Pollut Res Int*, 22, 8329-38.

Brown, D.R., Clark, B.W., Garner, L.V., Di Giulio, R.T. (2016). Embryonic cardiotoxicity of weak aryl hydrocarbon receptor agonists and CYP1A inhibitor fluoranthene in the Atlantic killifish (Fundulus heteroclitus). *Comp Biochem Physiol C Toxicol Pharmacol*, 188, 45-51.

Bull, M.J., Plummer, N.T. (2014). Part 1: The Human Gut Microbiome in Health and Disease. *Integr Med (Encinitas)*, 13, 17-22.

Denison, M.S., Rogers, J.M., Rushing, S.R., Jones, C.L., Tetangco, S.C., Heath-Pagliuso, S. (2002). Analysis of the aryl hydrocarbon receptor (AhR) signal transduction pathway. *Curr Protoc Toxicol*, Chapter 4, Unit4 8.

Dong, F., Hao, F., Murray, I.A., Smith, P.B., Koo, I., Tindall, A.M., Kris-Etherton, P.M., Gowda, K., Amin, S.G., Patterson, A.D., Perdew, G.H. (2020). Intestinal microbiota-derived tryptophan metabolites are predictive of Ah receptor activity. *Gut Microbes*, 12, 1-24.

Dvorak, Z., Kopp, F., Costello, C.M., Kemp, J.S., Li, H., Vrzalova, A., Stepankova, M., Bartonkova, I., Jiskrova, E., Poulikova, K., Vyhlidalova, B., Nordstroem, L.U., Karunaratne, C.V., Ranhotra, H.S., Mun, K.S., Naren, A.P., Murray, I.A., Perdew, G.H., Brtko, J., Toporova, L., Schon, A., Wallace, B.D., Walton, W.G., Redinbo, M.R., Sun, K., Beck, A., Kortagere, S., Neary, M.C., Chandran, A., Vishveshwara, S., Cavalluzzi, M.M., Lentini, G., Cui, J.Y., Gu, H., March, J.C., Chatterjee, S., Matson, A., Wright, D., Flannigan, K.L., Hirota, S.A.,

Sartor, R.B., Mani, S. (2020). Targeting the pregnane X receptor using microbial metabolite mimicry. *EMBO Mol Med*, 12, e11621.

Gao, J., Xu, K., Liu, H., Liu, G., Bai, M., Peng, C., Li, T., Yin, Y. (2018). Impact of the Gut Microbiota on Intestinal Immunity Mediated by Tryptophan Metabolism. *Front Cell Infect Microbiol*, 8, 13.

Gutierrez-Vazquez, C., Quintana, F.J. (2018). Regulation of the Immune Response by the Aryl Hydrocarbon Receptor. *Immunity*, 48, 19-33.

Hakkola, J., Rysa, J., Hukkanen, J. (2016). Regulation of hepatic energy metabolism by the nuclear receptor PXR. *Biochim Biophys Acta*, 1859, 1072-1082.

Heath-Pagliuso, S., Rogers, W.J., Tullis, K., Seidel, S.D., Cenijn, P.H., Brouwer, A., Denison, M.S. (1998). Activation of the Ah receptor by tryptophan and tryptophan metabolites. *Biochemistry*, 37, 11508-15.

Hubbard, T.D., Murray, I.A., Bisson, W.H., Lahoti, T.S., Gowda, K., Amin, S.G., Patterson, A.D., Perdew, G.H. (2015a). Adaptation of the human aryl hydrocarbon receptor to sense microbiota-derived indoles. *Sci Rep*, 5, 12689.

Hubbard, T.D., Murray, I.A., Perdew, G.H. (2015b). Indole and Tryptophan Metabolism: Endogenous and Dietary Routes to Ah Receptor Activation. *Drug Metab Dispos*, 43, 1522-35.

Chai, S.C., Wright, W.C., Chen, T. (2020). Strategies for developing pregnane X receptor antagonists: Implications from metabolism to cancer. *Med Res Rev*, 40, 1061-1083.

Illes, P., Krasulova, K., Vyhlidalova, B., Poulikova, K., Marcalikova, A., Pecinkova, P., Sirotova, N., Vrzal, R., Mani, S., Dvorak, Z. (2020). Indole microbial intestinal metabolites expand the repertoire of ligands and agonists of the human pregnane X receptor. *Toxicol Lett*, 334, 87-93.

Islam, J., Sato, S., Watanabe, K., Watanabe, T., Ardiansyah, Hirahara, K., Aoyama, Y., Tomita, S., Aso, H., Komai, M., Shirakawa, H. (2017). Dietary tryptophan alleviates dextran sodium sulfate-induced colitis through aryl hydrocarbon receptor in mice. *J Nutr Biochem*, 42, 43-50.

Isom, H.C., Secott, T., Georgoff, I., Woodworth, C., Mummaw, J. (1985). Maintenance of differentiated rat hepatocytes in primary culture. *Proc Natl Acad Sci U S A*, 82, 3252-6.

Jensen, M.T., Cox, R.P., Jensen, B.B. (1995). 3-Methylindole (skatole) and indole production by mixed populations of pig fecal bacteria. *Appl Environ Microbiol*, 61, 3180-4.

Jin, U.H., Lee, S.O., Sridharan, G., Lee, K., Davidson, L.A., Jayaraman, A., Chapkin, R.S., Alaniz, R., Safe, S. (2014). Microbiome-derived tryptophan metabolites and their aryl hydrocarbon receptor-dependent agonist and antagonist activities. *Mol Pharmacol*, 85, 777-88.

Kolluri, S.K., Jin, U.H., Safe, S. (2017). Role of the aryl hydrocarbon receptor in carcinogenesis and potential as an anti-cancer drug target. *Arch Toxicol*, 91, 2497-2513.

Kumar, P., Lee, J.H., Lee, J. (2021). Diverse roles of microbial indole compounds in eukaryotic systems. *Biol Rev Camb Philos Soc*, 96, 2522-2545.

Lamas, B., Richard, M.L., Leducq, V., Pham, H.P., Michel, M.L., Da Costa, G., Bridonneau, C., Jegou, S., Hoffmann, T.W., Natividad, J.M., Brot, L., Taleb, S., Couturier-Maillard, A., Nion-Larmurier, I., Merabtene, F., Seksik, P., Bourrier, A., Cosnes, J., Ryffel, B., Beaugerie, L., Launay, J.M., Langella, P., Xavier, R.J., Sokol, H. (2016). CARD9 impacts colitis by altering gut microbiota metabolism of tryptophan into aryl hydrocarbon receptor ligands. *Nat Med*, 22, 598-605.

Larigot, L., Juricek, L., Dairou, J., Coumoul, X. (2018). AhR signaling pathways and regulatory functions. *Biochim Open*, 7, 1-9.

Levy, M., Blacher, E., Elinav, E. (2017). Microbiome, metabolites and host immunity. *Curr Opin Microbiol*, 35, 8-15.

Li, G., Young, K.D. (2013). Indole production by the tryptophanase TnaA in Escherichia coli is determined by the amount of exogenous tryptophan. *Microbiology (Reading)*, 159, 402-410.

Mulero-Navarro, S., Fernandez-Salguero, P.M. (2016). New Trends in Aryl Hydrocarbon Receptor Biology. *Front Cell Dev Biol*, 4, 45.

Murray, I.A., Perdew, G.H. (2020). How Ah Receptor Ligand Specificity Became Important in Understanding Its Physiological Function. *International Journal of Molecular Sciences*, 21.

Novotna, A., Pavek, P., Dvorak, Z. (2011). Novel stably transfected gene reporter human hepatoma cell line for assessment of aryl hydrocarbon receptor transcriptional activity: construction and characterization. *Environ Sci Technol*, 45, 10133-9.

Pavek, P., Pospechova, K., Svecova, L., Syrova, Z., Stejskalova, L., Blazkova, J., Dvorak, Z., Blahos, J. (2010). Intestinal cell-specific vitamin D receptor (VDR)-mediated transcriptional regulation of CYP3A4 gene. *Biochem Pharmacol*, 79, 277-87.

Pichard-Garcia, L., Gerbal-Chaloin, S., Ferrini, J.B., Fabre, J.M., Maurel, P. (2002). Use of long-term cultures of human hepatocytes to study cytochrome P450 gene expression. *Methods Enzymol*, 357, 311-21.

Poulain-Godefroy, O., Boute, M., Carrard, J., Alvarez-Simon, D., Tsicopoulos, A., de Nadai, P. (2020). The Aryl Hydrocarbon Receptor in Asthma: Friend or Foe? *Int J Mol Sci*, 21.

Powell, D.N., Swimm, A., Sonowal, R., Bretin, A., Gewirtz, A.T., Jones, R.M., Kalman, D. (2020). Indoles from the commensal microbiota act via the AHR and IL-10 to tune the cellular composition of the colonic epithelium during aging. *Proc Natl Acad Sci U S A*, 117, 21519-21526.

Qiu, Z., Cervantes, J.L., Cicek, B.B., Mukherjee, S., Venkatesh, M., Maher, L.A., Salazar, J.C., Mani, S., Khanna, K.M. (2016). Pregnane X Receptor Regulates Pathogen-Induced Inflammation and Host Defense against an Intracellular Bacterial Infection through Toll-like Receptor 4. *Sci Rep*, 6, 31936.

Rasmussen, M.K., Balaguer, P., Ekstrand, B., Daujat-Chavanieu, M., Gerbal-Chaloin, S. (2016). Skatole (3-Methylindole) Is a Partial Aryl Hydrocarbon Receptor Agonist and Induces CYP1A1/2 and CYP1B1 Expression in Primary Human Hepatocytes. *PLoS One*, 11, e0154629.

Roager, H.M., Licht, T.R. (2018). Microbial tryptophan catabolites in health and disease. *Nat Commun*, 9, 3294.

Schiering, C., Wincent, E., Metidji, A., Iseppon, A., Li, Y., Potocnik, A.J., Omenetti, S., Henderson, C.J., Wolf, C.R., Neberts, D.W., Stockinger, B. (2017). Feedback control of AHR signalling regulates intestinal immunity. *Nature*, 542, 242-245.

Stejskalova, L., Dvorak, Z., Pavek, P. (2011). Endogenous and exogenous ligands of aryl hydrocarbon receptor: current state of art. *Curr Drug Metab*, 12, 198-212.

Stepankova, M., Bartonkova, I., Jiskrova, E., Vrzal, R., Mani, S., Kortagere, S., Dvorak, Z. (2018). Methylindoles and Methoxyindoles are Agonists and Antagonists of Human Aryl Hydrocarbon Receptor. *Mol Pharmacol*, 93, 631-644.

Takaki, M., Mawe, G.M., Barasch, J.M., Gershon, M.D., Gershon, M.D. (1985). Physiological responses of guinea-pig myenteric neurons secondary to the release of endogenous serotonin by tryptamine. *Neuroscience*, 16, 223-40.

Tourino, M.C., de Oliveira, E.M., Belle, L.P., Knebel, F.H., Albuquerque, R.C., Dorr, F.A., Okada, S.S., Migliorini, S., Soares, I.S., Campa, A. (2013). Tryptamine and dimethyltryptamine inhibit indoleamine 2,3 dioxygenase and increase the tumor-reactive effect of peripheral blood mononuclear cells. *Cell Biochem Funct*, 31, 361-4.

Venkatesh, M., Mukherjee, S., Wang, H., Li, H., Sun, K., Benechet, A.P., Qiu, Z., Maher, L., Redinbo, M.R., Phillips, R.S., Fleet, J.C., Kortagere, S., Mukherjee, P., Fasano, A., Le Ven, J., Nicholson, J.K., Dumas, M.E., Khanna, K.M., Mani, S. (2014). Symbiotic bacterial metabolites regulate gastrointestinal barrier function via the xenobiotic sensor PXR and Toll-like receptor 4. *Immunity*, 41, 296-310.

Vyhlidalova, B., Krasulova, K., Pecinkova, P., Marcalikova, A., Vrzal, R., Zemankova, L., Vanco, J., Travnicek, Z., Vondracek, J., Karasova, M., Mani, S., Dvorak, Z. (2020). Gut Microbial Catabolites of Tryptophan Are Ligands and Agonists of the Aryl Hydrocarbon Receptor: A Detailed Characterization. *Int J Mol Sci*, 21.

Vyhlidalova, B., Poulikova, K., Bartonkova, I., Krasulova, K., Vanco, J., Travnicek, Z., Mani, S., Dvorak, Z. (2019). Mono-methylindoles induce CYP1A genes and inhibit CYP1A1 enzyme activity in human hepatocytes and HepaRG cells. *Toxicol Lett*, 313, 66-76.

Weems, J.M., Yost, G.S. (2010). 3-Methylindole metabolites induce lung CYP1A1 and CYP2F1 enzymes by AhR and non-AhR mechanisms, respectively. *Chem Res Toxicol*, 23, 696-704.

Williams, B.B., Van Benschoten, A.H., Cimermancic, P., Donia, M.S., Zimmermann, M., Taketani, M., Ishihara, A., Kashyap, P.C., Fraser, J.S., Fischbach, M.A. (2014). Discovery and characterization of gut microbiota decarboxylases that can produce the neurotransmitter tryptamine. *Cell Host Microbe*, 16, 495-503.

Wishart, D.S. (2019). Metabolomics for Investigating Physiological and Pathophysiological Processes. *Physiol Rev*, 99, 1819-1875.

Wlodarska, M., Kostic, A.D., Xavier, R.J. (2015). An integrative view of microbiome-host interactions in inflammatory bowel diseases. *Cell Host Microbe*, 17, 577-91.

Yokoyama, M.T., Carlson, J.R. (1979). Microbial metabolites of tryptophan in the intestinal tract with special reference to skatole. *Am J Clin Nutr*, 32, 173-8.

Zelante, T., Iannitti, R.G., Cunha, C., De Luca, A., Giovannini, G., Pieraccini, G., Zecchi, R., D'Angelo, C., Massi-Benedetti, C., Fallarino, F., Carvalho, A., Puccetti, P., Romani, L. (2013). Tryptophan catabolites from microbiota engage aryl hydrocarbon receptor and balance mucosal reactivity via interleukin-22. *Immunity*, 39, 372-85.

Zhang, C.H., Ma, S.G., Delarosa, E.M., Tay, S., Sodhi, J., Musinipally, V., Chang, P., Pai, R., Halladay, J.S., Misner, D., Kenny, J.R., Hop, C.E.C.A., Khojasteh, S.C. (2014). For a series of methylindole analogs, reactive metabolite formation is a poor predictor of intrinsic cytotoxicity in human hepatocytes. *Toxicology Research*, 3, 184-190.

8 LIST OF PUBLICATIONS

Abbott K. L., Chaudhury C. S., Chandra, A., Vishveshwara S., Dvorak Z., Jiskrova E., Poulikova K., **Vyhlidalova B.**, Mani S. and Pondugula S. R. (2019). Belinostat, at Its Clinically Relevant Concentrations, Inhibits Rifampicin-Induced CYP3A4 and MDR1 Gene Expression. *Mol Pharmacol*, 95(3): 324-334 **[IF$_{2019}$ 3.664]**

Vyhlidalova B., Poulikova K., Bartonkova I., Krasulova K., Vanco J., Travnicek Z., Mani S. and Z. Dvorak (2019). Mono-methylindoles induce CYP1A genes and inhibit CYP1A1 enzyme activity in human hepatocytes and HepaRG cells. *Toxicol Lett*, 313, 66-76 **[IF$_{2019}$ 3.569]**

Vyhlidalova B., Bartonkova I., Jiskrova E., Li H., Mani S. and Dvorak Z. (2020). Differential activation of human pregnane X receptor PXR by isomeric mono-methylated indoles in intestinal and hepatic in vitro models. *Toxicol Lett*, 324: 104-110 **[IF$_{2020}$ 4.374]**

Dvorak Z., Kopp F., Costello C. M., Kemp J. S., Li H., Vrzalova A., Stepankova M., Bartonkova I., Jiskrova E., Poulikova K., **Vyhlidalova B.**, Nordstroem L. U., Karunaratne C. V., Ranhotra H. S., Mun K. S., Naren A. P., Murray I. A., Perdew G. H., Brtko J., Toporova L., Schon A., Wallace W. G., Walton W. G., Redinbo M. R., Sun K., Beck A., Kortagere S., Neary M. C., Chandran A., Vishveshwara S., Cavalluzzi M. M., Lentini G., Cui J. Y., Gu H., March J. C., Chatterjee S., Matson A., Wright D., Flannigan K. L., Hirota S. A., Sartor R. B. and Mani S. (2020). Targeting the pregnane X receptor using microbial metabolite mimicry. *EMBO Mol Med*, 12(4): e11621 **[IF$_{2020}$ 12.137]**

Vyhlidalova B., Krasulova K., Pecinkova P., Marcalikova A., Vrzal R., Zemankova L., Vanco J., Travnicek Z., Vondracek J., Karasova M., Mani S., Dvorak Z. (2020). Gut Microbial Catabolites of Tryptophan Are Ligands and Agonists of the Aryl Hydrocarbon Receptor: A Detailed Characterization. *Int J Mol Sci*, 21(7): 2614 **[IF$_{2020}$ 5.924]**

Vyhlidalova B., Krasulova K., Pecinkova P., Poulikova K., Vrzal R., Andrysik Z., Chandran A., Mani S. and Dvorak Z. (2020). Antimigraine Drug Avitriptan Is a Ligand and Agonist of Human Aryl Hydrocarbon Receptor that Induces CYP1A1 in Hepatic and Intestinal Cells. *Int J Mol Sci* 21(8):2799 **[IF$_{2020}$ 5.924]**

Illes P., Krasulova K., **Vyhlidalova B.**, Poulikova K., Marcalikova A., Pecinkova P., Sirotova N., Vrzal R., Mani S. and Dvorak Z. (2020). Indole microbial intestinal metabolites expand the repertoire of ligands and agonists of the human pregnane X receptor. *Toxicol Lett*, 334: 87-93 **[IF$_{2020}$ 4.374]**

Grycova A., Joo H., Maier V., Illes P., **Vyhlidalova B.**, Poulikova K., Sladekova L., Nadvornik P., Vrzal R., Zemankova L., Pecinkova P., Poruba M., Zapletalova I., Vecera R., Anzenbacher P., Ehrmann J., Ondra P., Jung J.-W., Mani S., Dvorak Z. (2022). Targeting the aryl hydrocarbon receptor with microbial metabolite mimics alleviates experimental colitis in mouse. *J Med Chem* 65(9):6859-6868 **[IF$_{2021}$ 8.039]**

Conference reports

Vyhlidalova B., Poulikova K., Bartonkova I., Dvorak Z.: Methylindoles activate human pregnane X receptor. *International Meeting on 22nd MDO and 33rd JSSX*; 2018 Oct 1-5; Kanazawa; Japan; p-183.

Poulikova K., **Vyhlidalova B.**, Bartonkova I., Dvorak, Z.: Antagonists effects of carvones at human AhR. *International Meeting on 22nd MDO and 33rd JSSX*; 2018 Oct 1-5; Kanazawa; Japan; p-182.

Vyhlidalova B., Krasulova K., Poulikova K., Bartonkova I., Dvorak Z.: Dual effects of methylated indoles on CYP1A1 in human hepatocytes. *12th International ISSX meeting*; 2019 July 28-31; Portland; Oregon; p-20.